foods

Special Issue Reprint

Postharvest Management of Fruits and Vegetables Series II

Edited by
Imahori Yoshihiro and Jinhe Bai

mdpi.com/journal/foods

MDPI

Postharvest Management of Fruits and Vegetables Series II

Postharvest Management of Fruits and Vegetables Series II

Editors

Imahori Yoshihiro
Jinhe Bai

MDPI

Basel • Beijing • Wuhan • Barcelona • Belgrade • Novi Sad • Cluj • Manchester

Editors

Imahori Yoshihiro
Osaka Metropolitan
University
Sakai
Japan

Jinhe Bai
Horticultural Research
Laboratory
Fort Pierce
USA

Editorial Office
MDPI
St. Alban-Anlage 66
4052 Basel, Switzerland

This is a reprint of articles from the Special Issue published online in the open access journal *Foods* (ISSN 2304-8158) (available at: https://www.mdpi.com/journal/foods/special_issues/Postharvest_Fruits_Vegetables_Series).

For citation purposes, cite each article independently as indicated on the article page online and as indicated below:

Lastname, A.A.; Lastname, B.B. Article Title. *Journal Name* **Year**, *Volume Number*, Page Range.

ISBN 978-3-7258-1363-6 (Hbk)
ISBN 978-3-7258-1364-3 (PDF)
doi.org/10.3390/books978-3-7258-1364-3

Contents

About the Editors

Imahori Yoshihiro

Imahori Yoshihiro, PhD, holds the title of Emeritus Professor at Osaka Prefecture University in Japan. He served as a professor there until 2022, specializing in post-harvest physiology and fruit and vegetable processing. Currently, he serves as a guest researcher at Osaka Metropolitan University in Japan. Dr. Imahori completed his BSc, MSc, and PhD in Agriculture at Osaka Prefecture University. His research primarily focuses on the metabolic regulating mechanisms of fruits and vegetables under various pre-harvest and post-harvest environmental conditions, such as temperature, atmosphere, and light. He has extensively studied topics such as low-temperature storage, controlled atmosphere storage, and post-harvest physiological disorders including chilling and low oxygen injury. Additionally, he has explored post-harvest treatments to prevent these disorders and the ascorbate metabolism in produce. Over his career, Dr. Imahori has published numerous papers both internationally and nationally and has contributed chapters and edited books on the post-harvest physiology of fruits and vegetables.

Jinhe Bai

Jinhe Bai, PhD, is a research chemist at the Horticultural Research Laboratory, Agricultural Research Service, United States Department of Agriculture, located in Fort Pierce, Florida. He earned his BSc and MSc in Horticulture from Shanxi Agriculture University and Northwest A&F University in China, respectively, and obtained his PhD from Osaka Prefecture University in Japan. Before his current role, Dr. Bai gained extensive experience across horticultural and food industries, research institutes, and academia. His research is primarily focused on the preservation of post-harvest fruit and vegetable quality. His expertise spans CA storage, MAP, and edible coating technologies. Additionally, he investigates how internal and environmental factors affect the metabolism of crops, influencing their flavor and nutritional value. His research is enhanced by the use of advanced laboratory equipment and technologies, including GC–MS and LC–MS/MS, to analyze volatile and non-volatile metabolites.

foods

MDPI

Editorial

Postharvest Management of Fruits and Vegetables—Series II

Yoshihiro Imahori [1,*] and Jinhe Bai [2,*]

[1] Graduate School of Agricultural, Osaka Metropolitan University, Osaka 599-8531, Japan
[2] Horticultural Research Laboratory (USDA-ARS), Fort Pierce, FL 34945, USA
* Correspondence: imahori@omu.ac.jp (Y.I.); jinhe.bai@usda.gov (J.B.)

Fruits and vegetables are crucial nutritional sources of carbohydrates, protein, minerals, vitamins, and dietary fiber, offering significant benefits to human health. Their high water content, however, makes them highly susceptible to dehydration and mechanical damage after harvest. Being living organisms, these horticultural crops undergo continuous physiological and biochemical changes, leading to extensive losses due to microbial effects, physical injury, and postharvest senescence. These losses significantly impact the quality and quantity of fruits and vegetables, affecting the balance between harvest and consumption. Effective postharvest management is therefore essential for maintaining quality and extending shelf life, thereby reducing economic losses.

This Special Issue compiles a collection of recent research in the field, featuring ten scientific papers, including eight research articles and two reviews, covering various aspects of postharvest management.

1. Ripening, Ethylene, and the Application of 1-Methylcyclopropene (1-MCP)

Rapid ripening significantly contributes to the swift deterioration of climacteric fruits post-harvest, a common occurrence in apples, pears, mangoes, and papayas. Ethylene is a crucial factor in this process, playing a pivotal role in promoting both respiration and ripening [1]. The chemical compound 1-methylcyclopropene (1-MCP) effectively binds to the ethylene receptors in plants, acting as a competitive inhibitor [2]. This binding mechanism helps mitigate the influence of ethylene, consequently reducing the loss of quality in fresh produce [2,3].

The application of 1-MCP, both before and after harvest, has achieved considerable success in various fruits, particularly in apples [3,4] and pears [3]. Recent efforts have expanded its use to fruits typically consumed at a ripe stage, such as European pears, mangoes, papayas, bananas, tomatoes, and kiwifruit [5]. In cases such as that of apples, where ripening is not required before consumption, it is crucial to maintain 1-MCP usage within the approved dosage limit of 1 ppm or lower [6]. For other fruits, the 1-MCP dosage must be carefully balanced; it should be high enough to extend storage life, yet low enough to allow for the fruit to ripen after storage, optionally with additional ripening treatments [5].

Research by Bai et al. [7] and Shu [8] has shown the importance of skillfully manipulating 1-MCP application for optimal results. Strategies such as delaying the application to stages of partial ripening [8] and reducing the dosage through a combined approach [7] have proven effective. Dias et al. [5] have further compiled the most effective methods for reversing the effects of 1-MCP, contributing valuable insights to the postharvest management of climacteric fruits.

Among the contributions in this issue, three articles involve the application of 1-MCP. Yuan et al. examined the treatment of 1-MCP with or without combination with melatonin on mangoes, observing improved visual quality and increased activities of antioxidant enzymes. Prange and Wright reviewed the additional effects of 1-MCP on apples and pears stored in controlled atmosphere (CA) conditions, finding that some cultivars can be stored at higher temperatures, potentially leading to energy savings and quality benefits. Shah

Citation: Imahori, Y.; Bai, J. Postharvest Management of Fruits and Vegetables—Series II. *Foods* **2024**, *13*, 1049. https://doi.org/10.3390/foods13071049

Received: 18 March 2024
Revised: 21 March 2024
Accepted: 26 March 2024
Published: 29 March 2024

et al. reviewed advances in loquat storage technology, showing that 1-MCP treatment alleviates chilling injury (CI) in loquat, inhibits reactive oxygen species (ROS) production, and maintains membrane integrity, thereby reducing internal browning and the incidence of fruit decay.

2. Controlled and Modified Atmosphere

CA is most commonly used on apples and pears, employing a combination of reduced oxygen and increased carbon dioxide, along with cold temperature and high relative humidity (RH), to reduce water loss, lower respiration rate, prevent decay development, and extend storage life [6]. In comparison with CA, modified atmosphere (MA) is used for film packaging in small-scale and short-term storage, making it more suitable for retailers. The atmosphere composition in MA packaging (MAP) is less precise. Bai et al. [9] demonstrated a perforated packaging which substantially enhanced the quality of small fruit in modified humidity packaging without considerable changes in the oxygen and carbon dioxide.

In this Special Issue, three articles relate to CA/MA. Sinde et al. investigated the effects of passive and active MA on the quality of fresh-cut melons, indicating the importance of packaging design for different melon types to avoid fermented off-flavor associated with ethanol and ethyl acetate. Shah et al. summarized the applications of controlled and modified atmospheres in loquat storage, emphasizing the specific oxygen concentration needs for different fruits. Compared to the low oxygen concentration of 1–3% in apples and pears [6], the required concentration for loquat is much higher, at 10–13%. Prange and Wright intensively examined the effects of CA on apples and pears. A dynamic controlled atmosphere (DCA) was introduced to indicate the ways in which to adjust the oxygen and carbon dioxide concentration during storage to fit the changing plant physiological status in fruit.

3. Natural Wax and Edible Coating Application

Natural wax on the fruit surface plays a key role in protecting against water loss from the fruit and partially creates low-oxygen and high-carbon dioxide conditions within the fruit [10]. Under modern postharvest handling systems, washing and brushing remove most of the natural wax cover, making the fruit more susceptible to water loss and reducing the effectiveness of CA. Edible coatings function similarly to natural wax but offer enhanced effects in terms of water protection and internal gas control [10].

Two articles in this Special Issue relate to natural wax and edible coatings. Bai et al. stored winter melons at 20 °C for four months. The natural wax was initially thin directly after harvest; however, its thickness increased gradually during storage. The nutritional and phytonutritional contents, along with the volatile profile, were well-maintained after four months of storage. The appearance remained good even after six months of storage at 20 °C (unpublished data). Obenland et al. explored the performance of a variety of coatings and found that the coatings did not effectively limit weight loss through either the cuticle or stem end of the blueberries. On the contrary, the application of coatings caused a loss of bloom on the blueberry surface, which negatively affected the appearance and marketability. Although fruits are covered with natural wax, the postharvest application of edible coatings is a standard procedure for many of them. This is carried out to reduce water loss, inhibit respiration, slow down postharvest deterioration, and enhance the appearance of apples, pears, citrus fruits, nectarines, and peaches [10].

4. Cold Storage and Chilling Injury

Cold storage is the most important technology in fresh fruit and vegetable storage. Many fruits originating from tropical and subtropical regions, as well as some from temperate regions, such as mangoes, grapefruits, winter melons, tomatoes, loquats, and even some apple varieties, are susceptible to chilling injury (CI). CI in fresh fruits refers to damage caused by exposing the fruit to low, but not freezing, temperatures. The symptoms vary

depending on the fruit type, but commonly observed signs include surface pitting, internal browning, water soaked appearance (translucency), abnormal ripening, off-flavors and odors, and increased susceptibility to decay [11].

Many fresh products discussed in this Special Issue face CI challenges, including loquats, melons, winter melons, and apples. Cold storage is used for the quality management of loquat fruit; however, the susceptibility of some cultivars to CI can lead to browning and other disorders. Although many melon cultivars are chilling-sensitive, fresh-cut melons do not exhibit clear CI phenomena. Winter melons are susceptible to CI when stored below 13 °C but retain a long storage life at room temperature. Prange and Wright reviewed updated storage temperature recommendations and the factors influencing these temperatures for apples and pears, based on the accumulated postharvest data from the last 20 years. Apple cultivars have been divided into two storage temperature groups (0 to 1 °C and >1 °C) based on chilling sensitivity. Gradual cooling, rather than rapid cooling, is recommended for apple cultivars, especially for chilling-sensitive cultivars. European pear cultivars are held at storage temperatures close to or just below 0 °C since they are not chilling-sensitive, and most cultivars require a cold temperature to induce ethylene production and ripening, especially if picked early for long-term storage. Asian pears apparently have higher-temperature requirements in CA, compared with European pears. The temperature recommendations for regular air (RA) and CA storage differ in some apple and European pear cultivars. The CA recommendation is, on average, approximately 0.9 °C higher for apple cultivars and approximately 0.5 °C higher for pear cultivars, compared with RA. Research evidence suggests that some apple and pear cultivars can be stored at higher temperatures in DCA than in CA, leading to possible energy savings and quality benefits.

5. Decay Control

Fresh produce contains 80–95% of water and rich nutrients, which is an ideal medium for infection and the growth of plant pathogens. In this issue, two articles focus on fruit postharvest decay. Gong et al. examined metabolic changes in apples during *Penicillium expansum* infection, offering insights into decay control strategies. Olmedo et al. explored the efficacy of thymol vapors in managing grapefruit diseases, demonstrating effectiveness and safety.

The application of low-residue chemicals or natural compounds in active packaging systems has been intensively researched for controlling postharvest food safety and decay. Sun et al. [12–14] used controlled-release chlorine dioxide and carvacrol to control microbial growth. Miranda et al. [15] applied coatings incorporated with ginger oil to preserve papaya postharvest quality and prevent decay in papaya.

6. Molecular Markers

The integration of Genome-Wide Association Studies (GWAS) [16], quantitative trait loci (QTL) [17], and single-nucleotide polymorphism (SNP)-based DNA markers [18] represents a cutting-edge approach in the genetic improvement of fruits and vegetables. The analyses are powerful tools used in the agricultural sector, particularly in the improvement of fruit and vegetable crops. GWAS involves scanning the genomes of many different plants to identify genetic variants associated with desirable traits, such as chilling injury tolerance, increased flavor quality, or disease resistance. In contrast, QTL analysis focuses on pinpointing specific regions in the genome (loci) that are responsible for quantifiable traits such as disease tolerance. SNP-based DNA markers are a crucial component in this process. These markers are variations at a single DNA base pair, and they serve as precise genetic signposts. They are used to track the inheritance of specific traits and facilitate marker-assisted selection in breeding programs. By combining GWAS, QTL, and SNP markers, researchers and breeders can more efficiently identify and select for genes that confer advantageous characteristics, leading to the development of fruit and vegetable varieties that are better-suited to various environmental conditions, such as chilling tem-

peratures [19] and plant pathogen pressure [20], and consumer preferences, such as certain volatile profiles [21,22]. This triad of genomic tools has significantly accelerated the pace of crop improvement, enabling more targeted and effective breeding strategies. In this Special Issue, Dos-Santos et al. investigated the effect of QTLs on the volatile compound composition in melons, showing the potential of molecular markers in crop improvement.

In summary, this Special Issue provides a comprehensive exploration of methods and advancements in preserving the quality and extending the shelf life of fruits and vegetables post-harvest. It underscores the critical roles of ripening management, atmospheric conditions, temperature control, and molecular genetics in crop improvement and postharvest quality. This collection of articles offers a detailed overview of the current and emerging postharvest management techniques, highlighting their essential role in maintaining the nutritional and economic value of fruits and vegetables.

Author Contributions: Y.I. and J.B. equally contributed to organizing, composing, and editing this Special Issue. All authors have read and agreed to the published version of the manuscript.

Acknowledgments: For the valuable contributions to this Special Issue, we thank all authors for submitting high-quality manuscripts, the reviewers for their careful evaluation of improving the papers, and the editorial staffs.

Conflicts of Interest: The authors declare no conflicts of interest.

List of Contributions:

1. Yuan, F.; Wang, C.; Yi, P.; Li, L.; Wu, G.; Huang, F.; Huang, M.; Gan, T. The Effects of Combined 1-Methylcyclopropene and Melatonin Treatment on the Quality Characteristics and Active Oxygen Metabolism of Mango Fruit during Storage. *Foods* **2023**, *12*, 1979. https://doi.org/10.3390/foods12101979.
2. Shinde, R.; Vinokur, Y.; Fallik, E.; Rodov, V. Effects of Genotype and Modified Atmosphere Packaging on the Quality of Fresh-Cut Melons. *Foods* **2024**, *13*, 256. https://doi.org/10.3390/foods13020256.
3. Obenland, D.; Leyva-Gutierrez, F.M.A.; Wang, T. Investigations into Determinants of Blueberry Coating Effectiveness. *Foods* **2023**, *12*, 174. https://doi.org/10.3390/foods12010174.
4. Prange, R.; and Wright, A.H. A Review of Storage Temperature Recommendations for Apples and Pears. *Foods* **2023**, *12*, 466. https://doi.org/10.3390/foods12030466.
5. Gong, D.; Bi, Y.; Zong, Y.; Li, Y.; Sionov, E.; Prusky, D. Dynamic Change of Carbon and Nitrogen Sources in Colonized Apples by *Penicillium expansum*. *Foods* **2022**, *11*, 3367. https://doi.org/10.3390/foods11213367.
6. Olmedo, G.M.; Zhang, J.; Zhao, W.; Mattia, M.; Rosskopf, E.N.; Ritenour, M.; Plotto, A.; Bai, J. Application of Thymol Vapors to Control Postharvest Decay Caused by *Penicillium digitatum* and *Lasiodiplodia theobromae* in Grapefruit. *Foods* **2023**, *12*, 3637. https://doi.org/10.3390/foods12193637.
7. Li, C.; He, M.; Cai, Z.; Qi, H.; Zhang, J.; Zhang, C. Hyperspectral Imaging with Machine Learning Approaches for Assessing Soluble Solids Content of Tribute Citru. *Foods* **2023**, *12*, 247. https://doi.org/10.3390/foods12020247.
8. Bai, J.; Rosskopf, E.N.; Jeffries, K.A.; Zhao, W.; Plotto, A. Soil Amendment and Storage Effect the Quality of Winter Melons (*Benincasa hispida* (Thunb) Cogn.) and Their Juice. *Foods* **2023**, *12*, 209. https://doi.org/10.3390/foods12010209.
9. Shah, H.M.S.; Khan, A.S.; Singh, Z.; Ayyub, S. Postharvest Biology and Technology of Loquat (*Eriobotrya japonica* Lindl.). *Foods* **2023**, *12*, 1329. https://doi.org/10.3390/foods12061329.
10. Dos-Santos, N.; Bueso, M.C.; Díaz, A.; Moreno, E.; Garcia-Mas, J.; Monforte, A.J.; Fernández-Trujillo, J.P. Thorough Characterization of *ETHQB3.5*, a QTL Involved in Melon Fruit Climacteric Behavior and Aroma Volatile Composition. *Foods* **2023**, *12*, 376. https://doi.org/10.3390/foods12020376.

References

1. Yang, S.F.; Hoffman, N.E. Ethylene biosynthesis and its regulation in higher plants. *Annu. Rev. Plant Physiol.* **1984**, *35*, 155–189. [CrossRef]
2. Sisler, E.; Serek, M. Inhibitors of ethylene responses in plants at the receptor level: Recent developments. *Physiol. Plant.* **1997**, *100*, 577–582. [CrossRef]

3. Watkins, C.B. The use of 1-methylcyclopropene (1-MCP) on fruits and vegetables. *Biotechnol. Adv.* **2006**, *24*, 389–409. [CrossRef] [PubMed]
4. Fan, X.; Blankenship, S.M.; Mattheis, J.P. 1-Methylcyclopropene inhibits apple ripening. *J. Am. Soc. Hortic. Sci.* **1999**, *124*, 690–695. [CrossRef]
5. Dias, C.; Ribeiro, T.; Rodrigues, A.C.; Ferrante, A.; Vasconcelos, M.W.; Pintado, M. Improving the ripening process after 1-MCP application: Implications and strategies. *Trends Food Sci. Technol.* **2021**, *113*, 382–396. [CrossRef]
6. Bai, J.; Prange, R.K.; Toivonen, P.A. Pome fruits. In *Modified and Controlled Atmospheres for the Storage, Transportation, and Packaging of Horticultural Commodities*; Yahia, E., Ed.; CRC Press: Boca Raton, FL, USA, 2009; pp. 267–285.
7. Bai, J.; Yin, X.; Whitaker, B.D.; Deschuytter, K.; Chen, P.M. Combination of 1-methylcyclopropene and ethoxyquin to control superficial scald of 'Anjou'pears. *HortTechnology* **2009**, *19*, 521–525. [CrossRef]
8. Shu, C.; Wall, M.M.; Follett, P.A.; Sugimoto, N.; Bai, J.; Sun, X. Effect of Humidity-Triggered Controlled-Release 1-Methylcyclopropene (1-MCP) on Postharvest Quality of Papaya Fruit. *Horticulturae* **2023**, *9*, 1062. [CrossRef]
9. Bai, J.; Baldwin, E.; Tsantili, E.; Plotto, A.; Sun, X.; Wang, L.; Kafkaletou, M.; Wang, Z.; Narciso, J.; Zhao, W.; et al. Modified humidity clamshells to reduce moisture loss and extend storage life of small fruits⋆. *Food Packag. Shelf Life* **2019**, *22*, 100376. [CrossRef]
10. Bai, J.; Plotto, A. Coatings for fresh fruits and vegetables. In *Edible Coatings and Films to Improve Food Quality*, 2nd ed.; Baldwin, E., Hagenmaier, R., Bai, J., Eds.; CRC Press: Boca Raton, FL, USA, 2011; pp. 185–242.
11. Sevillano, L.; Sanchez-Ballesta, M.T.; Romojaro, F.; Flores, F.B. Physiological, hormonal and molecular mechanisms regulating chilling injury in horticultural species. Postharvest technologies applied to reduce its impact. *J. Sci. Food Agric.* **2009**, *89*, 555–573. [CrossRef]
12. Sun, X.; Cameron, R.G.; Plotto, A.; Zhong, T.; Ference, C.M.; Bai, J. The Effect of Controlled-Release Carvacrol on Safety and Quality of Blueberries Stored in Perforated Packaging. *Foods* **2021**, *10*, 1487. [CrossRef] [PubMed]
13. Sun, X.; Zhou, B.; Luo, Y.; Ference, C.; Baldwin, E.; Harrison, K.; Bai, J. Effect of controlled-release chlorine dioxide on the quality and safety of cherry/grape tomatoes. *Food Control* **2017**, *82*, 26–30. [CrossRef]
14. Sun, X.; Baldwin, E.; Bai, J. Applications of gaseous chlorine dioxide on postharvest handling and storage of fruits and vegetables—A review. *Food Control* **2019**, *95*, 18–26. [CrossRef]
15. Miranda, M.; Sun, X.; Marín, A.; dos Santos, L.C.; Plotto, A.; Bai, J.; Benedito Garrido Assis, O.; David Ferreira, M.; Baldwin, E. Nano- and micro-sized carnauba wax emulsions-based coatings incorporated with ginger essential oil and hydroxypropyl methylcellulose on papaya: Preservation of quality and delay of post-harvest fruit decay. *Food Chem. X* **2022**, *13*, 100249. [CrossRef] [PubMed]
16. Uffelmann, E.; Huang, Q.Q.; Munung, N.S.; De Vries, J.; Okada, Y.; Martin, A.R.; Martin, H.C.; Lappalainen, T.; Posthuma, D. Genome-wide association studies. *Nat. Rev. Methods Primers* **2021**, *1*, 59. [CrossRef]
17. Nica, A.C.; Dermitzakis, E.T. Expression quantitative trait loci: Present and future. *Philos. Trans. R. Soc. B Biol. Sci.* **2013**, *368*, 20120362. [CrossRef] [PubMed]
18. Schork, N.J.; Fallin, D.; Lanchbury, J.S. Single nucleotide polymorphisms and the future of genetic epidemiology. *Clin. Genet.* **2000**, *58*, 250–264. [CrossRef] [PubMed]
19. Braun, S.R.; Endelman, J.B.; Haynes, K.G.; Jansky, S.H. Quantitative Trait Loci for Resistance to Common Scab and Cold-Induced Sweetening in Diploid Potato. *Plant Genome* **2017**, *10*, plantgenome2016-10. [CrossRef] [PubMed]
20. Khan, M.A.; Zhao, Y.; Korban, S.S. Identification of genetic loci associated with fire blight resistance in Malus through combined use of QTL and association mapping. *Physiol. Plant.* **2013**, *148*, 344–353. [CrossRef] [PubMed]
21. Fan, Z.; Jeffries, K.A.; Sun, X.; Olmedo, G.; Zhao, W.; Mattia, M.R.; Stover, E.; Manthey, J.A.; Baldwin, E.A.; Lee, S.; et al. Chemical and genetic basis of orange flavor. *Sci. Adv.* **2024**, *10*, eadk2051. [CrossRef] [PubMed]
22. Yu, Y.; Bai, J.; Chen, C.; Plotto, A.; Yu, Q.; Baldwin, E.A.; Gmitter, F.G. Identification of QTLs controlling aroma volatiles using a 'Fortune' x 'Murcott' (*Citrus reticulata*) population. *BMC Genom.* **2017**, *18*, 646. [CrossRef] [PubMed]

foods

MDPI

Article

Application of Thymol Vapors to Control Postharvest Decay Caused by *Penicillium digitatum* and *Lasiodiplodia theobromae* in Grapefruit

Gabriela M. Olmedo [1], Jiuxu Zhang [2], Wei Zhao [1], Matthew Mattia [1], Erin N. Rosskopf [1], Mark Ritenour [2], Anne Plotto [1] and Jinhe Bai [1,*]

[1] Horticultural Research Laboratory (USDA-ARS), 2001 S. Rock Rd, Ft. Pierce, FL 34945, USA; gabriela.olmedo@usda.gov (G.M.O.); wei.zhao@usda.gov (W.Z.); matthew.mattia@usda.gov (M.M.); erin.rosskopf@usda.gov (E.N.R.); anne.plotto@ars.usda.gov (A.P.)

[2] Indian River Research and Education Center, University of Florida, 2199 S. Rock Rd, Ft. Pierce, FL 34945, USA; jiuxuzhang@ufl.edu (J.Z.); ritenour@ufl.edu (M.R.)

* Correspondence: jinhe.bai@usda.gov

Abstract: Two of the major postharvest diseases impacting grapefruit shelf life and marketability in the state of Florida (USA) are stem-end rot (SER) caused by *Lasiodiplodia theobromae* and green mold (GM) caused by *Penicillium digitatum*. Here, we investigated the in vitro and in vivo efficacy of vapors of thymol, a natural compound found in the essential oil of various plants and the primary constituent of thyme (*Thymus vulgaris*) oil, as a potential solution for the management of GM and SER. Thymol vapors at concentrations lower than 10 mg L^{-1} significantly inhibited the mycelial growth of both pathogens, causing severe ultrastructural damage to *P. digitatum* conidia. In in vivo trials, the incidence and lesion area of GM and SER on inoculated grapefruit were significantly reduced after a 5 d exposure to 50 mg L^{-1} thymol vapors. In addition, the in vitro and in vivo sporulation of *P. digitatum* was suppressed by thymol. When applied in its vapor phase, thymol had no negative effect on the fruit, neither introducing perceivable off-flavor nor causing additional weight loss. Our findings support the pursuit of further studies on the use of thymol, recognized as safe for human health and the environment, as a promising strategy for grapefruit postharvest disease management.

Keywords: essential oil vapors; citrus; stem-end rot; green mold; sporulation

Citation: Olmedo, G.M.; Zhang, J.; Zhao, W.; Mattia, M.; Rosskopf, E.N.; Ritenour, M.; Plotto, A.; Bai, J. Application of Thymol Vapors to Control Postharvest Decay Caused by *Penicillium digitatum* and *Lasiodiplodia theobromae* in Grapefruit. *Foods* **2023**, *12*, 3637. https://doi.org/10.3390/foods12193637

Academic Editor: Juan Pablo Fernández-Trujillo

Received: 24 August 2023
Revised: 27 September 2023
Accepted: 28 September 2023
Published: 30 September 2023

1. Introduction

Grapefruit (*Citrus paradisi*) is a citrus fruit grown in tropical and subtropical countries around the globe and is highly valued for its sour-to-semisweet flavor and its anticarcinogenic, anti-inflammatory, and antioxidative properties [1–3]. One of the main problems affecting citrus for fresh consumption and juice production is the significant economic loss caused by fungal pathogens that infect fruit before, during, or after harvest, which lead to disease at the postharvest stage. In the state of Florida (USA), hot and humid weather conditions favor the development of several postharvest diseases, but Diplodia stem-end rot (SER), caused by *Lasiodiplodia theobromae* (Pat.) Griffon & Maubl., and green mold (GM), caused by *Penicillium digitatum* Sacc., have always been the most prevalent [4,5]. Moreover, since Huanglongbing (HLB) was confirmed in Florida in 2005, citrus production in Florida has declined significantly largely due to the HLB epidemic [6], while a significant increase in the preharvest *Lasiodiplodia* colonization of HLB-affected fruit tissues has also been reported [7–9]. HLB, attributed to the bacterium *Candidatus* Liberibacter asiaticus, affects citrus trees, generating a multitude of symptoms that include twig dieback, leaf chlorosis and fruit size reduction, asymmetrical shape, irregular color, and premature drop. Typically, *L. theobromae* infects the citrus calyx and floral disk (button) during development on the tree but remains quiescent until the fruit is harvested. In HLB-infected trees, a more

prolific *L. theobromae* presence was found in symptomatic fruit than in asymptomatic fruit, which may result not only in a higher postharvest SER incidence but also in exacerbated HLB-associated fruit drop in the field. A transcriptomic analysis revealed a gene expression profile in the abscission zone of HLB fruit that reflects typical characteristics of defense responses against necrotrophic fungal infection, which was validated by a phytohormone measurement and fungal detection [8]. Thus, the economic losses associated with SER appear to be aggravated in Florida since HLB spread throughout the state.

Traditionally, chemical fungicides have been the primary tool for the control of pre- and postharvest diseases. Postharvest fungicides thiabendazole, imazalil, and fludioxonil are effective in reducing GM, and they have also shown some efficacy against the SER causal agent [4]. However, the year-round usage of the same active ingredients is highly conducive to the selection and proliferation of resistant biotypes of fungal pathogens, such as *P. digitatum* [10]. Moreover, fungicide use is increasingly restricted due to the associated risks to human health and negative environmental impacts. Therefore, growers and packers are left with few effective and environmentally accepted fungicides, and there is an urgent need to search for other safe and effective alternatives that also can reduce the development of pathogen resistance [11,12]. One such alternative is the exploitation of essential oils (EOs), which are known to have little to no impact on human health or the environment. These plant aromatic compounds are generally recognized as safe (GRAS), and research into their use in postharvest disease control has expanded in the past decade. The utilization of EOs and their main chemical components has resulted in the control of postharvest diseases on a variety of fresh fruits and vegetables [13–16], but many were reported to have perceivable negative sensory impacts and/or induced phytotoxic damage to the peel [17–19]. While much previous work was conducted by incorporating EOs into wax coatings or dipping fruit into EO solutions, the application of EOs in the vapor phase has been shown to have certain advantages over that in the liquid phase, such as a minimal or no negative impact on products' organoleptic properties, improved penetration, rapid and homogeneous distribution, and enhanced antimicrobial activity [20–23]. Here, we evaluated the effect of thymol, the main constituent of thyme (*Thymus vulgaris*), in its vapor phase on *P. digitatum* and *L. theobromae*. For this purpose, pathogen mycelia and conidia were exposed to thymol vapors, and inhibitory concentrations were calculated. The in vivo efficacy of thymol treatments to control SER and GM was tested on grapefruit (*Citrus paradisi*) inoculated with fungal pathogens. After storage, weight loss and sensory perceptions were assessed.

2. Materials and Methods

2.1. Fungal Pathogens and Fruit

The isolates used in this study were obtained from the Department of Horticultural Sciences at the University of Florida, India River Research and Education Center, in Fort Pierce, FL (USA). *P. digitatum* (isolate PD-26) was originally collected by G.E. Brown (Florida Department of Citrus, Lake Alfred, FL, USA) and is resistant to thiabendazole [24]. *L. theobromae* (isolate D-36) was isolated from red grapefruit (*C. paradisi*) showing typical lesions of Diplodia stem-end rot (SER) from a grove located in Fort Pierce, FL. For both isolates, morphological identification and pathogenicity tests following Koch postulates on grapefruit were performed [25]. Isolate identities were confirmed via molecular methods using ITS4/ITS5 and EF1-728F/EF1-986R primer sets to amplify the internal transcribed spacer (ITS) region in both isolates and part of the translation elongation factor 1-alpha (TEF1-α) gene in *L. theobromae*. Briefly, mycelia grown on potato dextrose broth were homogenized under liquid nitrogen, and the DNA was extracted using a DNA easy Plant Mini Kit according to the manufacturer's protocol (Qiagen Inc., Germantown, MD, USA). A total of 50 µL PCR mixture was prepared for each isolate, containing 25 µL 2× GoTaq Green Master Mix (Promega, Madison, WI, USA), 2 µL forward and reverse primers (10 µM), 19 µL nuclease-free water, and 2 µL genomic DNA (25–65 ng mL^{-1}). PCR reactions were run in a T100 Thermal Cycler (Bio-Rad, Hercules, CA, USA) that was programmed for a

5 min initial denaturation step at 94 °C, followed by 40 cycles (each 45 s at 94 °C, 30 s at 52 °C, and 90 s at 72 °C) and a 6 min final extension at 72 °C. The amplified products were purified using a QIAquick PCR Purification Kit (Qiagen Inc., Germantown, MD, USA) and sequenced using a 3730xl DNA Analyzer (Applied Biosystems, Hercules, CA, USA). The obtained sequences were compared to the ones reported for *L. theobromae* and *P. digitatum* in GenBank.

The grapefruits (*C. paradisi*, var. 'Flame') used for the in vivo experiments were harvested from commercial groves in Saint Lucie County (FL, USA). Fruits with intact stems and no wounds were selected, taken to the US Horticultural Research Laboratory (USDA-ARS), superficially sanitized via immersion in 200 mg L^{-1} NaClO (pH 6) for 2 min, and then air-dried before use.

2.2. Chemical Compounds

Thymol (98.5%) was purchased from Sigma-Aldrich Co. (St. Louis, MO, USA) and kept at room temperature in the dark until use. For every assay, a thymol melting/crystallization cycle was performed by heating thymol powder above its melting point (49.6 °C) following a protocol reported by Cometa et al. [26] with slight modifications. Namely, thymol was subjected to a thermal treatment at 55 °C until melted onto a 20 mm diameter filter paper (No. 4, Whatman, Cleves, OH, USA). The filter paper was immediately attached to the inner surface of the top lid of the container that was used as indicated for each assay (Petri dishes or plastic 11 gal boxes). The containers were immediately closed and sealed.

2.3. Effective Inhibitory Concentration Determination

In vitro fungal growth inhibition using thymol was assayed following the same protocol for both pathogens, but the initial fungal structures differed (Figure 1). For *L. theobromae*, a 3 mm diameter mycelial plug was placed in the center of a Petri dish (9 cm diameter and 5 cm in height) containing potato dextrose agar (PDA), while for *P. digitatum*, a 5 µL spot of conidial suspension containing 10^4 conidia mL^{-1} was used for plate inoculation. The difference in methodology is based on each pathogen's disease cycle. The key role of conidia in *P. digitatum* spread and infection has been previously reported [27]. Asexual spores are the primary inoculum for GM during fruit–pathogen interaction since the germination of conidia occurs on the surface wounds of citrus. Conversely, *L. theobromae* development on fruit begins in the field, but mycelia remain quiescent until harvest. When the senescence of stem-end tissue post-abscission proceeds, which may be enhanced by postharvest ethylene degreening treatments and under conducive environmental conditions (such as high temperatures and relative humidity), fungal hyphae resume growth, colonize and infect fruit tissue adjacent to the stem-end, and develop through the fruit core tissues, causing whole fruit decay [4]. After inoculation, thymol treatments were applied by melting and crystalizing thymol as explained previously. To achieve the final concentrations of 1, 2, 4, 8, and 16 mg L^{-1} within plate headspaces, 0.32, 0.64, 1.28, 2.56, and 5.12 mg of thymol were used, respectively. The plates were sealed with parafilm and incubated at 25 °C in the dark. Colony diameters were measured daily until the mycelia in the control plates without thymol covered the entire plate. Thymol concentrations that inhibited 50 and 90% of the mycelial growth (effective concentrations, EC_{50} and EC_{90}) were calculated based on logarithmic models (based on the relationship between percent inhibition and compound concentration) [28].

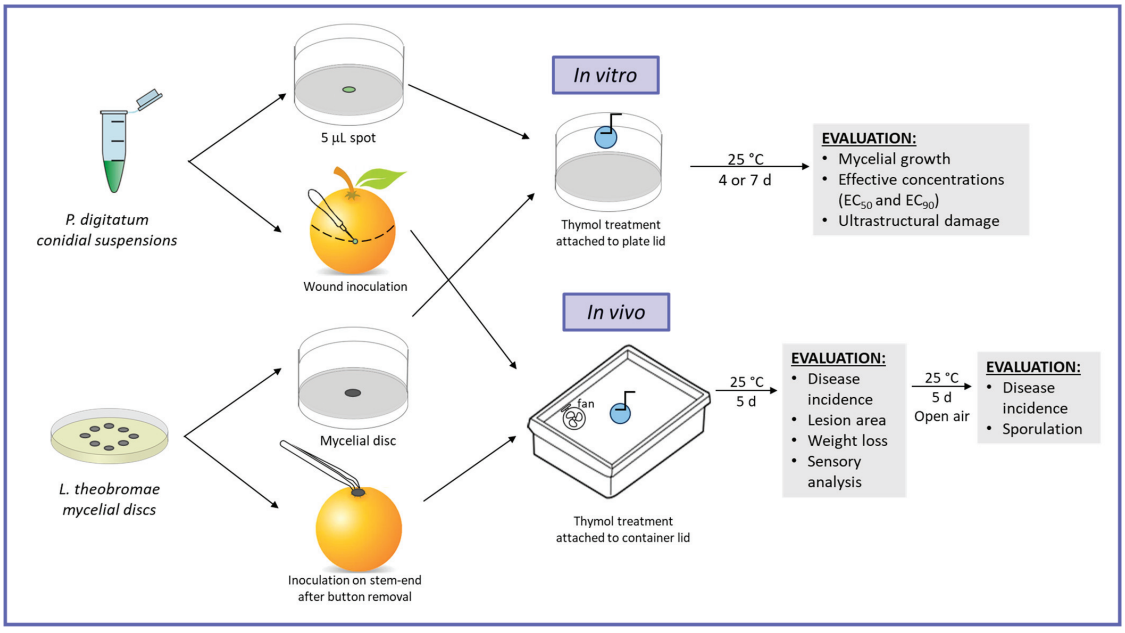

Figure 1. Protocols for the evaluation of the effect of thymol vapors on pathogens' in vitro growth and in vivo development on grapefruit. *P. digitatum* conidial suspensions (10^4 conidia mL^{-1}) and *L. theobromae* mycelial discs (3 mm diameter) were used to inoculate PDA plates and grapefruit. Thymol treatments were applied at 25 °C in air-tight conditions. After incubation, pathogens' in vitro growth and ultrastructural damage were evaluated. In in vivo experiments, disease incidence, lesion area, weight loss, and sensory analyses were performed after 5 d. Then, containers were opened, thymol discs were removed, and fruits were stored for 5 additional days to determine whether thymol vapor had fungicidal or fungistatic effects.

2.4. Scanning Electronic Microscopy (SEM) Observation

SEM was used to observe *P. digitatum* conidial morphology and cell wall integrity after treatment with thymol at sublethal concentrations. Conidial suspensions were exposed to 1 mg L^{-1} thymol treatment for 24 h and then observed under a microscope. Sample preparation was performed following a previously reported protocol [29], with some modifications. Cells were washed three times with deionized water and then covered with a fixative solution containing 2.5% glutaraldehyde and 4% paraformaldehyde in sodium cacodylate buffer 0.1 M (pH 7) (Sigma Aldrich Co., St. Louis, MO, USA). Tubes were incubated at 4 °C overnight. Then, the cells were again washed three times and dehydrated by consecutively transferring them to increasing ethanol concentrations from 30% to 100%. Incubation with 100% ethanol was carried out three times. Finally, the samples were transferred to solutions of ethanol:hexamethyldisilizane (HMDS, Sigma Aldrich Co., St. Louis, MO, USA) at ratios of 3:1, 2:1, and 1:1 with two final steps at 100% HMDS and allowed to evaporate in a chemical fume hood overnight. The cells were attached to SEM stubs, and observations were performed using an S-4800 scanning electron microscope (Hitachi High Technologies America, Inc., Pleasanton, CA, USA) with 1000× magnification and a 5 kV accelerating voltage.

2.5. In Vivo Assays in Airtight Conditions

For in vivo assays, the fruits were inoculated with the pathogens, as shown in Figure 1. For *L. theobromae*, the button on the stem-end of each fruit was removed to expose fresh tissue. A 3 mm diameter mycelial PDA plug from the margin of a 3 d old fungal colony was

placed with mycelia facing down on the wounded area. After 6 h at 25 °C, the plugs were removed. For *P. digitatum*, the fruits were inoculated using a 1 mm wide and 2 mm long sterile stainless steel rod previously immersed in a freshly prepared conidial suspension with a concentration of 10^4 conidia mL^{-1} [30]. After inoculation, the fruits were placed inside 11-gallon gasket-sealed storage boxes (Weather Shield Storage Box, Ziploc, S. C. Johnson & Son, Racine, WI, USA), with twelve fruits per container, arranged in a single layer. Thymol-containing filter papers were attached to the lids, as explained above, to achieve concentrations ranging from 1 to 100 mg L^{-1}. This concentration range was based on antifungal in vitro results, considering that antimicrobial in vivo efficacy is often lower than antimicrobial in vitro efficacy. A thymol slow-release treatment was included to determine whether a more extended inhibitory effect was achieved. This treatment consisted of a Miracloth (Calbiochem®, San Diego, CA, USA) sachet containing pectin–alginate microencapsulated thymol prepared following a protocol previously reported by our group [31]. A 40 mm USB cooling fan (5 V, 5300 rpm, Shenzhen Engesen Electronics Co., Ltd., Shenzhen, China) was attached to an inner wall of each container to ensure air circulation. The containers were closed and stored at 25 °C and 90% RH for 5 d prior to disease incidence and lesion area evaluation. The filter papers were then removed, and the fruits were maintained in the open air for an additional 5 d at 25 °C to determine whether the thymol vapor had a fungicidal or fungistatic effect. Controls consisted of inoculated fruit stored in the same conditions as treatments but not exposed to thymol.

2.6. Weight Loss and Sensory Evaluation

As a quality parameter of grapefruit after thymol treatment, individual fruit weights were determined before and after 5 d of storage at 25 °C. Weight loss was calculated as $(A_0 - A_x)/A_0) \times 100$, where A_0 is the initial fruit weight, and A_x is the weight at the corresponding evaluation time.

All treatments were first evaluated for the potential effects of the carryover of thymol on fruit flavor, and three treatments were chosen for a sensory evaluation test: (i) untreated control, (ii) 100 mg L^{-1} thymol, and (iii) 100 mg L^{-1} thymol encapsulated in pectin–alginate. Following storage, 10 grapefruits per treatment were washed, sanitized in 0.01% PAA, and air-dried at room temperature overnight. On the following day, the fruits were peeled, removing the stem and blossom ends, flavedo, and albedo, and cut into 14–16 pieces each. The pieces were first mixed in a fruit bowl to ensure that every panelist would obtain a 3-piece sample representing different fruits from each treatment. The samples were placed in 3-digit-coded 4 oz cups on a serving tray and served at 18 °C in a randomized order following a Williams design, with the order of presentation balanced across panelists. Testing took place in isolated booths equipped with positive air pressure and red lighting. Sensory evaluation was carried out by a panel of 24 untrained staff members, some of whom were familiar with tasting various citrus fruits. Every panel member was asked to rank the samples for overall preference ("like most" to "like least") [32]. In a second question, they were asked, for each sample, to indicate whether they could detect any off-flavor and describe that off-flavor if any was perceived.

2.7. Statistical Analysis

For in vitro assays, three Petri dish replicates were performed for each condition, and the entire panel of assays was performed three times. In vivo experiments were conducted with a completely randomized design, with two replicates consisting of 12 fruits per replicate (container with 12 grapefruits). The experiment was performed twice. In all cases, an analysis of variance was used to check homogeneity and normality, followed by Student's *t* least significant difference (LSD), and mean separations were based on p values ≤ 0.05. Sensory rank data were analyzed using the Friedman-type statistical test for rank data, with the non-parametric analog to Fisher's LSD for rank sums [32].

3. Results

3.1. Penicillium digitatum Conidia Germination and Lasiodiplodia theobromae Mycelial Growth Inhibition by Thymol Vapors In Vitro

The antifungal activity of EOs has become an important area of agricultural research due to the increasing awareness of the human and environmental toxicity associated with traditional fungicides, as well as the increasing appearance of multi-resistant fungal isolates in packinghouses throughout the world [33,34]. In this work, we evaluated the effect of thymol vapors on two major fungal pathogens affecting citrus in Florida (USA). As shown in Figure 2, fungal growth was significantly affected by exposure to thymol in a concentration-dependent manner. While both pathogens were completely inhibited by 8 mg L^{-1} of thymol, effective concentration calculations showed that *P. digitatum* (EC_{50} = 0.135 mg L^{-1} and EC_{90} = 1.235 mg L^{-1}) was more sensitive than *L. theobromae* (EC_{50} and EC_{90} of 1.13 and 5.42 mg L^{-1}, respectively).

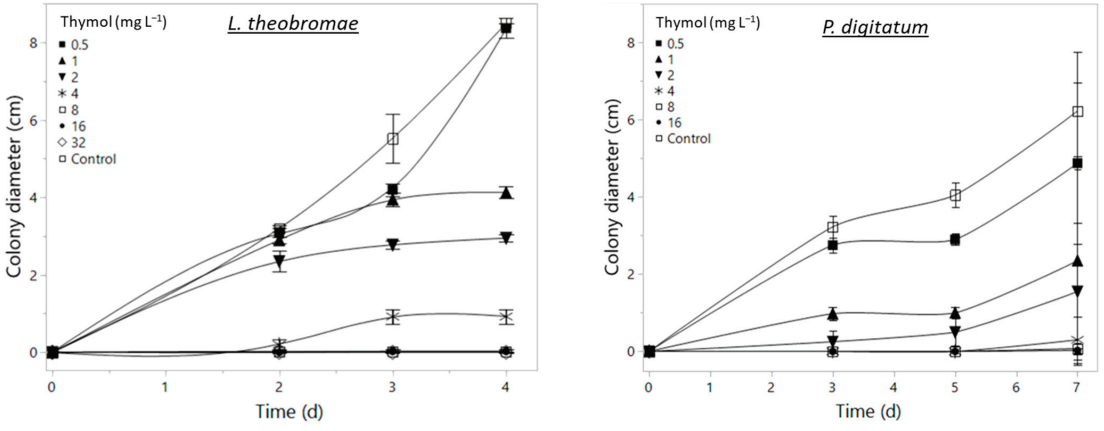

Figure 2. *Lasiodiplodia theobromae* and *Penicillium digitatum* growth inhibition resulting from increasing thymol vapor concentrations in sealed Petri dishes on potato dextrose agar. Plates were stored at 23 °C, and colony diameter was measured daily.

It is noteworthy that, while *P. digitatum* mycelial growth was not significantly inhibited by 1 mg L^{-1} thymol, sporulation was severely affected, leading to a plain white colony (Figure 3a), compared to the characteristic full green color associated with conidia in the control plates (Figure 3b), although this inhibition was not quantified. An SEM observation showed that EO at 1 mg L^{-1} (sublethal concentration) caused severe ultrastructural damage to *P. digitatum* conidia during the first 24 h. The conidia in control samples exhibited a regular and homogenous morphology consisting of smooth and continuous cell walls (Figure 3c), while after exposure to EO vapors, most cells were shrunken and abnormally shaped (Figure 3d). Also, considerable quantities of cellular debris were observed in the thymol-treated samples, as an indication of conidial lysis. As mentioned previously, *L. theobromae* growth was delayed by the thymol vapors (Figure 2); however, colony characteristics remained the same as those observed under control conditions.

The effective concentrations found in the present work were significantly lower than those reported by other authors. For instance, Ding et al. [35] found that EC_{50} values ranged between 29.8 and 55.33 mg L^{-1} for six different postharvest disease-causing fungi, including *Penicillium* sp. Also, Zhang et al. [36] reported a minimum inhibitory concentration of 65 mg L^{-1} against *B. cinerea*, and Yan et al. [37] reported an EC_{50} of 37 mg L^{-1} against *L. theobromae*. The primary difference between previous studies and the present one, other than the pathogen strains used, is the thymol application method used; previous authors added thymol directly into a liquid medium or dissolved it in ethanol before incorporating it into the medium (diffusion methods). Here, pathogens were directly exposed to the EO

vapors produced after heating at temperatures above thymol's melting point. The results of the current study are in agreement with the results of various studies in the medical field in which EO vapors exhibited greater antimicrobial effects than EOs delivered in liquid form applied by direct contact [38–41]. In addition, Boukhatem et al. [42] reported that micellar formation by lipophilic molecules in the aqueous phase reduces EO accessibility to microorganisms, whereas the vapor phase allows free attachment. These observations might explain the lower EC50 and EC90 concentrations observed here.

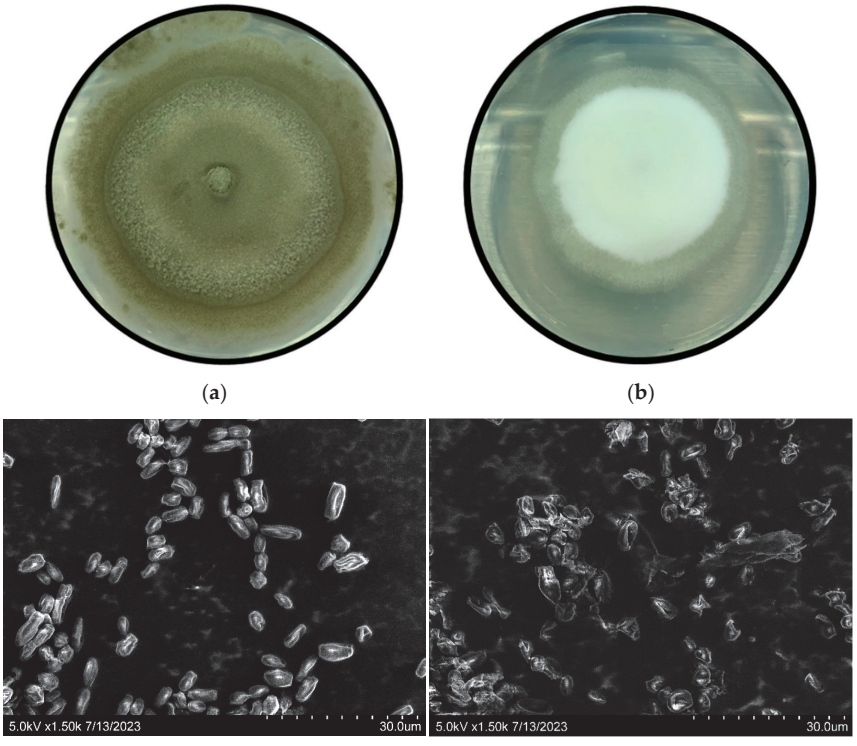

(**a**) (**b**)

(**c**) (**d**)

Figure 3. Effect of thymol vapor on *Penicillium digitatum* mycelia and conidia. Suspensions of 10^4 conidia mL^{-1} were exposed to thymol vapor at 23 °C. Top and lower panels represent colony morphology after 4 d and conidia ultrastructural characteristics (SEM photographs at 1500× magnification) after 24 h, respectively, for control condition (**a**,**c**) and 1 mg L^{-1} thymol treatment (**b**,**d**).

3.2. Postharvest Disease Control by Thymol Vapor on Inoculated Grapefruit

The evaluation of the potential of thymol to control postharvest diseases in grapefruit was assessed in airtight containers at room temperature over a period of 5 d. When the fruits were inoculated with *L. theobromae* or *P. digitatum* and exposed to direct EO vapors, concentration-dependent incidence reductions were observed (Figure 4). The effective concentrations required to reduce in vivo pathogen growth were 10 to 50 times higher than those in vitro. It is commonly reported that in vivo efficacy is often reduced when compared to in vitro studies, particularly in the application of antimicrobial compounds and specifically for EO vapors applied for antimicrobial treatments in fresh food studies, including citrus [43] and cherry tomatoes [44], as well as in processed food products, like cheese [45], bread [46], mushrooms [47], and coffee beans [48]. As was observed in the in vitro assays, *P. digitatum* was more sensitive to thymol than *L. theobromae*. For instance, 50 mg L^{-1} thymol treatment resulted in an 81% reduction in SER incidence and a 90%

reduction in visible lesion size (Figure 4, lower panels), while the same treatment on *P. digitatum*-inoculated fruit resulted in 90 and 99% reductions in GM incidence and lesion size, respectively (Figure 4, top panels). In contrast, the controlled-release treatment of thymol did not exhibit any inhibitory effect against the pathogens. This suggests that, after inoculation, fruit infection developed at a rate that did not allow the controlled-release thymol to prevent pathogen reproduction.

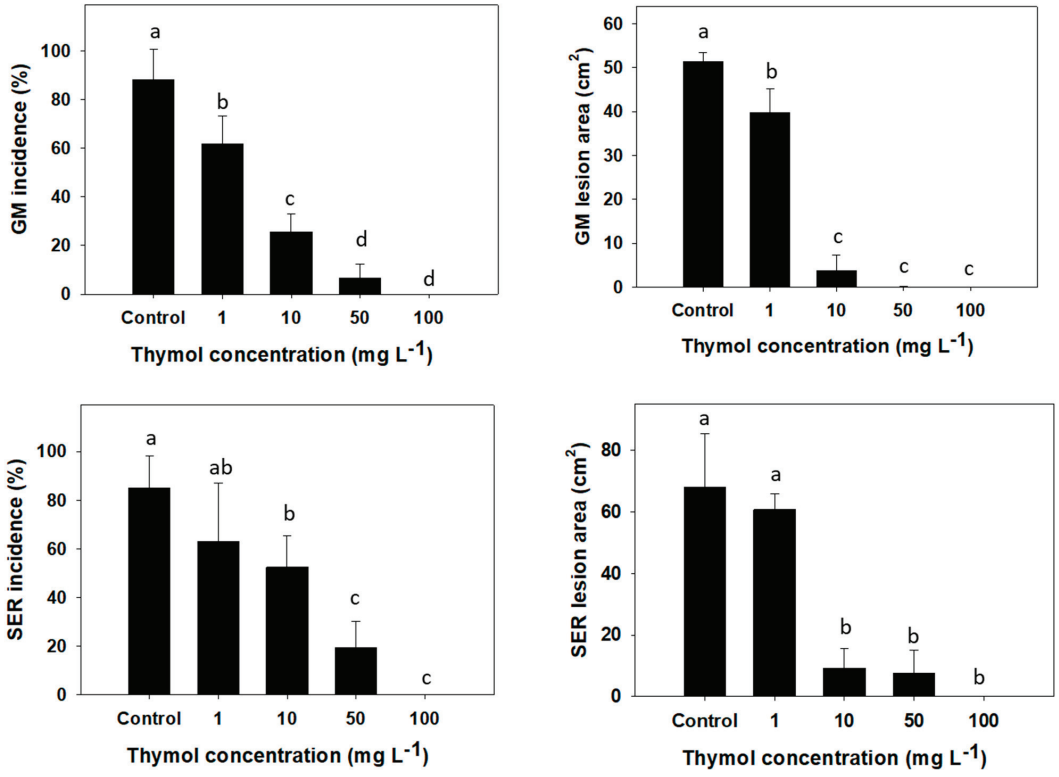

Figure 4. Incidence and lesion area of green mold (GM) and stem-end rot (SER) on grapefruit inoculated with *Penicillium digitatum* (GM) and *Lasiodiplodia theobromae* (SER), exposed to thymol vapors at 1, 10, 50, and 100 mg L^{-1} for 5 d at 23 °C. Top panels: GM; bottom panels: SER. Columns with different letters are significantly different according to Student's *t* LSD ($p \leq 0.05$).

The different effects of thymol vapors on the assayed pathogens in this study could be explained by the different growth patterns in fruit and, thus, how much vapor can reach the mycelia. Edris and Farrag [49] stated that superficial-growing molds are particularly susceptible to EO volatile compounds. It is known that *L. theobromae* infects fruit from the button at the stem-end and proceeds through the core more quickly than the rind [4]. However, *P. digitatum* infection begins with a wound on the rind and spreads on a number of skin oil glands through pores, remaining relatively superficial during the first few days [50]. Based on these characteristics, thymol vapors might be in direct contact with *P. digitatum* cells more readily than *L. theobromae* cells growing underneath the rind through the core.

After the 5 d initial storage, the fruits were kept for five additional days in the open air and again evaluated (Figure 5). After 10 d, the GM incidence in the untreated control remained around 90%, and decayed fruits were fully covered by olive-green conidia. In Figure 5, the lower left panel shows that, after five additional days, nearly all grapefruits

exposed to 10 mg L^{-1} thymol developed decay, which suggests that thymol's effect is fungistatic rather than fungicidal. However, the pathogen growing on these fruits was not able to produce conidia, confirming the anti-sporulating effect observed in in vitro trials (Figure 3a,b). When developing in a single fruit, *P. digitatum* usually produces one to two billion greenish conidial spores that are dispersed into the atmosphere, perpetuating disease [10]. These conidia are particularly difficult to inactivate due to their stability when exposed to heat, light, and chemical reagents [51]. While further assays are needed to elucidate the exact mechanism involved in the sporulation impairment achieved by thymol, this result is worth highlighting, as it may be crucial for improved postharvest disease control.

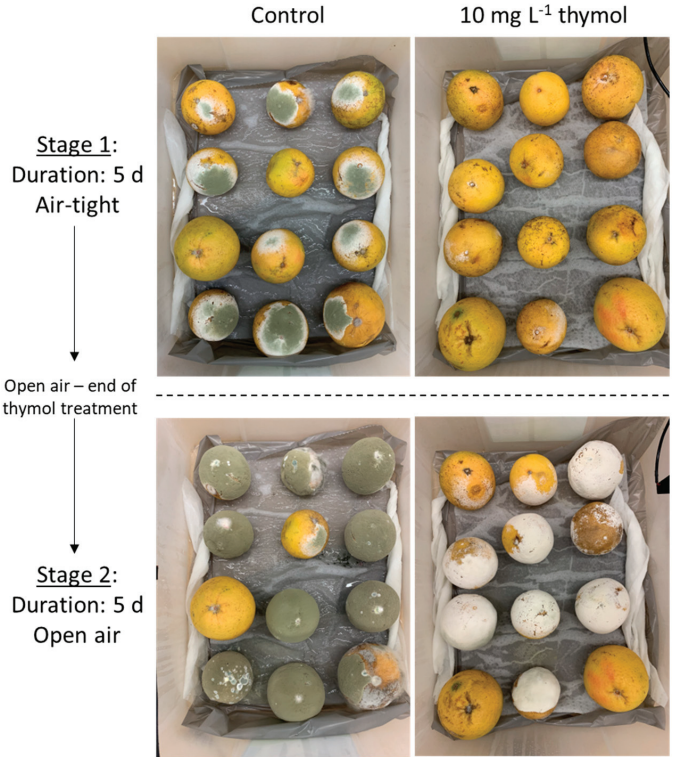

Figure 5. *Penicillium digitatum*-inoculated grapefruits exposed to 10 mg L^{-1} thymol. Pictures show control (**left** panels) and 10 mg L^{-1} thymol treatment (**right** panels) after 5 initial days in air-tight conditions (**top**) and 5 additional days in the open air (**bottom**) at 23 °C.

The *P. digitatum* isolate used in this work is resistant to thiabendazole [24]. This is, as mentioned before, one of the major challenges faced by the agricultural industry worldwide [52]. It has been reported that the mode of action of thymol is broad and non-specific; i.e., it induces changes in several metabolic pathways affecting DNA synthesis, cytoplasmic and outer membrane permeability, and fatty acid and volatile compound profiles [53]. Hence, microbial resistance development against thymol vapor treatments is unlikely to occur, which further supports their potential use as alternatives and/or complements to current postharvest microbial management strategies. Among the various advantages of the vapor-phase applications of EOs, the gas improves penetration and homogeneity and can potentially provide a more consistent and uniform pathogen exposure to thymol, even in hard-to-reach areas. Also, vapor treatments do not require solvents or

carriers that might be needed for solution-based treatments, and, thus, potential side effects or interactions between pathogens and those additional ingredients are reduced.

3.3. Fruit Weight Loss and Sensory Evaluation

The exposure of the grapefruit to different thymol concentrations did not alter the fruit weight loss when compared with the untreated fruit. The fruit weight loss was lower than 0.4% after 5 days at 25 °C in all cases. Also, no phytotoxicity was observed after the thymol vapor treatments. Previous research has shown that, when essential oil vapor is applied to fruits, the effects on weight loss can indeed be varied, depending on various factors, including the essential oil type, vapor concentration, fruit type, and environmental conditions. A weight loss reduction is most likely related to EOs' antimicrobial properties, as well as their ability to form a protective layer on the surface of the fruits, which prevents moisture loss [54]. Contrarily, an increase in weight loss is mostly due to phytotoxicity caused by a high EO dosage, which damages the fruit skin, or altered respiration [17,55]. Our observations indicate that the applied thymol vapor dosages did not harm the fruit surface. However, the low dosage also did not effectively prevent water loss.

As mentioned before, one of the main limitations for the use of EOs in food processing is the negative impact that they might have on organoleptic properties. Thus, we evaluated the panelists' sensory perception after grapefruit exposure to thymol vapors at 100 mg L^{-1} of thymol pure or microencapsulated in pectin–alginate. In the taste panels, the rank sums for preference were 51, 50, and 43 points for 100 mg L^{-1} of thymol, microencapsulated thymol, and the control, respectively, with no significant difference between treatments (T = 1.583, Friedman statistics for rank data). Furthermore, the panelists' comments after tasting suggested that there were no perceived off-flavors that could be related to the thymol treatments. The lack of undesired flavors observed in the present work is likely due to the dosages of the thymol vapors being low enough; thus, accumulation on the fruit surface did not exceed the threshold levels. Also, the treatment was applied to grapefruit, which has a rather thick peel acting as a barrier to the edible part. It would be appropriate to test the treatment in thinner-peel fruit such as mandarins. Nevertheless, our results agree with those of previous reports where essential oil vapors were used to inhibit different bacterial and fungal strains that cause food spoilage, without exceeding the acceptable flavor thresholds [56–58]. Under our experimental conditions, the application of thymol in the vapor phase would not lead to consumer rejection.

4. Conclusions

Our findings demonstrate the significant inhibitory effects of thymol vapors on the two primary postharvest pathogens responsible for decay in commercial grapefruit. While thymol alone may not completely control SER and GM, its application resulted in noteworthy reductions in disease incidence and hindered the production of conidia by *P. digitatum.* Also, under our experimental conditions, no negative effects, such as off-flavors or a weight loss increase, resulted from the thymol vapor applications. These positive outcomes support the potential implementation of this EO as part of a grapefruit postharvest management strategy. Future studies involving combinations of thymol vapors and postharvest fungicides, as well as other postharvest fruit handling processes, will be conducted to analyze the feasibility of its application at commercial scale. Considering this compound's known safety for human health and the environment and the several advantages of its application in the vapor phase compared to in liquid form, our work presents a promising option to complement current postharvest management approaches.

Author Contributions: Conceptualization, G.M.O., J.Z., W.Z., M.M., E.N.R., M.R., A.P. and J.B.; methodology, G.M.O. and J.Z.; formal analysis, G.M.O. and J.Z.; investigation, G.M.O., J.Z., W.Z., M.M., E.N.R., M.R., A.P. and J.B.; data curation, G.M.O.; writing—original draft preparation, G.M.O., J.Z., M.R., A.P. and J.B.; writing—review and editing, G.M.O., J.Z., W.Z., M.M., E.N.R., M.R., A.P. and J.B.; supervision, A.P. and J.B. All authors have read and agreed to the published version of the manuscript.

Funding: This research was funded in part by Florida Citrus Packers through a USDA Technical Assistance for Specialty Crops grant (TASC-2019-02) and the USDA National Institute of Food and Agriculture, USDA-NIFA-CDRE project 2018-70016-27387.

Data Availability Statement: The data presented in this study are included in the article. Further inquiries can be directed to the corresponding author.

Acknowledgments: We would like to thank the following people for their contribution to this study: Ric Stange, Wayne Hunter, Nancy Owens, and Maria Gonzalez.

Conflicts of Interest: The authors declare no conflict of interest.

References

1. Hung, W.-L.; Suh, J.H.; Wang, Y. Chemistry and health effects of furanocoumarins in grapefruit. *J. Food Drug Anal.* **2017**, *25*, 71–83. [CrossRef] [PubMed]
2. Murphy, M.M.; Barraj, L.M.; Rampersaud, G.C. Consumption of grapefruit is associated with higher nutrient intakes and diet quality among adults, and more favorable anthropometrics in women, NHANES 2003–2008. *Food Nutr. Res.* **2014**, *58*, 1–11. [CrossRef] [PubMed]
3. Reddy, P.J.; Ellington, D.R.; Zhu, Y.; Browne, K.F. The safety of grapefruit juice in patients taking atorvastatin. *Circulation* **2007**, *115*, E265.
4. Zhang, J. Chapter 10—Lasiodiplodia theobromae in Citrus Fruit (Diplodia Stem-End Rot). In *Postharvest Decay*; Bautista-Baños, S., Ed.; Academic Press: San Diego, CA, USA, 2014; pp. 309–335.
5. Shahzad, F.; Vashisth, T.; Ritenour, M.A.; Brecht, J.K. Huanglongbing disease symptoms and the postharvest quality of 'LB8-9' (Sugar Belle®) and 'Tango' mandarins as affected by ethylene treatment. *Sci. Hort.* **2023**, *310*, 111766. [CrossRef]
6. USDA-NASS. Florida Citrus Statistics 2021–2022. Available online: http://www.nass.usda.gov/Statistics_by_State/Florida/Publications/Citrus/cit/2013-14/cit0514.pdf (accessed on 20 July 2023).
7. Zhao, W.; Bai, J.; McCollum, G.; Baldwin, E. High incidence of preharvest colonization of huanglongbing-symptomatic citrus sinensis fruit by *Lasiodiplodia theobromae* (*Diplodia natalensis*) and exacerbation of postharvest fruit decay by that fungus. *Appl. Env. Microbiol.* **2015**, *81*, 364–372. [CrossRef]
8. Zhao, W.; Baldwin, E.A.; Bai, J.; Plotto, A.; Irey, M. Comparative analysis of the transcriptomes of the calyx abscission zone of sweet orange insights into the huanglongbing-associated fruit abscission. *Hortic. Res.* **2019**, *6*, 71. [CrossRef]
9. Zhao, W.; Gottwald, T.; Bai, J.; McCollum, G.; Irey, M.; Plotto, A.; Baldwin, E. Correlation of Diplodia (*Lasiodiplodia theobromae*) infection, huanglongbing, ethylene production, fruit removal force and pre-harvest fruit drop. *Sci. Hort.* **2016**, *212*, 162–170. [CrossRef]
10. Holmes, G.J.; Eckert, J.W. Sensitivity of *Penicillium digitatum* and *P. italicum* to Postharvest Citrus Fungicides in California. *Phytopathology* **1999**, *89*, 716–721. [CrossRef]
11. Wisniewski, M.; Droby, S.; Norelli, J.; Liu, J.; Schena, L. Alternative management technologies for postharvest disease control: The journey from simplicity to complexity. *Postharvest Biol. Technol.* **2016**, *122*, 3–10. [CrossRef]
12. Palou, L.; Ali, A.; Fallik, E.; Romanazzi, G. GRAS, plant- and animal-derived compounds as alternatives to conventional fungicides for the control of postharvest diseases of fresh horticultural produce. *Postharvest Biol. Technol.* **2016**, *122*, 41–52. [CrossRef]
13. Antunes, M.D.C.; Cavaco, A.M. The use of essential oils for postharvest decay control. A review. *Flavour. Fragr. J.* **2010**, *25*, 351–366. [CrossRef]
14. Khorram, F.; Ramezanian, A. Cinnamon essential oil incorporated in shellac, a novel bio-product to maintain quality of 'Thomson navel' orange fruit. *J. Food Sci. Technol.* **2021**, *58*, 2963–2972. [CrossRef] [PubMed]
15. Bhandari, N.; Bika, R.; Subedi, S.; Pandey, S. Essential oils amended coatings in citrus postharvest management. *J. Agric. Food Res.* **2022**, *10*, 100375. [CrossRef]
16. Jhalegar, M.D.J.; Sharma, R.R.; Singh, D. In vitro and in vivo activity of essential oils against major postharvest pathogens of Kinnow (*Citrus nobilis* × *C. deliciosa*) mandarin. *J. Food Sci. Technol.* **2015**, *52*, 2229–2237. [CrossRef] [PubMed]
17. Werrie, P.-Y.; Durenne, B.; Delaplace, P.; Fauconnier, M.-L. Phytotoxicity of essential oils: Opportunities and constraints for the development of biopesticides. A review. *Foods* **2020**, *9*, 1291. [CrossRef]
18. Guerreiro, A.C.; Gago, C.M.; Faleiro, M.L.; Miguel, M.G.; Antunes, M.D. Edible coatings enriched with essential oils for extending the shelf-life of 'Bravo de Esmolfe' fresh-cut apples. *Int. J. Food Sci. Technol.* **2016**, *51*, 87–95. [CrossRef]
19. Santos, S.M.d.; Malpass, G.R.P.; Okura, M.H.; Granato, A.C. Edible active coatings incorporated with *Cinnamomum cassia* and *Myristica fragrans* essential oils to improve shelf-life of minimally processed apples. *Ciência Rural* **2018**, *48*. [CrossRef]
20. Gurtler, J.B.; Garner, C.M. A review of essential oils as antimicrobials in foods with special emphasis on fresh produce. *J. Food Prot.* **2022**, *85*, 1300–1319. [CrossRef]
21. Kyoui, D.; Saito, Y.; Takahashi, A.; Tanaka, G.; Yoshida, R.; Maegaki, Y.; Kawarai, T.; Ogihara, H.; Suzuki, C. Antibacterial Activity of Hexanol Vapor In Vitro and on the Surface of Vegetables. *Foods* **2023**, *12*, 3097. [CrossRef]

22. Goñi, P.; López, P.; Sánchez, C.; Gómez-Lus, R.; Becerril, R.; Nerín, C. Antimicrobial activity in the vapour phase of a combination of cinnamon and clove essential oils. *Food Chem.* **2009**, *116*, 982–989. [CrossRef]
23. López-Gómez, A.; Ros-Chumillas, M.; Antolinos, V.; Buendía-Moreno, L.; Navarro-Segura, L.; Sánchez-Martínez, M.J.; Martínez-Hernández, G.B.; Soto-Jover, S. Fresh culinary herbs decontamination with essential oil vapours applied under vacuum conditions. *Postharvest Biol. Technol.* **2019**, *156*, 110942. [CrossRef]
24. Zhang, J. The potential of a new fungicide fludioxonil for stem-end rot and green mold control on Florida citrus fruit. *Postharvest Biol. Technol.* **2007**, *46*, 262–270. [CrossRef]
25. Koch, R. Verber Bakteriologische Forschung. In *Verhandlungen des X. Internationalen Medicinischen Congresses*; A. Hirschwald: Berlin, Germany, 1890; Volume 1, pp. 35–47.
26. Cometa, S.; Bonifacio, M.A.; Bellissimo, A.; Pinto, L.; Petrella, A.; De Vietro, N.; Iannaccone, G.; Baruzzi, F.; De Giglio, E. A green approach to develop zeolite-thymol antimicrobial composites: Analytical characterization and antimicrobial activity evaluation. *Heliyon* **2022**, *8*, e09551. [CrossRef] [PubMed]
27. de Ramón-Carbonell, M.; Sánchez-Torres, P. The transcription factor PdSte12 contributes to Penicillium digitatum virulence during citrus fruit infection. *Postharvest Biol. Technol.* **2017**, *125*, 129–139. [CrossRef]
28. Russell, P.E. *Sensitivity Baselines in Fungicide Resistance Research and Management*; Crop Life International: Brussels, Belgium, 2002.
29. Ali, R.; El-Boubbou, K.; Boudjelal, M. An easy, fast and inexpensive method of preparing a biological specimen for scanning electron microscopy (SEM). *MethodsX* **2021**, *8*, 101521. [CrossRef] [PubMed]
30. Olmedo, G.M.; Cerioni, L.; Sepulveda, M.; Ramallo, J.; Rapisarda, V.A.; Volentini, S.I. Polyhexamethylene guanidine as a fungicide, disinfectant and wound protector in lemons challenged with *Penicillium digitatum*. *Food Microbiol.* **2018**, *76*, 128–134. [CrossRef]
31. Sun, X.; Cameron, R.G.; Plotto, A.; Zhong, T.; Ference, C.M.; Bai, J. The Effect of Controlled-Release Carvacrol on Safety and Quality of Blueberries Stored in Perforated Packaging. *Foods* **2021**, *10*, 1487. [CrossRef]
32. Meilgaard, M.C.; Civille, G.V.; Carr, B.T. *Sensory Evaluation Techniques*, 4th ed.; CRC Press: Boca Raton, FL, USA, 2007; p. 448.
33. Sánchez-Torres, P. Molecular Mechanisms Underlying Fungicide Resistance in Citrus Postharvest Green Mold. *J. Fungi* **2021**, *7*, 783. [CrossRef]
34. Chen, D.; Förster, H.; Adaskaveg, J.E. Baseline Sensitivities of Major Citrus, Pome, and Stone Fruits Postharvest Pathogens to Natamycin and Estimation of the Resistance Potential in *Penicillium digitatum*. *Plant Dis.* **2021**, *105*, 2114–2121. [CrossRef]
35. Ding, J.; Liu, C.; Huang, P.; Zhang, Y.; Hu, X.; Li, H.; Liu, Y.; Chen, L.; Liu, Y.; Qin, W. Effects of thymol concentration on postharvest diseases and quality of blueberry fruit. *Food Chem.* **2023**, *402*, 134227. [CrossRef]
36. Zhang, J.; Ma, S.; Du, S.; Chen, S.; Sun, H. Antifungal activity of thymol and carvacrol against postharvest pathogens *Botrytis cinerea*. *J. Food Sci. Technol.* **2019**, *56*, 2611–2620. [CrossRef] [PubMed]
37. Yan, J.; Zhang, J.; Hu, C.; Deng, L.; Ritenour, M.A. Use of carvacrol and thymol in shellac coating to control stem-end rot on 'Ruby Red' grapefruit and maintain fruit quality during simulated storage and marketing. *Sci. Hort.* **2020**, *272*, 109606. [CrossRef]
38. Inouye, S.; Takizawa, T.; Yamaguchi, H. Antibacterial activity of essential oils and their major constituents against respiratory tract pathogens by gaseous contact. *J. Antimicrob. Chemother.* **2001**, *47*, 565–573. [CrossRef] [PubMed]
39. Nagoor Meeran, M.F.; Javed, H.; Al Taee, H.; Azimullah, S.; Ojha, S.K. Pharmacological Properties and Molecular Mechanisms of Thymol: Prospects for Its Therapeutic Potential and Pharmaceutical Development. *Front. Pharmacol.* **2017**, *8*, 380. [CrossRef]
40. Inouye, S.; Uchida, K.; Abe, S. Vapor activity of 72 essential oils against a *Trichophyton mentagrophytes*. *J. Infect. Chemother.* **2006**, *12*, 210–216. [CrossRef] [PubMed]
41. Fisher, K.; Phillips, C. Potential antimicrobial uses of essential oils in food: Is citrus the answer? *Trends Food Sci. Technol.* **2008**, *19*, 156–164. [CrossRef]
42. Boukhatem, M.N.; Ferhat, M.A.; Kameli, A.; Saidi, F.; Kebir, H.T. Lemon grass (*Cymbopogon citratus*) essential oil as a potent anti-inflammatory and antifungal drugs. *Libyan J. Med.* **2014**, *9*, 25431. [CrossRef]
43. Rahman, M.M.; Wills, R.B.H.; Bowyer, M.C.; Golding, J.B.; Kirkman, T.; Pristijono, P. Potential Control of Postharvest Fungal Decay of Citrus Fruits by Crude or Photochemically Changed Essential Oils—A Review. *Food Rev. Int.* **2023**, 1–18. [CrossRef]
44. Feng, W.; Chen, J.; Zheng, X.; Liu, Q. Thyme oil to control *Alternaria alternata* in vitro and in vivo as fumigant and contact treatments. *Food Control* **2011**, *22*, 78–81. [CrossRef]
45. Hlebová, M.; Foltinová, D.; Vešelényiová, D.; Medo, J.; Šramková, Z.; Tančinová, D.; Mrkvová, M.; Hleba, L. The Vapor Phase of Selected Essential Oils and Their Antifungal Activity In Vitro and In Situ against Penicillium commune, a Common Contaminant of Cheese. *Foods* **2022**, *11*, 3517. [CrossRef]
46. Císarová, M.; Hleba, L.; Medo, J.; Tančinová, D.; Mašková, Z.; Čuboň, J.; Kováčik, A.; Foltinová, D.; Božik, M.; Klouček, P. The in vitro and in situ effect of selected essential oils in vapour phase against bread spoilage toxicogenic aspergilli. *Food Control* **2020**, *110*, 107007. [CrossRef]
47. López-Gómez, A.; Ros-Chumillas, M.; Navarro-Martínez, A.; Barón, M.; Navarro-Segura, L.; Taboada-Rodríguez, A.; Marín-Iniesta, F.; Martínez-Hernández, G.B. Packaging of Fresh Sliced Mushrooms with Essential Oils Vapours: A New Technology for Maintaining Quality and Extending Shelf Life. *Foods* **2021**, *10*, 1196. [CrossRef] [PubMed]
48. Hlebová, M.; Hleba, L.; Medo, J.; Uzsakova, V.; Kloucek, P.; Bozik, M.; Haščík, P.; Čuboň, J. Antifungal and antitoxigenic effects of selected essential oils in vapors on green coffee beans with impact on consumer acceptability. *Foods* **2021**, *10*, 2993. [CrossRef] [PubMed]

49. Edris, A.E.; Farrag, E.S. Antifungal activity of peppermint and sweet basil essential oils and their major aroma constituents on some plant pathogenic fungi from the vapor phase. *Food Nahr.* **2003**, *47*, 117–121. [CrossRef]
50. Ghanei Ghooshkhaneh, N.; Golzarian, M.R.; Mamarabadi, M. Detection and classification of citrus green mold caused by *Penicillium digitatum* using multispectral imaging. *J. Sci. Food Agric.* **2018**, *98*, 3542–3550. [CrossRef]
51. Suhr, K.I.; Nielsen, P.V. Antifungal activity of essential oils evaluated by two different application techniques against rye bread spoilage fungi. *J. Appl. Microbiol.* **2003**, *94*, 665–674. [CrossRef] [PubMed]
52. Papoutsis, K.; Mathioudakis, M.M.; Hasperué, J.H.; Ziogas, V. Non-chemical treatments for preventing the postharvest fungal rotting of citrus caused by *Penicillium digitatum* (green mold) and *Penicillium italicum* (blue mold). *Trends Food Sci. Technol.* **2019**, *86*, 479–491. [CrossRef]
53. Barbosa, L.N.; Alves, F.C.B.; Andrade, B.F.M.T.; Albano, M.; Rall, V.L.M.; Fernandes, A.A.H.; Buzalaf, M.A.R.; Leite, A.d.L.; de Pontes, L.G.; dos Santos, L.D.; et al. Proteomic analysis and antibacterial resistance mechanisms of Salmonella Enteritidis submitted to the inhibitory effect of *Origanum vulgare* essential oil, thymol and carvacrol. *J. Proteom.* **2020**, *214*, 103625. [CrossRef] [PubMed]
54. Sharma, M.; Rani, P.; Nidhin, P.T.; Katoch, M. A polymer-based gel fumigator, having a combination of Monarda citriodora essential oil (MEO) and hexanal: A solution for the postharvest rot and phytotoxicity of apple during storage. *Postharvest Biol. Technol.* **2023**, *200*, 112248. [CrossRef]
55. Verdeguer, M.; Sánchez-Moreiras, A.M.; Araniti, F. Phytotoxic Effects and Mechanism of Action of Essential Oils and Terpenoids. *Plants* **2020**, *9*, 1571. [CrossRef]
56. Nazer, A.I.; Kobilinsky, A.; Tholozan, J.L.; Dubois-Brissonnet, F. Combinations of food antimicrobials at low levels to inhibit the growth of *Salmonella* sv. Typhimurium: A synergistic effect? *Food Microbiol.* **2005**, *22*, 391–398. [CrossRef]
57. Tyagi, A.K.; Malik, A. Antimicrobial potential and chemical composition of Eucalyptus globulus oil in liquid and vapour phase against food spoilage microorganisms. *Food Chem.* **2011**, *126*, 228–235. [CrossRef]
58. Perumal, A.B.; Nambiar, R.B.; Sellamuthu, P.S.; Emmanuel, R.S. Use of modified atmosphere packaging combined with essential oils for prolonging post-harvest shelf life of mango (cv. Banganapalli and cv. Totapuri). *LWT* **2021**, *148*, 111662. [CrossRef]

foods

MDPI

Article

The Effects of Combined 1-Methylcyclopropene and Melatonin Treatment on the Quality Characteristics and Active Oxygen Metabolism of Mango Fruit during Storage

Fang Yuan [1], Chunyan Wang [1,*], Ping Yi [2,3], Li Li [2,3,*], Guifen Wu [1], Fang Huang [2], Min Huang [2] and Ting Gan [2]

[1] College of Chemistry and Biological Engineering, Guangxi Minzu Normal University, Chongzuo 532200, China; yf2018yuyu@126.com (F.Y.)
[2] Agro-Food Science and Technology Research Institute, Guangxi Academy of Agricultural Sciences, Nanning 530007, China; pingyi@gxaas.net (P.Y.)
[3] Guangxi Key Laboratory of Fruits and Vegetables Storage-Processing Technology, Guangxi Academy of Agricultural Sciences, Nanning 530007, China
* Correspondence: wcy15100166681@163.com (C.W.); lili@gxaas.net (L.L.)

Abstract: AbstractIn this study, mango fruit (Tainong No. 1) was treated with either 0.1 mg/L 1-methylcyclopropene (1-MCP) alone or with a combination of 0.1 mg/L 1-MCP and 0.2 mM melatonin (MT). The mango fruit was then stored for 10 days at 25 °C and 85–90% relative humidity. Quality characteristics and the active oxygen metabolism of postharvest mangoes were evaluated every 2 days. Compared to untreated mango fruit, those with the treatments of 1-MCP alone or 1-MCP + MT had a better appearance and higher levels of soluble sugar, ascorbic acid, and titratable acidity. Moreover, these treatments prevented the loss of fruit firmness, successfully delayed the escalation of a^* and b^* values, and reduced malondialdehyde content and superoxide anion generation rate. After 10 days of storage, mango fruit treated by 1-MCP alone or 1-MCP + MT exhibited increased activities of antioxidant enzymes such as ascorbate peroxidase, catalase, superoxide dismutase, and other peroxidases; nevertheless, the two treatment protocols maintained higher mango total phenolic content only at the later stage of storage. These findings suggest that mango fruit treated with 1-MCP alone or with 1-MCP + MT improves the quality characteristics and antioxidant activities. Moreover, compared to 1-MCP treatment alone, 1-MCP + MT-treated mangoes exhibited higher quality and a stronger regulation of active metabolism during storage.

Keywords: 1-methylcyclopropene; melatonin; mango fruit; active oxygen metabolism; storage

Citation: Yuan, F.; Wang, C.; Yi, P.; Li, L.; Wu, G.; Huang, F.; Huang, M.; Gan, T. The Effects of Combined 1-Methylcyclopropene and Melatonin Treatment on the Quality Characteristics and Active Oxygen Metabolism of Mango Fruit during Storage. *Foods* **2023**, *12*, 1979. https://doi.org/10.3390/foods12101979

Academic Editors: Jinhe Bai and Imahori Yoshihiro

Received: 27 March 2023
Revised: 5 May 2023
Accepted: 9 May 2023
Published: 12 May 2023

1. Introduction

Mango (*Mangnifera indica* L.), the 'King of Fruits', is grown worldwide for its soft and juicy pulp, unique flavour and high nutritional content [1,2]. Mangoes can provide plenty of antioxidants for the human body such as phenolics and vitamins [3,4]. However, mango fruit is not postharvest-storage resistant because of its vigorous metabolism. It matures and softens quickly at room temperature and then decays [5], reducing its nutritional and commercial values.

Previous studies have indicated that active oxygen metabolism has a significant impact on fruit ripening, senescence, and softening [6,7]. For instance, the single or combined use of tea polyphenolics and 1-methylcyclopropene (1-MCP) coating impeded the senescence of bracken and improved its storage quality by modifying its active oxygen metabolism and reducing its malondialdehyde content [6]. Exogenous H_2O_2 treatment has been found to accelerate the senescence and ripening processes of kiwifruit during late storage periods by leading to an imbalance in redox homeostasis [7]. Similar findings were obtained in studies on muskmelon [8], sweet cherry [9], strawberry [10], and mango fruit [11]. Although higher plants have antioxidant defence systems that protect tissues from excessive reactive oxygen species (ROS), external factors may also regulate reactive oxygen species metabolism.

1-MCP, a competitive inhibitor of ethylene, is safe and widely applied for preserving fruits and vegetables. Studies on pear [12], apple [13], nectarine [14], kiwifruit [15–17], and banana [18] have shown that 1-MCP can enhance the antioxidant activity, preserve the quality of postharvest fruit, reduce ROS production, and delay the senescence of fresh produce.

Melatonin (N-acetyl-5-methoxytryptamine, MT) is synthesized from serotonin, which is metabolized from tryptophan [19,20]. MT is commonly present in plants and animals and has direct or indirect regulatory influences on the metabolism and growth of plants [21–24]. Exogenous MT has excellent ROS scavenging ability, which has been shown to maintain higher activities of antioxidant enzymes (e.g., ascorbate peroxidase, catalase, glutathione reductase, peroxidase, and superoxide dismutase) [25,26], enhance the contents of antioxidants (e.g., glutathione, ascorbic acid, and phenolics [24]), and reduce the production of ROS [27]. Moreover, MT can maintain better fruit quality [25–27] and is related to ethylene synthesis in fruit [28].

The single use of MT or 1-MCP to promote the quality and shelf-life of mango has been investigated in many studies. However, studies on the influences of the combination of 1-MCP and exogenous MT on active oxygen metabolism and the nutritional quality of mango are limited. The optimum concentrations of MT and 1-MCP were selected in a pre-experiment, and based on this, the objective of this work was to assess the effect of the combined treatment of 1-MCP and MT on the firmness, nutrients, and antioxidant activity of fresh mango fruit during storage.

2. Materials and Methods

2.1. Fruit Treatments

Mangoes (Tainong No. 1) were collected at commercial maturity (pulp hardness, 151.70 N; total soluble solids content, 6.9%; titratable acid content, 10.21 mg/g Fw; and soluble sugar content 26.46 mg/g Fw). These were collected at 6:00 a.m. on 2 July 2022, from a well-managed orchard in Baise City, Guangxi Province, China. On the same day, mangoes were harvested and delivered to the laboratory. Mangoes were handpicked to remove those with visual defects, diseases, or mechanical damage. Mangoes were soaked for 10 min in a 30 mg/L chlorine dioxide solution for sterilisation and then washed with distilled water. About 25 washed fruits were randomly chosen for quality evaluation. The remaining mangoes were stochastically separated into three different groups (150 mangoes/group): 1-MCP, 1-MCP combined with MT (1-MCP + MT), and a control group (CK). Fruits were individually soaked for 30 min in the dark in distilled water (control), 1-MCP (0.1 mg/L), and a mixture of 1-MCP (0.1 mg/L) and MT (0.2 mmol/L); all treatments contained 0.01 mL/L Tween 20. After being immersed, the fruits were air-dried for 60 min at 25 °C in the dark. Subsequently, the treated fruits were exposed to 0 (control group) and 0.1 mg/L 1-MCP (1-MCP and 1-MCP + MT groups) for 12 h at 25 °C. Afterwards, the fruits were stored for 10 days at 25 °C and 85–90% relative humidity.

2.2. Determination of Colour Characteristics and Fruit Firmness

The colour characteristics of the surface of the mango fruits were evaluated using the approach reported by Chen et al. [29]. Three different individual mangoes were used for determination. The colour of two points on opposite sides of the equatorial perimeter of each mango was determined.

The mango fruit firmness was quantified based on the methods reported by Lin et al. [30] and Yu et al. [31], with minor modifications. A texture instrument (FTC/TMS-Pilot, Sterling, Virginia, USA) equipped with a 10 mm diameter probe (test rate, 60 mm/s, starting force, 0.38 N; and puncture distance, 10 mm) was employed for assessing the fruit firmness without the peel. Eight peeled fruits were analysed. The pulp on two opposite sides of the equatorial region was cut into squares (1.8 cm × 1.8 cm × 1.3 cm), which were used to determine the firmness.

2.3. Measurement of Total Soluble Solids, Soluble Sugar Content and Titratable Acidity

The total soluble solid content, soluble sugar content, and titratable acidity were calculated using the methods reported by Ma et al. [32], with minor modifications. The determination of total soluble solids in the filtrate was repeated five times. Titratable acidity was extracted from 8 g of pulp and determined by acid–base titration. The pulp from five mangoes was frozen in liquid nitrogen and 1.0 g of pulp powder was used to determine soluble sugar content. Total soluble solid values are expressed as percentages, whereas titratable acidity and soluble sugar concentrations are presented as mg/g on a fresh weight basis.

2.4. Quantification of Ascorbic Acid and Total Phenolic Content

The pulp from five mangoes was frozen in liquid nitrogen and crushed into a frozen powder, then the powdered pulp (3 g) was used to quantify the level of ascorbic acid using the approach of Lin et al. [33] and Chen et al. [34]. The ascorbic acid level is presented as mg/100 g on a fresh weight basis.

The total phenolic level was determined using the approach reported by Chen et al. [35], with slight modifications. Anhydrous methanol with 1% hydrochloric acid was used to extract total phenolic from 5 g of frozen mango pulp powder. The standard for total phenolic level determination was gallic acid (GA). The level of total phenolic is presented as mg GAE/kg (gallic acid equivalent).

2.5. Quantification of the Malondialdehyde Level and Superoxide Anion ($O_2^{-\cdot}$) Generation Rate

The malondialdehyde level and $O_2^{-\cdot}$ generation rate were quantified using the methods reported by Lin et al. [36,37], with minor modifications.

The pulp from five mangoes was frozen in liquid nitrogen and crushed into a frozen powder, and the powdered pulp (5 g) was then used to determine the malondialdehyde level and $O_2^{-\cdot}$ generation rate. The level of malondialdehyde was calculated and shown as nmol/100 g on a fresh weight basis, and the $O_2^{-\cdot}$ generation rate was displayed as μmol/min/kg on a fresh weight basis.

2.6. Assays of the Activities of Superoxide Dismutase, Catalase, Ascorbate Peroxidase, and Peroxidase

Superoxide dismutase, catalase, ascorbate peroxidase, and peroxidase activities were evaluated using an ELISA kit (Jiangsu Meimian Industrial Co., Ltd., Yancheng, China). The standard curve was plotted according to the standard's activity and its corresponding OD value at 450 nm. The absorbance value of the enzyme activity in the sample was measured at 450 nm. The superoxide dismutase, catalase, ascorbate peroxidase, and peroxidase activities were reported as U/g on a fresh weight basis using the standard curve.

2.7. Statistical Analyses

All data are displayed as the average ± standard deviation. For statistical analysis, SPSS software (version 17.0) was employed to conduct a one-way analysis of variance. Different letters were applied to represent the statistical significance ($p < 0.05$).

3. Results

3.1. Colour Characteristics, Visual Appearance, and Fruit Firmness

The change in colour appearance is an important factor in determining fruit ripening and quality [29]. The noticeable change in mango after storage was that the peel turns yellow while the surface colour of the peel lightens (Figure 1E).

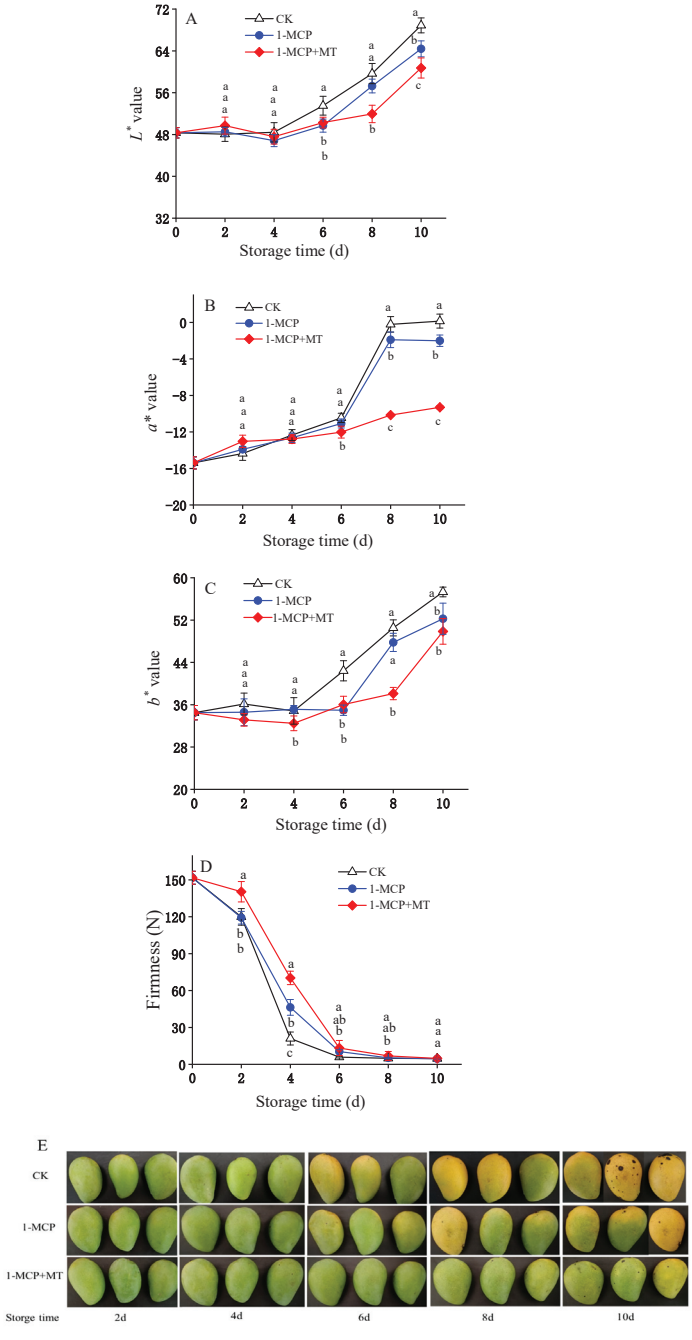

Figure 1. The effects of the 1-MCP and 1-MCP + MT treatments on L^* (**A**), a^* (**B**), and b^* (**C**) values of mango peel firmness (**D**) and visual appearance (**E**) of mango fruit during storage at 25 °C. Error bars indicate the standard deviation (SD) of six (L^*, a^*, and b^* value) or eight (firmness) replicates. Significant differences ($p < 0.05$) among different treatments on the same storage day are indicated by different lowercase letters.

Within 4 days of storage, no significant change was observed in the L^* value of the mango epidermis (Figure 1A, Table S1). However, after being stored for more than 4 days, the L^* value elevated. These results suggested that the colour of the mango epidermis became lighter (Figure 1E). Compared to the control mango, the L^* values increased more slowly in 1-MCP and 1-MCP + MT-treated mangoes. After a 6- to 10-day storage period, the control mango had a significantly higher L^* value than 1-MCP + MT-treated mango ($p < 0.05$). Furthermore, in the final 4 days of storage, the 1-MCP-treated mango also exhibited a higher L^* value than the 1-MCP + MT-treated mango.

The a^* value displayed an ascending trend with increased storage time (Figure 1B, Table S1). The a^* values changed slowly in the 1-MCP + MT group. During storage days 0–6, no significant difference ($p < 0.05$) was reported in the a^* value between the 1-MCP and the control groups. Between 6 and 8 days of storage, a^* values in these two groups escalated rapidly, indicating that the mango peel's greenish colour had reduced and quickly turned red during this time. A slow change in the a^* value was also observed in 1-MCP + MT-treated mango throughout the whole storage period. From the sixth day, the 1-MCP + MT group owned a significantly lower a^* value compared to the remaining two groups ($p < 0.05$).

During the 4-day storage, the b^* value changed slightly in all groups (Figure 1C, Table S1) and then escalated speedily from the 6th day, indicating that the colour of the mango peel had begun to turn yellow (Figure 1E). The order of turning yellow from less to more was: 1-MCP + MT group, 1-MCP group, and then the control group (Figure 1E).

Firmness is one of the most important indicators of fruit quality [12,15]. As shown in Figure 1D and Table S1, changes in mango firmness occurred along with the period of storage. The firmness of the mango decreased throughout the storage period, and rapid softening occurred within the storage duration (2–6 days). During the storage period, especially on the 4th day, the firmness degradation in mango fruits was significantly inhibited by 1-MCP + MT and 1-MCP. The firmness of mangoes treated with 1-MCP + MT and 1-MCP was higher than that of the untreated mangoes. Additionally, the firmness of the mangoes treated with 1-MCP + MT was considerably greater ($p < 0.05$) than that of the control mangoes during days 2–8 of storage.

3.2. Total Soluble Solids, Titratable Acidity, and Soluble Sugar Content

Total soluble solids content, titratable acidity and soluble sugar content are essential components of mango fruit that affect its taste, nutrition, and storage quality. As shown in Figure 2A and Table S1, after an initial increase, the total soluble solids content of untreated mango fruit decreased and then slightly increased again. The total soluble solids content in 1-MCP and 1-MCP + MT-treated mango fruit increased continuously during storage and was significantly higher than that of untreated mangoes from storage days 8 to 10 ($p < 0.05$). However, there was no significant difference between the total soluble solids level of the 1-MCP and the 1-MCP + MT-treated mango fruits.

Figure 2B and Table S1 displays an overall downward trend in the titratable acidity content of all samples during storage. All treatment groups experienced a gradual decline in titratable acidity content from days 0–4 before a sharp decline. Within the period of storage days 4–6, the titratable acidity content of the 1-MCP-treated mangoes remained at a notably higher level than the control. However, the titratable acidity content reduction was remarkably delayed by 1-MCP + MT treatment during storage. Interestingly, the 1-MCP + MT-treated mangoes demonstrated a significantly higher level of titratable acidity than the other two groups ($p < 0.05$).

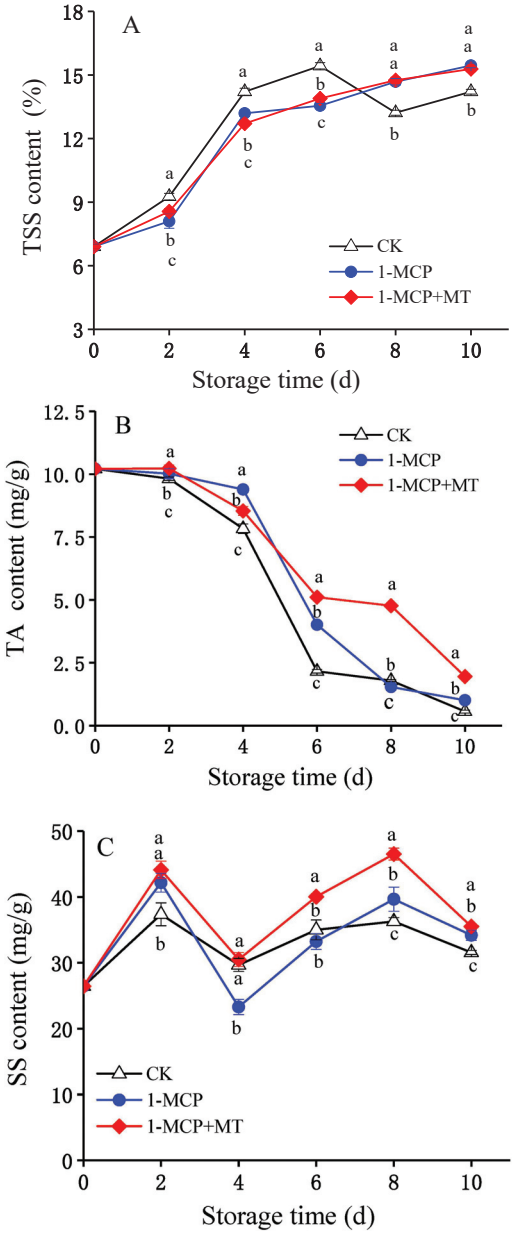

Figure 2. Effects of 1-MCP and 1-MCP + MT treatment on total soluble solids (TSS) content (**A**), titratable acidity (TA) (**B**), and soluble sugar (SS) content (**C**) in mango fruit during storage at 25 °C. Error bars indicate the SD of three replicates. Significant differences ($p < 0.05$) among different treatments on the same storage day are indicated by different lowercase letters.

The soluble sugar level of mango pulp among the three groups exhibited an increasing tendency during 0–2 days and 4–8 days but decreased during storage days 2–4 and days 8–10 (Figure 2C, Table S1). During storage, the 1-MCP + MT treatment produced more soluble sugar than the other two groups. Further analysis showed that within the 6–10-day storage period, the soluble sugar content of the 1-MCP + MT group had a significantly

higher ($p < 0.05$) soluble sugar level than the 1-MCP and control groups. Furthermore, the 1-MCP treatment only maintained a significantly elevated content of soluble sugar during the early and late periods compared to the control ($p < 0.05$).

3.3. Ascorbic Acid and Total Phenolic Content

Ascorbic acid serves as one of the most essential nutritional factors to estimate the quality of fruits and vegetables. Moreover, it functions effectively as an antioxidant in plants. The concentrations of ascorbic acid had a divergent downward trend throughout the storage process in all three groups, as shown in Figure 3A and Table S1. The ascorbic acid content decreased sharply in the control mangoes during days 2–4, resulting in a lower content of ascorbic acid than in the two treatment groups during days 4–10. Statistical analysis revealed that the 1-MCP group maintained a significantly higher content of ascorbic acid than the control group on day 4 and during days 0–3 of storage ($p < 0.05$). Within days 4–10 of storage, the 1-MCP + MT group retained the highest ascorbic acid content.

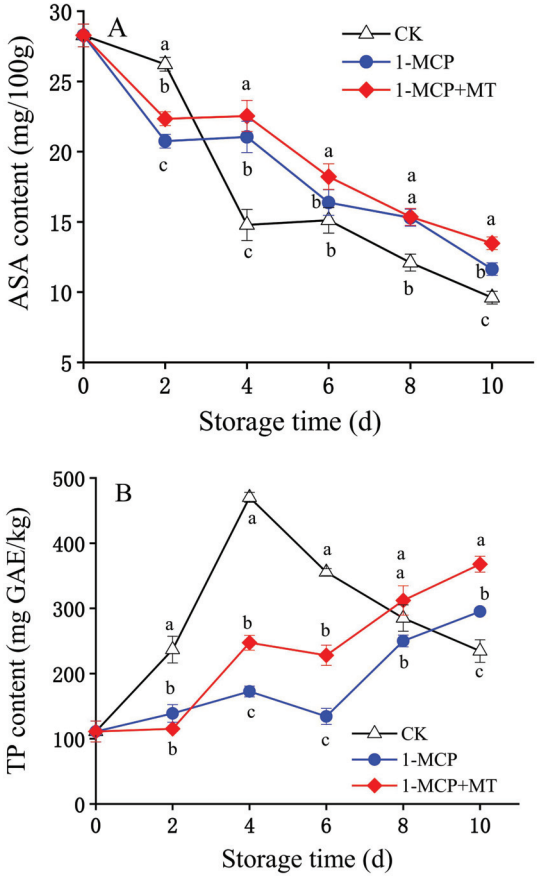

Figure 3. The effects of 1-MCP and 1-MCP + MT treatment on the ascorbic acid (ASA) content (**A**) and total phenolic content (TP) (**B**) of mango fruit during storage at 25 °C. Error bars indicate the SD of three replicates. Significant differences ($p < 0.05$) among different treatments on the same storage day are indicated by different lowercase letters.

The total phenolic content for the three groups during storage is shown in Figure 3B and Table S1. After 4 days of storage, the total phenolic content of mangoes without treatment increased rapidly to 407.26 mg GAE/kg and then declined quickly. However, the

total phenolic content in the two treatment groups raised comparatively slowly during the storage period, except for a slight decrease in storage days 0–6. It was also shown that the total phenolic content of the 1-MCP + MT and 1-MCP-treated mangoes was significantly lower than that of the control ($p < 0.05$) on days 2–6. Moreover, the total phenolic content of mangoes with 1-MCP + MT treatment differed significantly from that of the 1-MCP-treated mangoes at days 4–10 ($p < 0.05$).

3.4. $O_2^{-\cdot}$ Generation Rate and Malondialdehyde Content

$O_2^{-\cdot}$ as an intracellular ROS can cause irreversible damage to cells when excessively accumulated. Excess intracellular ROS such as $O_2^{-\cdot}$ may harm cells irreversibly. Figure 4A and Table S1 indicated that 1-MCP + MT treatment inhibited $O_2^{-\cdot}$ generation during storage ($p < 0.05$). The $O_2^{-\cdot}$ generation rate in 1-MCP-treated mango was dramatically different from that in control mango without 1-MCP on day 6. Nevertheless, the 1-MCP + MT treatment was more effective in decreasing $O_2^{-\cdot}$ accumulation.

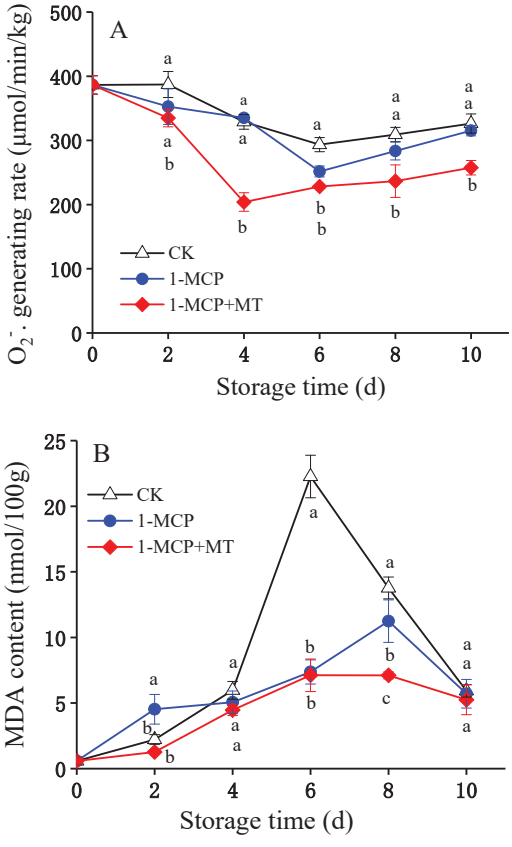

Figure 4. The effects of 1-MCP and 1-MCP + MT treatment on $O_2^{-\cdot}$ generating rate (**A**) and malondialdehyde (MDA) content (**B**) in mangoes during storage at 25 °C. Error bars indicate the SD of three replicates. Significant differences ($p < 0.05$) among different treatments on the same storage day are indicated by different lowercase letters.

The malondialdehyde content increased continuously over time but most notably during storage days 2–8 (Figure 4B, Table S1). The malondialdehyde level of the control mango was 22.28 nmol/100 g on day 6, which was 213% and 202% higher than that of

the 1-MCP + MT and 1-MCP-treated mango, respectively. These results revealed that the 1-MCP + MT-treated mangoes maintained the lowest malondialdehyde content.

3.5. Superoxide Dismutase, Catalase, Ascorbate Peroxidase, and Peroxidase Activities

Relatively higher superoxide dismutase activity was recorded in mango pulp with the 1-MCP and 1-MCP + MT treatments (Figure 5A, Table S1), and the 1-MCP + MT treatment was more prominent in stimulating superoxide dismutase activity. The superoxide dismutase activity of 1-MCP + MT-treated mango pulp was considerably higher at storage days 2–6 and 10 compared to mangoes in the 1-MCP treatment group and the control group ($p < 0.05$). Compared to the control group, a significantly higher superoxide dismutase activity in mango with 1-MCP treatment was recorded on storage days 4–6 and on storage day 10 ($p < 0.05$).

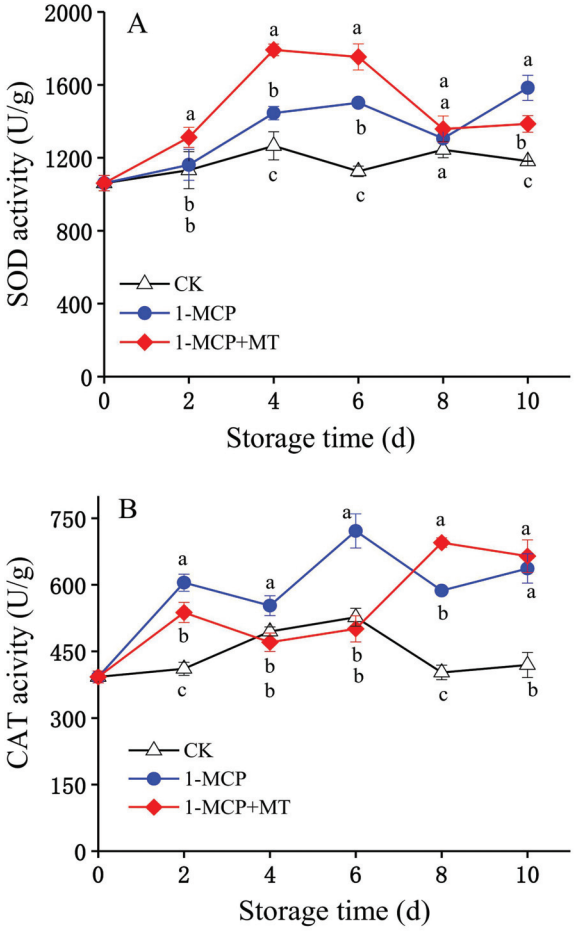

Figure 5. *Cont.*

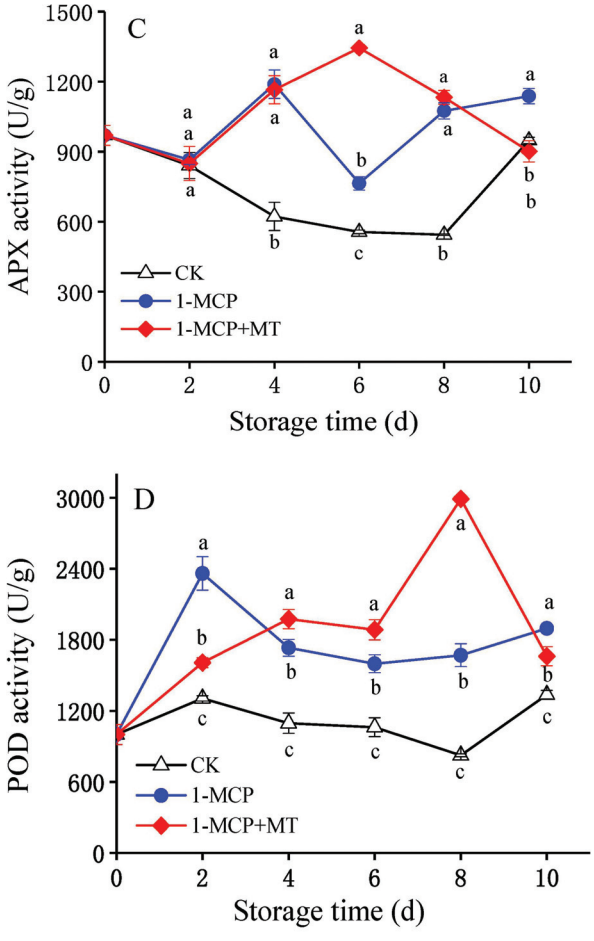

Figure 5. The effects of 1-MCP and 1-MCP + MT treatment on superoxide dismutase (SOD) (**A**), catalase (CAT) (**B**), ascorbate peroxidase (APX) (**C**), and peroxidase (POD) (**D**) activities in mangoes during storage at 25 °C. Error bars indicate the SD of three replicates. Significant differences ($p < 0.05$) among different treatments on the same storage day are indicated by different lowercase letters.

Throughout the storage period, the activity of catalase in the control mangoes was significantly lower than in mangoes with 1-MCP treatment. The catalase activity in 1-MCP-treated mangoes had a significantly higher value ($p < 0.05$) than that of control mango at storage days 2–10. Additionally, the catalase activity in 1-MCP + MT-treated mangoes exhibited lower values on storage days 2–6 and higher values on day 8 than mangoes with 1-MCP treatment (Figure 5B, Table S1). In the early (2 days) and late (8–10 days) of storage, 1-MCP + MT treatment significantly increased catalase activity compared to the control ($p < 0.05$).

The ascorbate peroxidase activity of the control mangoes consistently declined from 0 to 8 days and then increased (Figure 5C, Table S1). On storage day 8, the lowest activity of ascorbate peroxidase was achieved in the control group, which was 51.1% and 48.0% of the 1-MCP and 1-MCP + MT groups, respectively. After 4–8 days of storage, the ascorbate peroxidase activity in the control mangoes was significantly lower than that of 1-MCP + MT-treated mango ($p < 0.05$). In addition, on the 6th day, the ascorbate peroxidase activity in 1-MCP + MT-treated mangoes was also significantly higher than that of the 1-MCP-treated mangoes ($p < 0.05$). Figure 5C shows that, in comparison with the control,

the 1-MCP treatment had an impact on maintaining the ascorbate peroxidase activity at higher levels for days 4–10, and a significant difference was recorded ($p < 0.05$).

1-MCP and 1-MCP + MT treatments induced noticeably higher peroxidase activities ($p < 0.05$) during the mango storage period compared to the control group (Figure 5D, Table S1). During the storage period, the peroxidase activity in the control group was relatively stable. In the 1-MCP group, the peroxidase activity escalated at storage days 0–2, decreased during storage days 2–4, and then remained relatively stable from days 4 to 10. The 1-MCP + MT group showed two periods (days 0–4 and days 6–8) of increasing peroxidase activity. Further investigation demonstrated that the mangoes with 1-MCP + MT treatment had significantly higher peroxidase activity than the 1-MCP-treated mangoes on days 4–8 ($p < 0.05$).

4. Discussion

Exogenous MT exhibited a positive effect on regulating the ripeness of postharvest fruit while simultaneously having a negative effect on fruit senescence [21]. Previous studies have reported that MT accelerates the ripening of tomatoes [38] and grape berries [28] by promoting ethylene biosynthesis. However, contrary conclusions were drawn from the studies on bananas [39], strawberries [40], pears [41], and mangoes [42] in which the use of MT inhibited the production of ethylene and delayed the senescence and ripening of fruits. Fruit senescence is linked to a decrease in quality and an imbalance in active oxygen metabolism. In this study, throughout the storage at 25 °C, mangoes treated with 1-MCP + MT demonstrated greater antioxidant activity and quality than those treated with 1-MCP alone.

The mango in the 1-MCP + MT group maintained a stable a^* value and inhibited the increase in b^* during storage, which reduced the colour change in the mango epidermis and maintained good appearance quality. In particular, the 1-MCP + MT treatment only caused the smallest change in a^* values of the mango's epidermis, which meant that these mangoes remained green after 10 days of storage. The mangoes were significantly yellow in the 1-MCP and control groups. This result is inconsistent with the result reported by Rastegar et al. [43] in which the single use of MT showed no impact on the colour change in mangoes. The synergy of 1-MCP and MT could maintain mango firmness and produce greater titratable acidity and soluble sugar content than 1-MCP alone or in the control. The total soluble solids content of mangoes was reduced during days 2–6 of storage due to the addition of 1-MCP alone and 1-MCP + MT. The reason for this might be that the control mangoes matured faster after 6 days of storage. In other studies, employing MT alone had no effect on mango colour change, titratable acidity, or total soluble solids content [43]. Studies have shown that strawberries treated with MT alone have a lower ascorbic acid content [44], whereas, in this study, the 1-MCP + MT treatment effectively delayed the decrease in the ascorbic acid content of mangoes and had a higher content than that of the 1-MCP group. Therefore, in terms of obtaining higher-quality mangoes, the combination of 1-MCP and MT is superior to 1-MCP alone.

Exogenous MT has been proven in several studies to increase phenolic synthesis [27,45,46]. Nevertheless, in our investigation, the total phenolic content of the control mangoes significantly changed after storage but changed less in the 1-MCP and 1-MCP + MT-treated mangoes. Plant phenolic compounds assist in disease resistance via antibacterial and bactericidal activities, free radical removal, and anti-lipid peroxidation [47]. In the late period of storage, the reduction in total phenolic levels in the control mangoes reduced the ability of the fruit to resist pathogens, thereby accelerating decay (Figure 1E). At low concentrations, ROS act as signal molecules in plants and aid in defence responses; however, excessive amounts can lead to oxidative damage and enhance the ripening and senescence processes. Antioxidant enzymes and antioxidants in plants affect ROS removal [33,37]. In this study, we discovered that the combination of 1-MCP and MT played a primary role in promoting ascorbic acid and strengthening superoxide dismutase, ascorbate peroxidase, and peroxidase activities. In addition, their combination also inhibited the accumulation of

$O_2^{-\cdot}$ and malondialdehyde while increasing catalase activity in the latter storage period (Figure 5), which helped to decrease ROS damage to fruit tissue and delayed the process of senescence and ripening. Different storage stages were associated with the peak activities of different antioxidant enzymes, indicating that each of them played a role in scavenging ROS at different stages. The antioxidative effects of 1-MCP, which reduces ROS production in other fruits [13–15], are enhanced by MT.

5. Conclusions

The effects of the combined treatment of 1-MCP and MT improved the visual and quality characteristics of mangoes during storage, maintained higher ascorbic acid content, decreased $O_2^{-\cdot}$ generation rates, reduced the malondialdehyde content, and maintained higher antioxidant enzyme activity levels. Whether in terms of quality or the regulation of the active metabolism of mangoes, the effects of the combination of 1-MCP and MT were superior to those of 1-MCP alone. Hence, the 1-MCP and MT combined treatment may be a potential alternative in the postharvest technology of mango fruits during storage.

Supplementary Materials: The following supporting information can be downloaded at: https://www.mdpi.com/article/10.3390/foods12101979/s1, Table S1: the values of each evaluated parameter in Figures 1–5 at each storage time.

Author Contributions: Conceptualization, F.Y. and L.L.; validation, M.H., C.W. and F.Y.; formal analysis, G.W.; investigation, F.H.; data curation, L.L.; writing—original draft preparation, F.Y. and T.G.; writing—review and editing, C.W., P.Y. and L.L.; visualization, F.Y.; supervision, P.Y.; funding acquisition, L.L. All authors have read and agreed to the published version of the manuscript.

Funding: This research was financially supported by the Guangxi Natural Science Foundation (Grant Nos. 2020GXNSFBA297099 and 2021GXNSFAA075035), the earmarked fund for China Agriculture Research System (CARS-31), and the Special National Key Research and Development Plan (Grant No. 2021YFD1600105).

Data Availability Statement: The data are available from the corresponding author.

Conflicts of Interest: The authors declare no conflict of interest.

References

1. Sivakumar, D.; Jiang, Y.; Yahia, E.M. Maintaining mango (*Mangifera indica* L.) fruit quality during the export chain. *Food Res. Int.* **2011**, *44*, 1254–1263. [CrossRef]
2. Peng, Y.; Fei, L.; Liu, X.; Sun, G.; Hao, K.; Cui, N.; Zhao, L.; Liu, L.; Jie, F. Coupling of regulated deficit irrigation at maturity stage and moderate fertilization to improve soil quality, mango yield and water-fertilizer use efficiency. *Sci. Hortic.* **2023**, *307*, 111492. [CrossRef]
3. Akther, S.; Jothi, J.S.; Badsha, M.R.; Rahman, M.M.; Das, G.B.; Alim, M.A. Drying methods effect on bioactive compounds, phenolic profile, and antioxidant capacity of mango powder. *J. King Saud Univ. Sci.* **2023**, *35*, 102370. [CrossRef]
4. Ma, X.; Wu, H.; Liu, L.; Yao, Q.; Wang, S.; Zhan, R.; Xing, S.; Zhou, Y. Polyphenolic compounds and antioxidant properties in mango fruits. *Sci. Hortic.* **2011**, *129*, 102–107. [CrossRef]
5. Liu, B.; Xin, Q.; Zhang, M.; Chen, J.; Lu, Q.; Zhou, X.; Li, X.; Zhang, W.; Feng, W.; Pei, H.; et al. Research Progress on Mango Post-Harvest Ripening Physiology and the Regulatory Technologies. *Foods* **2023**, *12*, 173. [CrossRef]
6. Li, Z.; Zhang, W.; Li, X.; Liu, H.; Li, F.; Zhang, X. Combined effects of 1-methylcyclopropene and tea polyphenolics coating treatment on the postharvest senescence and reactive oxygen species metabolism of bracken (*Pteridium aquilinum var. latiusculum*). *Postharvest Biol. Technol.* **2022**, *185*, 111813. [CrossRef]
7. Yan, H.; Chen, H.; Zhao, J.; Yao, T.; Ding, X. Postharvest H_2O_2 treatment affects flavor quality, texture quality and ROS metabolism of '*Hongshi*' kiwifruit fruit kept at ambient conditions. *Food Chem.* **2023**, *405*, 134908. [CrossRef]
8. Xue, H.; Sun, Y.; Li, L.; Bi, Y.; Hussain, R.; Zhang, R.; Long, H.; Nan, M.; Pu, L. Acetylsalicylic acid (ASA) induced fusarium rot resistance and suppressed neosolaniol production by elevation of ROS metabolism in muskmelon fruit. *Sci. Hortic.* **2020**, *265*, 109264. [CrossRef]
9. Meng, X.; Chen, C.; Song, T.; Xu, J.; Zhang, X.; Wang, J.; Pan, Z.; Zhang, H.; Zhang, H. Effect of nano-silica coating combined with pressurized Ar treatment on postharvest quality and reactive oxygen species metabolism in sweet cherry fruit. *Food Chem.* **2022**, *374*, 131715. [CrossRef]
10. Xu, C.; Zhang, X.; Liang, J.; Fu, Y.; Wang, J.; Jiang, M.; Pan, L. Cell wall and reactive oxygen metabolism responses of strawberry fruit during storage to low voltage electrostatic field treatment. *Postharvest Biol. Technol.* **2022**, *192*, 112017. [CrossRef]

11. Jincy, M.; Djanaguiraman, M.; Jeyakumar, P.; Subramanian, K.S.; Jayasankar, S.; Paliyath, G. Inhibition of phospholipase D enzyme activity through hexanal leads to delayed mango (*Mangifera indica* L.) fruit ripening through changes in oxidants and antioxidant enzymes activity. *Sci. Hortic.* **2017**, *218*, 316–325. [CrossRef]
12. Seo, H.J.; Wang, Y.S.; Lwin, H.P.; Choi, J.H.; Chun, J.P.; Roan, S.F.; Chen, L.Z.; Lee, J. Early season '*Wonhwang*' pear fruit quality following international transport and storage is negatively impacted by fruitlet stage gibberellic acid$_{4+7}$ (GA_{4+7}) application but improved by postharvest 1-methylcyclopropene (1-MCP). *Sci. Hortic.* **2019**, *256*, 108549. [CrossRef]
13. Lv, J.; Zhang, J.; Han, X.; Bai, L.; Xu, D.; Ding, S.; Ge, Y.; Li, C.; Li, J. Genome wide identification of superoxide dismutase (SOD) genes and their expression profiles under 1-methylcyclopropene (1-MCP) treatment during ripening of apple fruit. *Sci. Hortic.* **2020**, *271*, 109471. [CrossRef]
14. Zhang, W.; Zhao, H.; Jiang, H.; Xu, Y.; Cao, J.; Jiang, W. Multiple 1-MCP treatment more effectively alleviated postharvest nectarine chilling injury than conventional one-time 1-MCP treatment by regulating ROS and energy metabolism. *Food Chem.* **2020**, *330*, 127256. [CrossRef] [PubMed]
15. Chai, J.; Wang, Y.; Liu, Y.; Yong, K.; Liu, Z. 1-MCP extends the shelf life of ready-to-eat '*Hayward*' and '*Qihong*' kiwifruit stored at room temperature. *Sci. Hortic.* **2021**, *289*, 110437. [CrossRef]
16. Salazar, J.; Jorquera, C.; Campos-Vargas, R.; Jorgensen, C.; Zapata, P.; Infante, R. Effect of the application timing of 1-MCP on postharvest traits and sensory quality of a yellow-fleshed kiwifruit. *Sci. Hortic.* **2019**, *244*, 82–87. [CrossRef]
17. Zhang, Y.; Wang, K.; Xiao, X.; Cao, S.; Chen, W.; Yang, Z.; Shi, L. Effect of 1-MCP on the regulation processes involved in ascorbate metabolism in kiwifruit. *Postharvest Biol. Technol.* **2021**, *179*, 111563. [CrossRef]
18. Chang, L.Y.; Brecht, J.K. Responses of 1-methylcyclopropene (1-MCP)-treated banana fruit to pre-and post-treatment ethylene exposure. *Sci. Hortic.* **2023**, *309*, 111636. [CrossRef]
19. Lee, K.; Back, K. Melatonin-deficient rice plants show a common semidwarf phenotype either dependent or independent of brassinosteroid biosynthesis. *J. Pineal Res.* **2019**, *66*, e12537. [CrossRef]
20. Adil, M.; Jeong, B.R. Role of melatonin and serotonin in plant stress tolerance. In *Plant Life under Changing Environment*; Academic Press: London, UK, 2020; pp. 775–791. [CrossRef]
21. Arnao, M.B.; Hernández-Ruiz, J. Melatonin in flowering, fruit set and fruit ripening. *Plant Reprod.* **2020**, *33*, 77–87. [CrossRef] [PubMed]
22. Sharafi, Y.; Aghdam, M.S.; Luo, Z.; Jannatizadeh, A.; Razavi, F.; Fard, J.R.; Farmani, B. Melatonin treatment promotes endogenous melatonin accumulation and triggers GABA shunt pathway activity in tomato fruits during cold storage. *Sci. Hortic.* **2019**, *254*, 222–227. [CrossRef]
23. Njie, A.; Zhang, W.E.; Dong, X.; Lu, C.; Pan, X.; Liu, Q. Effect of Melatonin on Fruit Quality via Decay Inhibition and Enhancement of Antioxidative Enzyme Activities and Genes Expression of Two Mango Cultivars during Cold Storage. *Foods* **2022**, *11*, 3209. [CrossRef]
24. Wang, L.; Luo, Z.; Ban, Z.; Jiang, N.; Yang, M.; Li, L. Role of exogenous melatonin involved in phenolic metabolism of *Zizyphus jujuba* fruit. *Food Chem.* **2021**, *341*, 128268. [CrossRef] [PubMed]
25. Onik, J.C.; Wai, S.C.; Li, A.; Lin, Q.; Sun, Q.; Wang, Z.; Duan, Y. Melatonin treatment reduces ethylene production and maintains fruit quality in apple during postharvest storage. *Food Chem.* **2021**, *337*, 127753. [CrossRef] [PubMed]
26. Dong, B.; Yao, Q.; Zhu, D.; Han, H.; Tang, H.; Ding, X. Exogenous melatonin maintains quality of postharvest *Rosa roxburghii* fruit by modulating reactive oxygen species metabolism and energy status. *Sci. Hortic.* **2022**, *304*, 111346. [CrossRef]
27. Shang, F.; Liu, R.; Wu, W.; Han, Y.; Fang, X.; Chen, H.; Gao, H. Effects of melatonin on the components, quality and antioxidant activities of blueberry fruits. *LWT-Food Sci. Technol.* **2021**, *147*, 111582. [CrossRef]
28. Xu, L.; Yue, Q.; Bian, F.E.; Sun, H.; Zhai, H.; Yao, Y. Melatonin enhances phenolics accumulation partially via ethylene signaling and resulted in high antioxidant capacity in grape berries. *Front. Plant Sci.* **2017**, *8*, 1426. [CrossRef] [PubMed]
29. Chen, Y.; Lin, H.; Shi, J.; Zhang, S.; Lin, Y.; Lin, T. Effects of a feasible 1-methylcyclopropene postharvest treatment on senescence and quality maintenance of harvested Huanghua pears during storage at ambient temperature. *LWT-Food Sci. Technol.* **2015**, *64*, 6–13. [CrossRef]
30. Lin, Y.; Lin, Y.; Lin, H.; Lin, M.; Li, H.; Yuan, F.; Chen, Y.; Xiao, J. Effects of paper containing 1-MCP postharvest treatment on the disassembly of cell wall polysaccharides and softening in *Younai* plum fruit during storage. *Food Chem.* **2018**, *264*, 1–8. [CrossRef]
31. Yu, K.; Xu, J.; Zhou, L.; Zou, L.; Liu, W. Effect of Chitosan Coatings with Cinnamon Essential Oil on Postharvest Quality of Mangoes. *Foods* **2021**, *10*, 3003. [CrossRef]
32. Ma, Q.; Lin, X.; Wei, Q.; Yang, X.; Zhang, Y.N.; Chen, J. Melatonin treatment delays postharvest senescence and maintains the organoleptic quality of '*Newhall*' navel orange (*Citrus sinensis* (L.) *Osbeck*) by inhibiting respiration and enhancing antioxidant capacity. *Sci. Hortic.* **2021**, *286*, 110236. [CrossRef]
33. Lin, Y.; Lin, H.; Fan, Z.; Wang, H.; Lin, M.; Chen, Y.; Hung, Y.C.; Lin, Y. Inhibitory effect of propyl gallate on pulp breakdown of longan fruit and its relationship with ROS metabolism. *Postharvest Biol. Technol.* **2020**, *168*, 111272. [CrossRef]
34. Chen, Y.; Lin, H.; Jiang, Y.; Zhang, S.; Lin, Y.; Wang, Z. Phomopsis longan Chi-induced pericarp browning and disease development of harvested longan fruit in association with energy status. *Postharvest Biol. Technol.* **2014**, *93*, 24–28. [CrossRef]
35. Chen, M.; Lin, H.; Zhang, S.; Lin, Y.; Chen, Y.; Lin, Y. Effects of adenosine triphosphate (ATP) treatment on postharvest physiology, quality and storage behavior of longan fruit. *Food Bioprocess Technol.* **2015**, *8*, 971–982. [CrossRef]

36. Lin, Y.; Lin, H.; Zhang, S.; Chen, Y.; Chen, M.; Lin, Y. The role of active oxygen metabolism in hydrogen peroxide-induced pericarp browning of harvested longan fruit. *Postharvest Biol. Technol.* **2014**, *96*, 42–48. [CrossRef]
37. Lin, Y.; Lin, Y.; Lin, H.; Zhang, S.; Chen, Y.; Shi, J. Inhibitory effects of propyl gallate on browning and its relationship to active oxygen metabolism in pericarp of harvested longan fruit. *LWT-Food Sci. Technol.* **2015**, *60*, 1122–1128. [CrossRef]
38. Sun, Q.; Zhang, N.; Wang, J.; Zhang, H.; Li, D.; Shi, J.; Lin, R.; Weeda, S.; Zhao, B.; Ren, S.; et al. Melatonin promotes ripening and improves quality of tomato fruit during postharvest life. *J. Exp. Bot.* **2015**, *66*, 657–668. [CrossRef]
39. Hu, W.; Yang, H.; Tie, W.; Yan, Y.; Ding, Z.; Liu, Y.; Wu, C.; Wang, J.; Reiter, R.J.; Tan, D.X.; et al. Natural variation in banana varieties highlights the role of melatonin in postharvest ripening and quality. *J. Agric. Food Chem.* **2017**, *65*, 9987–9994. [CrossRef]
40. Pang, L.; Wu, Y.; Pan, Y.; Ban, Z.; Li, L.; Li, X. Insights into exogenous melatonin associated with phenylalanine metabolism in postharvest strawberry. *Postharvest Biol. Technol.* **2020**, *168*, 111244. [CrossRef]
41. Liu, J.; Yang, J.; Zhang, H.; Cong, L.; Zhai, R.; Yang, C.; Wang, Z.; Ma, F.; Xu, L. Melatonin inhibits ethylene synthesis via nitric oxide regulation to delay postharvest senescence in pears. *J. Agric. Food Chem.* **2019**, *67*, 2279–2288. [CrossRef]
42. Liu, S.; Huang, H.; Huber, D.J.; Pan, Y.; Shi, X.; Zhang, Z. Delay of ripening and softening in '*Guifei*' mango fruit by postharvest application of melatonin. *Postharvest Biol. Technol.* **2020**, *163*, 111136. [CrossRef]
43. Rastegar, S.; Khankahdani, H.H.; Rahimzadeh, M. Effects of melatonin treatment on the biochemical changes and antioxidant enzyme activity of mango fruit during storage. *Sci. Hortic.* **2020**, *259*, 108835. [CrossRef]
44. Liu, C.; Zheng, H.; Sheng, K.; Liu, W.; Zheng, L. Effects of melatonin treatment on the postharvest quality of strawberry fruit. *Postharvest Biol. Technol.* **2018**, *139*, 47–55. [CrossRef]
45. Yan, R.; Xu, Q.; Dong, J.; Kebbeh, M.; Shen, S.; Huan, C.; Zheng, X. Effects of exogenous melatonin on ripening and decay incidence in plums (*Prunus salicina* L. *cv. Taoxingli*) during storage at room temperature. *Sci. Hortic.* **2022**, *292*, 110655. [CrossRef]
46. Wang, L.; Yang, M.; Dong, Y.; Reiter, R.J.; Xu, Y.; Lin, X.; Luo, Z.; Li, L. Melatonin confers enhanced polyamine metabolism and cell tolerance in *Vitis vinifera* against oxidative damage: Quantitative proteomic evidence. *Postharvest Biol. Technol.* **2022**, *184*, 111756. [CrossRef]
47. Ehlting, J.; Hamberger, B.; Million-Rousseau, R.; Werck-Reichhart, D. Cytochromes P450 in phenolic metabolism. *Phytochem. Rev.* **2006**, *5*, 239–270. [CrossRef]

foods

MDPI

Article

Thorough Characterization of *ETHQB3.5*, a QTL Involved in Melon Fruit Climacteric Behavior and Aroma Volatile Composition

Noelia Dos-Santos [1], María C. Bueso [2], Aurora Díaz [3,4,5], Eduard Moreno [6], Jordi Garcia-Mas [6,7], Antonio J. Monforte [5] and Juan Pablo Fernández-Trujillo [1,8,*]

1 Department of Agronomical Engineering, Technical University of Cartagena (UPCT), Paseo Alfonso XIII, 48. ETSIA, E-30203 Cartagena, Spain
2 Department of Applied Mathematics and Statistics, UPCT-Technical University of Cartagena, Doctor Fleming s/n. ETSII, E-30202 Cartagena, Spain
3 Department of Plant Sciences, Agrifood Research and Technology Centre of Aragon (CITA), Avda. Montañana 930, E-50059 Zaragoza, Spain
4 AgriFood Institute of Aragon—IA2, CITA-University of Zaragoza, E-50059 Zaragoza, Spain
5 IBMCP Instituto de Biología Molecular y Celular de Plantas, CSIC/Universidad Politécnica de València, Ciudad Politécnica de la Innovación—Edificio 8E Ingeniero Fausto Elio, s/n, E-46022 València, Spain
6 Center for Research in Agricultural Genomics (CRAG) CSIC-IRTA-UAB-UB, Edifici CRAG, Campus Universitat Autònoma de Barcelona (UAB), Bellaterra, E-08193 Barcelona, Spain
7 Institut de Recerca i Tecnologia Agroalimentàries (IRTA), Edifici CRAG, Campus UAB, Bellaterra, E-08193 Barcelona, Spain
8 Institute of Plant Biotechnology, UPCT-Technical University of Cartagena, Plaza del Hospital s/n, Campus Muralla del Mar, E-30202 Cartagena, Spain
* Correspondence: juanp.fdez@upct.es; Tel.: +34-968325436

Abstract: The effect of the QTL involved in climacteric ripening *ETHQB3.5* on the fruit VOC composition was studied using a set of Near-Isogenic Lines (NILs) containing overlapping introgressions from the Korean accession PI 16375 on the chromosome 3 in the climacteric 'Piel de Sapo' (PS) genetic background. *ETHQB3.5* was mapped in an interval of 1.24 Mb that contained a NAC transcription factor. NIL fruits also showed differences in VOC composition belonging to acetate esters, non-acetate esters, and sulfur-derived families. Cosegregation of VOC composition (23 out of 48 total QTLs were mapped) and climacteric ripening was observed, suggesting a pleiotropic effect of *ETHQB3.5*. On the other hand, other VOCs (mainly alkanes, aldehydes, and ketones) showed a pattern of variation independent of *ETHQB3.5* effects, indicating the presence of other genes controlling non-climacteric ripening VOCs. Network correlation analysis and hierarchical clustering found groups of highly correlated compounds and confirmed the involvement of the climacteric differences in compound classes and VOC differences. The modification of melon VOCs may be achieved with or without interfering with its physiological behavior, but it is likely that high relative concentrations of some type of ethylene-dependent esters could be achieved in climacteric cultivars.

Keywords: candidate genes; *Cucumis melo* L.; ethylene production; fruit quality; near-isogenic lines; respiration rate; quantitative trait loci; volatile organic compounds

Citation: Dos-Santos, N.; Bueso, M.C.; Díaz, A.; Moreno, E.; Garcia-Mas, J.; Monforte, A.J.; Fernández-Trujillo, J.P. Thorough Characterization of *ETHQB3.5*, a QTL Involved in Melon Fruit Climacteric Behavior and Aroma Volatile Composition. *Foods* **2023**, *12*, 376. https://doi.org/10.3390/foods12020376

Academic Editors: Imahori Yoshihiro and Jinhe Bai

Received: 25 November 2022
Revised: 3 January 2023
Accepted: 6 January 2023
Published: 13 January 2023

1. Introduction

Genetic dissection of fruit aroma volatiles is difficult because of the polygenic nature of these traits, which remains largely unknown [1]. Most of the Quantitative Trait Loci (QTLs) associated with volatile organic compounds (VOCs) have been mapped in climacteric fruits, such as apples [2], peaches [3–5], melons [6–8], or tomatoes [1,9–13], but also in non-climacteric ones such as grapes [14,15], strawberries [16], and raspberries [17]. One of the difficulties encountered in the genetic dissection of VOCs is the huge number of compounds involved and the difficulties associated with their analysis and quantification [18–20]. Multivariate

statistical tools, including correlation network analysis or clustering procedures, are useful for identifying interactions between VOCs and for grouping highly correlated compounds, allowing dimensionality reduction [20,21].

Melon germplasm displays a very high degree of genetic variability underlying its molecular, morphological, physiological, and compositional characters at plant and fruit levels, thus providing a reservoir of genetic variability for improving melon cultivars [22–28], although only a small part has been mapped in integrated maps [25].

Melons have been proposed as alternative models to tomatoes for studying climacteric fruit ripening because of the presence of climacteric and non-climacteric cultivars within the same species [29]. In the first attempt to decipher the genetic control of climacteric ripening, Périn et al. [30] described two major genes (*Al-3* and *Al-4*, located on chromosomes 8 and 9, respectively) as being responsible for the genetic control of climacteric ripening, together with other QTLs located in different chromosomes with lesser effects. Then, QTLs with a major effect on climacteric ripening have been mapped in different experimental populations [31–36]. Among them, *ETHQB3.5* was identified in the Near-Isogenic Line (NIL) SC3-5 that carries an introgression on chromosome 3 from the Korean accession PI 16375, cultivar Shongwan Charmi (SC), into the Spanish 'Piel de Sapo' (PS) genetic background [31,37]. Remarkably, both PS and SC are non-climacteric cultivars [38]. Additionally, another set of NILs with shorter introgressions in the same region of chromosome 3 from the same cross has been used to study the possible effects of *ETHQB3.5* on traits of interest for postharvest purposes, including the retention of certain flavors following cold storage [39] or the production of VOCs [38,40–42].

The main advantage of using NILs compared with other mapping populations is that QTLs can be located easily in defined introgressions flanked by molecular markers, where their effects can be studied in a homogeneous genomic background, normally from elite cultivars. Thus, NIL collections are considered efficient tools for studying the genetics of complex traits such as VOCs in agronomically important species, e.g., tomato [10,12,43] or melon [6,38,40,44].

The goal of the study was to map *ETHQB3.5* and examine its possible colocalization with other QTLs involved in the production of VOCs. This information will lead to classify VOCs as ethylene-dependent or independent. Putative candidate genes for climacteric ripening and VOC biosynthesis were tentatively located. Our null hypothesis is that the candidate gene involved in climacteric ripening boosts climacteric-dependent VOC biosynthesis.

2. Materials and Methods

2.1. Plant Materials, Crop Management, and Experimental Design

A set of melon NILs with a single homozygous introgression in chromosome 3 from the Korean accession SC in the genetic background of the Spanish cultivar PS was selected for the present study. All the NILs were developed from the NIL SC3-5 that harbors an introgression in chromosome 3 from SC [37], as explained in the mapping schedule of Figure 1. Based on previous data [38,39], the location of *ETHQB3.5* was defined between markers ECM208 and ECM125 [45]. SC3-5 was backcrossed with the recurrent parent PS and F1 plants were selfed for subsequent recombinant screening. F2 seedlings were screened with the aforementioned markers, and plants showing recombinations among them were transferred to the greenhouse to be self-fertilized. Additional research showed that original NIL SC3-5 contained an introgression in chromosome 6, including the QTL *ETHQV6.3*, that is also involved in climacteric ripening **[32]**. In fact, SC3-5 showed SC alleles at markers ECM178, CMCTN41, and A06-C03 [45–47] (Table S1). Recombinant plants were genotyped with those markers, and those showing SC alleles were discarded. The recombination events were fixed in the next generation, and the extension of the recombinant introgressions was determined by genotyping with previously published mapped makers [24,25,46–50]. A total of six recombinant Introgression Lines (ILs) were

obtained: SC3-5-7, SC3-5-8, SC3-5-12, SC3-5-13, and SC3-5-14) and were finally included in the experiments along with the recurrent parent PS.

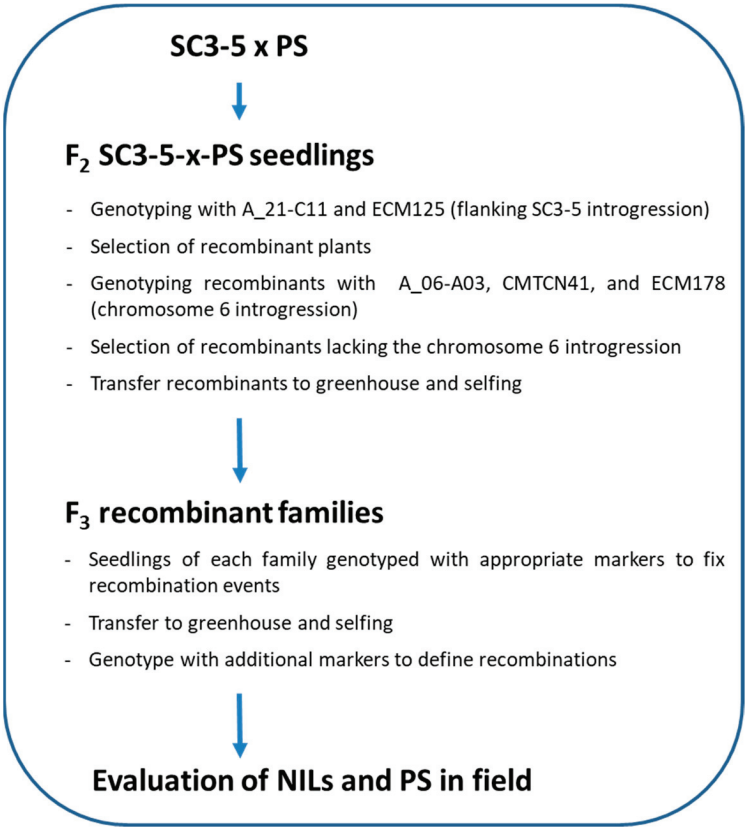

Figure 1. Mapping schedule used to obtain melon Near-Isogenic Lines (NILs) from SC3-5 and the parental PS.

Melon fruits used in this study were cultivated in an open field under Mediterranean conditions from April to July at the Integrated Center of Training and Agricultural Experimentation (CIFEA, in its Spanish acronym) located in Torre Pacheco (Murcia, Spain). The crop management techniques, harvesting practices, and harvest indices were those commonly used for this crop [39,40,51]. The numbers of replicates harvested (2–3 fruits per each of the replicate plants) were: $n = 5$ for SC3-5-7, $n = 7$ for SC3-5-8, and SC3-5-12 $n = 9$ for SC3-5-13 and SC3-5-14, and $n = 21$ for the parental PS used as reference. More replicates in PS were required to obtain better results using the Dunnett test after ANOVA. A completely randomized experimental design has been previously described [38,51,52].

2.2. Physiological Behavior and Maturity Indices at Harvest

The physiological behavior of the NILs and PS was confirmed during two seasons. According to [39,53], fruits were stored at 21 ± 1 °C and relative humidity of 66 ± 6% for at least 8 d. Respiration rate (CO_2) and ethylene production (C_2H_4) were measured by the static method in at least 5 individual fruits of different replicate plants. Fruits were harvested from 7 to 10 a.m. at their optimum stage of maturity according to common harvest criteria [52]. Fruit density was measured at harvest by water displacement and fruit weight every day. The measurements were conducted at least 2 h after harvest to temperate

and equilibrate the fruits with the environment. Fruits were enclosed in hermetic containers for 1 h and sampled for ethylene after 45 min and for CO_2 after 1 h (or the equivalent time in order to avoid accumulation beyond 1% *w*/*w* CO_2). The container was opened and the fruits were ventilated until the next-day measurement. Duplicate samples of 0.5 mL were removed every time from the headspace and analyzed via gas chromatography (GC) with Thermo Finnigan Trace GC 2000 (Milan, Italy) equipped with a thermal conductivity detector and 2-m Porapak N 80/100 column (Agilent J&W, EEUU, Santa Clara, CA, USA) for CO_2 and a GS-Q de 30 m × 0.530 mm column (J&W Scientific, Agilent Technologies Inc., EEUU) and flame ionization detector for ethylene.

GC conditions for CO_2 were: oven temperature of 100 °C for 3 min and post-run conditions of 160 °C for 5 min with 70 kPa pressure. The injector and detector temperatures were 150 °C. A constant flow was used by mixing 30 mL He min^{-1} as inert gas and nitrogen as make-up gas of 10 mL min^{-1}. The signal range was the maximum of 1.

For C_2H_4, oven temperature remained at 60 °C for 2.2 min, and then, a ramp of 80 °C·min^{-1} up to 80 °C was set. Every analysis lasted 2.45 min. The injector and detector temperatures were 200 °C and 250 °C, respectively. The split mode was 1:15 with a purge flow of 90 mL·min^{-1}. The constant flow was established (6 mL·min^{-1}) with a mixture of synthetic air (350 mL·min^{-1}), H_2 (35 mL·min^{-1}), He (4 mL·min^{-1}), and N_2 (30 mL·min^{-1}) as make-up gas. The signal range was 1.

The GCs were previously calibrated with external standards (1 ± 0.1 ppm for ethylene and 1 ± 0.1% *w*/*w* for CO_2 -Air Liquide, Valencia, Spain-). Calculations were programmed in an Excel worksheet according to [54]. In accordance with their physiological behavior (levels of respiration rate and ethylene production), the NILs and PS (control) were classified as non-climacteric (NC), light, or moderately climacteric (LC or MC) [52]. The physiological behavior of the NILs was verified in two different seasons and $n \geq 5$ fruits per season except for the NIL SC3-5-7 (only one season).

2.3. Juice Sampling and VOC Analysis

The methodology used to determine the VOC composition of melon juice by constant flow gas-chromatography mass-spectrometry (GC-MS) analysis was adapted from [38]. VOCs were tentatively identified and aligned by matching their mass spectra of individual components with those stored in the National Institute for Standards and Technology (NIST05a.L, search version 2.0) spectral database and by comparing with linear retention indices (LRI) reported in the literature or NIST database (http://webbook.nist.gov/chemistry/cas-ser.html (accessed on 1 January 2022)). VOCs were classified into ten classes of compounds (acetate esters, organic acids, alcohols, aldehydes, alkanes, ketones, non-acetate esters, sulfur-derived compounds, terpenes, and others). The variables of the compound classes and individual VOCs were obtained following a previously described method [44]. Consistently unidentified compounds (NID) of the untargeted GC-MS analysis were classified as unidentified and reported according to their mass spectra and/or LRI. The closest group of chemical compounds was tentatively reported from NID1 to NID4 compounds and used for the classification of compound classes. The NID1 compound with LRI 1143 was the same unidentified compound previously labeled as "NID3" [44].

2.4. Candidate Gene Selection

Molecular markers were anchored to the melon genome v4.0 [48,55] using the BLAST (Basic Local Alignment Search Tool) available at www.melonomics.net (accessed on 1 January 2022) (Table S1). Annotated genes included in the genomic regions defined by the markers were also retrieved from the Melonomics 4.0 website. The annotation of the genes was double-checked, also using BLAST to compare the annotated/predicted melon genes with the *Arabidopsis thaliana* database (TAIR; www.arabidopsis.org (accessed on 1 January 2022)) and the Uniref90 protein database (http://www.uniprot.org (accessed on 1 January 2022)). The annotation was retained when the significance of the BLAST

comparison was $p < 10^{-5}$. The role of transcription factors or other genes on the phenotype was not directly determined.

2.5. Statistical Analysis and QTL Mapping

The statistical analysis applied to the data from the compound classes and individual VOC variables has been explained previously in detail [44]. For each melon line, all individual VOCs and the classes of compounds were subjected to exploratory data analysis to detect possible outliers by using box-whisker plots allowing a visual comparison between NILs. The data were log-transformed (base 2) and, to apply this transformation, the zero values of VOCs were substituted by the minimum non-zero values observed in the whole dataset [12]. The transformed data were submitted to analysis of variance (ANOVA) with pedigree (NILs and PS) as a factor. The resulting *p*-values were corrected for multiple testing by using the Benjamini and Hochberg criterion [56]. Variables that showed significant differences at level $p = 0.05$ were selected for further analysis. NIL means were simultaneously compared with the control PS mean with a Dunnett's test at level $p = 0.05$. NILs showing significant differences were assumed to harbor a QTL for the trait under study in their respective introgression from SC on chromosome 3. The position of the QTL was established by substitution mapping based on the different lengths of the introgressed segments [57].

A correlation network analysis (CNA) by considering the Pearson correlation coefficient was performed to evaluate the interactions among VOCs and to find groups containing highly correlated VOCs, which were visualized by drawing graphs. The pairs of compounds with absolute Pearson correlation coefficient values higher than a given threshold were selected. Additionally, a hierarchical cluster analysis (HCA) was carried out to classify and identify either cluster of VOCs or NILs. Specifically, an agglomerative hierarchical clustering (AHC) procedure was performed for the individual VOCs of PS and NILs together, considering the similarity metric defined in terms of the Pearson correlation coefficient and using the Ward's minimum variance method. In general, AHC starts with the definition of each VOC belonging to a cluster. In each step, the closest pair of clusters are merged into a new cluster until all of the compounds are in a single cluster. In order to visualize the clustering procedure, a heatmap and a tree diagram (dendrogram) are represented by including the ordering of the clusters and the level of similarity or distance between clusters.

All statistical techniques were performed using free R environment software version 4.1.3 (R Foundation for Statistical Computing, Vienna, Austria) and the flashClust package for HCA and CNA [58]. The correlation networks and the heatmaps were visualized by using the igraph [59] and the gplot [60] packages, respectively.

2.6. Classification of VOCs According to Ethylene Dependence

The volatile compounds were classified as dependent or independent of ethylene action according to different criteria: (i) their levels in the NILs compared with PS and the physiological behavior of each NIL resulting from respiration and ethylene production measurements in separate fruits (climacteric or non-climacteric behavior) as reported above; and (ii) the colocalization of QTLs of VOCs and *ETHQB3.5*.

3. Results

3.1. Ideogram of the NILs. Physiological Behavior, Mapping of ETHQB3.5 and Putative Candidate Genes

An ideogram showing the five NILs under study was obtained (Figure 2).

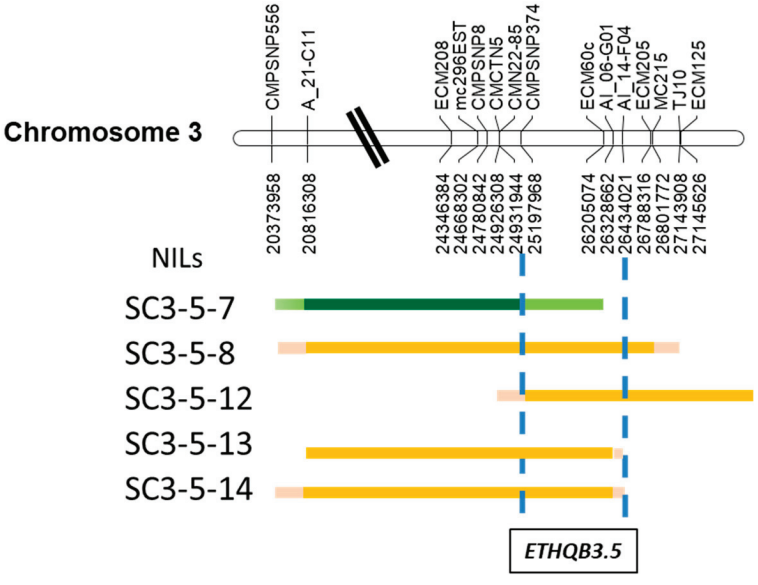

Figure 2. Ideogram showing the extent of the SC introgression on chromosome 3 among the Near-Isogenic Lines (NILs) and classification of their climacteric behavior (green—non-climacteric, orange—climacteric). Molecular markers are anchored to the melon genome v4.0. All the molecular markers are reported in Table S1. Pale or deep green color indicates introgressed region covered by non-climacteric NILs and pink–orange color by climacteric ones, according to Figures 3 and S1. Pink and light green indicate the regions between markers where the recombination occurred in each NIL.

The parental PS and the NIL SC3-5-7 showed non-climacteric behavior, whereas three NILs (SC3-5-8, SC3-5-12, and SC3-5-14) were classified as climacteric. The NIL SC3-5-13 showed a climacteric respiration peak but was not accompanied by a consistent peak of ethylene production in the main season of the experiments (Figure 3). However, the climacteric pattern accompanied by the ethylene peak was confirmed during an additional season (Figure S1). The climacteric NILs showed moderate respiration rate levels of 250–1400 nmol·kg^{-1}·s^{-1} of CO_2 and a slight peak of ethylene production of 5–70 pmol·kg^{-1}·s^{-1} of C_2H_4 (Figure 3).

In accordance with the above-mentioned classification of climacteric behavior (Figure 3), the QTL *ETHQB3.5* was mapped (Figure 2) between the molecular markers CMPSNP374 and AI_14-F04 of the melon genome v4.0 and separated by 1.24 Mb (physical positions from 25.197.968 to 26.434.021), e.g., less than 0.32% of the 400 Mb of the version 4.0 of the melon genome (Figure 2; Tables S1–S3).

Because the role of transcription factor or genes on the phenotype was not directly determined, only a summary of the genes contained in the regions of potential interest in the genetic map were reported. One hundred and forty-seven genes were annotated within the genetic region that included *ETHQB3.5*, e.g., from MELO3C011093 to MELO3C011239, thirteen of them were with unknown functions that would require further characterization (Table S3). One hundred and forty-six additional genes were located in the introgression area studied outside of the *ETHQB3.5* region (forty-five genes from markers CMN22-85 and CMPSNP374; one hundred and one genes from markers AI_14-F04 and TJ10; Tables S2 and S3).

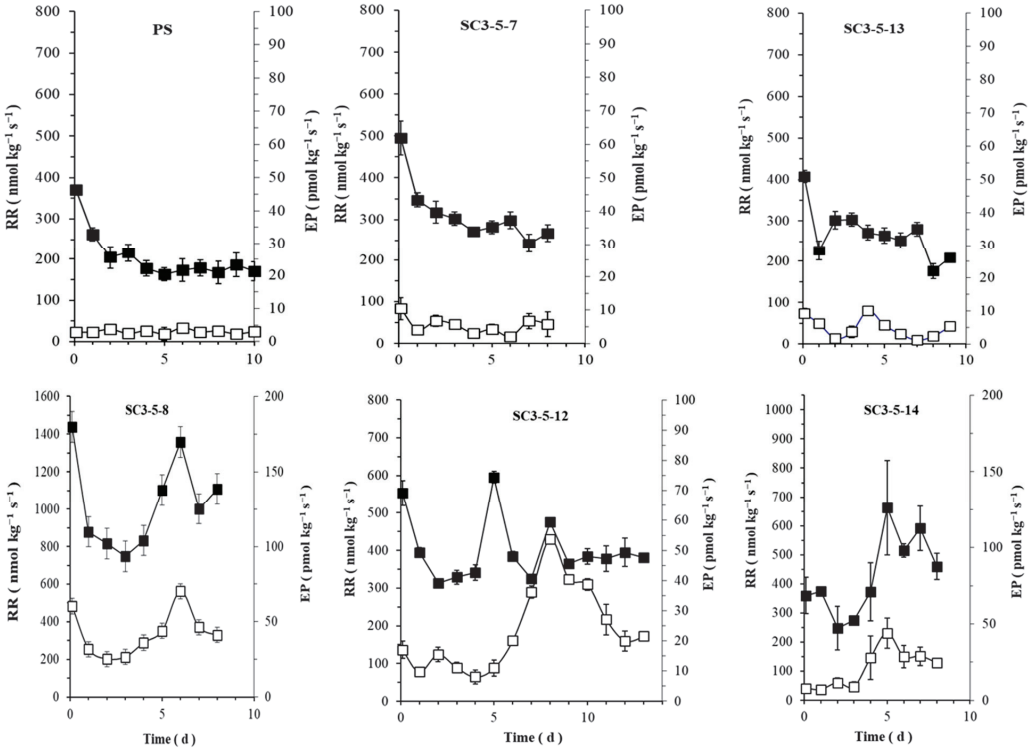

Figure 3. Respiration rate (CO_2, ■) and ethylene production (C_2H_4, □) (RR and EP, respectively; mean ± S.E.) during postharvest ripening at 21 °C and relative humidity of 66 ± 6%. Non-climacteric fruits of parental PS (n = 21) and NIL SC3-5-7 (n = 5). Light–moderate climacteric fruits of NILs SC3-5-8, SC3-5-12 (n = 7), SC3-5-13 (n = 9), and SC3-5-14 (n = 9).

3.2. Volatile Organic Compounds

3.2.1. Compound Classes of VOCs and Univariate Analysis

NILs and PS showed differences in compound classes and individual VOCs (Tables 1 and 2). Aldehydes, alcohols, and ketones were the major VOC classes in PS and the NIL SC3-5-7. Ketones were significantly higher in the parental PS than in the NILs. Furthermore, higher aldehyde content was found in the NIL SC3-5-7 compared with PS. On the other hand, acetate esters and sulfur-derived compounds were more prominent among NILs except for SC3-5-7. The NIL SC3-5-8 showed relatively low levels of alkanes and terpenes compared with PS, whereas the level of compounds classified as "others" in all NILs (except for SC3-5-7) was lower than in PS (Table 1).

3.2.2. Univariate Analysis of Individual VOCs

A total of 161 consistent volatiles were identified and subjected to univariate and multivariate analysis. One hundred and ten individual volatile compounds pointed out the main differences in aroma between PS and NIL (Tables 2 and S4). They were mainly acetate esters, sulfur-derived compounds, and non-acetate esters, which showed values above those of PS or the non-climacteric NIL. Twenty-nine of the one hundred and ten compounds were absent in PS (mainly non-acetate esters and sulfur-derived compounds), and another thirty-five were present in one or several NILs irrespective of their physiological behavior (e.g., associated with this introgression in chromosome 3, Table 2).

Table 1. Main compound classes identified for QTL mapping in melon chromosome 3 using five Near-Isogenic Lines (NILs) with different physiological behavior. Data are expressed as percentages of each compound class with respect to the total normalized areas.

	NILs. Replicates and Classification of Climacteric Behavior [a]																					
Compound Class [b]	PS $n = 21$ (NC)		SC3-5-7 $n = 5$ (NC)		SC3-5-8 $n = 7$ (LC/MC)		SC3-5-12 $n = 7$ (LC/MC)		SC3-5-13 $n = 9$ (LC/MC)		SC3-5-14 $n = 9$ (LC/MC)		p-Value [c]	*ETHQB3.5* Association [d]
ACE	5.89		7.24		43.24	*	46.39	*	15.73	*	24.56	*	****	Full
NAE	6.31		5.38		4.90		5.47		6.36		6.00		NS	No
ALD	33.30		52.02	*	19.24		13.64	*	35.82		29.44		***	No
ALC	16.80		17.17		14.78		11.40		15.54		16.05		NS	No
KET	19.80		9.48	*	6.79	*	6.35	*	13.00	*	10.06	*	****	No
ACD	0.24		0.38		0.36		0.30		0.23		1.02		NS	No
SDC	1.50		2.22		7.79	*	7.25	*	4.84	*	6.99	*	****	Full
TER	1.40		1.01		0.73	*	0.97		1.36		1.31		***	No
AHA	2.08		1.69		0.58	*	1.20		1.96		1.27		**	No
OTH	6.42		3.51		1.63	*	2.62	*	4.36		3.36	*	****	No

[a] Non-climacteric, NC; LC or MC Light or moderate climacteric, respectively. [b] Compound classes: ACE, acetate esters; NAE, non-acetate esters; ALD, aldehydes; ALC, alcohols; KET, ketones; ACD, organic acids; SDC, sulfur-derived compounds; TER, terpenes; AHA, alkanes; OTH, others. Underlined terms indicate absence of QTL mapped in melon chromosome 3 due to the lack of interpretation of the results. [c] NIL means followed by an asterisk were significantly different from the control PS according to one-way ANOVA with pedigree effect followed by a Dunnett test ($p = 0.05$). *, **, ***, ****: significance at $p \leq 0.05$, 0.01, 0.001, and 0.0001, respectively. NS, non-significant. [d] Association of the group of aroma volatiles with the presence of *ETHQB3.5* in the map (Figure 3) without taking into account SC3-5-13.

Hexanal was the most relevant in the percentage of total area (close to 8–20%), particularly above the upper level in parental PS and the non-climacteric NIL SC3-5-7. In PS, the content of the three volatile compounds, ethenylbenzene, (1-hydroxy-2,4,4-trimethylpentan-3-yl) 2-methylpropanoate, and 2-ethyl-3-hydroxyhexyl 2-methylpropanoate, was particularly high compared with the NIL.

Eight individual volatile compounds with higher levels in the climacteric NILs compared with PS (and one, ethenylbenzene, with a lower level in climacteric NILs than in PS) reflected the differences in physiological behavior between the climacteric NILs and PS. The eight individual compounds with higher relative levels in all the climacteric NILs were as follows: two acetate esters (benzyl acetate, butan-2-yl acetate), three non-acetate esters (methyl propanoate, 1-methylethyl acetate, 2-methylpropyl acetate), one sulfur-derived compound (1-(3-Hydroxypropylsulfanyl)ethanone), one alcohol (2-Methylbutan-1-ol), and one unidentified (NID1).

The difference in the aldehyde content between the non-climacteric NIL SC3-5-7 and PS was mainly due to NID4 and two aldehydes (2,4-dimethylbenzaldehyde; 4-methylbenzaldehyde) that were undetectable in PS. The other two aldehydes, (E)-hept-4-enal and (E)-non-2-enal, had a higher content in the NIL SC3-5-7 and other NILs (SC3-5-13 for (E)-hept-4-enal and SC3-5-14 for both compounds) than in PS (Table 2). On the other hand, the aldehydes (2E,6E)-nona-2,6-dienal and decanal were absent or present in lower concentrations, respectively, in NIL SC3-5-7 compared with PS (Table S5).

3.2.3. Genes Located in the Region Mapped of ETHQB3.5 or Covered by the Introgression

The 1-deoxy-D-xylulose-5-phosphate synthase gene, a putative candidate gene for VOC biosynthesis, was mapped in the *ETHQB3.5* region (Table S3). The other two genes were found in the surrounding region of the SC introgression in melon chromosome 3, such as aspartate aminotransferase (MELO3C011284.2; data obtained from MELOGEN from physical positions 24913797 to 24917594), and a phospholipase (MELO3C011257) (Table S3).

Table 2. Main fruit volatile compounds identified for QTL mapping in melon chromosome 3 using five Near-Isogenic Lines (NILs) with different physiological behavior (SC3-5-7, $n = 5$; SC3-5-8 and SC3-5-12, $n = 7$; SC3-5-13 and SC3-5-14, $n = 9$) and the parental control 'Piel de Sapo' (PS) ($n = 21$). Volatile compounds were selected for significance of the univariate statistical criterion described. Data are the mean relative content in percentage with respect to the total of the probable aromatic volatile compounds identified. NIL means in bold followed by an asterisk were significantly different from the control PS mean according to one-way ANOVA with pedigree effect followed by a Dunnett test ($p = 0.05$). *, **, ***, **** significance at $p \leq 0.05$, 0.01, 0.001, and 0.0001, respectively.

Order [b]	CAS [c] Number	IUPAC [d] Name	Compound Class [e]	Compound IDN [f]	NILs and Classification of Climacteric Behavior [a] PS (NC)	SC3-5-7 (NC)	SC3-5-8 (LC/MC)	SC3-5-12 (LC/MC)	SC3-5-13 (LC/MC)	SC3-5-14 (LC/MC)	*p*-Value [g]	MQ [h]
1	000554-12-1	Methyl propanoate	NAE	17	0.06	0.13	**0.3** *	**0.24** *	**0.12** *	**0.45** *	****	95
2	000108-21-4	1-Methylethyl acetate	ACE	21	0.05	0.15	**0.36** *	**0.37** *	**0.31** *	**0.47** *	****	81
3	001534-08-3	S-Methyl ethanethioate	SDC	27	0.05	**0.82** *	**0.92** *	**0.74** *	**0.98** *	**1.44** *	****	87
4	000109-60-4	Propyl acetate	ACE	32	0.16	0.41	**1.61** *	0.85	0.25	0.21	**	83
5	000623-42-7	Methyl butanoate	NAE	33	0	0.02	**0.11** *	**0.07** *	0.02	**0.08** *	****	91
6	000137-32-6	2-Methylbutan-1-ol	ALC	34	0	0.03	**0.09** *	**0.15** *	**0.04** *	**0.16** *	****	86
7	000110-19-0	2-Methylpropyl acetate	ACE	44	0.06	1.79	**8.33** *	**6.17** *	**2.39** *	**5.45** *	****	83
8	000868-57-5	Methyl 2-methylbutanoate	NAE	45	0	**0.07** *	**0.46** *	**0.42** *	**0.06** *	**0.24** *	****	76
9	000105-54-4	Ethyl butanoate	NAE	49	0.18	0.82	**0.54** *	0.85	0.39	0.13	****	97
10	000106-36-5	Propyl propanoate	NAE	50	0	0.03	**0.32** *	**0.11** *	0.09	**0.11** *	****	78
11	000123-86-4	Butyl acetate	ACE	51	0.17	0.41	**2.31** *	**1.99** *	0.39	**0.46** *	***	90
12	002432-51-1	1-Methylsulfanylbutan-1-one	SDC	55	0	0.05	**0.12** *	**0.06** *	0.04	**0.1** *	****	63
13	000123-92-2	3-Methylbutyl acetate	ACE	64	0.02	0.03	**0.27** *	**0.16** *	0.04	**0.05** *	****	90
14	000624-41-9	2-Methylbutyl acetate	ACE	65	0.13	**1.19** *	**10.04** *	**9.16** *	**1.24** *	**4.18** *	****	83
15	000100-42-5	Ethenylbenzene	OTH	66	5.21	3.14	**2.17** *	**2.37** *	**3.12** *	**3.24** *	***	97
16	016630-66-3	Methyl 2-methylsulfanylacetate	SDC	72	0	0.01	**0.05** *	**0.09** *	0.01	**0.03** *	****	87
17	001191-16-8	3-Methylbut-2-enyl acetate	ACE	73	0	0.01	**0.06** *	**0.06** *	0.01	0.01	****	72
18	023747-45-7	3-Methyl-1-methylsulfanyl-butan-1-one	SDC	74	0	0.04	**0.18** *	**0.08** *	0.04	**0.13** *	****	64
19	000111-70-6	Heptan-1-ol	ALC	83	0	**0.03** *	0.01	**0.03** *	**0.05** *	**0.06** *	***	80
20	115051-66-6	1-(3-Hydroxypropylsulfanyl) ethanone	SDC	94	0.07	0.72	**3.82** *	**4** *	**0.59** *	**1.16** *	****	64
21	000142-92-7	Hexyl acetate	ACE	96	0.02	**0.1** *	**0.81** *	**1.2** *	**0.11** *	**0.25** *	****	85
22	000470-82-6	1,8,8-Trimethyl-7-oxabicyclo[2-2-2]octane	TER	98	0.01	0.04	**0.11** *	**0.13** *	0.04	**0.1** *	****	96
23	019780-39-3	(2R,3S)-3-Ethylheptan-2-ol	ALC	106	0.03	**0.14** *	0.03	**0.2** *	**0.16** *	**0.25** *	****	50
24	NID1	NID1 (LRI 1143; RT 20.871) (m/z 43, 88, 73, 61, 148, 41, 45)	NID	122	0.02	0.15	**1.67** *	**1.58** *	**0.27** *	**0.8** *	****	55
25	3901-95-9	1-Methyl-4-propan-2-ylcyclohexan-1-ol	ALC	125	0.1	**0.21** *	0.06	0.11	**0.17** *	**0.29** *	****	71
26	000140-11-4	Benzyl acetate	ACE	132	0.18	0.16	**5.08** *	**2.97** *	**3.21** *	**3.34** *	****	97
27	056805-23-3	(3Z,6Z)-Nona-3.6-dien-1-ol	ALC	137	0.02	**0.15** *	**0.3** *	**0.26** *	0.12	0.23	***	80
28	007371-86-0	4-Acetyloxypentan-2-yl acetate	ALC	141	0.02	**0.28** *	**0.43** *	**0.59** *	0.06	**0.18** *	****	73

Table 2. *Cont.*

Order [b]	CAS [c] Number	IUPAC [d] Name	Compound Class [e]	Compound IDN [f]	NILs and Classification of Climacteric Behavior [a] PS (NC)	SC3-5-7 (NC)		SC3-5-8 (LC/MC)		SC3-5-12 (LC/MC)		SC3-5-13 (LC/MC)		SC3-5-14 (LC/MC)		*p*-Value [g]	MQ [h]
29	015764-16-6	2,4-Dimethylbenzaldehyde	ALD	149	0	**0.13**	*	0.03		0.06		0.1		0.04		**	93
30	000103-45-7	2-Phenylethyl acetate	ACE	151	0.12	**0.77**	*	**1.73**	*	**1.07**	*	**0.84**	*	**1.01**	*	****	72
31	074367-33-2	(1-Hydroxy-2.4.4-trimethyl-pentan-3-yl) 2-methylpropanoate	NAE	153	1.42	0.55		**0.34**	*	**0.45**	*	1.02		0.87		***	78
32	000067-64-1	Acetone	KET	4	6.26	2.62		**1.06**	*	4.96		4.96		3.99		**	72
33	000079-20-9	Methyl acetate	ACE	6	0.69	0.58		**2.25**	*	1.13		1.13		**1.77**	*	*	86
34	000078-84-2	2-Methylpropanal	ALD	7	0	0.02		**0.06**	*	0.02		0.02		**0.17**	*	****	81
35	000078-83-1	2-Methylpropan-1-ol	ALC	16	0	0.04		0.01		**0.04**	*	**0.04**	*	**0.27**	*	**	68
36	000108-88-3	Methylbenzene	OTH	41	1.59	**0.33**	*	**0.25**	*	1.4		0.87		0.93		**	76
37	003214-41-3	Octane-2-5-dione	KET	87	0.03	**0.1**	*	0.04		0.09		**0.09**	*	**0.08**	*	**	71
38	000111-87-5	Octan-1-ol	ALC	110	0.05	**0.51**	*	0.1		**0.21**	*	0.18		**0.51**	*	****	72
39	000079-77-6	(E)-4-(2,6,6-Trimethyl-1-cyclohexenyl)but-3-en-2-one	KET	160	0.02	**0.11**	*	**0.06**	*	0.02		**0.07**	*	**0.09**	*	****	71
40	000075-07-0	Acetaldehyde	ALD	1	0.25	0.38		0.36		0.28		**0.48**	*	**0.48**	*	*	83
41	000074-93-1	Methanethiol	SDC	2	0.35	0.21		**0.16**	*	**0.17**	*	0.22		0.3		**	90
42	00064-17-5	Ethanol	ALC	3	0.43	**0.12**	*	0.17		0.27		0.38		0.37		**	86
43	009057-02-7	Propanal	ALD	5	0.08	0		**0.21**	*	0		0		0		**	90
44	000075-15-0	Methanedithione	SDC	8	0.07	0		0		0.06		**0.18**	*	0.05		**	69
45	000071-23-8	Propan-1-ol	ALC	9	0.06	0.03		**0**	*	0.01		0.07		**0**	*	****	60
46	000123-72-8	Butanal	ALD	10	0.35	0.2		**0.13**	*	**0.12**	*	0.28		0.25		**	82
47	000078-93-3	Butan-2-one	KET	11	0.16	0.12		**0**	*	0.14		0.2		0.16		****	64
48	092112-69-1	Hexane	AHA	13	0	**0.1**	*	0.05		0.01		0.04		**0.07**	*	**	72
49	000123-73-9	But-2-enal	ALD	18	0.25	0.2		**0.11**	*	**0.09**	*	0.18		0.16		***	86
50	000590-86-3	3-Methylbutanal	ALD	19	0	0.01		0		0.01		**0.03**	*	**0.06**	*	****	60
51	068411-77-8	Cyclohexane	AHA	20	0.42	0.14		**0.03**	*	0.29		0.53		0.37		*	50
52	000110-62-3	Pentanal	ALC	22	0.04	0.07		0.07		0.08		**0.1**	*	**0.14**	*	**	90
53	000616-25-1	Pent-1-en-3-ol	ALC	23	0.1	0.1		**0.04**	*	0.07		0.12		0.08		**	78
54	017528-72-2	Pent-1-en-3-one	KET	24	0.38	0.3		**0.17**	*	**0.17**	*	0.32		0.26		*	51
55	000600-14-6	Pentane-2.3-dione	KET	25	0	**0.13**	*	0		0		0		**0.44**	*	****	85
56	003208-16-0	2-Ethylfuran	OTH	28	0.5	0.3		**0.07**	*	0.27		0.52		0.56		**	53
57	000108-10-1	4-Methylpentan-2-one	KET	29	0.04	0.02		**0**	*	**0**	*	0.03		**0.01**	*	****	50
58	068920-64-9	Methyldisulfanylmethane	SDC	35	0.33	0.22		0.22		**0.12**	*	0.33		0.54		**	94
59	000565-69-5	2-Methylpentan-3-one	KET	36	0.07	0.05		**0.03**	*	0.03		0.09		0.07		*	80
60	NID4	NID4 (LRI 734; RT 3.229) (m/z 41, 98, 69, 55, 83)	ALD	37	0	**0.02**	*	**0.01**	*	0		**0.01**	*	**0.02**	*	**	-
61	000105-46-4	Butan-2-yl acetate	ACE	40	0	0		**0.04**	*	**0.03**	*	**0.02**	*	**0.07**	*	****	72
62	025044-01-3	2-Methylpent-1-en-3-one	KET	43	0.03	0.02		0.51		0.05		0.06		**0.08**	*	*	70
63	000820-71-3	2-methylprop-2-enyl acetate	ACE	47	0	0		**0.38**	*	**0.43**	*	0.04		**0.17**	*	****	79

Table 2. *Cont.*

Order [b]	CAS [c] Number	IUPAC [d] Name	Compound Class [e]	Compound IDN [f]	NILs and Classification of Climacteric Behavior [a] PS (NC)	SC3-5-7 (NC)	SC3-5-8 (LC/MC)	SC3-5-12 (LC/MC)	SC3-5-13 (LC/MC)	SC3-5-14 (LC/MC)	*p*-Value [g]	MQ [h]
64	000066-25-1	Hexanal	ALD	48	19.68	19.64	8.27	**8.37** *	15.04	13.39	*	90
65	NID2	NID2 (LRI 908; RT 8.645) (m/z 71, 41, 58, 55, 56)	NID	54	0	0	**0.1** *	0	0	0	****	-
66	005271-38-5	2-Methylsulfanylethanol	SDC	56	0	0	0.01	**0.02** *	0.01	**0.05** *	****	86
67	018729-48-1	3-Methylcyclopentan-1-ol	ALC	57	0.08	0.04	**0.01** *	0.03	0.05	0.06	*	52
68	007452-79-1	Ethyl 2-methylbutanoate	NAE	58	0.01	0.24	**0.24** *	0	0.19	0	***	95
69	000816-11-5	Methyl 2-ethylbutanoate	NAE	59	0.01	0	0	**0.27** *	0	0.06	**	96
70	000540-42-1	2-Methylpropyl propanoate	NAE	62	0	0.02	**0.06** *	**0.06** *	0.04	**0.23** *	****	82
71	000929-22-6	(E)-Hept-4-enal	ALD	69	0.03	**0.05** *	0	0	**0.04** *	**0.04** *	****	67
72	000628-63-7	Pentyl acetate	ACE	71	0	0	**0.18** *	**0.29** *	0.02	**0.04** *	****	78
73	000591-23-1	3-Methylcyclohexan-1-ol	ALC	76	0.23	0.15	**0.14** *	**0.11** *	0.17	0.16	**	80
74	000105-68-0	1-Butanol, 3-methyl-, propanoate	NAE	77	0	0	0	0.02	0.01	**0.04** *	***	75
75	000100-52-7	Benzaldehyde	ALD	79	0.39	0.34	**0.07** *	0.21	0.42	0.34	****	81
76	000108-83-8	2,6-Dimethylheptan-4-one	KET	81	0.03	0.01	**0.01** *	**0** *	0.02	0.01	*	64
77	005441-52-1	3,5-Dimethylcyclohexan-1-ol	ALC	90	0.38	0.31	**0.19** *	0.23	0.27	0.32	**	74
78	000104-76-7	2-Acetyloxypropyl acetate	ACE	99	1.32	2.25	2.03	1.45	1.6	**2.72** *	***	90
79	000623-84-7	1-Acetyloxypropan-2-yl acetate	ACE	100	0.01	0.03	**0.07** *	0.04	0.01	0.02	**	72
80	001193-81-3	(2-Methylcyclohexyl)methanol	ALC	102	0.85	0.65	0.43	**0.51** *	0.59	0.68	*	74
81	001114-92-7 (meso)	3-Acetyloxybutan-2-yl acetate, meso	ACE	104	0.07	0.09	0.16	**0.35** *	0.08	0.04	*	-
82	000098-86-2	1-Phenylethanone	KET	105	1.17	0.51	**0.11** *	0.53	1.11	0.86	*	65
83	001114-92-7 (rac)	3-Acetyloxybutan-2-yl acetate, rac	ACE	107	0	0	**0.05** *	**0.14** *	0	0	****	88
84	000617-94-7	2-Phenylpropan-2-ol	ALC	109	2.53	2.06	**0.35** *	1.71	1.77	1.94	***	72
85	001565-75-9	2-Phenylbutan-2-ol	ALC	111	0.33	0	**0.94** *	0	0	0	****	72
86	000104-87-0	4-Methylbenzaldehyde	ALD	112	0	**0.12** *	0	**0.06** *	0.06	0.04	**	83
87	061193-21-3	Undecane	AHA	117	0.1	0.3	**0.04** *	0.14	0.21	0.18	*	64
88	000628-66-0	3-Acetyloxypropyl acetate	ACE	120	0	0	0.02	0.07	0	0.01	****	60
89	000112-06-1	Heptyl acetate	ACE	121	0.01	0	0.02	**0.3** *	0	0.02	***	60
90	000577-16-2	1-(2-methylphenyl)ethanone	KET	127	0.36	0.35	**0.05** *	0.29	0.29	0.28	***	70
91	004621-04-10	4-Propan-2-ylcyclohexan-1-ol	ALC	128	0.3	0.3	0.14	0.27	**0** *	**0.25** *	****	70
92	000464-49-3	1,7,7-trimethylbicyclo[2.2.1] heptan-2-one	TER	129	0.98	0.66	**0.37** *	0.58	0.75	0.8	****	98
93	31502-19-9	(E)-Non-6-en-1-ol	ALC	130	0.04	**0.19** *	0	0	0	0	****	83
94	018829-56-6	(E)-Non-2-enal	ALD	133	0.14	**0.46** *	0.07	0.02	0.15	**0.16** *	**	80
95	000103-09-3	2-Ethylhexyl acetate	ACE	134	0	**0.4** *	**0.26** *	**0.14** *	0	0.01	****	86
96	000557-48-2	(2E,6E)-Nona-2,6-dienal	ALD	135	0.09	**0** *	**0** *	**0** *	**0** *	0.15	***	72
97	143-08-8	Nonan-1-ol	AHA	138	0.03	0	**0.07** *	0	0	0.06	**	79
98	002040-07-5	1-(2,4,5-Trimethylphenyl)ethanone	KET	140	0	0	**0.16** *	0	0	0	****	83

Table 2. *Cont.*

Order [b]	CAS [c] Number	IUPAC [d] Name	Compound Class [e]	Compound IDN [f]	NILs and Classification of Climacteric Behavior [a] PS (NC)	SC3-5-7 (NC)		SC3-5-8 (LC/MC)		SC3-5-12 (LC/MC)		SC3-5-13 (LC/MC)	SC3-5-14 (LC/MC)		*p*-Value [g]	MQ [h]
99	93-92-5	1-Phenylethyl acetate	ACE	142	0.22	**0.05**	*	0.12		0.24		0.22	0.19		*	81
100	094094-93-6	Dodecane	AHA	143	0.03	**0.45**	*	0.03		0.07		0.05	0.08		**	87
101	000112-31-2	Decanal	ALD	144	0.49	**0.13**	*	0.26		0.27		0.32	0.45		****	97
102	000112-14-1	Octyl acetate	ACE	145	0.03	**0.47**	*	0		0.05		0	0.02		****	86
103	052844-21-0	1-Cyclohexene-1-carboxaldehyde, 2,6,6-trimethyl-	ALD	147	0	**0.07**	*	0		0		0.01	**0.05**	*	**	95
104	NID3	NID3 (LRI 1258, RT 22.147) (m/z 175, 190, 176, 57, 147)	ALD	150	0.06	0		**0.17**	*	0		0	0		**	-
105	000629-62-9	Pentadecane	AHA	159	0.07	0.14		0.01		0.02		0.01	0.07		**	96
106	000767-54-4	3,3,5-trimethylcyclohexan-1-ol	ALC	100	0.07	0.09		**0.05**	*	0.07		0.11	0.1		***	55
107	471-01-2	3,5,5-trimethylcyclohex-3-en-1-one	KET	123	0.28	0.14		0.03		0.18		0.25	0.18		*	57
108	492-37-5	2-phenylpropanoic acid	ACD	125	0.43	0.49		**0.19**	*	0.4		0.41	0.41		*	66
109	10340-23-5	(Z)-non-3-en-1-ol	ALC	135	0.15	0.08		0.27		0.27		0.28	**0.41**	*	*	81
110	74367-31-0	2-Ethyl-3-hydroxyhexyl 2-methylpropanoate	NAE	153	2.28	1.35		**0.6**	*	**0.9**	*	1.69	1.69		***	75

[a] Non-climacteric, NC; LC or MC Light or moderate climacteric, respectively. [b] Order of report. Underlined numbers are compounds not interpretable in Table 4 for QTL mapping in melon chromosome 3. [c] Chemistry Abstract Service. [d] IUPAC, International Union of Pure and Applied Chemistry. [e] Compound classes: ACD, organic acids; ACE, acetate esters; AHA, alkanes; ALC, alcohols; ALD, aldehydes; KET, ketones; NAE, non-acetate esters; SDC, sulfur-derived compounds; TER, terpenes; OTH, others. [f] IDN: Identification number assigned to each volatile compound in the analysis according to its increasing order of retention time in the chromatogram. [g] The raw *p* values of the ANOVA were corrected for the multiple tests using the Benjamini and Hochberg (1995) false discovery rate criterion [56]. Original data were transformed for statistical analysis by applying the log transformation (base 2). [h] MQ: Match quality (0–100 units) of spectra compared with those of the National Institute for Standards and Technology (NIST05a.L, search version 2.0) data bank.

3.2.4. VOC QTL Mapping

Several scenarios were obtained when we tried to map compound classes or individual volatiles (Tables 3 and 4) by substitution mapping: (i) the inferred map position of the volatile QTL colocalized with *ETHQB3.5*, (ii) the QTL mapped in a different position than *ETHQB3.5* QTL, (iii) the segregation of the trait and introgressions among NILs was not compatible with the presence of a single QTL in the studied region. QTLs included in the (i) scenario are climacteric dependent and may be due to pleiotropic effects of *ETHQB3.5*, whereas QTLs included in the (ii) scenario would be genes linked to *ETHQB3.5* whose effects would be largely climacteric-independent. For example, QTLs for VOCs belonging to the acetate esters and sulfur-derived compounds classes colocalized with *ETHQB3.5*, whereas QTLs associated with aldehydes and ketones classes were mapped independently to *ETHQB3.5* (Tables 1 and 3).

Forty-four VOC QTL could be mapped (only one per individual VOC) out of the one hundred and ten with some significant NIL effect in Table 2, and in thirty-one of which SC alleles increased volatile synthesis (Table 4). Twenty-one QTLs of individual VOCs colocalized with the region of *ETHQB3.5* (plus two more for compound classes of acetate esters and sulfur-derived compounds), and in nineteen of them (plus two of the compound classes mentioned above), the SC alleles increased the VOCs synthesis (Tables 4 and S2). Most of them altered the composition of acetate and non-acetate esters and sulfur-derived compounds (Tables 2, 4 and S2).

For VOCs without a QTL mapped in chromosome 3 (Table 2), a more complex genetic control was assumed. For example, for 25 VOCs, only SC3-5-8 showed significant differences compared to PS (Table 2). In another case, only SC3-5-7 showed an increased level of 2,4-dimethylbenzaldehyde or octyl acetate or a reduction in ethanol or decanal (Table 2), suggesting that *ETHQB3.5* or another tightly linked QTL present in the other NILs, modulates the effects of a QTL that is to the left part of the introgression that is covered by SC-3-5-7 (Table 4).

Twenty-five QTLs of VOCs were mapped in regions outside the region of *ETHQB3.5* in chromosome 3. Seventeen of the former QTLs (including aldehydes, ketones, and the rest of individual VOCs) were mapped to the right of the molecular marker AI_14-F04 (Table S2), and thirteen of them, including aldehydes, had a negative effect on the PS levels of VOCs. On the other hand, eight of the QTLs (seven VOCs plus ketones as compound classes) were mapped to the left of the molecular marker CMPSNP374 and showed a positive effect on VOC levels in PS, except for ketones as compound classes (Tables 1, 2 and S2).

Table 3. QTL mapping of compound classes of aroma volatiles in melon chromosome 3 is depicted at the top according to [49] using the conventional nomenclature [61] for the chromosomes. For each aroma volatile, the estimated position of the QTL is indicated by a shadowed area and is colored dark when the SC [SC = 'Shongwan Charmi' (PI161375)] allele increased the trait or light color when it decreased the trait. Dark colors indicate values above PS, while light colors indicate values below PS levels. *ETHQB3.5* is the region containing the QTL of the climacteric. I/D: Ethylene dependence (1) and independence (−1).

Physical Distance in the Genetic Map	Molecular Marker Position																							
	20,373,958	20,816,308	24,346,383	24,668,302	24,780,842	24,926,308	24,931,945		25,197,968		26,205,074	26,328,662		26,434,021	26,788,316	26,801,772		27,143,907	27,145,624					
Compound Classes	**CMPSNP556**	**A_21-C11**	**ECM208**	**mc296EST**	**CMPSNP8**	**CMCTN5**	**CMN22-85**		**CMPSNP374**		**ECM60c**	**AI_06_G01**		**AI_14-F04**	**ECM205**	**MC215**		**TJ10**	**ECM125**	N Confirmed > PS	N Confirmed < PS	N QTLclim > PS	N QTLclim < PS	Significance ($p < 0.05$)	Ethylene I/D
Acetate Esters																				1	–	1	–	****	1
Sulfur Derived Compounds																				1	–	1	–	****	1
Aldehydes																				–	1	–	–	***	–1
Ketones																				–	1	–	–	****	–1
	Climacteric QTL position (*ETHQB3.5*)																							

Table 4. QTL mapping of individual aroma volatile compounds in melon chromosome 3 is depicted at the top according to [49] using the conventional nomenclature [61] for the chromosomes. For each aroma volatile, the estimated position of the QTL is indicated by a shadowed area (grey or black) when the SC ['Shongwan Charmi' (PI161375)] allele increased or decreased the trait, respectively. Question mark indicates position of mapping in doubt.

IUPAC [a] Name of Aroma Volatile Compounds	CMPSNP556	A_21—C11	ECM208	mc296EST	CMPSNP8	CMCTN5	CMN22—85	CMPSNP374	ECM60c	AI_06—G01	AI_14—F04	ECM205	MC215	TJ10	ECM125	N QTL Confirmed > PS	N QTL Confirmed < PS	N QTL in ETHQB3.5 Region > PS	N QTL in ETHQB3.5 Region < PS	CAS Number [b]	Ethylene I/D [c]
IDN [d] QTL Climacteric position									*ETHQB3.5*									Colocalization with *ETHQB3.5*			
1 Methyl propanoate																1	–	1	–	000554-12-1	1
2 1-Methylethyl acetate																1	–	1	–	000108-21-4	1
3 S-Methylmet ethanethioate																1	–	–	–	001534-08-3	−1
5 Methyl butanoate																1	–	1	–	000623-42-7	1
6 2-Methylbutan-1-ol																1	–	1	–	000137-32-6	1
7 2-methylpropyl acetate																1	–	1	–	000110-19-0	1
8 Methyl 2-methylbutanoate																1	–	–	–	000868-57-5	−1
10 Propyl propanoate																1	–	1	–	000106-36-5	1
11 Butyl acetate																1	–	1	–	000123-86-4	1
12 1-Methylsulfanylbutan-1-one																1	–	1	–	002432-51-1	1
13 3-Methylbutyl acetate																1	–	1	–	000123-92-2	1
14 2-Methylbutyl acetate																1	–	–	–	000624-41-9	−1
15 Ethenylbenzene																–	1	–	1	000100-42-5	1
16 Methyl 2-methylsulfanylacetate																1	–	1	–	016630-66-3	1
17 3-Methylbut-2-enyl acetate																1	–	–	–	001191-16-8	−1
18 3-Methyl-1-methylsulfanyl-butan-1-one																1	–	1	–	023747-45-7	1
20 1-(3-Hydroxypropylsulfanyl)ethanone																1	–	1	–	115051-66-6	1
21 Hexyl acetate																1	–	–	–	000142-92-7	−1

Table 4. *Cont.*

IDN [d]	IUPAC [a] Name of Aroma Volatile Compounds	CMPSNP556	A_21—C11	ECM208	mc296EST	CMPSNP8	CMCTN5	CMN22—85	CMPSNP374	ECM60c	AI_06—G01	AI_14—F04	ECM205	MC215	TJ10	ECM125	N QTL Confirmed > PS	N QTL Confirmed < PS	N QTL in ETHQB3.5 Region > PS	N QTL in ETHQB3.5 Region < PS	CAS Number [b]	Ethylene I/D [c]
	QTL / Climacteric position									*ETHQB3.5*									Colocalization with *ETHQB3.5*			
22	1,8,8-Trimethyl-7-oxabicyclo[2-2-2]octane									■	■						1	–	1	–	000470-82-6	1
24	NID1 (LRI 1143; RT 20.871) (*m*/*z* 43, 88, 73, 61, 148, 41, 45)									■	■						1	–	1	–	NID1	1
26	Benzyl acetate									■	■						1	–	1	–	000140-11-4	1
30	2-Phenylethyl acetate								■	■							1	–	–	–	000103-45-7	−1
31	(1-Hydroxy-2,4,4-trimethyl-pentan-3-yl) 2-methylpropanoate											■	■	■	■		–	1	–	–	074367-33-2	−1
39	(E)-4-(2,6,6-Trimethyl-1-cyclohexenyl)but-3-en-2-one		■	■	■	■	■	■									1	–	–	–	000079-77-6	−1
41	Methanethiol											■	■	■	■		–	1	–	–	000074-93-1	−1
46	Butanal											■	■	■	■		–	1	–	–	000123-72-8	−1
49	But-2-enal											■	■	■	■		–	1	–	–	000123-73-9	−1
54	Pent-1-en-3-one											■	■	■	■		–	1	–	–	017528-72-2	−1
57	4-Methylpentan-2-one									■	■	■					–	1	–	1	000108-10-1	1
58	Methyldisulfanylmethane														■	■	–	1	–	–	068920-64-9	−1
60	NID4 (LRI 734; RT 3.229) (*m*/*z* 41, 98, 69, 55, 83)		■	■	■	■	■	■									1	–	–	–	NID4	−1
61	Butan-2-yl acetate									■	■						1	–	1	–	000105-46-4	1
63	2-methylprop-2-enyl acetate									■	■						1	–	1	–	000820-71-3	1
64	Hexanal														■	■	–	1	–	–	000066-25-1	−1
69	Methyl 2-ethylbutanoate														■	■	1	–	–	–	000816-11-5	−1

Table 4. *Cont.*

IDN [d]	IUPAC [a] Name of Aroma Volatile Compounds	CMPSNP556	A_21—C11	ECM208	mc296EST	CMPSNP8	CMCTN5	CMN22—85		CMPSNP374		ECM60c	AI_06—G01		AI_14—F04	ECM205	MC215		TJ10	ECM125	N QTL Confirmed > PS	N QTL Confirmed < PS	N QTL in ETHQB3.5 Region > PS	N QTL in ETHQB3.5 Region < PS	CAS Number [b]	Ethylene I/D [c]
	QTL / Climacteric position											*ETHQB3.5*											Colocalization with *ETHQB3.5*			
70	2-Methylpropyl propanoate																				1	–	1	–	000540-42-1	1
72	Pentyl acetate																				1	–	1	–	000628-63-7	1
73	3-Methylcyclohexan-1-ol																				–	1	–	–	000591-23-1	−1
76	2,6-Dimethylheptan-4-one																				–	1	–	–	000108-83-8	−1
80	(2-Methylcyclohexyl)methanol																				–	1	–	–	001193-81-3	−1
81	3-Acetyloxybutan-2-yl acetate, meso																				1	–	–	–	001114-92-7 (meso)	−1
83	3-Acetyloxybutan-2-yl acetate, rac																				1	–	–	–	001114-92-7 (rac)	−1
89	Heptyl acetate																				1	–	–	–	000112-06-1	−1
110	2-Ethyl-3-hydroxyhexyl 2-methylpropanoate																				–	1	–	–	74367-31-0	−1
	Total QTLs																				31	13	19	2		

Abbreviations: NID, unidentified compound. [a] IUPAC, International Union of Pure and Applied Chemistry. [b] Chemical Abstracts Service. [c] Numbers indicate the ethylene dependence classification of QTLs. (−1) Fully independent. (1) Fully dependent. [d] Identification number is assigned to each volatile compound in the analysis according to its increasing order of retention time in the chromatogram (as in Table 2).

3.2.5. Correlation Network and Hierarchical Clustering Analysis

The CNA built sixty-seven groups (Figure 4), five of which had at least three compounds (G1, G2, G3, G4, and G5) (Table 5), and the remaining only had one compound. In the most numerous group (G1), a network was established among twenty-eight volatile compounds (Tables 2, 5 and S6; Figure 5); twenty-three of them were signed as important in the QTL identification in chromosome 3 (seventeen of them with QTLs colocalized with *ETHQB3.5*; Tables 4, 5 and S6). Three sub-groups were obtained within G1, mainly associated with acetate esters, non-acetate esters, and sulfur-derived compounds, respectively. In G2, aldehyde, alcohol, and ketones were present. In the other groups, the grouping of VOCs was more difficult to classify, except in G5 (alcohol and non-acetate esters particularly, plus one terpene and one classified as another VOC type). In G2 and G5, most of the VOCs with QTL that mapped in chromosome 3 (four per group) were located to the right of *ETHQB3.5* and only for ethenylbenzene (in G5) colocalized with *ETHQB3.5*. The VOCs of G3 and G4 include compounds not interpretable in Table 4 for QTL mapping in chromosome 3 (Tables 4, 5, S2 and S6).

Table 5. Groups with at least two compounds and correlations above 0.7 in absolute value were obtained by correlation network analysis (CNA) applied to melon aroma volatile compounds. The chemical and sensory attributes of the compounds are in Table S6.

Order [a]	CAS [b] and Group	IUPAC [c] Name
	Group 1	
1	000079-20-9	Methyl acetate
2	000078-83-1	2-Methylpropan-1-ol
3	000554-12-1	Methyl propanoate
4	001534-08-3	S-Methyl ethanethioate
5	000109-60-4	Propyl acetate
6	000623-42-7	Methyl butanoate
7	000137-32-6	2-Methylbutan-1-ol
8	000110-19-0	2-Methylpropyl acetate
9	000868-57-5	Methyl 2-methylbutanoate
10	000820-71-3	2-Methylprop-2-enyl acetate
11	000106-36-5	Propyl propanoate
12	000123-86-4	Butyl acetate
13	002432-51-1	1-Methylsulfanylbutan-1-one
14	005271-38-5	2-Methylsulfanylethanol
15	000540-42-1	2-Methylpropyl propanoate
16	000123-92-2	3-Methylbutyl acetate
17	000624-41-9	2-Methylbutyl acetate
18	000628-63-7	Pentyl acetate
19	016630-66-3	Methyl 2-methylsulfanylacetate
20	001191-16-8	3-Methylbut-2-enyl acetate
21	023747-45-7	3-Methyl-1-methylsulfanyl-butan-1-one
22	115051-66-6	1-(3-Hydroxypropylsulfanyl)ethanone
23	000142-92-7	Hexyl acetate
24	000470-82-6	1,8,8-Trimethyl-7-oxabicyclo[2-2-2]octane
25	NID1 [d]	NID1 (LRI 1143; RT 20.871) (m/z 43, 88, 73, 61, 148, 41, 45)
26	000140-11-4	Benzyl acetate
27	007371-86-0	4-Acetyloxypentan-2-yl acetate
28	000103-45-7	2-Phenylethyl acetate

Table 5. *Cont.*

Order [a]	CAS [b] and Group	IUPAC [c] Name
	Group 2	
1	000123-72-8	Butanal
2	000123-73-9	But-2-enal
3	000616-25-1	Pent-1-en-3-ol
4	017528-72-2	Pent-1-en-3-one
5	000565-69-5	2-Methylpentan-3-one
6	000066-25-1	Hexanal
	Group 3	
1	068411-77-8	Cyclohexane
2	000108-88-3	Methylbenzene
3	018729-48-1	3-Methylcyclopentan-1-ol
4	000105-54-4	Ethyl butanoate
	Group 4	
1	NID2 [d]	NID2 (LRI 908; RT 8.645) (*m*/*z* 71, 41, 58, 55, 56)
2	001565-75-9	2-Phenylbutan-2-ol
3	002040-07-5	1-(2,4,5-Trimethylphenyl)ethanone
	Group 5	
1	000100-42-5	Ethenylbenzene
2	000591-23-1	3-Methylcyclohexan-1-ol
3	005441-52-1	3,5-Dimethylcyclohexan-1-ol
4	001193-81-3	(2-Methylcyclohexyl)methanol
5	000464-49-3	1,7,7-Trimethylnorbornan-2-one
6	074367-33-2	(1-Hydroxy-2,4,4-trimethyl-pentan-3-yl) 2-methylpropanoate
7	74367-31-0	2-Ethyl-3-hydroxyhexyl 2-methylpropanoate

[a] Arbitrary order within each group according to correlation network analysis. Underlined numbers are compounds not interpretable in Table 4 for QTL mapping in melon chromosome 3. [b] CAS, Chemical Abstracts Service (number of compounds). [c] IUPAC, International Union of Pure and Applied Chemistry. [d] All unidentified compounds are identified with linear retention index, retention time (min), and main ions.

Six clustering VOCs can be clearly identified in the heatmap (Figure 6): C1, C2, C3, C4, C5, C6, and the detailed VOCs per cluster are shown in Figure 7. Twenty-six of the VOCs in C1 also belong to the most numerous group (G1) identified by correlation network analysis. As we mentioned above, these were important VOCs for QTL mapping and many colocalized with *ETHQB3.5* (Table 4). The VOCs included in the groups G3 and G5 were assigned to the same cluster, C3, while all VOCs in the groups G2 and G4 were identified into C6 and C5, respectively. Clusters C2 and C4 had no intercorrelated VOCs with higher correlation absolute values than 0.7.

A heatmap for two-way HCA of melon fruits and their VOCs indicates that cluster C1 showed more evident associations with climacteric NILs because the VOCs included in the cluster were related to esters (acetate and non-acetate) and sulfur-derived compounds (mostly esters) (Figure 8). These VOCs were produced via amino acids and, particularly, methionine. In fact, at the bottom left of the heatmap, the compounds that differentiate PS from the NILs are found, mostly esters, as expected. At this position, the separation between SC3-5-8, SC3-5-14, and SC3-5-12 from the rest was evident.

The VOCs in a sub-cluster C4 were mainly related to aldehydes (4-methylbenzaldehyde; 1-cyclohexene-1-carboxaldehyde, 2,6,6-trimethyl-; (E)-hept-4-enal) and ketones (pentane-2.3-dione; octane-2-5-dione) and were associated to the non-climacteric NIL SC3-5-7, while the VOCs included in cluster C5 (top of Figure 8, VOCs located on the right), such as propanal, 2-phenylbutan-2-ol, 1-(2,4,5-trimethylphenyl)ethanone or butan-2-one, were associated with the climacteric NIL SC3-5-8, which showed an exclusive different level of these VOCs versus PS (Table 2). Consequently, these VOCs were not interpretable for QTL mapping (Tables 2 and 4).

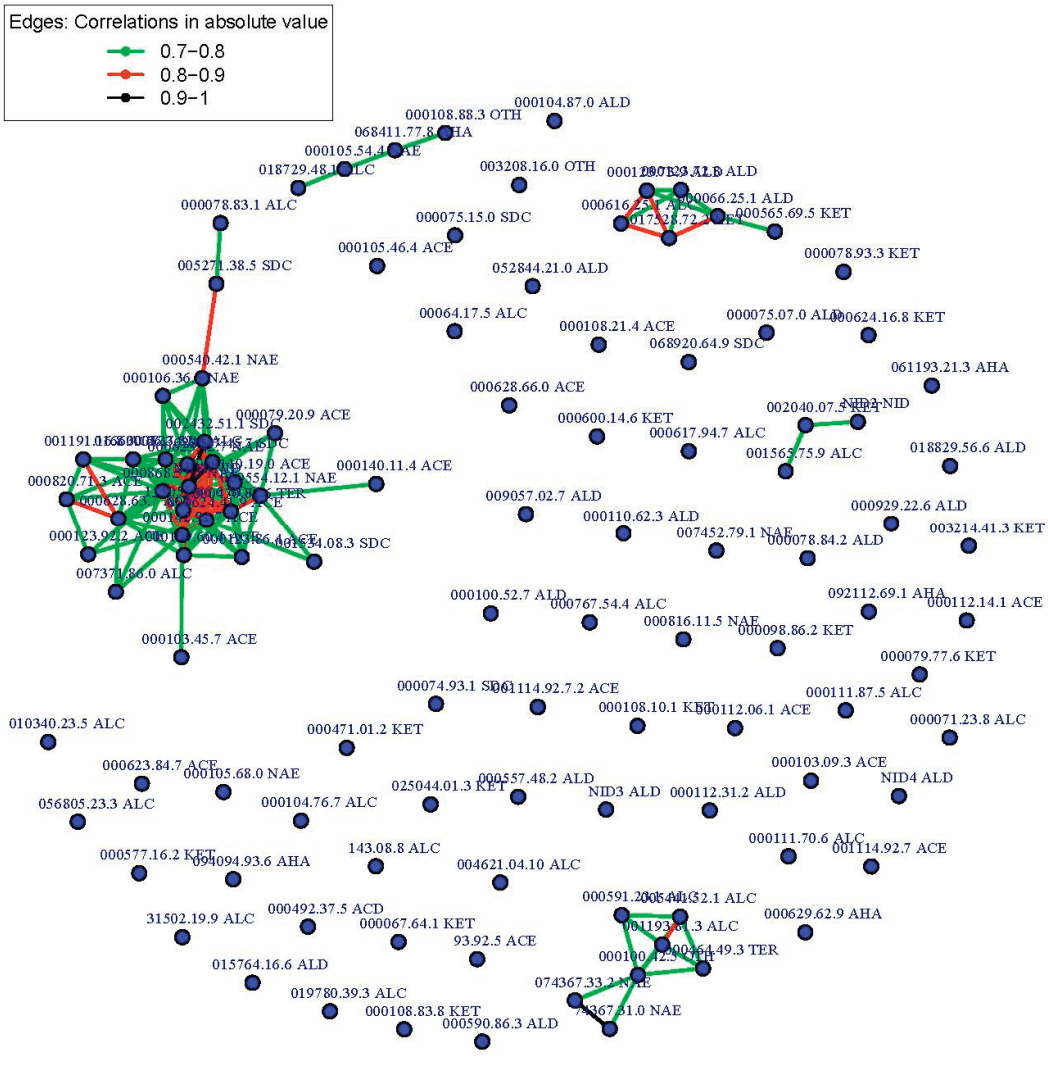

Figure 4. Correlation network analysis (CNA) based on absolute Pearson correlation coefficient with cut-off value greater than 0.7. Groups identified from individual volatile compounds analyzed for the Near-Isogenic Lines (NILs) with introgression on melon chromosome 3 (SC3-5-7, SC3-5-8, SC3-5-12, SC3-5-13, and SC3-5-14) and the parental control 'Piel de Sapo' (PS). CAS numbers use dots instead of dashes. ACE, acetate esters; NAE, non-acetate esters; SDC, sulfur-derived compounds; ALD, aldehydes; KET, ketones; ALC, alcohols; TER, terpenes; AHA, aliphatic compounds; OTH, other compounds; NID, unidentified compound.

3.3. Association between VOCs and Climacteric Behavior

The QTL of twenty-one individual VOCs mapped in the *ETHQB3.5* region exclusively showed ethylene dependence (plus the acetate esters and sulfur-derived compounds as compound classes). Twenty-three QTLs (plus the aldehydes and ketones as compounds classes) showed full ethylene independence (Tables 3, 4 and S2).

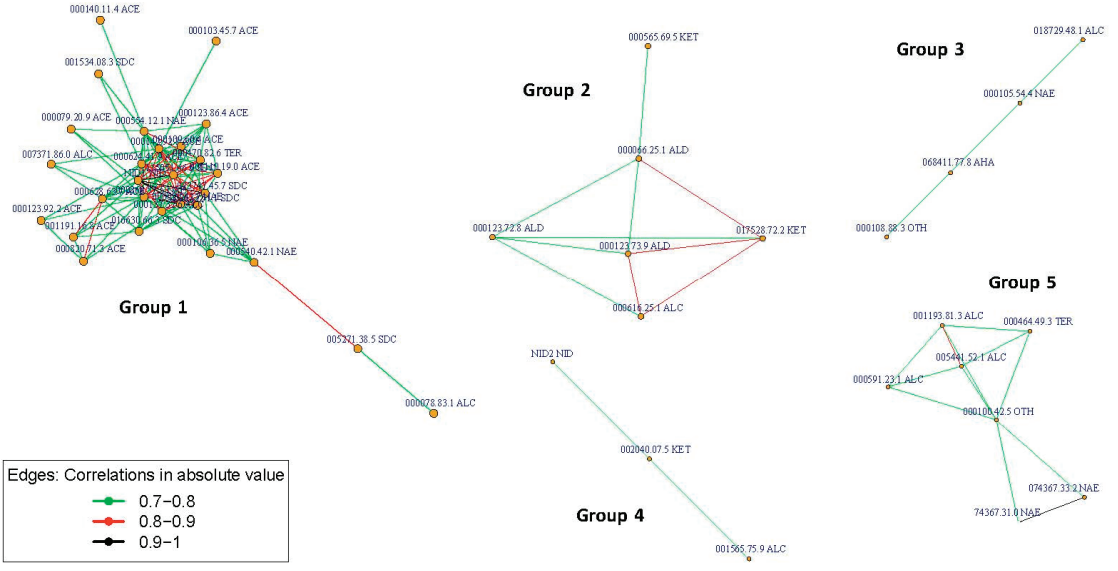

Figure 5. Grouping of individual volatile compounds with six or more compounds in each group obtained by correlation network analysis (CNA) applied to individual volatile compounds analyzed for Near-Isogenic Lines (NILs) with introgression on melon chromosome 3 (SC3-5-7, SC3-5-8, SC3-5-12, SC3-5-13, and SC3-5-14) and the parental control 'Piel de Sapo' (PS). CAS numbers use dots instead of dashes. ACE, acetate esters; NAE, non-acetate esters; SDC, sulfur-derived compounds; ALD, aldehydes; KET, ketones; ALC, alcohols; TER, terpenes; AHA, aliphatic compounds; OTH, other compounds; NID, unidentified compound.

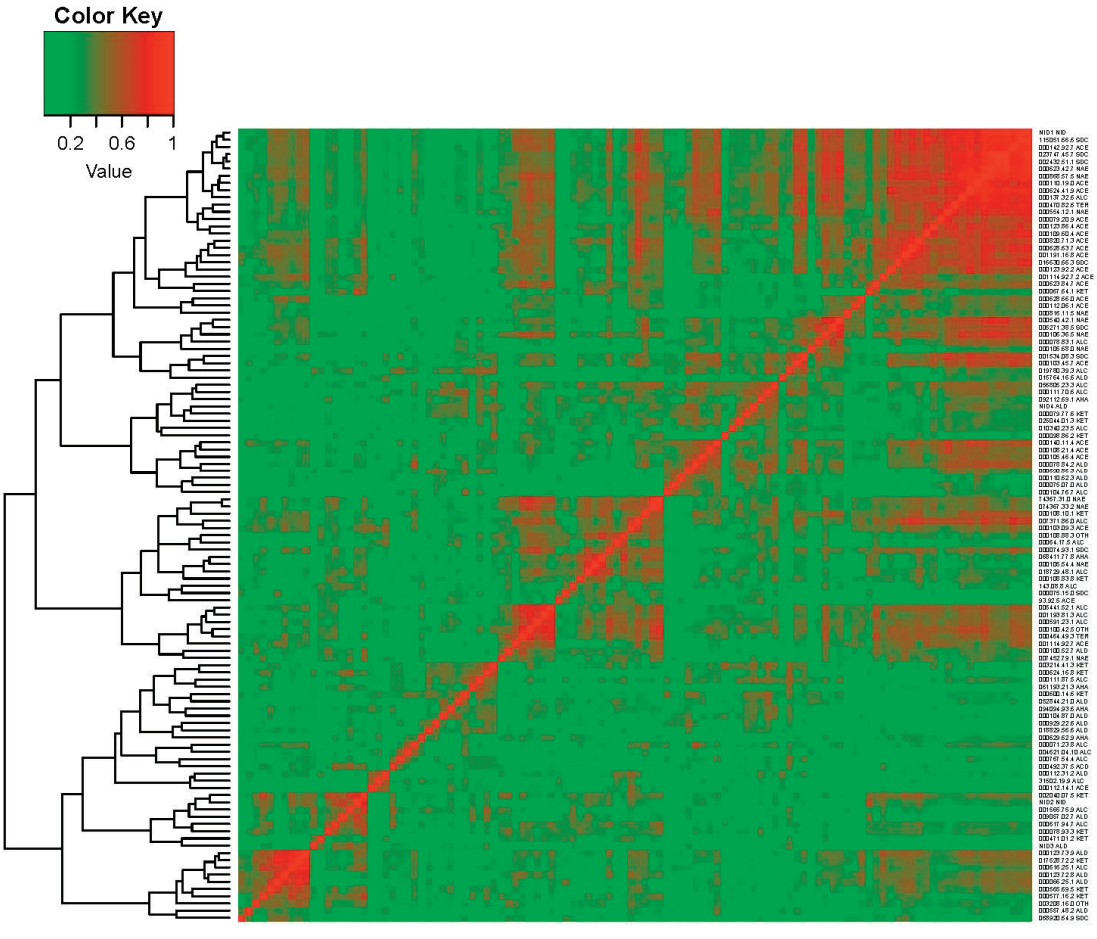

Figure 6. Heatmap of absolute Pearson correlation coefficients between pairs of individual volatile compounds was analyzed for the Near-Isogenic Lines (NILs) with introgression on melon chromosome 3 (SC3-5-7, SC3-5-8, SC3-5-12, SC3-5-13, and SC3-5-14) and the parental control 'Piel de Sapo' (PS). Dendrogram obtained by Ward's hierarchical clustering method was applied to the log_2-transformed data. The individual volatiles are plotted by their respective CAS numbers (dots instead of dashes) on the right of the heatmap.

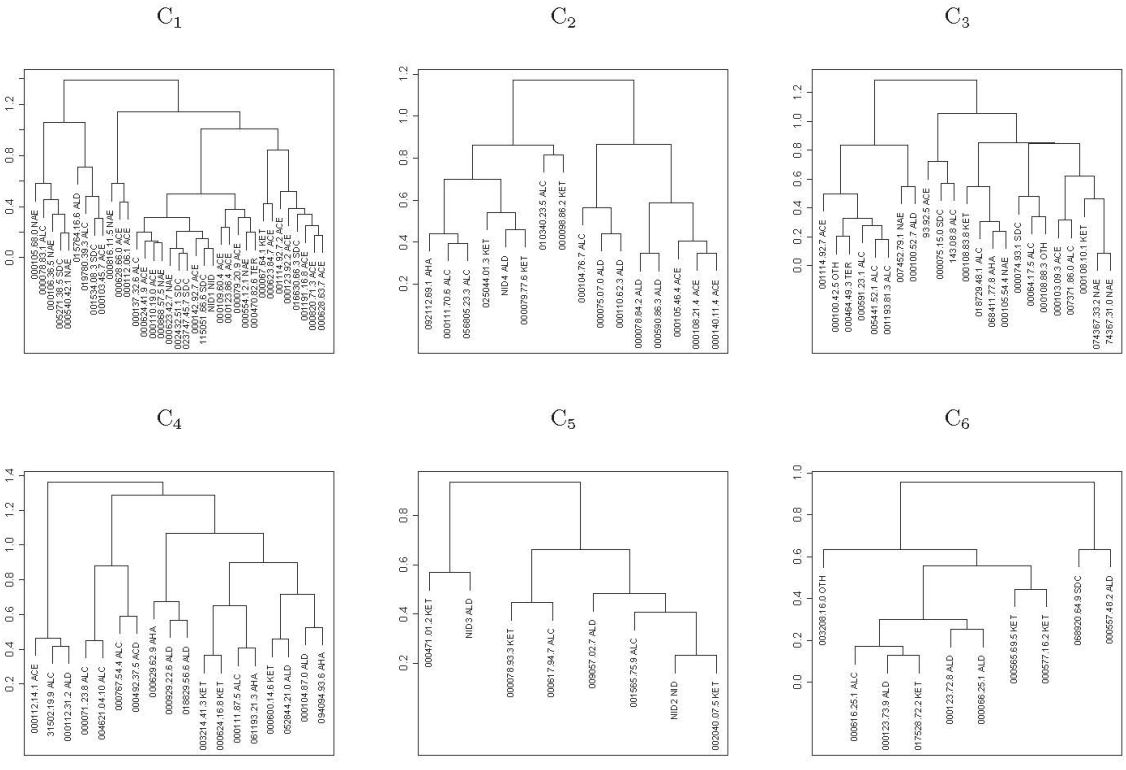

Figure 7. Detailed dendrograms of the six clusters (**C1**–**C6**) identified by hierarchical clustering applied to individual volatile compounds analyzed for the near-isogenic lines (NILs) with introgression on melon chromosome 3 (SC3-5-7, SC3-5-8, SC3-5-12, SC3-5-13, and SC3-5-14) and the parental control 'Piel de Sapo' (PS). The individual volatiles are plotted by their respective CAS numbers (dots instead of dashes) plus their chemical compound classes. ACE, acetate esters; NAE, non-acetate esters; SDC, sulfur derived compounds; ALD, aldehydes; KET, ketones; ALC, alcohols; TER, terpenes; AHA, aliphatic compounds; OTH, other compounds; NID, unidentified compound.

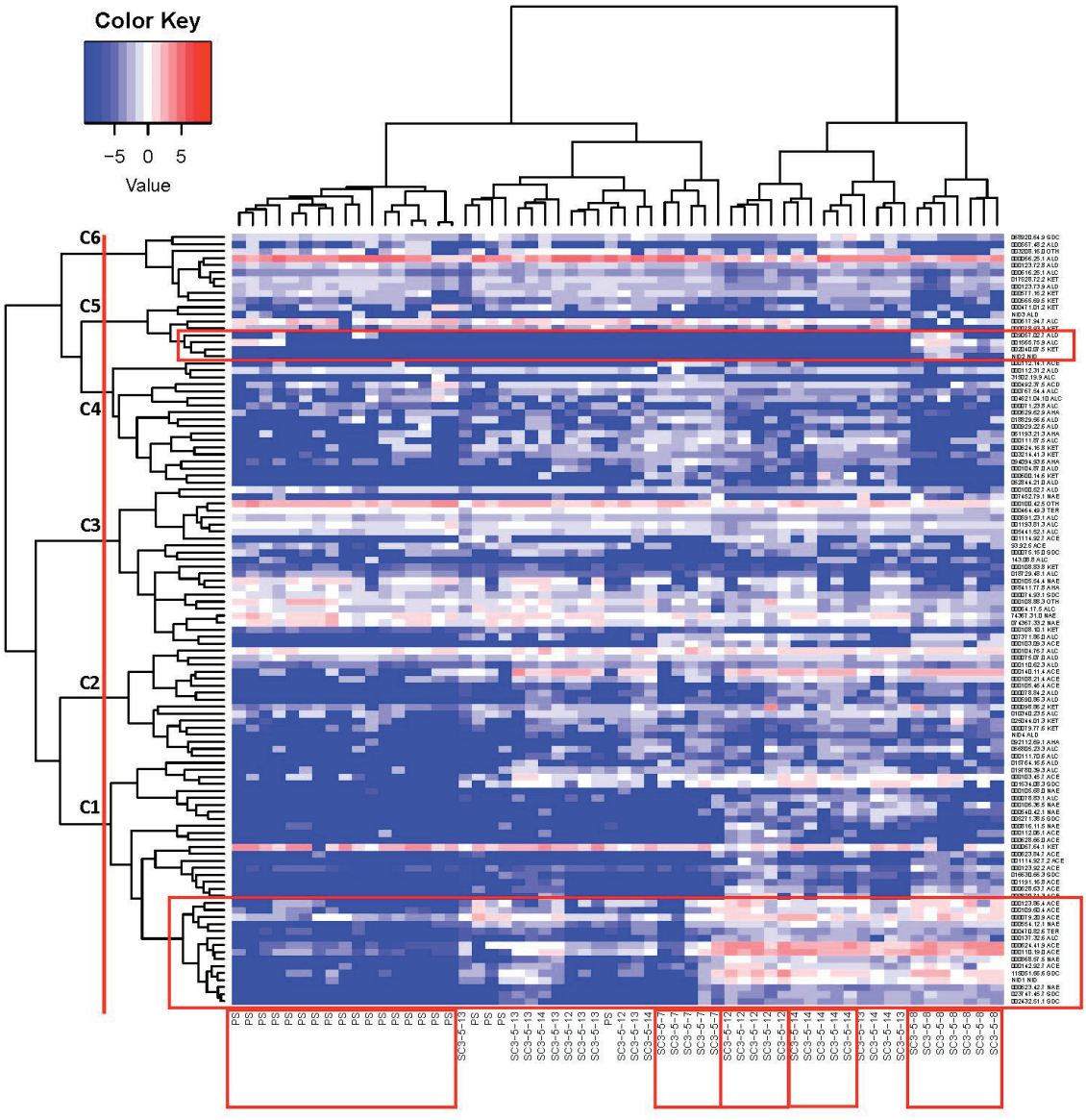

Figure 8. Heatmap for two-way hierarchical clustering applied to melon fruits and their aroma volatiles analyzed for the Near-Isogenic Lines (NILs) with introgression of melon chromosome 3 (SC3-5-7, SC3-5-8, SC3-5-12, SC3-5-13, and SC3-5-14) and the parental control 'Piel de Sapo' (PS). Dendrograms obtained by Ward's hierarchical clustering method were applied to the $\log_2$-transformed data analyzed. The individual volatiles are plotted by their respective CAS numbers (dots instead of dashes) on the right of the heatmap.

4. Discussion

The melon aroma was complex and strongly dependent on the NIL or cultivar studied, but also on physiological behavior (Figure 3), in agreement with previous results [6,20,38,40,43,62]. Many studies comparing climacteric and non-climacteric cultivars of different origins reached a similar conclusion concerning the predominance of aldehydes

and ketones in non-climacteric types and different levels of esters in climacteric ones [62–66], all in a ripening-dependent manner [18,36,40,67]. However, the present study details that the components of climacteric melon aroma, such as acetate esters and sulfur-derived compound classes (and several individual VOCs) colocalized with *ETHQB3.5* (Tables 3 and 4). The former results are supporting the link between this QTL and QTLs of individual VOC production.

In detail, climacteric NILs and PS showed different accumulation levels of certain individual VOCs, mainly acetate esters (e.g., 1-methylethyl acetate or 2-methylpropyl acetate) and sulfur-derived compounds (e.g., 1-methylsulfanylbutan-1-one or 3-methyl-1-methylsulfanyl-butan-1-one) (Table 2). Three of these acetate esters (1-methylethyl acetate, 2-methylpropyl acetate, and benzyl acetate), which are related to the climacteric behavior of NILs and their QTLs colocalized with *ETHQB3.5* (Table 4), and three acetate esters identified from our results (hexyl acetate, propyl acetate, and methyl acetate) (Table 2) have been previously reported in NILs with introgression in chromosomes 3 and/or 6 [38,40]. In general, as in [38,40], all these compounds, except 1-methylethyl acetate with its lower values, showed higher values in the NILs than in PS.

The importance of ethylene-dependent esters (particularly acetate esters) and sulfur-derived compounds (collectively or individually) has also been outlined in the flesh of intact fruits of the climacteric NIL SC3-5-1 containing both introgression in melon chromosomes 3 and 6 (and the corresponding QTLs *ETHQB3.5* and *ETHQV6.3*), which indicated that our results using melon flesh in these NILs are not an artifact [20,36,42]. In addition, thirteen of the compounds reported in intact fruit are described as important in chromosome 3 in the present investigation with VOCs obtained from pulp juice, but not all of them have QTLs that colocalized with *ETHQB3.5* (Tables 2, 4 and S2). Among them, the QTLs of 2-methylbutyl acetate, hexyl acetate, 2-phenylethyl acetate, or S-methyl ethanethioate did not colocalize with *ETHQB3.5*, while butyl acetate and 3-methyl-1-methylsulfanyl-butan-1-one colocalized with *ETHQB3.5* (Tables 2, 4 and S2). This result is an indication of potential ethylene dependence and independence of VOCs of interest in melons.

Several of the esters (acetate and non-acetate) identified (Tables 2 and S4) have been described as predominant in climacteric orange-flesh cantaloupes (*C. melo* var. reticulatus, Naudin, cv. Sol Real) but are also important in oriental melons. In cantaloupes, most of them were acetate ester-type: methylbutyl (e.g., 2-methylbutyl acetate, 3-methylbutyl acetate), ethyl (e.g., ethyl butanoate), hexyl (e.g., hexyl acetate), nonenyl and benzyl (e.g., benzyl acetate), and non-acetate ester-type: butanoates (e.g., ethyl butanoate), methylpropanotaes, and hexanoates. Alcohols (e.g., 2-methylbutan-1-ol) and aldehydes were described as important precursors in the synthesis of key esters of melon aroma [67–70]. In climacteric oriental Hami-type melon, acetate esters (e.g., ester 2-methylpropyl acetate) and non-acetate esters (e.g., methyl 2-methylbutanoate) have also been reported [71]. The former authors reported a profile with many other VOCs similar to those in the climacteric NILs under study (Tables 2 and S4), probably due to the origin of the introgression of the Korean accession PI161375 [37].

Essentially, *ETHQB3.5* in the PS genetic background (Figure 2) enhanced overall ester VOCs, including acetate and sulfur-derived esters and some non-acetate esters. Santo Domingo et al. [36] suggested that *ETHQB3.5* in PS background does not produce a strong effect in the main contributors to the melon aroma, at least compared with the other genetic backgrounds, such as 'Védrantais', and that the introduction of other climacteric QTLs is necessary for designing a strong aromatic melon line. However, the study of *ETHQB3.5* is enough to study VOC's ethylene dependence or independence. We compared our results with VOCs obtained via hybrids of/and ACO (antisense aminocyclopropane-1-carboxylic acid oxidase) in 'Védrantais' [72,73] or antisense suppression of alcohol acetyltransferase in Hami melons [74]. In general, the agreement with the enhancement of many ester VOCs and those of the antisense ACO could be due to the concomitant increase of many volatiles of the same pathway and the coordinated expression of the genes associated with this pathway (Table 4). Even so, some discrepancies are apparent when comparing some ester VOCs classified as ethylene-independent (Tables 2 and 4) and the apparent full ethylene-

dependence of esters apparently synthesized from alcohols by alcohol acetyl transferases (*Cm*AAT) [73]. The potential explanation for this apparent discrepancy (for example, for 2-methylbutyl acetate, a VOC with QTL classified as ethylene-independent, Tables 4 and S2) is the presence of alternative pathways for ester biosynthesis in melon (yet to be confirmed), similar to how it happens in apple [75].

On the other hand, the antisense Hami oriental melons that affected the last step of conversion of alcohols into esters [74], reduced the level of many esters (2-methylpropyl acetate, butyl acetate, 1-methylsulfanylbutan-1-one, 3-methylbutyl acetate, hexyl acetate, benzyl acetate, 2-phenylethyl acetate, and methyl acetate). They were characteristic compounds in the climacteric NILs with high levels in general, but not in all of them their QTLs were mapped within the *ETHQB3.5* region (Table 4).

One possible hypothesis for discrepancies with the former authors is the differences due to the genetic background [36], or that the alteration of climacteric ripening by *ETHQB3.5* had pleiotropic effects on the ethylene and VOC biosynthesis that could be controlled by genes widely distributed across the melon genome [36], as it has been revealed by the presence of potential *cis* e-QTLs [76].

In climacteric NILs, the higher content of individual non-acetate esters (e.g., propyl propanoate and methyl butanoate) absent from PS and absent in non-climacteric NILs suggests again a pleiotropic effect and only partial dependence on ethylene of this compound class, as has been outlined for other quality traits with the QTLs of chromosome 3 [32,52]. The non-acetate esters methyl propanoate and methyl butanoate, have previously been reported in climacteric NILs with higher values than in PS [38,40], and both were classified as ethylene-dependent here (Tables 4 and S2). The non-acetate esters methyl 2-methylbutanoate and ethyl butanoate have also been previously reported by [38,40] where they showed higher values in NILs (climacteric and non-climacteric) than in PS. In fact, this could be the reason for ethylene-independence or lack of classification, respectively, in our case (Tables 2, 4 and S2).

Although the climacteric trait in our NILs acts as a powerful enhancer in the production of many VOCs (Table 2), some of them also increased in non-climacteric NILs compared to parental PS. This suggests an additional explanation, which is that at least two QTLs could exist for this compound, the main one, ethylene-dependent, and the minor one, ethylene-independent. Unfortunately, we were unable to map two QTLs with this pattern, though this might be the case of a lack of QTL interpretation associated with the production of certain VOCs, particularly esters (Table 2). We hypothesize that this might be due to an additional QTL in other non-target introgressions that may also segregate in the genetic background.

The production of aldehydes, ketones, and alcohols was partly ethylene-independent because the levels of the individual volatile compounds belonging to these classes of compounds (Tables 1 and 2) were directly related to the separation according to climacteric or non-climacteric behavior of the NILs, in agreement with many authors [65,66,77]. One relevant case was 2-methylbutan-1-ol with relative levels higher in climacteric NILs, a reason why its QTL mapped within the *ETHQB3.5* region (Tables 2 and 4). In this sense, the introgression in non-climacteric NIL SC3-5-7 induced an increase in the aldehyde content compared with PS aroma, particularly in several individual compounds, as also observed in HCA figures (Tables 2, S4 and S5; Figures 7 and 8). Thus, this introgression, without carrying any QTL or gene that alters the climacteric behavior, had the potential to change the aroma of PS, as has been detected in NILs with introgression in chromosome 3 or other chromosomes [6,38,44]. Furthermore, the NIL SC3-5-7 showed reduced terpene content (Table 1), which might be affected by 1-deoxy-D-xylulose-5-phosphate synthase [15], a gene that maps in the region of recombination of this NIL located between the molecular markers CMPSNP374 and ECM60c (Tables 4 and S3).

The coexistence of the dependence and independence of VOC production on ethylene suggested that our results agreed with [78] and are partly due to the different pathways to produce branched-chain ester or straight-chain esters, also depending on their precursors.

According to [67], the metabolism of branched-chain amino acids, including Val, Leu, Ile, as well as the Phe as an aromatic amino acid, and Cys as a sulfur-containing amino acid, are under the regulation of ethylene. When Flores et al. [78] studied the formation of hexyl acetate from hexanal or butyl acetate from butanal, they concluded that the reduction of fatty acids and aldehydes was essentially an ethylene-dependent process, while the following process of ester-formation included ethylene-independent components too. In fact, we located a QTL ethylene-independent for hexanal, hexyl acetate, or butanal, but for butyl acetate, the QTL mapped was fully ethylene-dependent (Tables 4 and S2). Factors, other than their physiological behavior but associated with the genotype of each NIL (such as internal characteristics of the different NILs) and conditioned by the introgression, could be critical in the production of these VOCs.

The use of mapping in this experiment found clustering of QTLs that apparently controlled the levels of VOCs, belonging to similar compound classes linked to the genomic region that contain the climacteric QTL *ETHQB3.5* (Figures 4–8). Linkage of *ETHQB3.5* to other VOC QTLs in the original SC3-5 introgression could be the reason for the ethylene independence of some VOCs found in this work that have been previously reported as ethylene-dependent [36]. Additionally, the correlations of VOCs in HCA or CNA (Figures 4–8) are consistent with the existence of a few genomic regions controlling the levels of most of the investigated VOCs and with the clustering of QTLs for the same compound class, in agreement with results in peach [5]. Clustering of QTLs controlling VOCs with similar chemical structures has been found in apples [2], tomatoes [79], strawberries [16], and peaches [5], but this pattern could also be associated with pleiotropic effects of a single locus or a tight linkage between different loci. Though this genetic variation in climacteric pattern and VOC production could be important and has significant agricultural value by using DNA-based molecular markers in plant breeding programs, new findings on epigenetic variation controlling fruit development and ripening should be considered for future studies [80,81].

The potential precursors of the VOCs, depending on their chemical groups, are relevant for the discussion of the HCA (Figures 6 and 7; Tables 5 and S6). Some amino acids (Val, Phe, Ile, Leu, Thr, Ala and Met) are the main precursors involved in metabolic pathways of some of the aroma volatiles according to the literature (Tables S4 and S6). The amino acids Val, Ile, Met, and Ala have been postulated as the precursors of most of the esters found in our melon fruits (Tables 2, S4 and S6; [67]). The amino acids Val, Ile, and Met were the main precursors putatively responsible for the production of the volatiles that colocalized with *ETHQB3.5* (Table S4). More specifically, the data and references of Table S4 suggest that the metabolism of amino acids (mainly Met in sulfur-derived compounds, Ile in non-acetate esters and Ala, and Phe in acetate esters) is associated with volatile production. Treatment with 1-methylcyclopropene (1-MCP), a competitor of ethylene for binding to the ethylene receptor, affects the biosynthesis of flavor volatiles, such as acetate esters derived from the amino acids Ile and Phe, in cut climacteric Cantaloupe melons stored at 5 °C, but also reduced the amount of sulfur-derived compounds [82]. In general, our results (Table 1) are consistent with those former findings, but in our study, the effect of 1-MCP was not significant with some individual VOCs tightly linked to *ETHQB3.5* (e.g., for butyl acetate or 2-methylpropyl acetate), or even its effect was the opposite (e.g., for 2-methylbutyl acetate).

On the other hand, linolenic and linoleic fatty acids have also been described as the main substrates involved in the synthesis of acetate and non-acetate esters [63,83,84]. The amino acids (mainly Ala) and linolenic acid have been reported by the former authors (Table S6) to act as precursors of acetate esters (first subcluster in HCA). Three important compounds were located in this subcluster. The 2-methylbutyl acetate is an odorant with an intermediate intensity, very abundant in climacteric Cantaloupe-type, Charentais-type, and oriental Jiashi-type melons [68,71,77], and is predominant, together with butyl acetate and hexyl acetate, in Galia-type melons, both in the whole fruit and in the flesh [42,77,85]. According to the literature, the precursors of 2-methylbutyl acetate are the amino acids

L-Ala and L-Ile, whereas linolenic acid is the precursor of hexyl acetate (CAS 142-92-7) and butyl acetate (CAS 123-86-4) (Table S4).

Among the above CNA subclusters (Figure 8), sulfur-derived compounds are probably more important because of their potential involvement in the regulation of Yang's cycle [86], which uses L-Met as a precursor. Sulfur-derived compounds are important volatiles in melon aroma, L-Met degradation via methionine-γ-lyase, and the catabolic route through methionine aminotransferase being key features in the formation of such compounds and other melon volatiles [63,84,87]. One of these sulfur-derived compounds, methyl 2-methylsulfanylacetate, was present at very high levels in our climacteric NILs (Tables 2 and S4) and in other climacteric cultivars [64]. The important presence of sulfur-derived ester volatiles in climacteric NILs suggests the possible regulation of ethylene production in climacteric NILs through the conversion of excess L-Met into sulfur-derived volatiles by this degradation pathway. A similar hypothesis regarding the regulation of some esters by precursor availability has been suggested in *Actinidia chinensis* [88]. Some sulfur-derived compounds have been found in intact climacteric NILs containing the QTLs *ETHQB3.5* and *ETHQV6.3*, such as the SC3-5-1 [42], and are, therefore, not artifacts associated with the extraction and analysis procedures reported in other systems [89].

Among the candidate genes located in the *ETHQ3.5* QTL region, MELO3C011118, involved in the ethylene-activated signaling pathway [90] and stress response (Table S3), could also be directly involved in ethylene production associated with the climacteric pattern because, according to UNIPROT database (http://www.uniprot.org/uniprot/Q8RY59 (accessed on 1 January 2022)), the gene also interacts with dehydration-responsive DREB2 proteins and several transcription factors belonging to several protein families.

On the other hand, MELO3C011229 codifies an EG45-like domain-containing protein involved in alternative respiration (Table S3) and can be of interest because the cyanide-insensitive respiration contributes to the rise in respiration rates reported in several fruits in climacteric and ethylene-mediated ripening [91,92]. Another gene (MELO3C011217) codifies the Protein TIFY 8 involved in the jasmonic-acid-mediated signaling pathway in *Arabidopsis thaliana* (Table S3). Furthermore, MELO3C011093 is a MADS-box protein, and MELO3C011103 is a MADS-box interactor-like, and these genes play a major role in fruit development and ripening [93]. MELO3C011118 is associated with stress response, particularly the ethylene-activated signaling pathway (Table S3). Finally, there were other genes in the *ETHQB3.5* region (Table S3) that could be of interest. MELO3C011164 is a NAC domain-containing protein 92, and, interestingly, the gene underlying the climacteric QTL *ETHQV6.3* encodes the NAC transcription factor *Cm*NAC-NOR [32,94]. Therefore, this NAC transcription factor should be taken into consideration to be included in the NAC positive feedback loop that operates in climacteric melons [95,96].

5. Conclusions

ETHQB3.5 has been mapped in a 1.24 Mb genome region, setting the basis for its future molecular cloning. The accumulation of VOCs, mostly from the acetate esters, non-acetate esters, and sulfur-derived compound families, most likely has been associated with pleiotropic effects of the alteration of climacteric ripening by *ETHQB3.5* rather than structural genes located in this region of melon chromosome 3.

Some QTLs for the VOCs (twenty-three in total) colocalized with *ETHQB3.5* (e.g., 3-methylbutyl acetate, benzyl acetate, 2-methylbutan-1-ol, 2-methylpropyl acetate, and 1-methylsulfanylbutan-1-one), while others did not map on chromosome 3 (ethyl butanoate and methyl acetate) or mapped nearby (2-methylbutyl acetate, hexyl acetate, and 2-phenylethyl acetate). Therefore, the ethylene dependence of many VOCs must be considered in future breeding programs.

VOCs from the ketones and aldehyde compound families showed an accumulation independent of *ETHQB3.5*, indicating that genes involved in the content of these VOCs would be present in other regions of the same chromosome 3. Taken together, the results show that the modification of melon aroma may be achieved with or without interfering

with its physiological behavior. The production of high levels of some ethylene-dependent esters and sulfur-derived compounds identified here would require the active participation of the climacteric QTL *ETHQB3.5*.

Supplementary Materials: The following supporting information can be downloaded at: https://www.mdpi.com/article/10.3390/foods12020376/s1, Table S1. A list of molecular markers was used in this study and is located in MELOGEN v4.0; Table S2. The melon graphical genotype of the NILs was used in this study; Table S3. A list of genes, descriptions, and properties was obtained from the MELOGEN database v4.0 that were covered by molecular markers in the region of the QTL of the climacteric *ETHQB3.5*, and the introgressions were covered by this experiment; Table S4 [97–176]. Chemical and sensory attributes of the main melon fruit volatile compounds were used for QTL mapping in melon chromosome 3, identified in the five melon Near-Isogenic Lines (NILs) and the parental control 'Piel de Sapo' (PS).; Table S5. Main fruit volatile compounds were identified for QTL mapping on melon chromosome 3 identified in the headspace of the fruit of the non-climacteric Near-Isogenic Line SC3-5-7 and the parental line 'Piel de Sapo' (PS); Table S6. Chemical and sensory attributes of the most numerous grouping of the individual volatile compounds were obtained in the correlation network analysis applied to Near-Isogenic Lines (NILs) with introgression on melon chromosome 3 and the parental control 'Piel de Sapo' (PS); Figure S1. Respiration rate (RR) and ethylene production (EP) were obtained via Near-Isogenic Line SC3-5-13 (mean ± SE, $n = 3$) during postharvest ripening at 21 °C and relative humidity of 66 ± 6% for 10 days (season 2).

Author Contributions: N.D.-S., volatile data, integration, and analysis of the data; writing—review and editing; M.C.B., statistical analysis and derived graphs, data interpretation, and writing. A.D., E.M., and J.G.-M., development of the NILs and genetic, physical map, and funding acquisition; A.J.M., conceptualization, QTL mapping, review, editing, and funding-acquisition project management; J.P.F.-T., conceptualization, harvest, crop, laboratory management, funding acquisition, and project management and coordination; VOC analysis, analysis of the data; QTL mapping, writing, and editing. All authors have read and agreed to the published version of the manuscript.

Funding: This research was supported by the Ministry of Innovation and Science (at present, Ministry of Economy and Competitiveness) and Regional Development of European Union FEDER funds (AGL2010-20858, AGL2012-40130-C02-02, AGL2003-09175-C02-01, and AGL2003-09175-C02-02), Fundación Séneca de la Región de Murcia (projects 11784/PI/09, 05676/PI/07 and 00620/PI/04), and Consejería de Educación de la Región de Murcia (BIO-AGR06/02-0011). N. Dos-Santos was supported by an FPU-MEC AP2006-01565 fellowship (Ministry of Education, Spain). A. Díaz was supported by a JAE-Doc contract from CSIC.

Data Availability Statement: The data used to support the findings of this study can be made available by the corresponding author upon request.

Acknowledgments: We acknowledge the assistance of P. Varó and his team in CIFEA-Torre Pacheco (Consejería de Agricultura de la Región de Murcia) for crop management. Thanks are due to C. Miranda, M.J. Ferrer, J.A. Martínez, and J. Obando for fruit harvest, sampling, quality traits, and GC analysis, to J. Forment (Bioinformatics service of IBMCP) for *A. thaliana* and protein BLAST analysis, and M.A. Quesada and SAIT-UPCT for the GC-MS analysis.

Conflicts of Interest: The authors declare no conflict of interest.

References

1. Klee, H.J. Improving the flavor of fresh fruits: Genomics, biochemistry, and biotechnology. *New Phytol.* **2010**, *187*, 44–56. [CrossRef] [PubMed]
2. Dunemann, F.; Ulrich, D.; Boudichevskaia, A.; Grafe, C.; Weber, W.E. QTL mapping of aroma compounds analysed by headspace solid-phase microextraction gas chromatography in the apple progeny 'Discovery' × 'Prima'. *Mol. Breed.* **2009**, *23*, 501–521. [CrossRef]
3. Illa, E.; Eduardo, I.; Audergon, J.M.; Barale, F.; Dirlewanger, E.; Li, X.W.; Moing, A.; Lambert, P.; Le Dantec, L.; Gao, Z.S.; et al. Saturating the *Prunus* (stone fruits) genome with candidate genes for fruit quality. *Mol. Breed.* **2011**, *28*, 667–682. [CrossRef]
4. Sánchez, G.; Besada, C.; Badenes, M.L.; Monforte, A.J.; Granell, A. A non-targeted approach unravels the volatile network in peach fruit. *PLoS ONE* **2012**, *7*, e38992. [CrossRef]

5. Eduardo, I.; Chietera, G.; Pirona, R.; Pacheco, I.; Troggio, M.; Banchi, E.; Bassi, D.; Rossini, L.; Vecchietti, A.; Pozzi, C. Genetic dissection of aroma volatile compounds from the essential oil of peach fruit: QTL analysis and identification of candidate genes using dense SNP maps. *Tree Genet. Genomes* **2013**, *9*, 189–204. [CrossRef]
6. Obando-Ulloa, J.M.; Ruiz, J.; Monforte, A.J.; Fernández-Trujillo, J.P. Aroma profile of a collection of near-isogenic lines of melon. *Food Chem.* **2010**, *118*, 815–822. [CrossRef]
7. Galpaz, N.; Gonda, I.; Shem-Tov, D.; Barad, O.; Tzuri, G.; Lev, S.; Fei, Z.; Xu, Y.; Mao, L.; Jiao, C.; et al. Deciphering genetic factors that determine melon fruit-quality traits using RNA-Seqbased high-resolution QTL and eQTL mapping. *Plant J.* **2018**, *94*, 169–191. [CrossRef]
8. Mayobre, C.; Pereira, L.; Eltahiri, A.; Bar, E.; Lewinsohn, E.; Garcia-Mas, J. Genetic dissection of aroma biosynthesis in melon and its relationship with climacteric ripening. *Food Chem.* **2021**, *353*, 129484. [CrossRef]
9. Saliba-Colombani, V.; Causse, M.; Langlois, D.; Philouze, J.; Buret, M. Genetic analysis of organoleptic quality in fresh market tomato. 1. Mapping QTLs for physical and chemical traits. *Theor. Appl. Genet.* **2001**, *102*, 259–272. [CrossRef]
10. Tadmor, Y.; Fridman, E.; Gur, A.; Larkov, O.; Lastochkin, E.; Ravid, U.; Zamir, D.; Lewinsohn, E. Identification of malodorous, a wild species allele affecting tomato aroma that was selected against during domestication. *J. Agric. Food Chem.* **2002**, *50*, 2005–2009. [CrossRef]
11. Tieman, D.M.; Zeigler, M.; Schmelz, E.A.; Taylor, M.G.; Bliss, P.; Kirst, M.; Klee, H.J. Identification of loci affecting flavour volatile emissions in tomato fruits. *J. Exp. Bot.* **2006**, *57*, 887–896. [CrossRef]
12. Mathieu, S.; Cin, V.D.; Fei, Z.J.; Li, H.; Bliss, P.; Taylor, M.G.; Klee, H.J.; Tieman, D.M. Flavour compounds in tomato fruits: Identification of loci and potential pathways affecting volatile composition. *J. Exp. Bot.* **2009**, *60*, 325–337. [CrossRef] [PubMed]
13. Garbowicz, K.; Liu, Z.; Alseekh, S.; Tieman, D.; Taylor, M.; Kuhalskaya, A.; Ofner, I.; Zamir, D.; Klee, H.J.; Fernie, A.R.; et al. Quantitative trait loci analysis identifies a prominent gene involved in the production of fatty acid-derived flavor volatiles in tomato. *Mol. Plant.* **2018**, *11*, 1147–1165. [CrossRef] [PubMed]
14. Doligez, A.; Audiot, E.; Baumes, R. This, PQTLs for muscat flavor and monoterpenic odorant content in grapevine (*Vitis vinifera* L.). *Mol. Breed.* **2006**, *18*, 109–125. [CrossRef]
15. Battilana, J.; Costantini, L.; Emanuelli, F.; Sevini, F.; Segala, C.; Moser, S.; Velasco, R.; Versini, G.; Grando, M.S. The 1-deoxy-d-xylulose 5-phosphate synthase gene co-localizes with a major QTL affecting monoterpene content in grapevine. *Theor. Appl. Genet.* **2009**, *118*, 653–669. [CrossRef] [PubMed]
16. Zorrilla-Fontanesi, Y.; Rambla, J.L.; Cabeza, A.; Medina, J.J.; Sánchez-Sevilla, J.F.; Valpuesta, V.; Botella, M.A.; Granell, A.; Amaya, I. Genetic analysis of strawberry fruit aroma and identification of o-methyltransferase faOMT as the locus controlling natural variation in mesifurane content. *Plant Physiol.* **2012**, *159*, 851–870. [CrossRef] [PubMed]
17. Paterson, A.; Kassim, A.; McCallum, S.; Woodhead, M.; Smith, K.; Zait, D.; Graham, J. Environmental and seasonal influences on red raspberry flavour volatiles and identification of quantitative trait loci (QTL) and candidate genes. *Theor. Appl. Genet.* **2013**, *126*, 33–48. [CrossRef]
18. Vallone, S.; Sivertsen, H.; Anthon, G.E.; Barrett, D.M.; Mitcham, E.J.; Ebeler, S.E.; Zakharov, F. An integrated approach for flavour quality evaluation in muskmelon (*Cucumis melo* L. reticulatus group) during ripening. *Food Chem.* **2013**, *139*, 171–183. [CrossRef]
19. Verzera, A.; Dima, G.; Tripodi, G.; Ziino, M.; Lanza, C.M.; Mazzaglia, A. Fast quantitative determination of aroma volatile constituents in melon fruits by headspace-solid-phase microextraction and gas chromatography-mass spectrometry. *Food Anal. Meth.* **2011**, *4*, 141–149. [CrossRef]
20. Chaparro-Torres, L.A.; Bueso, M.C.; Fernández-Trujillo, J.P. Aroma volatiles at harvest obtained by HSSPME/GC-MS and INDEX/MS-E-nose fingerprint discriminate climacteric behavior in melon fruit. *J. Sci. Food Agric.* **2016**, *96*, 2352–2365. [CrossRef]
21. Sánchez, G.; Venegas-Calerón, M.; Salas, J.J.; Monforte, A.; Badenes, M.L.; Granell, A. An integrative "omics" approach identifies new candidate genes to impact aroma volatiles in peach fruit. *BMC Genom.* **2013**, *14*, 343. [CrossRef] [PubMed]
22. Aggelis, A.; John, I.; Grierson, D. Analysis of physiological and molecular changes in melon (*Cucumis melo* L.) varieties with different rates of ripening. *J. Exp. Bot.* **1997**, *48*, 769–778. [CrossRef]
23. Nuñez-Palenius, H.G.; Gomez-Lim, M.; Ochoa-Alejo, N.; Grumet, R.; Lester, G.; Cantliffe, D.J. Melon fruits: Genetic, diversity, physiology, and biotechnology features. *Crit. Biotechnol.* **2008**, *28*, 13–55. [CrossRef]
24. Blanca, J.; Esteras, C.; Ziarsolo, P.; Pérez, D.; Fernández-Pedrosa, V.; Collado, C.; de Pablos, R.R.; Ballester, A.; Roig, C.; Cañizares, J.; et al. Transcriptome sequencing for SNP discovery across *Cucumis melo*. *BMC Genom.* **2012**, *13*, 280. [CrossRef] [PubMed]
25. Diaz, A.; Fergany, M.; Formisano, G.; Ziarsolo, P.; Blanca, J.; Fei, Z.; Staub, J.E.; Zalapa, J.E.; Cuevas, H.E.; Dace, G.; et al. A consensus linkage map for molecular markers and quantitative trait loci associated with economically important traits in melon (*Cucumis melo* L.). *BMC Plant Biol.* **2011**, *11*, 111. [CrossRef] [PubMed]
26. Esteras, C.; Rambla, J.L.; Sánchez, G.; López-Gresa, M.P.; González-Mas, M.C.; Fernández-Trujillo, J.P.; Bellés, J.M.; Granell, A.; Picó, M.B. Fruit flesh volatile and carotenoid profile analysis within the *Cucumis melo* L. species reveals unexploited variability for future genetic breeding. *J. Sci. Food Agric.* **2018**, *98*, 3915–3925. [CrossRef]
27. Roy, A.; Bal, S.S.; Fergany, M.; Kaur, S.; Singh, H.; Malik, A.A.; Singh, J.; Monforte, A.J.; Dhillon, N.P.S. Wild melon diversity in India (Punjab State). *Gen. Resour. Crop. Evol.* **2012**, *59*, 755–767. [CrossRef]
28. Raghami, M.; López-Sesé, A.I.; Hasandokht, M.R.; Zamani, Z.; Moghadam, M.R.F.; Kashi, A. Genetic diversity among melon accessions from Iran and their relationships with melon germplasm of diverse origins using microsatellite markers. *Plant Syst. Evol.* **2014**, *300*, 139–151. [CrossRef]

29. Ezura, H.; Owino, W.O. Melon, an alternative model plant for elucidating fruit ripening. *Plant Sci.* **2008**, *175*, 121–129. [CrossRef]
30. Périn, C.; Gomez-Jimenez, M.C.; Hagen, L.; Dogimont, C.; Pech, J.C.; Latché, A.; Pitrat, M.; Lelièvre, J.M. Molecular and genetic characterization of a nonclimacteric phenotype in melon reveals two loci conferring altered ethylene response in fruit. *Plant Physiol.* **2002**, *129*, 300–309. [CrossRef]
31. Moreno, E.; Obando, J.; Dos-Santos, N.; Fernández-Trujillo, J.P.; Monforte, A.J.; García-Mas, J. Candidate genes and QTLs for fruit ripening and softening in melon. *Theor. Appl. Genet.* **2008**, *116*, 589–602. [CrossRef]
32. Vegas, J.; Garcia-Mas, J.; Monforte, A.J. Interaction between QTLs induces an advance in ethylene biosynthesis during melon fruit ripening. *Theor. Appl. Genet.* **2013**, *126*, 1531–1544. [CrossRef] [PubMed]
33. Pereira, L.; Santo Domingo, M.; Ruggieri, V.; Argyris, J.; Phillips, M.A.; Zhao, G.; Lian, Q.; Xu, Y.; He, Y.; Huang, S.; et al. Genetic dissection of climacteric fruit ripening in a melon population segregating for ripening behavior. *Hortic. Res.* **2020**, *7*, 187. [CrossRef] [PubMed]
34. Pereira, L.; Santo Domingo, M.; Argyris, J.; Mayobre, C.; Valverde, L.; Martín-Hernández, M.; Pujol, M.; Garcia-Mas, J. A novel introgression line collection to unravel the genetics of climacteric ripening and fruit quality in melon. *Sci. Rep.* **2021**, *11*, 11364. [CrossRef] [PubMed]
35. Oren, E.; Tzuri, G.; Dafna, A.; Rees, E.R.; Song, B.X.; Freilich, S.; Elkind, Y.; Isaacson, T.; Schaffer, A.A.; Tadmor, Y.; et al. QTL mapping and genomic analyses of earliness and fruit ripening traits in a melon recombinant inbred lines population supported by de novo assembly of their parental genomes. *Hortic. Res.* **2022**, *9*, uhabo81. [CrossRef]
36. Santo Domingo, M.; Areco, L.; Mayobre, C.; Valverde, L.; Martín-Hernández, A.M.; Pujol, M.; Garcia-Mas, J. Modulating climacteric intensity in melon through QTL stacking. *Hortic. Res.* **2022**, *9*, uhac131. [CrossRef]
37. Eduardo, I.; Arús, P.; Monforte, A.J. Development of a genomic library of near isogenic lines (NILs) in melon (*Cucumis melo* L.) from the exotic accession PI 161375. *Theor. Appl. Genet.* **2005**, *112*, 139–148. [CrossRef]
38. Obando-Ulloa, J.M.; Moreno, E.; García-Mas, J.; Nicolai, B.; Lammertyn, J.; Monforte, A.J.; Fernández-Trujillo, J.P. Climacteric or non-climacteric behavior in melon fruit. 1. Aroma volatiles. *Postharvest Biol. Technol.* **2008**, *49*, 27–37. [CrossRef]
39. Fernández-Trujillo, J.P.; Obando-Ulloa, J.M.; Martínez, J.A.; Moreno, E.; García-Mas, J.; Monforte, A.J. Climacteric and non-climacteric behavior in melon fruit 2. Linking climacteric pattern and main postharvest disorders and decay in a set of near-isogenic lines. *Postharvest Biol. Technol.* **2008**, *50*, 125–134. [CrossRef]
40. Obando-Ulloa, J.M.; Nicolai, B.; Lammertyn, J.; Bueso, M.C.; Monforte, A.J.; Fernández-Trujillo, J.P. Aroma volatiles associated with the senescence of climacteric or non-climacteric melon fruit. *Postharvest Biol. Technol.* **2009**, *52*, 146–156. [CrossRef]
41. Fernández-Trujillo, J.P.; Fernández-Talavera, M.; Ruiz-León, M.T.; Roca, M.J.; Dos-Santos, N. Aroma volatiles during whole melon ripening in a climacteric near-isogenic line and its inbred non-climacteric parents. *Acta Hort.* **2012**, *934*, 951–958. [CrossRef]
42. Fernández-Trujillo, J.P.; Dos-Santos, N.; Martínez-Alcaraz, R.; Le Bléis, I. Non-destructive assessment of aroma volatiles from a climacteric near-isogenic line of melon obtained by headspace sorptive bar extraction. *Foods* **2013**, *2*, 401–414. [CrossRef]
43. Matsui, K.; Ishii, M.; Sasaki, M.; Rabinowitch, H.D.; Ben-Oliel, G. Identification of an allele attributable to formation of cucumber-like flavor in wild tomato species (*Solanum pennellii*) that was inactivated during domestication. *J. Agric. Food Chem.* **2007**, *55*, 4080–4086. [CrossRef] [PubMed]
44. Dos-Santos, N.; Bueso, M.C.; Fernández-Trujillo, J.P. Aroma volatiles biomarkers of textural differences at harvest in non-climacteric near-isogenic lines of melon. *Food Res. Int.* **2013**, *54*, 1801–1812. [CrossRef]
45. Fernández-Silva, I.; Eduardo, I.; Blanca, J.; Esteras, C.; Picó, B.; Nuez, F.; Arús, P.; Garcia-Mas, J.; Monforte, A.J. Bin mapping of genomic and EST-derived SSRs in melon (*Cucumis melo* L.). *Theor. Appl. Genet.* **2008**, *118*, 139–150. [CrossRef] [PubMed]
46. Gonzalo, M.J.; Oliver, M.; Garcia-Mas, J.; Monfort, A.; Dolçet-Sanjuan, R.; Katzir, N.; Arús, P.; Monforte, A.J. Simple sequence repeat markers used in merging linkage maps of melon (*Cucumis melo* L.). *Theor. Appl. Genet.* **2005**, *110*, 802–811. [CrossRef]
47. Deleu, W.; Esteras, C.; Roig, C.; Gonzalez-To, M.; Fernandez-Silva, I.; Gonzalez-Ibeas, D.; Blanca, J.; Aranda, M.A.; Arus, P.; Nuez, F.; et al. A set of EST-SNPs for map saturation and cultivar identification in melon. *BMC Plant Biol.* **2009**, *9*, 90. [CrossRef]
48. Garcia-Mas, J.; Benjak, A.; Sanseverino, W.; Bourgeois, M.; Mir, G.; González, V.M.; Henaff, E.; Cámara, F.; Cozzuto, L.; Lowy, E.; et al. The genome of melon (*Cucumis melo* L.). *Proc. Natl. Acad. Sci. USA* **2012**, *109*, 11872–11877. [CrossRef]
49. Esteras, C.; Formisano, G.; Roig, C.; Diaz, A.; Blanca, J.; Garcia-Mas, J.; Gómez-Guillamón, M.L.; López-Sesé, A.I.; Lázaro, A.; Monforte, A.J.; et al. SNP genotyping in melons: Genetic variation, population structure, and linkage disequilibrium. *Theor. Appl. Genet.* **2013**, *126*, 1285–1303. [CrossRef]
50. Fukino, N.; Sakata, Y.; Kunihisa, M.; Matsumoto, S. Characterisation of novel simple sequence repeat (SSR) markers for melon (*Cucumis melo* L.) and their use for genotype identification. *J. Hort. Sci. Biotechnol.* **2007**, *82*, 330–334. [CrossRef]
51. Tijskens, L.M.M.; Dos-Santos, N.; Jowkar, M.M.; Obando, J.; Moreno, E.; Schouten, R.E.; Monforte, A.J.; Fernández-Trujillo, J.P. Postharvest fruit firmness behavior of near-isogenic lines of melon. *Postharvest Biol. Technol.* **2009**, *51*, 320–326. [CrossRef]
52. Obando-Ulloa, J.M.; Jowkar, M.M.; Moreno, E.; Souri, M.K.; Martínez, J.A.; Bueso, M.C.; Monforte, A.J.; Fernández-Trujillo, J.P. Discrimination of climacteric and non-climacteric fruit at harvest and at senescence stage by quality traits. *J. Sci. Food Agric.* **2009**, *89*, 1743–1753. [CrossRef]
53. Fernández-Trujillo, J.P.; Obando, J.; Martínez, J.Á.; Alarcón, A.; Eduardo, I.; Arús, P.; Monforte, A.J. Quality management of experiments with a collection of near-isogenic lines of melon. In *Proceedings of the III IBEROLAB—Third Virtual Iberoamerican Congress on Laboratory Quality Management, Virtual, 30 June 2005*; Atienza, J., Rabasseda, J., Eds.; Ministry of Environment and Rural and Marine Environment: Madrid, Spain, 2005; pp. 149–158.

54. Kader, A.A. Methods of gas mixing, sampling and analysis. In *Postharvest Technology of Horticultural Crops*, 3rd ed.; Kader, A.A., Ed.; University of California: Oakland, CA, USA, 2000; pp. 145–148.
55. Castanera, R.; Ruggieri, V.; Pujol, M.; Garcia-Mas, J.; Casacuberta, J. An Improved melon reference genome with single-molecule sequencing uncovers a recent burst of transposable elements with potential impact on genes. *Front. Plant Sci.* **2020**, *10*, 1815. [CrossRef]
56. Benjamini, Y.; Hochberg, Y. Controlling the false discovery rate: A practical and powerful approach to multiple testing. *J. Roy. Stat. Soc. B* **1995**, *57*, 289–300. [CrossRef]
57. Paterson, A.H.; DeVerna, J.; Lanini, B.; Tanksley, S. Fine mapping of Quantitative loci using selected overlapping recombinant chromosomes, in an interspecies cross of tomato. *Genetics* **1990**, *24*, 735–742. [CrossRef] [PubMed]
58. Langfelder, P.; Horvath, S. Fast R functions for robust correlations and hierarchical clustering. *J. Stat. Soft.* **2012**, *46*, i11. Available online: http://www.jstatsoft.org/v46/i11 (accessed on 20 November 2022). [CrossRef]
59. Csardi, G.; Nepusz, T. The igraph software package for complex network research. *InterJ. Complex Syst.* **2006**, *1695*, 1–9. Available online: http://igraph.org (accessed on 20 November 2022).
60. Warnes, G.R.; Bolker, B.; Bonebakker, L.; Gentleman, R.; Huber, W.; Liaw, A.; Lumley, T.; Maechler, M.; Magnusson, A.; Moeller, S.; et al. gplots: Various R Programming Tools for Plotting Data. R Package Version 3.1.3. 2022. Available online: https://CRAN.R-project.org/package=gplots (accessed on 20 November 2022).
61. Périn, C.; Hagen, L.S.; De Conto, V.; Katzir, N.; Danin-Poleg, Y.; Portnoy, V.; Baudracco-Arnas, S.; Chadoeuf, J.; Dogimont, C.; Pitrat, M. A reference map of *Cucumis melo* based on two recombinant inbred line populations. *Theor. Appl. Genet.* **2002**, *104*, 1017–1034. [CrossRef]
62. Allwood, J.W.; Cheung, W.; Xu, Y.; Mumm, R.; De Vos, R.; Deborde, C.; Biais, B.; Maucourt, M.; Berger, Y.; Schaffer, A.A.; et al. Metabolomics in melon: A new opportunity for aroma analysis. *Phytochemistry* **2014**, *99*, 61–72. [CrossRef]
63. Gonda, I.; Bar, E.; Portnoy, V.; Lev, S.; Burger, J.; Schaffer, A.A.; Tadmor, Y.; Gepstein, S.; Giovannoni, J.J.; Katzir, N.; et al. Branched-chain and aromatic amino acid catabolism into aroma volatiles in *Cucumis melo* L. fruit. *J. Exp. Bot.* **2010**, *61*, 1111–1123. [CrossRef]
64. Gonda, I.; Lev, S.; Bar, E.; Sikron, N.; Portnoy, V.; Davidovich-Rikanati, R.; Burger, J.; Schaffer, A.A.; Tadmor, Y.; Giovannonni, J.J.; et al. Catabolism of l-methionine in the formation of sulfur and other volatiles in melon (*Cucumis melo* L.) fruit. *Plant J.* **2013**, *74*, 458–472. [CrossRef] [PubMed]
65. Guler, Z.; Karaca, F.; Yetisir, H. Volatile compounds and sensory properties in various melons, which were chosen from different species and different locations, grown in Turkey. *Int. J. Food Prop.* **2013**, *16*, 168–179. [CrossRef]
66. Freilich, S.; Lev, S.; Gonda, I.; Reuveni, E.; Portnoy, V.; Oren, E.; Lohse, M.; Galpaz, N.; Bar, E.; Tzuri, G.; et al. Systems approach for exploring the intricate associations between sweetness, color and aroma in melon fruits. *BMC Plant Biol.* **2015**, *15*, 71. [CrossRef] [PubMed]
67. Li, Y.; Qi, H.; Jin, Y.; Tian, X.; Sui, L.; Qiu, Y. Role of ethylene in biosynthetic pathway of related-aroma volatiles derived from amino acids in oriental sweet melons (*Cucumis melo* var. makuwa Makino). *Scientia Hort.* **2016**, *201*, 24–35. [CrossRef]
68. Beaulieu, J.C. Volatile changes in cantaloupe during growth, maturation, and in stored fresh-cuts prepared from fruit harvested at various maturities. *J. Amer. Soc. Hort. Sci.* **2006**, *131*, 127–139. [CrossRef]
69. Beaulieu, J.C.; Lancaster, V.A. Correlating volatile compounds, sensory attributes, and quality parameters in stored fresh-cut cantaloupe. *J. Agric. Food Chem.* **2007**, *55*, 9503–9513. [CrossRef]
70. Song, J.; Forney, C.F. Flavour volatile production and regulation in fruit. *Can. J. Plant Sci.* **2008**, *88*, 537–550. [CrossRef]
71. Pang, X.; Guo, X.; Qin, Z.; Yao, Y.; Hu, X.; Wu, J. Identification of aroma-active compounds in Jiashi muskmelon juice by GC-O-MS and OAV calculation. *J. Agric. Food Chem.* **2012**, *60*, 4179–4185. [CrossRef]
72. Bauchot, A.D.; Mottram, D.S.; Dodson, A.T.; John, P. Effect of aminocyclopropane-1-carboxylic acid oxidase antisense gene on the formation of volatile esters in cantaloupe *Charentais* melon (Cv. *Vedrantais*). *J. Agric. Food Chem.* **1998**, *46*, 4787–4792. [CrossRef]
73. El-Sharkawy, I.; Manríquez, D.; Flores, B.; Regad, F.; Bouzayen, M.; Latché, A.; Pech, J.C. Functional characterization of a melon alcohol acyl-transferase gene family involved in the biosynthesis of ester volatiles. Identification of the crucial role of a threonine r esidue for enzyme activity. *Plant Mol. Biol.* **2005**, *59*, 345–362. [CrossRef]
74. Shan, W.Y.; Zhao, C.; Fan, J.G.; Cong, H.Z.; Liang, S.C.; Yu, X.Y. Antisense suppression of alcohol acetyltransferase gene in ripening melon fruit alters volatile composition. *Sci. Hort.* **2012**, *139*, 96–101. [CrossRef]
75. Sugimoto, N.; Engelgau, P.; Jones, A.D.; Song, J.; Beaudry, R. Citramalate synthase yields a biosynthetic pathway for isoleucine and straight- and branched-chain ester formation in ripening apple fruit. *Proc. Natl. Acad. Sci. USA* **2021**, *118*, e2009988118. [CrossRef] [PubMed]
76. Cubillos, F.A.; Coustham, V.; Loudet, O. Lessons from eQTL mapping studies: Non-coding regions and their role behind natural phenotypic variation in plants. *Curr. Opin. Plant Biol.* **2012**, *15*, 192–198. [CrossRef] [PubMed]
77. Kourkoutas, D.; Elmore, J.S.; Mottram, D.S. Comparison of the volatile compositions and flavour properties of cantaloupe, Galia and honeydew muskmelons. *Food Chem.* **2006**, *97*, 95–102. [CrossRef]
78. Flores, F.; El-Yahyaoui, F.; de Billerbeck, G.; Romojaro, F.; Latché, A.; Bouzayen, M.; Pech, J.C.; Ambid, C. Role of ethylene in the biosynthetic pathway of aliphatic ester aroma volatiles in *Charentais* Cantaloupe melons. *J. Exp. Bot.* **2002**, *53*, 201–206. [CrossRef]

79. Zanor, M.I.; Rambla, J.L.; Chaib, J.; Steppa, A.; Medina, A.; Granell, A.; Fernie, A.R.; Causse, M. Metabolic characterization of loci affecting sensory attributes in tomato allows an assessment of the influence of the levels of primary metabolites and volatile organic contents. *J. Exp. Bot.* **2009**, *60*, 2139–2154. [CrossRef]
80. Giordano, A.; Santo Domingo, M.; Quadrana, L.; Pujol, M.; Martín-Hernández, M.; Garcia-Mas, J. CRISPR/Cas9 gene editing uncovers the roles of constitutive triple response 1 and repressor of silencing 1 in melon fruit ripening and epigenetic regulation. *J. Exp. Bot.* **2022**, *73*, 4022–4033. [CrossRef]
81. Zhong, S.; Fei, Z.; Chen, Y.R.; Zheng, Y.; Huang, M.; Vrebalov, J.; McQuinn, R.; Gapper, N.; Liu, B.; Xiang, J.; et al. Single-base resolution methylomes of tomato fruit development reveal epigenome modifications associated with ripening. *Nat. Biotechnol.* **2013**, *31*, 154–159. [CrossRef]
82. Amaro, A.L.; Fundo, J.F.; Oliveira, A.; Beaulieu, J.C.; Fernández-Trujillo, J.P.; Almeida, D.P.F. 1-Methylcyclopropene effects on temporal changes of aroma volatiles and phytochemicals of fresh-cut cantaloupe. *J. Sci. Food Agric.* **2013**, *93*, 828–837. [CrossRef]
83. Rowan, D.D.; Hunt, M.B.; Alspach, P.A.; Whitworth, C.J.; Oraguzie, N.C. Heritability and genetic and phenotypic correlations of apple (*Malus x domestica*) fruit volatiles in a genetically diverse breeding population. *J. Agric. Food Chem.* **2009**, *57*, 7944–7952. [CrossRef]
84. Dávila-Aviña, J.E.D.; González-Aguilar, G.A.; Ayala-Zavala, J.F.; Sepulveda, D.R.; Olivas, G.I. Volatile compounds responsible of tomato flavor. *Rev. Fitotec. Mex.* **2011**, *34*, 133–143.
85. García-Gutiérrez, M.; Dos-Santos, N.; Chaparro-Torres, L.; Fernández-Trujillo, J.P. Optimización de un método no destructivo para determinar la evolución del aroma en postcosecha del fruto de melón entero. In Proceedings of the VI IBEROLAB—VI Iberoamerican Virtual Congress on Laboratory Quality Management, Virtual, 4 July 2011; Alsina, I., Martín de la Hinojosa, M.I., Hooghuis, H., Eds.; Ministry of Environment and Rural and Marine Environment: Madrid, Spain, 2011; pp. 103–111.
86. Van de Poel, B.; Bulens, I.; Markoula, A.; Hertog, M.L.A.T.; Dreesen, R.; Wirtz, M.; Vandoninck, S.; Oppermann, Y.; Keulemans, J.; Hell, R.; et al. Targeted systems biology profiling of tomato fruit reveals coordination of the Yang cycle and a distinct regulation of ethylene biosynthesis during postclimacteric ripening. *Plant Physiol.* **2012**, *160*, 1498–1514. [CrossRef] [PubMed]
87. Varlet, X.; Fernández, X. Sulfur-containing volatile compounds in seafood: Occurrence, odorant properties and mechanisms of formation. *Food Sci. Technol. Int.* **2010**, *16*, 463–503. [CrossRef] [PubMed]
88. Günther, C.S.; Heinemann, K.; Laing, W.A.; Nicolau, L.; Marsh, K.B. Ethylene-regulated (methylsulfanyl) alkanoate ester biosynthesis is likely to be modulated by precursor availability in *Actinidia chinensis* genotypes. *J. Plant Physiol.* **2011**, *168*, 629–638. [CrossRef]
89. Mandin, O.; Duckham, S.C.; Ames, J.M. Volatile compounds from potato-like model systems. *J. Agric. Food Chem.* **1999**, *47*, 2355–2359. [CrossRef]
90. Merchante, C.; Alonso, J.M.; Stepanova, N.A. Ethylene signaling: Simple ligand, complex regulation. *Curr. Opin. Plant Biol.* **2013**, *16*, 554–560. [CrossRef]
91. Paul, V.; Pandey, R.; Srivstava, G.C. The fading distinctions between classical patterns of ripening in climacteric and non-climacteric fruit and the ubiquity of ethylene—An overview. *J. Food Sci. Technol.* **2012**, *9*, 1–21. [CrossRef]
92. Xu, F.; Yuan, S.; Zhang, D.W.; Lv, X.; Lin, H.H. The role of alternative oxidase in tomato fruit ripening and its regulatory interaction with ethylene. *J. Exp. Bot.* **2012**, *63*, 5705–5716. [CrossRef]
93. Dong, T.; Chen, G.; Tian, S.; Xie, Q.; Yin, W.; Zhang, Y.; Hu, Z. A non-climacteric fruit gene CaMADS-RIN regulates fruit ripening and ethylene biosynthesis in climacteric fruit. *PLoS ONE* **2014**, *9*, e95559. [CrossRef]
94. Ríos, P.; Argyris, J.; Vegas, J.; Leida, C.; Kenigswald, M.; Tzuri, G.; Troadec, C.; Bendahmane, A.; Katzir, N.; Picó, B.; et al. *ETHQV6.3* is involved in melon climacteric fruit ripening and is encoded by a NAC domain transcription factor. *Plant J.* **2017**, *91*, 671–683. [CrossRef]
95. Lü, P.; Yu, S.; Zhu, N.; Chen, Y.R.; Zhou, B.; Pan, Y.; Tzeng, D.; Fabi, J.P.; Argyris, J.; Garcia-Mas, J.; et al. Genome encode analyses reveal the basis of convergent evolution of fleshy fruit ripening. *Nat. Plants* **2018**, *4*, 784–791. [CrossRef]
96. Bin, B.; Santo Domingo, M.; Mayobre, C.; Martín-Hernández, A.M.; Pujol, M.; Garcia-Mas, J. Knock-out of *CmNAC-NOR* affects melon climacteric fruit ripening. *Front. Plant Sci.* **2022**, *13*, 878037. [CrossRef]
97. U.S. Secretary of Commerce United States of America. Data Searches by CAS Registry. 2011. Available online: http://webbook.nist.gov/chemistry/cas-ser (accessed on 1 January 2022).
98. Wyllie, S.G.; Leach, D.N.; Wang, Y.M.; Shewfelt, R.L. Key aroma compounds in melons—Their development and cultivar dependence. *Fruit Flavors* **1995**, *596*, 248–257. [CrossRef]
99. Lessner, D.J.; Lhu, L.; Wahal, C.S.; Ferry, J.G. An engineered methanogenic pathway derived from the domains Bacteria and Archea. *Mbio* **2010**, *1*, 1–5. [CrossRef] [PubMed]
100. El-Sayed, A.M. The Pherobase: Database of Pheromones and Semiochemicals. Available online: http://www.pherobase.com (accessed on 25 July 2013).
101. The Good Scents Company Information System. Available online: http://www.thegoodscentscompany.com (accessed on 23 October 2022).
102. Nattaporn, W.; Pranee, A. Effect of pectinase on volatile and functional bioactive compounds in the flesh and placenta of 'Sunlady' cantaloupe. *Int. Food Res. J.* **2011**, *18*, 819–827. Available online: http://www.ifrj.upm.edu.my/18%20(02)%202011/(49)%20IFRJ-2010-004.pdf (accessed on 20 November 2022).
103. Biocycle.org. Available online: http://biocyc-org/META/NEW-IMAGE?type=NIL&object=PWY-5410 (accessed on 16 December 2013).

104. Singh, T.K.; Drake, M.A.; Cadwallade, K.R. Flavor of Cheddar cheese: A chemical and sensory perspective. *Compr. Rev. Food Sci. Food Saf.* **2003**, *2*, 139–162. [CrossRef]
105. Wyllie, S.G.; Leach, D.N. Aroma volatiles of *Cucumis melo* cv. *Golden Crispy. J. Agric. Food Chem.* **1990**, *38*, 2042–2044. [CrossRef]
106. Wikipedia. Propyl acetate. 2013. Available online: http://en.wikipedia.org/wiki/Propyl_acetate (accessed on 16 December 2013).
107. Goldenberg, L.; Feygenberg, O.; Samach, A.; Pesis, E. Ripening attributes of new passion fruit line featuring seasonal non-climacteric behavior. *J. Agric. Food Chem.* **2012**, *60*, 1810–1821. [CrossRef]
108. Cann, A.F.; Liao, J.C. Pentanol isomer synthesis in engineered microorganisms. *Appl. Microbiol. Biotechnol.* **2010**, *85*, 893–899. [CrossRef]
109. Neilson, H. The hydrolisis and synthesis of etylbutyrate by platinum black. *Science* **1902**, *XV*, 715–716. Available online: http://www.jstor.org/stable/1628613 (accessed on 25 July 2013).
110. Fantastic Flavours. Available online: http://www.flavours.asia/aromas.html (accessed on 25 July 2013).
111. Acree, T.; Arn, H. Flavornet and Human Odor Space. 2004. Available online: https://www.scirp.org/(S(czeh2tfqyw2orz553k1w0r45))/reference/referencespapers.aspx?referenceid=1708978 (accessed on 25 July 2013).
112. Rossouw, D.; Naes, T.; Bauer, F.F. Linking gene regulation and the exo-metabolome: A comparative transcriptomics approach to identify genes that impact on the production of volatile aroma compounds in yeast. *Bmc Genom.* **2008**, *9*, 530. [CrossRef]
113. Hayata, Y.; Sakamoto, T.; Maneerat, C.; Li, X.; Kozuka, H.; Sakamoto, K. Evaluation of aroma compounds Contributing to muskmelon flavor in Porapak Q extracts by aroma extract dilution analysis. *J. Agric. Food Chem.* **2003**, *51*, 3415–3418. [CrossRef] [PubMed]
114. Matich, A.; Rowan, D. Pathway analysis of branched-chain ester biosynthesis in apple using deuterium labeling and enantioselective gas chromatography-mass spectrometry. *J. Agric. Food Chem.* **2007**, *55*, 2727–2735. [CrossRef] [PubMed]
115. McLeish, R. Styrene Graphical Pathway Map. 2011. Available online: http://www.umbbd.ethz.ch/sty/sty_image_map.html (accessed on 25 July 2013).
116. Bedoukian Research Inc. Prenyl acetate. Product Information. 2013. Available online: http://www.bedoukian.com/products/product.asp?id=151 (accessed on 16 December 2013).
117. Seybold, S.J.; Vanderwel, D. Biosynthesis and endocrine regulation of pheromone production in the Coleoptera. In *Insect Pheromone Biochemistry and Molecular Biology. The Biosynthesis and Detection of Pheromones and Plant Volatiles*; Blomquist, G.J., Vogt, R.G., Eds.; Elsevier Academic Press: London, UK, 2003; Chapter 6; pp. 137–200. [CrossRef]
118. Van Moerkercke, A.; Schauvinhold, I.; Pichersky, E.; Haring, M.A.; Schuurink, R.C. A plant thiolase involved in benzoic acid biosynthesis and volatile benzenoid production. *Plant J.* **2009**, *60*, 292–302. [CrossRef] [PubMed]
119. Ribnicky, D.M.; Shulaev, V.; Raskin, I. Intermediates of salicylic acid biosynthesis in tobacco. *Plant Physiol.* **1998**, *118*, 565–572. [CrossRef]
120. Trinh, T.T.T.; Woon, W.Y.; Yu, B.; Curran, P.; Liu, S.Q. Effect of L-isoleucine and L-phenylalanine Addition on aroma compound formation during longan juice fermentation by a co-culture of *Saccharomyces cerevisiae* and *Williopsis saturnus*. *S. Afr. J. Enol. Vitic.* **2010**, *31*, 116–124. [CrossRef]
121. Kanehisa Laboratories. Propanoate Metabolism. 00640. 11/13/13. 2013. Available online: http://www.genome.jp/dbget-bin/show_pathway?map00640+C00207 (accessed on 25 July 2013).
122. Smit, B.A.; Engels, W.J.M.; Smit, G. Branched chain aldehydes: Production and breakdown pathways and relevance for flavour in foods. *Appl. Microbiol. Biotechnol.* **2009**, *81*, 987–999. [CrossRef]
123. Arfi, K.; Landaud, S.; Bonnarme, P. Evidence for distinct L-methionine catabolic pathways in the yeast *Geotrichum candidum* and the bacterium *Brevibacterium linens*. *Appl. Environ. Microbiol.* **2006**, *72*, 2155–2162. [CrossRef]
124. Liu, J.K.; Tang, X.; Zhang, Y.Z.; Zhao, W. Determination of the volatile composition in brown millet, milled millet and millet bran by gas chromatography-mass spectrometry. *Molecules* **2012**, *17*, 2271–2282. [CrossRef]
125. Wikipedia. Ionone. 2013. Available online: http://en.wikipedia.org/wiki/Ionone (accessed on 25 July 2013).
126. Jardine, K.J.; Sommer, E.D.; Saleska, S.R.; Huxman, T.E.; Harley, P.C.; Abrell, L. Gas phase measurements of pyruvic acid and its volatile metabolites. *Environ. Sci. Technol.* **2010**, *44*, 2454–2460. [CrossRef]
127. Croteau, R.; Karp, F. Biosynthesis of monoterpenes: Partial purification and characterization of 1,8-cineole synthetase from Salvia officinalis. *Archiv. Biochem. Biophys.* **1977**, *179*, 257–265. [CrossRef]
128. Pérez, A.G.; Sanz, C. Formation of fruit flavor. In *Fruit and Vegetable Flavour*; Bruckner, B., Grant, W.S., Eds.; Woodhead Publishing Ltd.: Cambridge, UK, 2008; pp. 41–70. [CrossRef]
129. Sanz, C.; Olías, J.M.; Pérez, A.G. Aroma biochemistry of fruits and vegetables. In *Phytochemistry of Fruit and Vegetables*; Tomás-Barberán, F.A., Robins, R.J., Eds.; Clarendon Press: Oxford, UK, 1997; pp. 125–155.
130. Perfumer Flavorist Library. Available online: http://www.perfumerflavorist.com/flavor/library (accessed on 25 July 2013).
131. Goodner, K.L. Practical retention index models of OV-101, DB-1, DB-5, and DB-Wax for flavor and fragrance compounds. *LWT-Food Sci. Technol.* **2008**, *41*, 951–958. [CrossRef]
132. Acree, T.; Arn, H. Flavornet and Human Odor Space. 2013. Available online: http://www.flavornet.org (accessed on 25 July 2013).
133. Mahattanatawee, K.; Ruiz, P.; Davenport, T.; Rouseff, R. Comparison of three lychee cultivar odor profiles using gas chromatography-olfactometry and gas chromatography-sulfur detection. *J. Agric. Food Chem.* **2007**, *55*, 1939–1944. [CrossRef] [PubMed]

134. ChemicalDictionary.org. Undecane. Chemical Dictionary. 2009. Available online: http://www.chemicaldictionary.org/dic/U/Undecane_429.html (accessed on 15 December 2013).
135. Wikipedia. Undecane. 2013. Available online: http://en.wikipedia.org/wiki/Undecane (accessed on 15 December 2013).
136. Weldegergis, T.B. Application of Modern Chromatographic Technologies for the Analysis of Volatile Compounds in South African Wines. Ph.D. Thesis, Stellenbosch University, Stellenbosch, South Africa, 2009. Available online: http://hdl.handle.net/10019.1/1129 (accessed on 13 December 2013).
137. Wikipedia. Cyclohexane. 2013. Available online: http://en.wikipedia.org/wiki/Cyclohexane (accessed on 13 December 2013).
138. Anonymous. Ethyl Benzene Pathway. UM-BBD Pathway Map. Starting with Reaction r0234. (University of Minnessota. Updated 27 May 2013). 2013. Available online: http://www.umbbd.ethz.ch/servlets/dynamicpathway?ptype=p&reacID=r0234&max_rows=5 (accessed on 13 December 2013).
139. Kniemeyer, O.; Heider, J. (S)-1-Phenylethanol dehydrogenase of Azoarcus sp strain EbN1, an enzyme of anaerobic ethylbenzene catabolism. *Archiv. Microbiol.* **2001**, *176*, 129–135. [CrossRef]
140. Kunst, L.; Jetter, R.; Samuels, A.L. Biosynthesis and transport of plant cuticular waxes. In *Annual Plant Reviews: Biology of the Plant Cuticle*; Riederer, M., Mülle, M., Eds.; Blackwell: Oxford, UK, 2006; pp. 182–215. [CrossRef]
141. Josephson, O.B.; Lindsay, R.C.; Stuiber, D.A. Variations in the occurrences of enzymatically derived volatile aroma compounds in salt- and freshwater fish. *J. Agric. Food Chem.* **1984**, *32*, 1344–1347. [CrossRef]
142. Wills, D.; Stephen, S.; Bryan, E. N-Octane Pathway Map. University Minnessota. (Updated 20 April 2013). 2012. Available online: http://umbbd.ethz.ch/oct/oct_map.html (accessed on 13 December 2013).
143. Dennis, E.G.; Keyzers, R.A.; Kalua, C.M.; Maffei, S.M.; Nicholson, E.L.; Boss, P.K. Grape contribution to wine aroma: Production of hexyl acetate, octyl acetate, and benzyl acetate during yeast fermentation is dependent upon precursors in the must. *J. Agric. Food Chem.* **2012**, *60*, 2638–2646. [CrossRef]
144. National Center for Biotechnology Information, U.S. National Library of Medicine. Methyl 2-ethylbutyrate—Substance Summary (SID 479764). 2013. Available online: http://pubchem.ncbi.nlm.nih.gov/summary/summary.cgi?sid=479764#x27 (accessed on 15 December 2013).
145. Fauconnier, M.L.; Marlier, M. Fatty acid hydroperoxides pathways in plants. A review. *Grasas Aceites* **1998**, *48*, 30–37. [CrossRef]
146. Leffingwell, J.C. Carotenoids as Flavor and Fragance Precursors. 2001. Available online: http://www.leffingwell.com/caroten.htm (accessed on 15 December 2013).
147. Kaiser, B.K.; Carleton, M.; Hickman, J.W.; Miller, C.; Lawson, D.; Budde, M.; Warrener, P.; Paredes, A.; Mullapudi, S.; Navarro, P.; et al. Fatty aldehydes in cyanobacteria are a metabolically flexible precursor for a diversity of biofuel products. *PLoS ONE* **2013**, *8*, e58307. [CrossRef] [PubMed]
148. Mayer, F.; Takeoka, G.R.; Buttery, R.G.; Whiterhand, L.C.; Naim, M.; Rabionowitch, H.D. Studies on the aroma of five fresh tomato cultivars and the precursors of cis- and trans-4,5-epoxy-(E)-2-decenals and methional. *J. Agric. Food Chem.* **2008**, *56*, 3749–3757. [CrossRef]
149. Vranová, J.; Ciesarová, Z. Furan in Food—A review. *Czech J. Food Sci.* **2009**, *27*, 1–10. [CrossRef]
150. Pesis, E. The role of the anaerobic metabolites, acetaldehyde and ethanol, in fruit ripening, enhancement of fruit quality and fruit deterioration. *Postharvest Biol. Technol.* **2005**, *37*, 1–19. [CrossRef]
151. Cameron, D.C.; Altaras, N.E.; Hoffman, M.L.; Shaw, A.J. Metabolic engineering of propanediol pathways. *Biotechnol. Prog.* **2008**, *14*, 116–125. [CrossRef] [PubMed]
152. Wikipedia. Camphor. 2013. Available online: http://en.wikipedia.org/wiki/Camphor (accessed on 15 December 2013).
153. Kanehisa Laboratories. Glycerolipid Metabolism. 2013. Available online: http://www.genome.jp/kegg-bin/show_pathway?map00561+C00479.005618/30/13 (accessed on 15 December 2013).
154. Stipanuk, M.H.; Ueki, I. Dealing with methionine/homocysteine sulfur: Cysteine metabolism to taurine and inorganic sulfur. *J. Inherit. Metabol. Dis.* **2011**, *34*, 17–32. [CrossRef] [PubMed]
155. Keen, A.R.; Walker, N.J.; Peberdy, M.F. The formation of 2-butanone and 2-butanol in Cheddar cheese. *J. Dairy Res.* **1974**, *41*, 249–257. [CrossRef]
156. Peterson, D.; Renieccius, G.A. Biological pathways for the formation of oxygen-containing aroma compounds. In: Heteroatomic aroma compounds. *ACS Symp. Ser.* **2002**, *826*, 227–242. [CrossRef]
157. Rychlik, M.; Schieberle, P.; Grosch, W. (Eds.) *Compilation of Odor Thresholds, Odor Qualities and Retention Indices of Key Food Odorants*; Technischen Universitat München: Garching, Germany, 1998.
158. Josephson, D.B.; Lindsay, R.C. Retro-aldol degradations of unsaturated aldehydes: Role in the formation of c 4-heptenal from t 2, c 6-nonadienal in fish, oyster and other flavors. *J. Am. Chem. Soc.* **1987**, *64*, 132–138. [CrossRef]
159. Grosch, W.; Schwarz, J.M. Linoleic and linolenic acid as precursors of the cucumber flavor. *Lipids* **1971**, *6*, 351–352. [CrossRef]
160. Hui, Y.H. (Ed.) *Handbook of Fruit and Vegetable Flavors*; John Wiley & Sons: Hoboken, NJ, USA, 2010.
161. Wikipedia. Cyclohexanol. 2013. Available online: http://en.wikipedia.org/wiki/Cyclohexanol (accessed on 15 December 2013).
162. Anonymous. Diisobutyl Ketone. Available online: http://www.chemicalland21.com/industrialchem/solalc/VALERONE.htm (accessed on 15 December 2013).
163. Rudell, D.R.; Mattinson, D.S.; Mattheis, J.P.; Wyllie, S.G.; Fellman, J.K. Investigations of aroma volatile biosynthesis under anoxic conditions and in different tissues of "Redchief Delicious" apple fruit (*Malus domestica* Borkh.). *J. Agric. Food Chem.* **2002**, *50*, 2627–2632. [CrossRef]

164. Colquhoun, T.A.; Marciniak, D.M.; Wedde, A.E.; Kim, J.Y.; Schwieterman, M.L.; Levin, L.A.; Van Moerkercke, A.; Schuurink, R.C.; Clark, D.G. A peroxisomally localized acyl-activating enzyme is required for volatile benzenoid formation in a Petuniaxhybrida cv. Mitchell Diploid' flower. *J. Exp. Bot.* **2012**, *63*, 4821–4833. [CrossRef]
165. Stueven, R. Technical note: Down with Diacetyl! 2003. Available online: http://www.beerme.com/graphics/pics/diacetyl.gif (accessed on 15 December 2013).
166. Hughes, P.S.; Baxter, E.D. (Eds.) *Beer Quality, Safety, and Nutritional Aspects*; RSC Paperbacks; The Royal Society of Chemistry: Cambridge, UK, 2001.
167. Rodríguez-Nogales, J.M.; Roura, E.; Contreras, E. Biosynthesis of ethyl butyrate using immobilized lipases: A statistical approach. *Process. Biochem.* **2005**, *40*, 63–68. [CrossRef]
168. Maeda, H.; Dudareva, N. The Shikimate pathway and aromatic amino acid biosynthesis in plants. *Ann. Rev. Plant Biol.* **2012**, *63*, 73–105. [CrossRef]
169. Suzuki, H.; Ohnishi, Y.; Furusho, Y.; Sakuda, S.; Horinouchi, S. Novel benzene ring biosynthesis from C3 and C4 primary metabolites by two enzymes. *J. Biol. Chem.* **2006**, *281*, 36944–36951. [CrossRef] [PubMed]
170. Stolle, A.; Ondruschka, B.; Bonrath, W.; Netscher, T.; Findeisen, M.; Hoffmann, M.M. Thermal isomerization of (+)-cis- and (-)-trans-pinane leading to (-)-beta-citronellene and (+)-isocitronellene. *Chemistry* **2008**, *14*, 6805–6814. [CrossRef] [PubMed]
171. Feldman, J.; Nugent, W.A. Process for the Preparation of Optically Active Cycloolefins. European Patent EP 0749406B1, PCT/US95/02393, 27 December 1996.
172. Fernández-Trujillo, J.P. Linear retention index of VOCs found in near-isogenic line SC12-1. Unpublished.
173. Stein, S.; Mirokhin, Y.; Tchekhovskoi, D.; Mallard, G. The NIST Mass Spectral Search Program for the NIST/EPA/NIH Mass Spectral Library. Version 2.0. 4 December 2012. Available online: https://chemdata.nist.gov/mass-spc/ms-search/docs/Ver20Man.pdf (accessed on 20 November 2022).
174. AMDIS32. 2.0g. Estimated Non-Polar Retention Index (n-alkane Scale). NIST. 2012. Available online: https://chemdata.nist.gov/mass-spc/ms-search/docs/Ver20Man.pdf (accessed on 20 November 2022).
175. Panighel, A.; Maoz, I.; De Rosso, M.; De Marchi, F.; Dalla Vedova, A.; Gardiman, M.; Bavaresco, L.; Flamini, R. Identification of saffron aroma compound β-isophorone (3,5,5-trimethyl-3-cyclohexen-1-one) in some *V. vinifera* grape varieties. *Food Chem.* **2014**, *145*, 186–190. [CrossRef] [PubMed]
176. Wikipedia. 3,3,5-Trimethylcyclohexanol. Available online: https://en.wikipedia.org/wiki/3,3,5-Trimethylcyclohexanol (accessed on 20 November 2022).

foods

MDPI

Article

Hyperspectral Imaging with Machine Learning Approaches for Assessing Soluble Solids Content of Tribute Citru

Cheng Li, Mengyu He, Zeyi Cai, Hengnian Qi, Jianhong Zhang and Chu Zhang *

School of Information Engineering, Huzhou University, Huzhou 313000, China
* Correspondence: chuzh@zjhu.edu.cn

Abstract: Tribute Citru is a natural citrus hybrid with plenty of vitamins and nutrients. Fruits' soluble solids content (SSC) is a critical quality index. This study used hyperspectral imaging at two spectral ranges (400–1000 nm and 900–1700 nm) to determine SSC in Tribute Citru. Partial least squares regression (PLSR) and support vector regression (SVR) models were established in order to determine SSC using the spectral information of the calyx and blossom ends. The average spectra of both ends as well as their fusion was studied. The successive projections algorithm (SPA) and the correlation coefficient analysis (CCA) were used to examine the differences in characteristic wavelengths between the two ends. Most models achieved performances with the correlation coefficient of the training, validation, and testing sets over 0.6. Results showed that differences in the performances among the models using the one-sided and two-sided spectral information. No particular regulation could be found for the differences in model performances and characteristic wavelengths. The results illustrated that the sampling side was an influencing factor but not the determinant factor for SSC determination. These results would help with the development of real-world applications for citrus quality inspection without concerning the sampling sides and the spectral ranges.

Keywords: hyperspectral images; soluble solids content; machine learning; sampling sides; data fusion

Citation: Li, C.; He, M.; Cai, Z.; Qi, H.; Zhang, J.; Zhang, C. Hyperspectral Imaging with Machine Learning Approaches for Assessing Soluble Solids Content of Tribute Citru. *Foods* **2023**, *12*, 247. https://doi.org/10.3390/foods12020247

Academic Editors: Imahori Yoshihiro and Jinhe Bai

Received: 8 November 2022
Revised: 22 December 2022
Accepted: 24 December 2022
Published: 5 January 2023

1. Introduction

China is now the country with the largest production of citrus. Citrus is a popular fruit not only for its unique taste but also for its high nutritional content. There are many excellent cultivars of citrus throughout the world. As one of them, Tribute Citru, also known as emperor citrus or Gong citrus, is a kind of citrus with high contents of carbohydrates, fiber, protein, calcium, etc. [1].

The soluble solids content (SSC) is a crucial indicator for evaluating the quality of Tribute Citru. SSC is the primary and most important quality parameter of concern to consumers. The common method of measuring SSC is to use a refractometer to measure the squeezed juice, which is time-consuming and damaging to the sample. Moreover, it cannot meet the demands for large-scale non-destructive measurement. Thus, rapid and non-destructive analytical techniques are needed.

Visible/near-infrared spectroscopy is a rapid and non-destructive technique that does not produce chemical contamination or damage to the sample(s) and has been applied in detecting fruit SSC [2–4]. Hyperspectral imaging technology combines imaging and spectroscopy technology, which can obtain spatial information at continuous spectral bands with high spectral resolution. Many research papers have been published based upon using hyperspectral imaging technology to detect SSC in fruits [5–9].

There are variations to the physiochemical characteristics within different parts of the fruit. VIS/NIR spectroscopy conducts point scan. When collecting spectral information of fruits, the different sampling points along with the equator or other representative regions were generally collected [10–13]. Some studies have also discussed the influence of spectra acquisition from different areas for SSC measurement [14–16].

The impact of variation within the samples should be considered in order to create a more accurate and robust SSC evaluation method. Hyperspectral imaging (HSI) can acquire the image of one side of the sample, covering the variations within the side of the sample. However, most studies acquired hyperspectral images of only one side of the samples [5–7]. Rare studies have considered using different sides of the fruits for SSC determination [8,9,17].

The SSC values were generally obtained to establish prediction models by averaging the measured values of different sample parts. The spectrum of each sample was also averaged by the spectra of different scanning points. Thus, it would be better if both the SSC value and the spectrum represent the corresponding sample. Given that different areas have both variations and similarities, it was worth investigating whether measuring both sides of samples for HSI was necessary. On the other hand, researchers have shown that hyperspectral imaging at different spectral ranges could be used to determine the SSC of fruits. The spectral ranges were also investigated to explore the influence of sampling sides.

In this study, hyperspectral imaging was used to determine SSC in Tribute Citru. The specific objectives were to (1) explore and compare the performances of hyperspectral imaging for SSC determination at two different spectral ranges (400–1000 nm and 900–1700 nm); (2) explore and compare the performances of sampling sides (the calyx end and the blossom end) for SSC determination; (3) explore the performances for SSC determination using the average spectra of the two sides and fused spectra of the two sides; (4) explore the characteristic wavelengths for SSC determination using the spectra of two sides to evaluate the performance consistency by the two sides.

2. Materials and Methods

2.1. Sample Preparation

Tribute Citru fruits were purchased from a local orchard in Liuzhou, Guangxi Province, China. A total of 458 samples of Tribute Citru fruits with similar sizes and no apparent damage on the surface were harvested on 22 November 2021. Before image acquisition, the fruits were stored at transported for four days and stored in the experimental room at a relatively stable temperature (15 $\pm$ 1 °C) for three days. All the samples were numbered sequentially and awaited the acquisition of hyperspectral images and subsequent SSC measurement. Figure 1 shows the RGB (red, green, and blue) images of citrus taken by the hyperspectral imaging system. The image of the fruit blossom end and the calyx end are shown in Figure 1a,b, respectively.

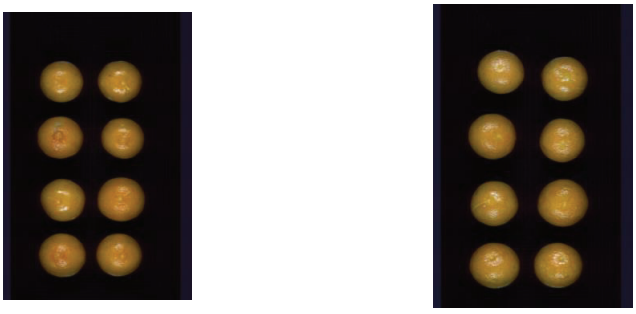

(**a**) (**b**)

Figure 1. RGB images of Tribute Citru. (**a**): the fruit blossom end; (**b**) the fruit calyx end.

2.2. SSC Measurement

The experimental arrangement for measuring SSC of Tribute Citru included a WIGGENS BR0035 Digital Brix Refractometer (WIGGENS Technology Ltd., Beijing, China) with an accuracy of 0.1 and °Brix range of 0–35%. For each of the 458 samples, the fruit was cut into

three pieces by the axis of the calyx and the blossom. Each piece was squeezed, and the juice was used to measure the SSC value. To avoid contamination, the refractometer was washed with distilled water after each measurement and dried with clean paper before the next reading. The average SSC value of the three pieces was used as the SSC of the sample.

2.3. Hyperspectral Imaging Systems

In this study, hyperspectral imaging systems at two spectral ranges were used for image acquisition of citrus. The two hyperspectral imaging systems differed in the hyperspectral camera. One hyperspectral camera was FX10 (Spectral Imaging Ltd., Oulu, Finland) with a spectral range of 400–1000 nm (VIS/NIR), and the other hyperspectral camera was FX17 (Spectral Imaging Ltd., Oulu, Finland) with a spectral range of 900–1700 nm. The two hyperspectral imaging systems shared the same light source (covering the spectral range of 35–2500 nm), moving platform, computer, and image acquisition software. First, the hyperspectral images of all the samples were acquired by FX10 camera. Next, the camera was changed to FX17 without changing the other hardware, and the hyperspectral images of the samples were then acquired by FX17 camera. The hyperspectral images were generated by pushbroom imaging (line scanning).

2.4. Hyperspectral Image Acquisition and Spectra Extraction

2.4.1. Hyperspectral Image Acquisition

The samples were placed on the mobile platform in sequence for hyperspectral image acquisition, as shown in Figure 1. The system parameters were adjusted for hyperspectral image acquisition. For FX10, the moving speed of the mobile platform was 17 mm/s, and the exposure time was set as 13.59 ms. For FX17, the moving speed of the mobile platform was set as 25 mm/s, and the exposure time was set as 8.26 ms. The difference in speed was because the imaging time of the two cameras was inconsistent. The hyperspectral camera will scan the calyx and blossom ends of Tribute Citru as side A and side B samples, respectively.

2.4.2. Spectra Extraction

Eight or fewer fruits were acquired in one hyperspectral image. Each fruit within the hyperspectral image was first cut as sub-hyperspectral images. The ENVI 4.7 software (ITT, Visual Information Solutions, Boulder, CO, USA) was used to cut each of the 458 samples from the original hyperspectral images, after which each sub-hyperspectral image contained only one fruit. The entire fruit region was defined as the region of interest (ROI), and the average spectrum of all pixel-wise spectra within the ROI was extracted.

Due to the noise at the beginning and end of the original spectra, the wavelength range of 487–974 nm was selected for FX10 and 933–1690 nm for FX17 of each sample. To eliminate the background interference and reduce the sample shape influence, wavelet transformation and area normalization preprocessing algorithms were used to preprocess the spectra. The spectral dataset of the fruit calyx end was named SP-A, and the spectral dataset of the fruit blossom end was named SP-B. By measuring the two sides of the samples, information of the entire fruit could be obtained, and more variations could be covered.

2.5. Data Analysis Methods

2.5.1. Regression Models

Support vector regression (SVR) is an important applied branch of support vector machine (SVM), a supervised learning algorithm for predicting discrete values [18]. The goal of SVR is to construct a hyperplane to fit the samples to minimize the overall distance between all samples and the hyperplane. SVR assumes that an error between the output value and the predicted value can be tolerated, and only the loss is calculated when the absolute value of the difference between the two is larger than the error. Therefore, SVR has a certain degree of tolerance to outliers, robustness, and excellent generalization ability. SVR can solve both

linear and non-linear issues. For non-linear problems, kernel functions are crucial to map the original data into high-dimensional spaces. In this study, the radial basis function (RBF) was used as the kernel function. The regularization parameters and kernel function coefficients were optimized by the grid-search method in the range of $[10^{-6}, 10^{6}]$.

Partial least squares regression (PLSR) is used to seek the underlying linear relationship between two matrices (independent matrix X and dependent matrix Y), which is a hidden variable approach to modeling the covariance structure in these two vector spaces. In order to explain the multidimensional direction with the biggest variance in the Y-space, the PLSR model tries to identify the multidimensional direction of the X-space [19]. PLSR decomposes both variables X and Y to extract factors, then the latent factors are arranged in descending order of their correlation. In contrast to conventional mulblossomle linear regression (MLR) models, PLSR can be constructed with mulblossomle correlated independent variables. The model can also be built if the number of samples is less than that of variables.

2.5.2. Wavelength Selection Methods

Successive projections algorithm (SPA) is a forward feature variable selection method. By projecting wavelengths onto other wavelengths, SPA compares the projection vectors, and the wavelength with the largest projection vector is selected into the candidate subset of characteristic wavelengths. The regression model is then used to evaluate the performances of different subsets. Therefore, SPA selects the combination of variables that contains the least redundant information and the least covariance [20].

Correlation coefficient analysis (CCA) is used to evaluate the degree of linear correlation between the independent and dependent variables [21]. Its value range is $[-1, 1]$. A positive value means positive correlation, a negative value means negative correlation, and a larger absolute value means a higher linear correlation. In this study, the correlation coefficient between each wavelength and the SSC content was examined in order to identify the characteristic wavelengths for SSC determination. The Pearson correlation coefficient was used in this study shown as Equation (1):

$$\rho_{x,y} = \frac{cov(x,y)}{\sigma_x \sigma_y} \quad (1)$$

where $\rho_{x,y}$ stands for the correlation coefficient between the variables x and y, $cov(x,y)$ stands for the covariance between the variables x and y, and σ_x and σ_y stand for the standard deviation of x and y.

2.6. Model Evaluation and Software

Six indicators were used to evaluate model performance, including correlation coefficient and root mean square errors of calibration (Rc and RMSEC), correlation coefficient and root mean square errors of validation (Rv and RMSEV), and correlation coefficient and root mean square errors of prediction (Rp and RMSEP) were assessed. Generally, the closer Rc, Rv, and Rp are to 1, the higher the stability and fit of the model, while the closer RMSEC, RMSEV, and RMSEP are to 0, the stronger the predictive ability of the model is.

In this study, the ENVI 4.7 software was used to cut the image of each fruit from hyperspectral images. Matlab R2017b (The Math Works, Natick, MA, USA) software was applied to group the samples and select effective wavelengths by SPA and CCA. The SVR model was developed on PyCharm Community Edition (version 2021.2.1) (JetBrains, Prague, Czech Republic) with Python (version 3.7.12), and the PLSR model was conducted on the Unscrambler X10.1 software (CAMO AS, Oslo, Norway). Specifically, the Origin 2017 64Bit (OriginLab, Northampton, MA, USA) was used to draw spectrograms and dotted line drawings.

3. Results

3.1. Outlier Removal

In this study, 458 fruits were studied. To further establish prediction models, outliers were first identified and removed. The outliers were identified in two steps. First, since SSC value of each sample was averaged by three manual measurements. To avoid manual measurement errors, the average SSC of each fruit was first calculated, and the difference between each measurement and the average value was then calculated. Indeed, there was no particular criterion for this kind of outlier removal. In this study, when the difference between the measurement and the averaged value was larger than 15%, the sample was regarded as an outlier sample. In total, 38 samples were identified as outliers in this step. Second, the remaining 420 samples were all used to build a PLSR model, and the predictive error of each sample was calculated. In the end, 20 samples with larger predictive errors were manually identified as outliers (with a negative impact on model performances) in the second step. Next, the 400 samples were subsequently randomly divided into the calibration set (300 samples), the validation set (50 samples), and the prediction set (50 samples) at a ratio of 6:1:1. It should be noted that outlier removal was conducted using the spectra of the calyx end. As for the two hyperspectral imaging systems, the identified outlier samples were different due to the fact that the PLSR model performed differently. The statistical analysis of SSC content in different sets is shown in Table 1.

Table 1. Statistical analysis of reference values of samples in the calibration, validation, and prediction sets.

Camera	Calibration Set (°Brix)			Validation Set (°Brix)			Prediction Set (°Brix)		
	Number	Min	Max	Number	Min	Max	Number	Min	Max
FX10	300	10.2	14.6	50	10.6	15.0	50	10.7	14.2
FX17	300	10.1	14.6	50	10.5	14.6	50	10.6	14.4

3.2. Spectral Profiles

Figure 2 shows the VIS/NIR reflectance spectra (obtained by FX10) and NIR reflectance spectra (obtained by NIR), with the horizontal coordinates indicating the 487–974 nm bands and the 933–1690 nm bands and the vertical coordinates indicating the reflectance of the spectra. Figure 2a,b shows the VIS/NIR spectra of the fruit calyx end (abbreviated as FX10-SP-A) and the fruit blossom end (abbreviated as FX10-SP-B) after removing the outlier samples. Figure 2c,d shows the spectral curves of the two sampling sides at the NIR range (FX17-SP-A and FX17-SP-B, respectively) after removing the outlier samples. It could be seen that the trends of the SP-A and SP-B curves were quite similar for each hyperspectral imaging system. From the spectral profiles, exploring the differences between the two sides for SSC measurement was difficult.

3.3. Regression Models

PLSR and SVR were used to establish regression models with the FX10 and FX17 datasets of the fruit calyx and blossom ends. The regression results are shown in Table 2.

For the SVR model and PLSR model, the samples were shot in the same order on the fruit calyx end and fruit blossom end. For both sides of the fruits, the samples in the calibration, validation, and prediction sets were the same. No samples were in the three sets at the same time.

For spectra extracted from the FX10 hyperspectral images, SVR and PLSR models obtained close results for each sampling side. Regression models for the calyx end (FX10-SP-A) showed slightly better performances than those for the blossom end (FX10-SP-B), with Rc, Rv, and Rp all over 0.7, as shown in Figure 3. However, the differences in the performances between the two sides were not significant. For spectra extracted from the FX17 hyperspectral images, SVR and PLSR models also obtained close results for each sampling side. The overall prediction performances of the models for the calyx end (FX17-SP-A) were close to

those for the blossom end (FX17-SP-B). The overall results of the regression models for the two sides showed differences in the performances between the sides, and the differences were insignificant. These results matched the literature [17].

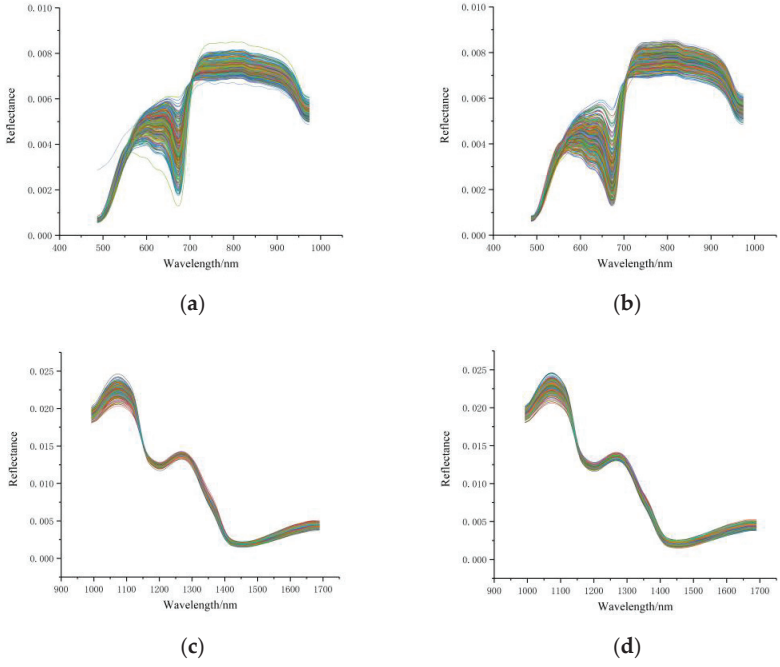

Figure 2. VIS/NIR spectra and NIR spectra of the fruit calyx and blossom ends. (**a**) VIS/NIR spectra of the fruit calyx end (FX10-SP-A); (**b**) VIS/NIR spectra of the fruit blossom end (FX10-SP-B); (**c**) NIR spectra of the fruit calyx end (FX17-SP-A); (**d**) NIR spectra of the fruit blossom end (FX17-SP-B).

It was worth investigating whether it was better to use the information of both sides instead of a single side. Thus, two different approaches to use the spectral information of the two sides were implemented. First, the average spectrum of the spectra of the two sides was calculated for each sample. Second, the low-level fusion of the spectrum of each side by directly concatenating the two spectra ranges was conducted. The results of models using average spectra and low-level fusion are shown in Table 2. For the average spectra of FX10, the PLSR model showed slightly better performances than the SVR model. For the average spectra of FX17, the SVR model showed slightly better performances than the PLSR model. For the low-level fusion of FX10, the PLSR model outperformed the SVR model. For low-level fusion of FX17, SVR, and PLSR models obtained close results.

For different datasets, the performances of the PLSR and SVR models varied. For the two sides, the performances of the same regression model were close. Moreover, the models using the average spectra of the two sides and the low-level fusion did not show significant improvement over the models using spectral profiles of a single side.

Indeed, the differences in the performances of models using a single side illustrated that there were variations of spectral profiles between the two sides. The close performances of models showed that these variations were not significant. It was a fact that both sides were in the same fruit, and the differences in spectral profiles might not be significant unless the color and maturity degree of the two sides were significantly different. When building regression models using spectra, it would be better to collect enough representative samples covering the variations of spectral profiles and SSC values. In this study, the performances of the two sides for SSC measurement did not show significant differences using different

regression models, indicating no significant variations in spectral profiles. On the other hand, the two spectral ranges obtained close performances with differences, which matched the previous studies [17,22–24].

The close results of models using the spectra of a single side and the spectra of two sides (by averaging and fusing) indicated that the spectral profiles were similar within one fruit. In this study, the color and maturity degree of the two sides was close, resulting in the similarity of the spectral profiles in the visible and NIR ranges, respectively. Thus, as for the hyperspectral image, acquiring one side of the fruits might be enough to represent the sample unless the internal quality varied significantly within one fruit.

Table 2. Results and parameters of the calibration, validation, and prediction sets by SVR and PLSR models.

Dataset	Model	Model Parameter	Calibration Set		Validation Set		Prediction Set	
			Rc [k]	RMSEC [n] (°Brix)	Rv [l]	RMSEV [o] (°Brix)	Rp [m]	RMSEP [p] (°Brix)
FX10-SP-A [a]	SVR [i]	Gamma: 1000.0 C: 10^6 Eps: 10^{-5}	0.810	0.435	0.750	0.511	0.705	0.53
	PLSR [j]	Factor: 19	0.786	0.451	0.769	0.497	0.731	0.51
FX10-SP-B [b]	SVR	Gamma: 10.0 C: 10^6 Eps: 10^{-5}	0.654	0.562	0.702	0.548	0.672	0.557
	PLSR	Factor: 16	0.744	0.487	0.705	0.558	0.655	0.571
FX17-SP-A [c]	SVR	Gamma: 10,000.0 C: 1000.0 Eps: 10^{-5}	0.725	0.497	0.744	0.578	0.588	0.567
	PLSR	Factor: 11	0.738	0.486	0.752	0.561	0.639	0.514
FX17-SP-B [d]	SVR	Gamma: 100.0 C: 10^6 Eps: 0.001	0.700	0.516	0.769	0.544	0.529	0.591
	PLSR	Factor: 8	0.685	0.524	0.772	0.540	0.596	0.556
FX10-average [e]	SVR	Gamma: 100.0 C: 10^6 Eps: 0.001	0.726	0.503	0.733	0.523	0.513	0.658
	PLSR	Factor: 17	0.782	0.455	0.751	0.515	0.736	0.515
FX17-average [f]	SVR	Gamma: 10,000.0 C: 10^4 Eps: 0.001	0.796	0.437	0.765	0.546	0.720	0.484
	PLSR	Factor: 11	0.747	0.479	0.773	0.540	0.611	0.540
FX10-fusion [g]	SVR	Gamma: 1000.0 C: 10^5 Eps: 0.001	0.882	0.344	0.707	0.566	0.529	0.675
	PLSR	Factor: 18	0.753	0.480	0.711	0.539	0.680	0.552
FX17-fusion [h]	SVR	Gamma: 10.0 C: 10^6 Eps: 0.0001	0.708	0.510	0.770	0.543	0.599	0.534
	PLSR	Factor: 12	0.720	0.499	0.734	0.582	0.597	0.547

[a] FX10-SP-A: data of the calyx end obtained by FX10 camera; [b] FX10-SP-B: data of the blossom end obtained by FX10 camera; [c] FX17-SP-A: data of the calyx end obtained by FX17 camera; [d] FX17-SP-B: data of the blossom end obtained by FX17 camera; [e] FX10-average: the average spectra of the two sides obtained by FX10 camera; [f] FX17-average: the average spectra of the two sides obtained by FX17 camera; [g] FX10-fusion: the fusion spectra of the two sides obtained by FX10 camera; [h] FX17-fusion: the fusion spectra of the two sides obtained by FX17 camera; [i] SVR: support vector regression; [j] PLSR: partial least squares regression; [k] Rc: correlation coefficient of calibration; [l] Rv: correlation coefficient of validation; [m] Rp: correlation coefficient of prediction; [n] RMSEC: root mean square errors of calibration; [o] RMSEV: root mean square errors of validation; [p] RMSEP: root mean square errors of prediction.

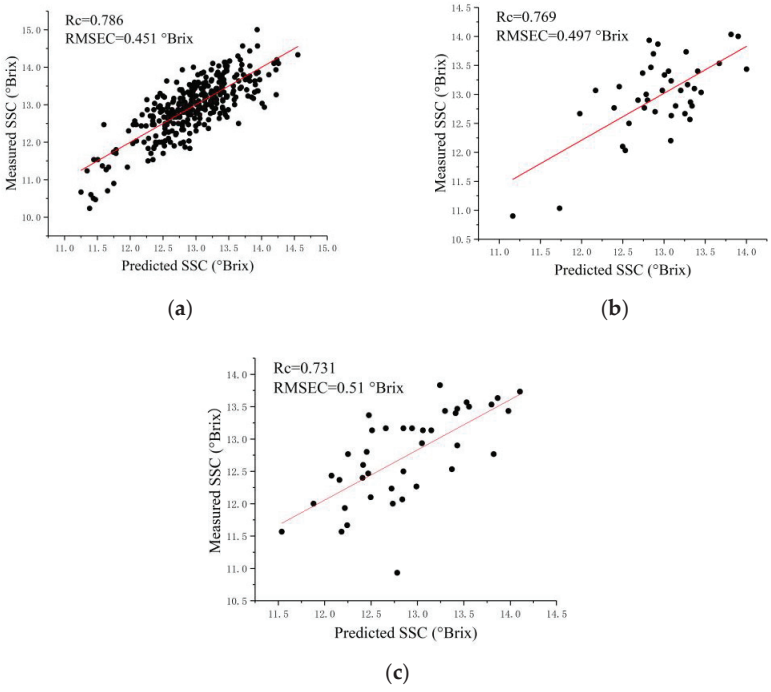

Figure 3. Scatter plots of the measured SSC values and predicted SSC values by SVR. (**a**) FX10-SP-A of calibration set; (**b**) FX10-SP-A of validation set; (**c**) FX10-SP-A of prediction set.

3.4. Analysis of Characteristic Wavelengths

The performances of models using the spectral information of a single side were close. In order to further explore the influence of spectral variations on characteristic wavelengths for SSC measurement, two variable selection methods, SPA and CCA, were used to select the characteristic wavelengths. The characteristic wavelengths of the two sides selected by SPA are shown in Table 3.

Table 3. Characteristic wavelengths selected by SPA for the datasets of the two sides of the two hyperspectral image systems.

Datasets	Number	Characteristic Wavelengths (nm)
FX10-SP-A	18	494, 516, 545, 574, 596, 674, 699, 704, 707, 713, 721, 743, 754, 765, 803, 877, 902, 944
FX10-SP-B	10	516, 526, 540, 548, 765, 800, 817, 872, 905, 927
FX17-SP-A	19	993, 1111, 1139, 1153, 1167, 1202, 1230, 1244, 1251, 1265, 1342, 1363, 1384, 1413, 1427, 1462, 1505, 1554, 1611
FX17-SP-B	20	1020, 1111, 1139, 1146, 1188, 1209, 1237, 1251, 1286, 1321, 1335, 1356, 1377, 1413, 1427, 1455, 1490, 1604, 1626, 1647

As shown in Table 3, the number of selected wavelengths accounted for 10%, 6%, 19% and 20% of the total number of wavelengths at the two spectral ranges, respectively. Figure 4 shows the characteristic wavelengths selected by SPA. Although the number of characteristic wavelengths for FX10-SP-A was more than that for FX10-SP-B, they were quite similar for the selected wavelengths. The characteristic wavelengths at 516 and 765 nm of FX10 were the same for the two sides, and the characteristic wavelengths at 545, 803, 877, and 902 nm of FX10-SP-A and the characteristic wavelengths at 540, 800, 872, and 905 nm of FX10-SP-B were close. A similar phenomenon could be found for FX17 datasets. The characteristic wavelengths at 1111, 1139, 1251, 1413, and 1427 nm were the same for both sides of FX17. The characteristic wavelengths at 1202, 1230, 1342, 1462, and 1611 nm of FX17-SP-A and 1209, 1237, 1335, 1455, and 1604 nm of FX17-SP-B were quite close.

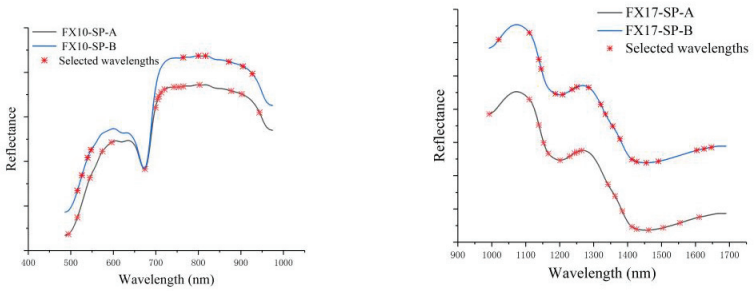

(**a**) (**b**)

Figure 4. Characteristic wavelengths obtained with SPA. (**a**) Selected wavelengths of VIS/NIR spectra including SP-A and SP-B; (**b**) selected wavelengths of NIR spectra including SP-A and SP-B. (Note: Given that the average spectra of the two sides partially overlap and are not convenient for observation, the reflectance values of the SP-B spectra of FX10 were averaged and increased by 0.01, and the reflectance values of the SP-B spectra of FX17 were averaged and increased by 0.001).

Figure 5 shows the correlation coefficient between each wavelength and the corresponding SSC values. Similarities could be found for the correlation coefficient curves of both sides. The peaks of the correlation coefficient curves of the two sides indicated the larger correlation coefficients, and these wavelengths had the potential to contribute more to SSC measurement. The wavelengths with higher correlation coefficients were 529–569 nm, 620–680 nm, 699–724 nm, and 952–974 nm for both FX10-SP-A and FX10-SP-B. For FX17, the correlation coefficient curves of both sides showed similar trends. The wavelengths at 1153–1279 nm and 1398–1547 nm showed higher correlation coefficients.

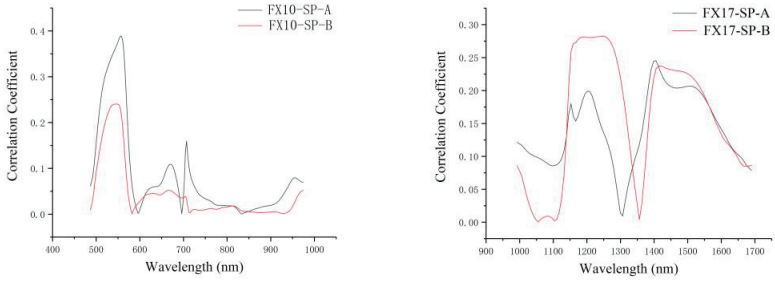

(**a**) (**b**)

Figure 5. Correlation coefficient corresponding to the wavelengths. (**a**) Correlation coefficient curves of VIS/NIR averaging spectra (FX10); (**b**) correlation coefficient curves of NIR averaging spectra (FX17).

The wavelengths in the visible range (400–780 nm) were mainly related to the color information of the fruits. The wavelength bands in the range of 780–1100 nm can be assigned as second and third overtone of C–H stretching and the second overtone of O–H stretching [25]. The wavelengths between 1200–1389 nm can be attributed to the third and second overtone of C–H stretch [25]. The wavelengths between 1400 nm and 1440 nm were related to water [26]. The wavelengths in the range of 1460–1600 nm might be related to cellulose [27]. The wavelengths between 1569 nm and 1604 nm can also be attributed to the O–H stretching of the first overtone in carbohydrates [28]. The wavelength of 1647 nm was attributed to the C–H stretching modes of aromatic C–H [29].

According to Table 3, Figures 2, 4 and 5, it can be seen that the spectral data of the two sides of Tribute Citru were similar, and the characteristic wavelengths that contributed

more to the SSC detection were also quite similar. These results also indicated that a single side of the fruit might be enough for the SSC measurement of Tribute Citru.

SVR and PLSR were built using the characteristic wavelengths identified by SPA and CCA. The results are shown in Table 4. For characteristic wavelengths of FX10 selected by SPA, the correlation coefficients of the SVR and PLSR models of the calyx and blossom ends were around 0.6. Similar results could be observed for characteristic wavelengths of FX17 selected by SPA.

Table 4. Results and parameters of the calibration, validation, and prediction sets by SVR and PLSR models using identified characteristic wavelengths.

Dataset	Model	Model Parameter	Calibration Set		Validation Set		Prediction Set	
			Rc [k]	RMSEC [n] (°Brix)	Rv [l]	RMSEV [o] (°Brix)	Rp [m]	RMSEP [p] (°Brix)
SPA-FX10-SP-A [a]	SVR [i]	Gamma: 10^5 C: 10^5 Eps: 10^{-3}	0.891	0.333	0.824	0.474	0.596	1.459
	PLSR [j]	Factor: 15	0.771	0.465	0.767	0.495	0.678	0.544
SPA-FX10-SP-B [b]	SVR	Gamma: 1000.0 C: 10^6 Eps: 10^{-5}	0.683	0.535	0.704	0.544	0.636	0.592
	PLSR	Factor: 9	0.704	0.518	0.675	0.564	0.664	0.568
SPA-FX17-SP-A [c]	SVR	Gamma: 10^4 C: 10^3 Eps: 10^{-5}	0.636	0.558	0.737	0.588	0.546	0.561
	PLSR	Factor: 14	0.743	0.482	0.718	0.592	0.670	0.498
SPA-FX17-SP-B [d]	SVR	Gamma: 10^3 C: 10^5 Eps: 10^{-3}	0.681	0.529	0.777	0.541	0.596	0.540
	PLSR	Factor: 8	0.689	0.522	0.774	0.537	0.594	0.559
CCA-FX10-SP-A [e]	SVR	Gamma: 10 C: 10^6 Eps: 10^{-5}	0.571	0.603	0.686	0.560	0.456	0.650
	PLSR	Factor: 14	0.685	0.531	0.699	0.553	0.672	0.564
CCA-FX10-SP-B [f]	SVR	Gamma: 10^3 C: 10^5 Eps: 10^{-3}	0.667	0.550	0.604	0.609	0.663	0.560
	PLSR	Factor: 15	0.705	0.517	0.665	0.607	0.629	0.594
CCA-FX17-SP-A [g]	SVR	Gamma: 10^5 C: 10^3 Eps: 10^{-4}	0.714	0.507	0.794	0.533	0.555	0.565
	PLSR	Factor: 9	0.699	0.514	0.758	0.553	0.658	0.499
CCA-FX17-SP-B [h]	SVR	Gamma: 10^4 C: 10^5 Eps: 10^{-3}	0.697	0.517	0.778	0.534	0.519	0.626
	PLSR	Factor: 9	0.668	0.535	0.788	0.527	0.506	0.644

[a] SPA-FX10-SP-A: data of the calyx end obtained by FX10 camera using SPA; [b] SPA-FX10-SP-B: data of the blossom end obtained by FX10 camera using SPA; [c] SPA-FX17-SP-A: data of the calyx end obtained by FX17 camera using SPA; [d] SPA-FX17-SP-B: data of the blossom end obtained by FX17 camera using SPA; [e] CCA-FX10-SP-A: data of the calyx end obtained by FX10 camera using CCA; [f] CCA-FX10-SP-B: data of the blossom end obtained by FX10 camera using CCA; [g] CCA-FX17-SP-A: data of the calyx end obtained by FX17camera using CCA; [h] CCA-FX17-SP-B: data of the blossom end obtained by FX17 camera using CCA; [i] SVR: support vector regression; [j] PLSR: partial least squares regression; [k] Rc: correlation coefficient of calibration; [l] Rv: correlation coefficient of validation; [m] Rp: correlation coefficient of prediction; [n] RMSEC: root mean square errors of calibration; [o] RMSEV: root mean square errors of validation; [p] RMSEP: root mean square errors of prediction.

For the characteristic wavelengths of FX10 identified by the CCA method, the wavelength ranges of 529–569 nm, 620–680 nm, 699–724 nm, and 952–974 nm with similar trends of the calyx and blossom ends were selected to build PLSR and SVR models. Relatively poor performances were obtained. The correlation coefficients of the training sets of the SVR and PLSR models were below 0.7. For the characteristic wavelengths of FX17 identified by the CCA method, the bands at 1153–1279 nm and 1398–1547 nm with similar trends of

the calyx and blossom ends were selected to build PLSR and SVR models. The results were not good enough.

Compared with the results in Table 3, the regression models using full range spectra performed slightly better than the corresponding models using identified characteristic wavelengths. Although characteristic wavelength selection can reduce the number of input variables and simplify the models, some useful information may also be lost.

4. Discussion

SSC is the most important quality attribute of concern to consumers. This study used hyperspectral imaging at two different spectral ranges to estimate the SSC in Tribute Citru, and the effect of the sampling sides of fruits was also investigated.

The physicochemical properties within one fruit varied in different regions resulting in differences in the corresponding spectral profiles. As for point-scan near-infrared spectroscopy, spectral profiles were generally acquired from different sampling regions, and corresponding SSC values of the same sampling area were measured. Guthire et al. (2006) showed the importance of the uniformity of the spectra measurement and quality attributes measurement [30]. The influence of sampling regions has also been discussed [14–16]. Unlike point-scan near-infrared spectroscopy, hyperspectral imaging can acquire images of one side of the fruit facing the camera, and each pixel contains a spectrum. Based on this characteristic, HSI was generally used to acquire images of only one side of the fruits [5–7]. An issue should be addressed that there might also be variations of the physicochemical properties between different sides of the fruits. In this study, hyperspectral images of the two different sides of Tribute Citru fruits were acquired and compared. The overall results of the SSC prediction of the two sides showed insignificant differences using different regression methods. Further analysis of the characteristic wavelengths for SSC determination by SPA and CCA showed great similarities between the two sides. Similar results could be found in previous research, and the performances of SSC prediction using the hyperspectral images of two opposite sides of plum showed insignificant differences [17].

Two approaches to using the information of the two sides were explored, including averaging the spectra of the two sides and concatenating the spectra of the two sides. The results did not show significant improvements using the two approaches compared with models using one side. Some reasons for this might be that averaging of the spectra of the two sides could use the information of the entire fruit, and some of the variations might be reduced by averaging; concatenating the spectra of the two sides might keep the variations; and some redundant information was used, due to the fact that the spectral features of the two sides were similar.

Relatively poor performances were obtained for the SSC determination of Tribute Citru. Some other studies have also obtained results that were not good enough [31–33]. Various factors affected the prediction performances (such as samples, instruments, and experimental operations, etc.), and more efforts should be made to improve the prediction performances.

This study showed that either side (the calyx and blossom ends) of the Tribute Citru could be used for SSC measurement of fruits. Although there were variations in the spectral profiles and physicochemical properties between the two sides of the Tribute Citru, future real-world applications can be developed by acquiring the hyperspectral images of either side of the fruits, which will reduce the cost of model development and online detection.

5. Conclusions

In this study, the influence of the sampling side of fruit for SSC determination using HSI was explored. The average of the spectra of the two sampling sides (the calyx end and the blossom end) and the fusion (direct concatenation) of the spectra of the two sampling sides were also investigated. The overall results of the two regression methods (PLSR and SVR) illustrated that the sampling sides might not significantly affect the prediction performances. Moreover, the average of the spectra of the two sampling sides

and the fusion of the spectra of the two sampling sides did not significantly improve the prediction performances. The performances of the two regression methods validated the results. The characteristic wavelengths for the SSC prediction using different sampling sides by the same characteristic wavelength selection method were quite similar, indicating that sampling on either side (the calyx end and the blossom end) might be used to predict SSC. The performances of hyperspectral imaging at two different spectral ranges showed no significant differences, illustrating that both could be used for the SSC prediction of Tribute Citru. In future studies, more samples should be used to develop more robust and accurate models with machine learning methods, such as deep learning. The real-world applications of hyperspectral imaging to inspect quality and safety of Tribute Citru might then be developed in the future by scanning either side (the calyx end and the blossom end) of the samples at different spectral ranges.

Author Contributions: Conceptualization, C.Z.; data curation, C.Z.; formal analysis, C.L.; funding acquisition, H.Q.; investigation, C.L., M.H. and Z.C.; methodology, C.Z.; project administration, H.Q.; resources, C.Z.; software, C.L., Z.C. and J.Z.; supervision, H.Q.; Validation, C.L. and M.H.; visualization, C.Z.; writing—original draft, C.L.; writing—review and editing, C.Z. All authors have read and agreed to the published version of the manuscript.

Funding: This work was supported by Zhejiang Province Key Laboratory of Smart Management and Application of Modern Agricultural Resources under Grant 2020E10017.

Institutional Review Board Statement: Not applicable.

Informed Consent Statement: Not applicable.

Data Availability Statement: The data can be requested by contacting the corresponding authors via E-mail.

Acknowledgments: We would like to thank Guangyan Wen, Qian Li, and Manjing Zhang from the School of Information Engineering, Huzhou University, for their help in this research.

Conflicts of Interest: The authors declare no conflict of interest.

References

1. Li, G.; Liu, S.; Zhou, Q.; Han, J.; Qian, C.; Li, Y.; Meng, X.; Gao, X.; Zhou, T.; Li, P. Effect of Response Surface Methodology-Optimized Ultrasound-Assisted Pretreatment Extraction on the Composition of Essential Oil Released From Tribute citrus Peels. *Front. Nutr.* **2022**, *9*, 840780. [CrossRef]
2. Liu, Y.; Chen, X.; Ouyang, A. Nondestructive determination of pear internal quality indices by visible and near-infrared spectrometry. *LWT-FOOD* **2008**, *41*, 1720–1725. [CrossRef]
3. Jamshidi, B.; Minaei, S.; Mohajerani, E.; Ghassemian, H. Prediction of Soluble Solids in Oranges Using Visible/Near-Infrared Spectroscopy: Effect of Peel. *Int. J. Food Prop.* **2014**, *17*, 1460–1468. [CrossRef]
4. Masithoh, R.E.; Pahlawan, M.F.R.; Wati, R.K. Non-destructive determination of SSC and pH of banana using a modular Vis/NIR spectroscopy: Comparison of Partial Least Square (PLS) and Principle Component Regression (PCR). In Proceedings of the IOP Conference Series: Earth and Environmental Science, Yogyakarta, Indonesia, 13–14 October 2020. [CrossRef]
5. Zhang, H.; Zhan, B.; Pan, F.; Luo, W. Determination of soluble solids content in oranges using visible and near infrared full transmittance hyperspectral imaging with comparative analysis of models. *Postharvest Biol. Technol.* **2020**, *163*, 111148. [CrossRef]
6. Wei, X.; He, J.; Zheng, S.; Ye, D. Modeling for SSC and firmness detection of persimmon based on NIR hyperspectral imaging by sample partitioning and variables selection. *Infrared Phys. Technol.* **2020**, *105*, 103099. [CrossRef]
7. Zhang, D.; Xu, Y.; Huang, W.; Tian, X.; Xia, Y.; Xu, L.; Fan, S. Nondestructive measurement of soluble solids content in apple using near infrared hyperspectral imaging coupled with wavelength selection algorithm. *Infrared Phys. Technol.* **2019**, *98*, 297–304. [CrossRef]
8. Gabrielli, M.; Lançon-Verdier, V.; Picouet, P.; Maury, C. Hyperspectral Imaging to Characterize Table Grapes. *Chemosensors* **2021**, *9*, 71. [CrossRef]
9. Ma, T.; Xia, Y.; Inagaki, T.; Tsuchikawa, S. Non-destructive and fast method of mapping the distribution of the soluble solids content and pH in kiwifruit using object rotation near-infrared hyperspectral imaging approach. *Postharvest Biol. Technol.* **2021**, *174*, 111440. [CrossRef]
10. Zou, X.; Zhao, J.; Li, Y. Selection of the efficient wavelength regions in FT-NIR spectroscopy for determination of SSC of 'Fuji' apple based on BiPLS and FiPLS models. *Vib. Spectrosc.* **2007**, *44*, 220–227. [CrossRef]

11. Pissard, A.; Marques, E.J.N.; Dardenne, P.; Lateur, M.; Pasquini, C.; Pimentel, M.F.; Fernández Pierna, J.A.; Baeten, V. Evaluation of a handheld ultra-compact NIR spectrometer for rapid and non-destructive determination of apple fruit quality. *Postharvest Biol. Technol.* **2021**, *172*, 111375. [CrossRef]
12. Liu, C.; Yang, S.X.; Li, X.; Xu, L.; Deng, L. Noise level penalizing robust Gaussian process regression for NIR spectroscopy quantitative analysis. *Chemom. Intell. Lab. Syst.* **2020**, *201*, 104014. [CrossRef]
13. Liu, Y.; Zhang, Y.; Jiang, X.; Liu, H. Detection of the quality of juicy peach during storage by visible/near infrared spectroscopy. *Vib. Spectrosc.* **2020**, *111*, 103152. [CrossRef]
14. Cayuela, J.A. Vis/NIR soluble solids prediction in intact oranges (Citrus sinensis L.) cv. Valencia Late by reflectance. *Postharvest Biol. Technol.* **2008**, *47*, 75–80. [CrossRef]
15. Xu, X.; Mo, J.; Xie, L.; Ying, Y. Influences of Detection Position and Double Detection Regions on Determining Soluble Solids Content (SSC) for Apples Using Online Visible/Near-Infrared (Vis/NIR) Spectroscopy. *Food Anal. Method* **2019**, *12*, 2078–2085. [CrossRef]
16. Castrignanò, A.; Buttafuoco, G.; Malegori, C.; Genorini, E.; Iorio, R.; Sblossomic, M.; Girone, G.; Venezia, A. Assessing the Feasibility of a Miniaturized Near-Infrared Spectrometer in Determining Quality Attributes of San Marzano Tomato. *Food Anal. Method* **2019**, *12*, 1497–1510. [CrossRef]
17. Li, B.; Cobo-Medina, M.; Lecourt, J.; Harrison, N.; Harrison, R.J.; Cross, J.V. Application of hyperspectral imaging for nondestructive measurement of plum quality attributes. *Postharvest Biol. Technol.* **2018**, *141*, 8–15. [CrossRef]
18. Huang, F.-H.; Liu, Y.-H.; Sun, X.; Yang, H. Quality inspection of nectarine based on hyperspectral imaging technology. *Syst. Sci. Control Eng.* **2021**, *9*, 350–357. [CrossRef]
19. Rajkumar, P.; Wang, N.; Eimasry, G.; Raghavan, G.S.V.; Gariepy, Y. Studies on banana fruit quality and maturity stages using hyperspectral imaging. *J. Food Eng.* **2012**, *108*, 194–200. [CrossRef]
20. Yuan, Y.; Wang, W.; Chu, X.; Xi, M.-j. Selection of Characteristic Wavelengths Using SPA and Qualitative Discrimination of Mildew Degree of Corn Kernels Based on SVM. *Spectrosc. Spectr. Anal.* **2016**, *36*, 226–230. [CrossRef]
21. Jiang, W.; Lu, C.; Zhang, Y.; Ju, W.; Wang, J.; Xiao, M. Molecular spectroscopic wavelength selection using combined interval partial least squares and correlation coefficient optimization. *Anal. Methods* **2019**, *11*, 3108–3116. [CrossRef]
22. Ye, W.; Yan, T.; Zhang, C.; Duan, L.; Chen, W.; Song, H.; Zhang, Y.; Xu, W.; Gao, P. Detection of Pesticide Residue Level in Grape Using Hyperspectral Imaging with Machine Learning. *Foods* **2022**, *11*, 1609. [CrossRef] [PubMed]
23. Zhu, H.; Chu, B.; Fan, Y.; Tao, X.; Yin, W.; He, Y. Hyperspectral Imaging for Predicting the Internal Quality of Kiwifruits Based on Variable Selection Algorithms and Chemometric Models. *Sci. Rep.* **2017**, *7*, 7845. [CrossRef] [PubMed]
24. Yan, T.; Duan, L.; Chen, X.; Gao, P.; Xu, W. Application and interpretation of deep learning methods for the geographical origin identification of Radix Glycyrrhizae using hyperspectral imaging. *RSC Adv.* **2020**, *10*, 41936–41945. [CrossRef]
25. Daneshvar, A.; Tigabu, M.; Karimidoost, A.; Oden, P.C. Single seed Near Infrared Spectroscopy discriminates viable and non-viable seeds of Juniperus polycarpos. *Silva Fennica* **2015**, *49*, 1334. [CrossRef]
26. Büning-Pfaue, H. Analysis of water in food by near infrared spectroscopy. *Food Chem.* **2003**, *82*, 107–115. [CrossRef]
27. Jochemsen, A.; Alfredsen, G.; Burud, I. Hyperspectral imaging as a tool for profiling basidiomycete decay of *Pinus sylvestris* L. *Int. Biodeterior. Biodegrad.* **2022**, *174*, 105464. [CrossRef]
28. Bowler, A.L.; Ozturk, S.; Rady, A.; Watson, N. Domain Adaptation for In-Line Allergen Classification of Agri-Food Powders Using Near-Infrared Spectroscopy. *Sensors* **2022**, *22*, 7239. [CrossRef]
29. Okparanma, R.N.; Mouazen, A.M. Visible and Near-Infrared Spectroscopy Analysis of a Polycyclic Aromatic Hydrocarbon in Soils. *Sci. World J.* **2013**, *2013*, 160360. [CrossRef]
30. Guthrie, J.A.; Liebenberg, C.J.; Walsh, K.B. NIR model development and robustness in prediction of melon fruit total soluble solids. *Aust. J. Agric. Res.* **2006**, *57*, 411. [CrossRef]
31. Sánchez, M.-T.; De la Haba, M.-J.; Pérez-Marín, D. Internal and external quality assessment of mandarins on-tree and at harvest using a portable NIR spectrophotometer. *Comput. Electron. Agr.* **2013**, *92*, 66–74. [CrossRef]
32. Wang, A.; Hu, D.; Xie, L. Comparison of detection modes in terms of the necessity of visible region (VIS) and influence of the peel on soluble solids content (SSC) determination of calyx orange using VIS–SWNIR spectroscopy. *J. Food Eng.* **2014**, *126*, 126–132. [CrossRef]
33. Fu, X.; Wang, X.; Rao, X. An LED-based spectrally tuneable light source for visible and near-infrared spectroscopy analysis: A case study for sugar content estimation of citrus. *Biosyst. Eng.* **2017**, *163*, 87–93. [CrossRef]

foods

MDPI

Article

Soil Amendment and Storage Effect the Quality of Winter Melons (*Benincasa hispida* (Thunb) Cogn.) and Their Juice

Jinhe Bai *, Erin N. Rosskopf, Kristen A. Jeffries, Wei Zhao and Anne Plotto

USDA, ARS, U.S. Horticultural Research Laboratory, 2001 S. Rock Rd, Fort Pierce, FL 34945, USA
* Correspondence: jinhe.bai@usda.gov; Tel.: +1-772-462-5880; Fax: +1-772-462-5986

Abstract: Winter melon fruits were grown in the field using anaerobic soil disinfestation (ASD) and conventional fertilizer alone as the control treatment. Fruits were harvested and stored at 20 °C for 120 d, the juice was processed on day one and day 120, and the effects of soil amendment and 120 d storage on the juice's physical and chemical (sugars, acids, volatile and nutritional compounds) properties were evaluated. Fruit juice extracted from ASD-grown fruit had greater magnitude of zeta potential than the control juice, indicating it was physically more stable than the juice obtained from the control conditions. ASD fruit juice had lower soluble solids content (SSC), and lower volatile compounds that contribute green, grass, and sulfur notes, and negatively influence flavor quality. ASD fruit juice had higher vitamin B5 and cytidine. Juice processed from 120 d stored fruit had less yield due to 12.4–15.6% weight loss. The non-soluble solids content was higher and particle size was larger, and the SSC and individual sugars decreased. However, titratable acidity (TA) increased primarily due to increased citric acid. Out of 16 free amino acids, 6 increased and only 1 decreased. However, three out of five nucleosides decreased; vitamins B1 and B6 increased; vitamins B2, B3 and C decreased. Overall, juice derived from fruit produced using ASD was physically more stable and had less SSC and off-odor volatiles than the control, while the fruit juice of those stored for 120 d had lower SSC and higher TA and nutritional profiles, comparable to freshly harvested fruit.

Keywords: *Benincasa hispida*; anaerobic soil disinfestation; ASD; volatile; soluble solids content; brix; acid; zeta potential; particle size; amino acid; vitamin; nucleoside; long storage

Citation: Bai, J.; Rosskopf, E.N.; Jeffries, K.A.; Zhao, W.; Plotto, A. Soil Amendment and Storage Effect the Quality of Winter Melons (*Benincasa hispida* (Thunb) Cogn.) and Their Juice. *Foods* **2023**, *12*, 209. https://doi.org/10.3390/foods12010209

Academic Editor: Rinaldo Botondi

Received: 17 November 2022
Revised: 23 December 2022
Accepted: 26 December 2022
Published: 3 January 2023

1. Introduction

There is sufficient scientific research and surveys showing that decreasing sugar-sweetened beverage (SSB) intake will reduce the prevalence of overweight individuals and obesity [1–4]. In contrast, increased fruit and vegetable intake lowers the risk of serious health problems, such as cardiovascular diseases and cancer [5–7]. Some fruit juice has similar energy density and sugar content to SSBs, and high fruit juice intake can be associated with an increased risk of diabetes in spite of the fact that fruit juices also contain vitamins, fibers, and minerals [8–10]. Thus, the search for low-sugar juices and drinks is motivated by public health concerns [11].

Different from the sweet cucurbits, such as melons [12] and watermelon [13], winter melon (*Benincasa hispida* (Thunb) Cogn.) is a non-sweet cucurbit (<3% sugars) with >90% of water content [14,15]. It is grown in temperate to tropical regions worldwide [14] and the crop grows well in Florida [16]. Winter melon is often recognized for its nutritional and medicinal properties, especially in Asian countries [14,17]. It is a good source of amino acids (such as three phenolic amino acids [18]), organic acids (tartronic acid with great potential to play a role in inhibiting the conversion of carbohydrates into fats [19,20]), mineral elements (such as Ca, K, Mg, Fe, Se [14,21]) and vitamins (such as vitamin C, riboflavin and Niacin [14]). A number of medicinal properties such as anxiolytic, anticonvulsant, antidepressant, anti-inflammatory and analgesic, antiasthmatic, hypolipidemic effects have been observed from winter melon fruit [14,17,21,22]. Pharmacological activities have also been revealed in seeds, fruit peel and plant stems [22].

Previous research showed that winter melon juice contains less than 3% soluble solids content (SSC), and the juice has potential for stand-alone and blends with other fruit and vegetable juices [18,23]. For this study, we compared different winter melon cultivars and selected a waxy-coated, round cultivar that produces low sugar, with physically stable juice (less cloudloss) and less off-odor [18].

Anaerobic soil disinfestation (ASD) is a method of soil disinfestation that is under development for use in crops that were previously produced using the fumigant methyl bromide prior to planting. In Florida, ASD is based on the incorporation of a labile carbon source combined with pasteurized poultry litter, irrigation to soil saturation, and tarping with gas-impermeable film for about three weeks [24]. The growth of soil anaerobic microorganisms increases as a direct response to a readily available carbon source and anaerobic conditions, producing organic acids as a result of anaerobic decomposition. These compounds are often lethal to soil-borne plant pathogens and plant-parasitic nematodes. Moreover, changes in resident soil microbial communities, fostered by resource availability in soil and the rhizosphere, may actively contribute to disease suppression. While it was reported that ASD affected plant growth and increased tomato yield [25], there are no published reports on the effects of ASD on fruit quality of winter melons.

In Florida, winter melon harvest season starts in late May/early June and ends in late January/early February [16]. To secure a stable supply of fruit for processors, technology needs to be developed to provide fruit during the four-month off-season. Typically, fruit are stored in cold temperatures for extended periods of time. However, similarly to other chilling sensitive fruit, such as mango [26] and Japanese apricot [27], winter melons suffer chilling injury when stored below 13 °C [15,28,29]; therefore room temperature is recommended for long-term storage [15]. A long-term storage experiment showed that many winter melon breeding lines could be stored at ambient temperature up to 120 d [30]. During storage, sugar, crude fiber, calcium and dry matter content increased while ascorbic acid and pectin content decreased [30]. However, to date, there is limited knowledge of how fruit quality and its juice are affected by long-term storage.

The objectives of the current research were to determine (1) if soil amendment by ASD affects winter melon fruit storability and juice processing properties and (2) the effects of long-term storage of the fruit on juice quality.

2. Materials and Methods

Winter melon [*Benincasa hispida* (Thunb.) Cogn] cv. 'Large Round' (round type with thick waxy coating) was directly seeded into raised beds treated with either ASD or fertilizer only, at the USDA Horticultural Research Laboratory Picos Farm in Fort Pierce, Florida, USA in fall 2020. After 120 d, fruit were harvested on 3 February 2021 and stored in a 20 °C dark room for up to 120 d. Fruit weight was measured during storage, and juice was extracted from 1-day and 120-day stored fruit. Juice processing properties and physicochemical attributes were determined, and effects of soil amendment and storage time on fruit and juice quality were compared. The experiment was designed with three field replicates.

2.1. Plant Materials and Field Treatment

Six raised beds (30 m long, 0.9 m wide, 0.25 m high and 1.8 m between centers) were constructed and three each randomly assigned to ASD or control to represent three field replications. Each control bed received a commonly implemented application of pre-plant compound fertilizer (10N-10P_2O_5-10K_2O) at a rate of 560 kg ha^{-1}; supplemental liquid fertilizer was applied via irrigation as needed. Pasteurized, pelleted poultry litter (ChickMagic, Cold Spring Egg Farm, Inc., Whitewater, WI, USA) applied at 15 mg ha^{-1} and feed-grade, black strap molasses (Double S Liquid Feed Service, Danville, IL, USA) at 13.9 m^3 ha^{-1} was used to establish ASD treatments [31]. Amendments were applied to the bed top and incorporated to a soil depth of 15 cm using a rotary cultivator. VaporSafe® totally impermeable film (TIF, 0.03 mm white on black, Raven Industries Inc., Sioux Falls,

SD, USA) was used to cover all the beds. Each ASD-treated bed was irrigated with 5 cm of water applied through two drip lines established on each bed [32]. Winter melon was direct-seeded four weeks after ASD treatments were initiated using in-bed spacing of 1.22 m between holes and three seeds per hole. Plants were thinned to two plants per hole after emergence. Each replicate contained 50 plants. A single harvest of fruit sized larger than 4.54 kg was conducted 120 d after planting.

2.2. Fruit Storage and Weight Loss

Melons were held on trellis shelves without packaging, and space between melons was maintained in storage (Figure 1A,B). Storage temperature was 20 °C, with relative humidity of 80%. After one or 120 d storage, three melons × three replicates per treatment were processed. For weight loss measurement, fruit weight was measured weekly.

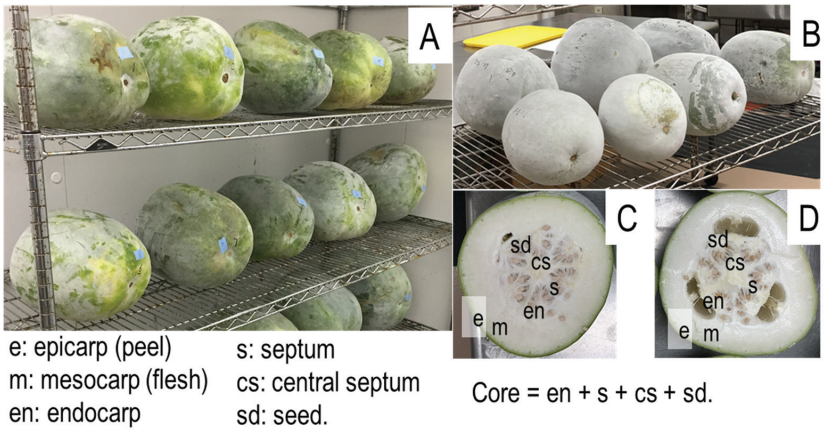

Figure 1. Surface waxy coat and internal structure of winter melon fruit at harvest and after 120 d storage at 20 °C. (**A**): Fruit, at harvest, covered with different levels of waxy coating; (**B**): Fruit, after 120 d storage at 20 °C, fully covered with thick waxy coating; (**C**,**D**): Transverse section of fruit at harvest (**C**) and after 120 d storage at 20 °C (**D**).

2.3. Juice Processing

Juice samples were extracted from melons in a lab-scale processing system. Briefly, after careful washing with fruit detergent (Fruit Cleaner 395, JBT Food Tech., Lakeland, FL, USA), melons were rinsed, and air-dried. After removing the peel (about 3 mm) and core (Figure 1C,D), the flesh was cut into 2 cm cubes, and juiced using a Juicerator (Model 6001, Acme Juicer Mfg Co, Sierra Madre, CA, USA) with a milk filter (Schwartz Manufacturing Co., Two Rivers, WI, USA) at 2500–3000× *g* for 1 min. Then, the juice was centrifuged at 17,000× *g* for 30 min, and pulp-free juice samples were collected for further quality analysis. Pulp from the filter and centrifuged pellets were merged as "pulp". Aliquots of the supernatant were taken for dry juice weight, soluble solids content (SSC), titratable acidity (TA), volatiles and non-volatiles analysis, and the measurements were taken from freshly harvested fruit or after storage at −80 °C (volatiles) for up to 4 months.

2.4. Juice Yield and Processing Waste

Material weight was taken at each processing stage, including whole fruit after wash, peel, flesh and core, filtered pulp and centrifuged pellet (pulp) and pulp-free juice. Thus, juice production, edible portion (flesh), and waste were calculated.

2.5. Physicochemical Quality Attributes

2.5.1. Particle Size and Juice Stability

In order to study the particle size, zeta potential, and juice stability, juice samples, 15 mL × 3 test tubes per replicate, were heated at 100 °C in a water bath for 10 min to inactivate the enzymes. After cooling the juice samples to 25 °C under tap water, 45 mL juice sample per replicate was collected and centrifuged for 10 min at 360× *g*. The supernatant was used for particle size, zeta potential, and juice opacity measurements. For particle size and zeta potential, the samples were analyzed using a Zetasizer (Malvern Panalytical, Malvern, UK). For juice opacity, juice samples were transferred to a cuvette and absorbance at 660 nm was recorded using a UV–visible spectrophotometer (UV-2401PC, Shimadzu, Columbia, MD, USA) [33]. High absorbance readings correspond to high opacity.

2.5.2. Juice Dry Matter and Non-Soluble Dry Matter

Juice, 100 g per replicate, was vacuum-dried at 55 °C. The total dry matter was directly measured, and non-soluble dry matter was obtained by subtracting SSC from the total dry matter. All were expressed as percentage of total juice.

2.5.3. SSC, pH and TA

Juice SSC was measured from the supernatant with a refractometer (RX5000α, Atago, Tokyo, Japan). TA and pH were measured by using a titrator equipped with a robotic autosampler (model 855, Metrohm, Herisau, Switzerland), a dosing interface (Dosino model 800, Metrohm, Herisau, Switzerland) and controlling software (Tiamo v. 2.5, Metrohm, Herisau, Switzerland). The principle procedure for TA determination was to titrate 10 mL of juice sample with 0.1 N NaOH to pH 8.1, the TA value was expressed as $[H^+]$ concentration, mmol L^{-1} [34].

2.5.4. Measurement of Volatile Compounds

Juice sample, 6 mL, was transferred to a 20-mL vial sealed with Teflon-lined septa (Gerstel Inc., Linthicum, MD, USA). Volatiles were analyzed by headspace (HS)—solid phase microextraction (SPME)—gas chromatography (GC)—mass spectrometry (MS) system, equipped with an autosampler and a cooling system to maintain samples at 4 °C [35,36]. Juice samples were pre-heated for 30 min at 40 °C. A 2 cm SPME fiber (50/30 μm DVB/Carboxen/PDMS, Supelco, Bellefonte, PA, USA) was then exposed to the headspace for 60 min at 40 °C. After exposure, the SPME fiber was inserted into the GC-MS (Model 7890 GC and 5975 N MS, Agilent, Santa Clara, CA, USA) injector to desorb the extract for 15 min at 250 °C. A DB-5 column (60 m × 0.25 mm i.d., 1.00 μm film thickness, J&W Scientific, Folsom, CA, USA) was used to separate volatiles. MS settings were from 30 to 250 *m/z* and ionized at 70 eV. Volatile compounds were identified by matching their spectra with those from the National Institute of Standards and Technology (NIST)/Environmental Protection Agency (EPA)/National Institutes of Health (NIH) Mass Spectral Library (NIST 14; WebBook, SRD69) and authentic volatile compound standards, as well as by comparing their RIs with corresponding literature data [23]. The concentrations of volatiles in the juices were calculated from the total ion current (TIC) of headspace samples, using the regression equations, determined by injecting five sequential concentrations of each standard to obtain a TIC calibration [37]. The calibration curves were constructed by adding chemical standards (Sigma-Aldrich, St. Louis, MO, USA) to a deodorized juice matrix. Deodorization of juice was performed by a rotary evaporator (R-215, Büchi, Flawil, Switzerland) equipped with a heating bath (B-491) set at 40 °C, a recirculating chiller (F-114) set at −3 °C, and a vacuum controller (V-855) operated under 70–20 mbar with a rotary speed 200–240 rpm until SSC reached 45%. Deodorized juice was then reconstituted to SSC 2.14% (original SSC level) by using DI water as the deodorized juice matrix. The chemical standards with C6 or smaller molecules were added directly into the deodorized juice matrix. The chemicals with >C6 molecules were prepared in two steps, first adding the standards into methanol to make a 1% stock solution; then, the stock solutions were added to the deodorized juice matrix.

All chemicals were mixed, and the concentrations were based on the abundance of each chemical in the juice samples. The concentration ranges were 31.25–500 μL L^{-1} in hexanal, (*E*)-2-hexenal and 1-hexanol, 0.3125–5 μL L^{-1} in acetaldehyde, methanethiol, dimethyl sulfide, pentanal, and dimethyl disulfide, and 1.5625–25 μL L^{-1} in all others. Each mixture had three replicates that were averaged.

2.5.5. Measurement of Nonvolatile Compounds

Juice (supernatant) was filtered with a 0.2 μm PES syringe and spiked with an internal standard, $^{13}C_6$-D-fructose, at a final concentration of 40 mg L^{-1}. LC-MS/MS analyses were performed with an 1290 Infinity II UPLC coupled with a 6470 triple quadrupole MS (Agilent, Santa Clara, CA, USA). The InfinityLab Poroshell 120 HILIC-Z column (2.1 × 150 mm, 2.7 μm, Agilent, Santa Clara, CA, USA) was held at 15 °C. Mobile A consisted of water, 20 mM ammonium acetate (pH 9.3), 5 μM medronic acid and mobile B was acetonitrile. Initial UPLC conditions were 90% B, 10% A for 1 min, followed by a linear gradient to 78% B at 8 min, 60% B at 12 min, and 10% B at 15 min. After flushing with 10% B for 3 min, the column was re-equilibrated with initial conditions (90% B, 10% A) for 10 min. The flow rate was kept constant at 0.4 mL min^{-1}. The Agilent Jet Stream ESI source was operated with a gas temperature of 225 °C, gas flow of 9 L min^{-1}, nebulizer pressure of 30 psi, sheath gas temperature of 375 °C, sheath gas flow of 12 L min^{-1}, and a capillary voltage (+ and −) of 3000 V. The MS was operated in dMRM mode and compound-specific fragmentor and collision energy voltages are listed in Supplementary Table S1. Compounds were identified by the comparison of MRM transitions listed in Supplementary Table S1 and retention times with analytical standards. Quantification of the identified compounds was performed by integrating the area under the chromatographic peak and calculating the amount of each compound based on standard curves. Standard curves were run in groups according to abundance levels [amino acids (1–90 mg L^{-1}); higher abundant sugars (150–12,500 mg L^{-1}); lower abundant sugars and organic acids (10–250 mg L^{-1}); nucleosides (0.004–6 mg L^{-1}); vitamins B2 and B7 (0.02–1 mg L^{-1}); vitamins B1, B3, B5, B6 and B12 (0.03–1 mg L^{-1}); vitamin C and malic acid (90–5000 mg L^{-1})]. A minimum of five points were used in each standard curve ($R^2 \geq 0.99$). The vitamin C and malic acid standards were prepared fresh immediately before their injection while the other standards were stored as stock solutions and then diluted with LC/MS water before injection. Each treatment group had three replicates that were averaged. MassHunter Quantitative Analysis software (Agilent, Santa Clara, CA, USA) was used for data analysis.

2.6. Statistical Analysis

All measurements were replicated three times using the three field replications. JMP Version 16 (SAS Institute, Gary, NC, USA) was used for analysis of data. Analysis of variance (ANOVA), and principal component analysis (PCA) was used to evaluate the effect of soil treatment and storage time on juice processing and quality attributes. Two independent samples *t*-Test (TTEST) was used to compare the effect of soil and storage treatments.

3. Results and Discussion

3.1. Weight Loss during Fruit Storage

Fruit harvested from the ASD treatment lost 15.6% of the total weight after 120 d storage, 3.2% more than the control fruit (Figure 2). The greater weight loss in ASD fruit was observed from the beginning and throughout the entire storage time (Figure 2). In the first week, the daily weight loss in ASD fruit was 0.39%, decreased to 0.24% in the next three weeks, further decreased to 0.10–0.18% until 87 d storage and finally decreased to 0.05–0.06% daily (Figure 2). The control fruit had a 0.30% daily weight loss in the first week, decreased to 0.10–0.16% in the following seven weeks, and further decreased to 0.03–0.09% in the last ten weeks (Figure 2). The higher weight loss rate for ASD fruit could be attributed to the lower maturity of the fruit at harvest as observed by a reduced waxy coating cover (Figure 1). Nevertheless, the difference in daily weight loss between the two

soil treatments remained even after 60 d storage after the waxy coating had fully developed on both ASD and control fruit (Figure 1).

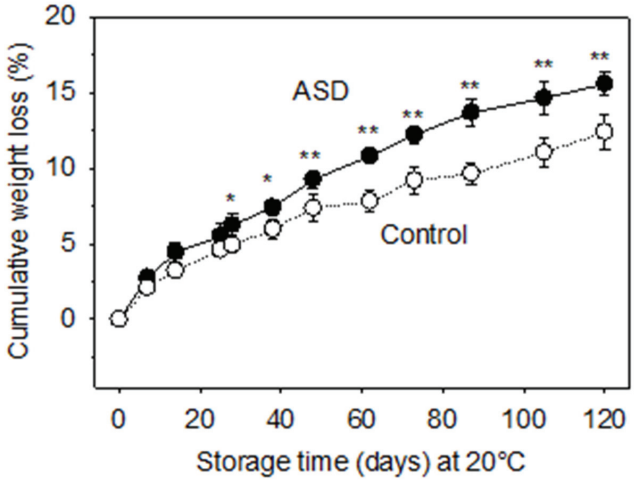

Figure 2. Comparison of weight loss of fruit grown in ASD (black dots) and non-treated soils (white dots). Fruit was stored at 20 °C for up to 120 d. * or ** indicate significant difference at 0.05 or 0.01, respectively, between ASD and control at each storage time.

The transversal section of fresh fruit showed that the cavity was full of endocarp tissue, septum, central septum and seeds at harvest, but after 120 d storage, the endocarp tissue shrank (Figure 1C,D). However, soil treatment and storage did not significantly affect the total core tissue weight (Table 1).

Table 1. Effect of soil treatment and storage time on juice production and waste of winter melons.

Storage Time (d)	Percentage of Each Fruit Portion (%)				ANOVA (Prob > |t|)		
	1		120		Soil Treatment (S)	Storage Time (T)	S × T
Soil Treatment	ASD	Control	ASD	Control			
Flesh	67.05	65.02	67.58	66.84	0.033 * [z]	0.060	0.263
Juice	56.68	53.70	55.43	54.62	0.008 **	0.772	0.081
Peel	11.48	11.69	12.01	12.36	0.693	0.401	0.922
Core	21.47	23.29	20.41	20.80	0.309	0.118	0.503
Pulp	10.36	11.33	12.15	12.22	0.170	0.005 **	0.231
Total waste	43.32	46.30	44.57	45.38	0.009 **	0.741	0.081

[z] *, ** represent significant levels at 0.05, and 0.01, respectively.

Water loss leads to softening, shriveling, discoloration, and general deterioration of appearance for most fruits and vegetables. Generally, when weight loss exceeds 4 to 6% of total fresh weight, the fresh produce becomes unmarketable or unappetizing [38,39]. However, we did not observe visible deterioration on the surface or in the flesh of fruit after 120 d storage even when the cumulative weight loss was over 15.6%. Similar results were reported in pumpkins that lost 18–21% weight during 120 d storage at 27–31 °C without visible deterioration [40].

3.2. Juice Production and Waste

The control and ASD-produced fresh fruit had 67% and 65% flesh (mesocarp, Figure 1C,D), respectively, and changed little during the 120 d storage (Table 1). Juice production was 11.33% and 10.36% lower by weight than the flesh in control and ASD fresh fruit, respec-

tively, due to the pulp being removed by filtration and centrifugation of pellets (Table 1). The pulp had more than 90% water content (data not shown) and could possibly be reduced by increasing filtration pressure; pulp waste could also potentially be used as a source of fiber-rich food supplement. The winter melon juice yield was between 53.70–56.68% of total fruit weight regardless of the soil treatments or storage time, much higher than orange juice yield, which is lower than 50% of total fruit weight [41]. ASD fruit produced more juice with less pulp (Table 1). During the long storage period at 20 °C, fruit maturation progressed, resulting in more pulp (Table 1).

3.3. Particle Size and Stability of Juice

Cloud stability is a desirable attribute in fruit juices; it depends on the surface charge of particles in the juice (charge repulsion can keep the cloud particles from aggregating) and the particle size. The zeta potential is a key indicator of the stability of particles in juice, which characterizes the charge of the particle surfaces that affect the precipitation of particles in juice. The higher the absolute value of the zeta potential (negative or positive), the less likely the particles in a cloudy juice will adhere together to form aggregates (flocculation) and sediment, resulting in more stable the juice. Zeta potential and particle size analyses have been proven to be valuable tools for prediction of juice stability and shelf life [42–44].

At the same storage time, particle size in ASD juice was smaller than in control juice; and the absolute values of zeta potential of ASD juice samples were larger than those of the control juice samples (Table 2), indicating ASD juice was more stable than control juice. However, based on the criterion that particles with an absolute value of zeta-potential larger than 15 mV are expected to be stable [45], both the ASD and the control juice could not be considered as "stable", because their absolute values of zeta potential were less than 15 mV, which were 11.58–11.68 mV and 8.77 mV, respectively, for ASD and control juice. Storing fruit for 120 d did not affect the zeta potential value of the juice, though storage increased the particle size in both ASD and control fruit juice (Table 2). Taking the particle size and zeta potential data together, the juice from fresh ASD-grown fruit was more stable than that derived from the control fruit.

Table 2. Effect of soil treatment and storage time on particle size and juice stability of winter melon juice samples.

Storage Time (d)	Percentage of Each Fruit Portion (%)				ANOVA (Prob > |t|)		
	1		120		Soil Treatment (S)	Storage Time (T)	S × T
Soil Treatment	ASD	Control	ASD	Control			
Absorbance of supernatant (OD 660 nm)	0.122	0.063	0.214	0.154	0.0001 *** [z]	0.0048 **	0.0064 **
Particle size (nm)	533.1	682.4	700.4	748.2	0.0001 ***	0.0001 ***	0.0215 *
Zeta potential (mV)	−11.580	−8.769	−11.680	−8.767	0.0008 ***	0.2614	0.1843

[z] *, **, *** represent significant levels at 0.05, 0.01 and 0.001, respectively.

3.4. Sugars, Acids and Non-Soluble Dry Matter of Juice

The SSC of fresh ASD fruit was 2.14 °Bx, and remained during 120 day storage, however, the value was 2.43 °Bx in the control juice, significantly higher than the ASD fruit juice (Table 3). Interestingly, SSC in the control juice decreased during the 120 d storage period, in spite of the 13–16% fruit water loss (Figure 2 and Table 3). Our results do not agree with the Pandey et al. [30] report, which showed that the SSC increased in all 19 genotypes of winter melons stored at room temperature. In many fruits, the increase in SSC is usually due to the hydrolysis of starch into soluble sugars or as a consequence of water loss [46,47]. The cultivar used in this experiment underwent a decrease in soluble solids likely due to increased respiration and/or metabolic reactions that convert soluble solids to insoluble, as has been reported for many other fruits and vegetables [47]. Fructose and glucose, which

account for about 40–50% of SSC in fresh juice, decreased to approximately 35–40% after 120 d storage (Table 3). Wills et al. [48] reported that glucose and fructose in mature winter melon fruit were 0.5% each—similar to our results (Table 3), however, the levels were as high as 0.8–0.9% in immature fruit, indicating that mature fruit should be used if juice with low sugar content is desired. Arabinose, galactose, and xylose, the non-cellulosic neutral sugar components of cell walls were detected, and arabinose was the predominant component (approx. 0.1%), followed by galactose (approx. 0.015%) and xylose (approx. 0.0005%) (Table 3). The results are different from Gross and Sams [49] who reported that galactose was the major component in cucurbit fruit.

Table 3. Effect of soil treatment and storage time on total dry matter, soluble solids content, pH, titratable acidity, non-soluble dry matter and individual sugars and acids of winter melon juice samples.

Storage Time (d)	Percentage of Each Fruit Portion (%)				ANOVA (Prob > |t|)		
	1		120		Soil Treatment (S)	Storage Time (T)	S × T
Soil Treatment	ASD	Control	ASD	Control			
Total dry matter (%)	2.23	2.57	2.25	2.42	0.0010 *** [z]	0.1229	0.0630
Soluble solids content (°Bx)	2.14	2.43	2.11	2.27	0.0010 ***	0.0448 *	0.1241
Non-soluble dry matter (%)	0.093	0.143	0.136	0.146	0.0010 ***	0.0026 **	0.0046 **
pH	5.45	5.60	5.19	5.21	0.1909	0.001 ***	0.3238
Titratable acidity (H^+ mmol L^{-1})	7.71	6.09	13.94	14.21	0.5065	0.001 ***	0.3624
Fructose (%)	0.5525	0.5246	0.4081	0.4433	0.8879	0.0019 **	0.2416
Glucose (%)	0.4162	0.4291	0.3124	0.3447	0.4730	0.0140 *	0.7553
Sucrose (%)	n.d. [y]	n.d.	n.d	n.d.			
Arabinose (%)	0.1060	0.1031	0.0822	0.0879	0.7569	0.0022 **	0.3625
Galactose (%)	0.0161	0.0193	0.0132	0.0137	0.2527	0.0202 *	0.3708
Xylose (%)	0.0005	0.0007	0.0004	0.0004	0.1382	0.0152 *	0.0827
Mannose (%)	n.d.	n.d	n.d.	n.d			
Rhamnose (%)	n.d.	n.d	n.d.	n.d			
Malic acid (%)	0.1297	0.1023	0.0836	0.0702	0.1327	0.0125 *	0.5850
Citric acid (%)	0.0056	0.0124	0.0643	0.0639	0.4688	0.0001 ***	0.4210
Succinic acid (%)	n.d.	n.d	n.d.	n.d			
Tartronic acid (%)	0.0017	0.0017	0.0016	0.0016	0.6643	0.0690	0.9398
Galacturonic acid (%)	n.d.	n.d	n.d.	n.d			

[z] *, **, *** represent significant levels at 0.05, 0.01 and 0.001, respectively. [y] Not detectable.

Winter melon juice was slightly acidic, with a pH value of 5.5 when fruit was fresh, and increased in acidity to pH 5.2 after 120 d storage (Table 3). The TA was 7.71 and 6.09 mmol L^{-1} in fresh ASD and control juice samples, respectively, and almost doubled after 120 d storage (Table 3). However, malic acid, the most abundant acid, decreased approximately 30% after 120 d storage. Conversely, citric acid increased 5–11 times during storage, and became almost comparable to malic acid; thus the sum of malic and citric acids increased by 10–15% following storage (Table 3).

Tartronic acid occurs naturally in cucumber and winter melon, and may play a critical role in inhibiting the conversion of carbohydrates into fats in animal studies [19,20]. Cucumber and winter melon breeders often set tartronic acid content as a quality attribute [50]. However, our data showed that tartronic acid contents were about 1% of the total acids, and storage did not significantly alter this content (Table 3).

The non-soluble dry matter, an attribute closely correlated to the dietary fiber content [18], was significantly higher in the control juice, and the content significantly increased during storage (Table 3), indicating that along with maturity progress and water loss during storage, cell wall cellulose, hemicelluloses and lignin accumulated (Table 3). Similar results were found in many plants [51], and confirmed with the storage of winter squash [52].

3.5. Nutritional Composition of Juice

Six vitamins, 17 free amino acids and five nucleosides were detected by LC-MS/MS (Table 4). Vitamin C content in fresh juice was 135–140 mg L^{-1}, which agrees with a previous report in which the extraction solvent was 3% metaphosphoric acid [53]. After 120 d storage at 20 °C, vitamin C was reduced by 25% (Table 4). Five B vitamins were detected: vitamin B5, B1, B6, B2 and B3 (Table 4). The abundant vitamin B5 was higher in ASD fruit samples (Table 4). After 120 d storage, vitamins B1 and B6 increased, but B2 and B3 decreased (Table 4). B7 was not detected in winter melon juice.

Table 4. Effect of soil treatment and storage time on vitamins, amino acids and nucleosides of winter melon juice samples.

Storage Time (d)	Concentration (mg L^{-1})				ANOVA (Prob > |t|)		
	1		120		Soil Treatment (S)	Storage Time (T)	S × T
Soil Treatment	ASD	Control	ASD	Control			
Thiamine (Vitamin B1)	0.113	0.066	0.141	0.121	0.0690	0.0287 * [z]	0.4166
Riboflavin (Vitamin B2)	0.031	0.031	0.019	0.017	0.7735	0.0005 ***	0.7573
Niacin (Vitamin B3)	0.022	0.032	0.011	0.010	0.3773	0.0063 **	0.2311
Pantothenic acid (Vitamin B5)	0.682	0.510	0.695	0.604	0.0155 *	0.2437	0.3746
Pyridoxine (Vitamin B6)	0.012	0.009	0.052	0.052	0.8732	0.0020 **	0.8610
Biotin (Vitamin B7)	n.d. [y]	n.d.	n.d.	n.d.			
Cobalamin (Vitamin B12)	n.d.	n.d.	n.d.	n.d.			
Ascorbic acid (Vitamin C)	139.988	135.279	104.342	101.150	0.4560	0.0001 ***	0.8841
Total vitamins	140.848	135.928	105.260	101.955	0.0798	0.0001 ***	0.6582
Alanine	0.667	0.653	0.757	0.737	0.6947	0.0733	0.9371
Arginine	59.121	91.057	122.451	113.350	0.5127	0.0332 *	0.2533
Aspartate	21.612	15.943	76.286	60.589	0.1267	0.0001 ***	0.4468
Cysteine	n.d.	n.d.	n.d.	n.d.			
Glutamate	0.557	0.582	2.179	2.158	0.2843	0.0001 ***	0.3952
Glutamine	279.663	406.499	397.641	415.866	0.2718	0.3305	0.4027
Glycine	4.356	6.104	5.044	5.453	0.1770	0.9802	0.3849
Isoleucine	22.341	27.581	33.444	33.015	0.4255	0.0203 *	0.3514
Leucine	22.126	28.325	17.219	18.030	0.0942	0.0034 **	0.1828
Lysine	12.824	13.489	16.022	16.675	0.6045	0.0311 *	0.9964
Methionine	3.722	5.060	4.689	5.607	0.0632	0.1859	0.6983
Phenylalanine	27.227	33.834	46.009	48.373	0.3701	0.0078 **	0.6653
Proline	3.142	4.750	4.053	3.815	0.1108	0.9742	0.0422 *
Serine	10.367	9.597	10.685	11.062	0.7763	0.2176	0.4143
Threonine	6.981	8.930	9.710	9.941	0.3525	0.1289	0.4587
Tryptophan	75.083	75.835	77.331	77.424	0.9668	0.8504	0.9741
Tyrosine	34.093	41.208	48.777	48.932	0.2902	0.0082 **	0.3098
Valine	20.936	25.544	27.458	28.440	0.4517	0.2194	0.6217
Total amino acids	604.817	794.990	899.755	899.468	0.2591	0.0062 **	0.3564
Adenosine	29.619	26.295	14.651	13.459	0.1360	0.0001 ***	0.4565
Cytidine	1.671	0.700	1.558	0.940	0.0104 *	0.7972	0.4801
Guanosine	8.167	4.249	4.263	2.955	0.0743	0.0755	0.3353
Inosine	0.014	0.015	0.003	0.002	0.9147	0.0001 ***	0.5193
5-Methyluridine	n.d.	n.d.	n.d.	n.d.			
Uridine	2.319	2.432	1.167	0.834	0.7391	0.0027 **	0.5064
Total nucleosides	41.790	33.691	21.641	18.189	0.0262 *	0.0001 ***	0.2628

[z] *, **, *** represent significant levels at 0.05, 0.01 and 0.001, respectively. [y] Not detectable.

Glutamine was the most abundant amino acid, followed by arginine, tryptophan, aspartate, tyrosine, phenylalanine, isoleucine, and valine (Table 4). The total amino acids were 604 and 794 mg L^{-1} at day 1 and increased to 900 and 899 mg L^{-1} after 120 d storage, in ASD and control fruit juice samples, respectively, with no significant differences between the two soil treatments (Table 4). The data agreed with previous reports: tryptophan, tyrosine, phenylalanine, the three phenolic amino acids were major components [18,23].

Dong et al. [54] reported similar total amino acids in winter melon pulp, although the major components were different [14,54].

Nucleosides and nucleotides are essential in a large number of biological processes. They are the precursors of the nucleic acids that make up DNA and RNA. Moreover, nucleosides and nucleotides participate in other metabolic functions as they form part of biosynthetic routes, operate in the transfer of chemical energy, are components of some co-enzymes, and play an important role as biological regulators [55]. Five nucleosides were detected, with adenosine as the greatest component, followed by guanosine (Table 4). Adenosine, inosine and uridine decreased after 120 d storage, and cytidine and total nucleosides were higher in the ASD-derived fruit juice samples than in the control (Table 4).

A PCA was performed to project the juice nutritional components onto a 2-component plot (Figure 3). The PCA discriminated 120 d storage fruit samples from 1 d storage on both Component 1 and Component 2, explaining 71.3% of the variation in the first two components (Figure 3a,b). Nutritional components from fresh fruit were on the upper-left side, including vitamin C, B2 and B3, leucine, and all nucleosides (guanosine and cytidine being on the lower left part of the quadrant) (Figure 3b). However, most of the amino acids, located on the right side (Figure 3b), were associated with 120 d stored samples.

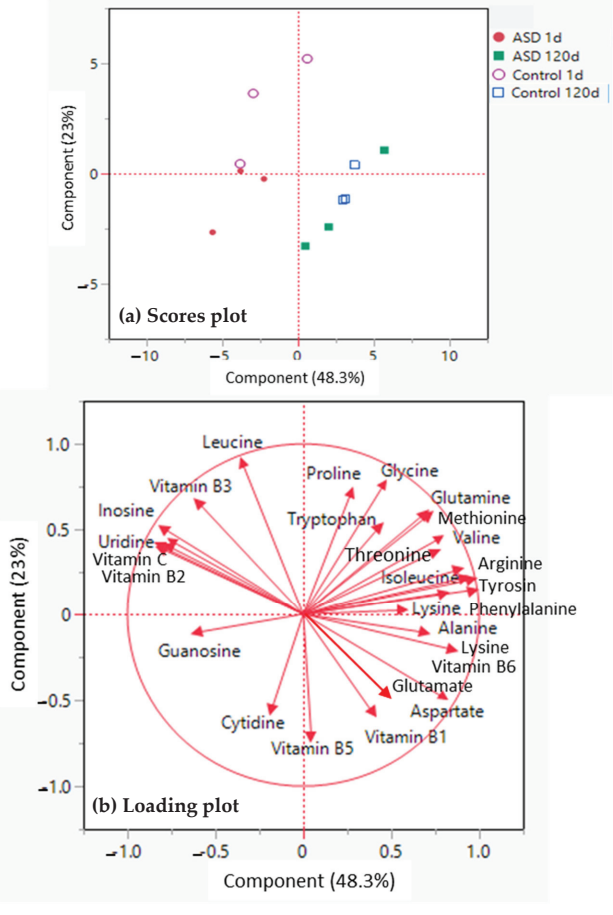

Figure 3. Principal components analysis (PCA) of 6 vitamins, 17 amino acids, and 5 nucleosides in winter melon juice samples extracted from ASD treated or control fruit that were stored at 20 °C for 1 or 120 d. (**a**) Scores plot and (**b**) Loading plot.

3.6. Volatile and Non-Volatile Profile of Juice

Fifteen volatile compounds were identified by GC-MS (Table 5). The major compounds were aldehydes, including acetaldehyde, pentanal, (*Z*)-3-hexenal, hexanal, (*E*)-2-hexenal, (*E*,*E*)-2,4-hexadienal, nonanal, (*E*,*Z*)-2,6-nonadienal, and (*E*)-2-nonenal. They accounted for about 97% of the total volatiles as measured by total ion current (Table 5). The key flavor notes associated with these volatiles include green, grass, fat and vegetable soup, descriptors which are not favorable in stand-alone juice or juice blends [56,57]. There were three sulfur compounds, methanethiol, dimethyl sulfide, and dimethyl disulfide, which were very low in concentration, but could potentially contribute strong off-odor [58,59]. There was one monoterpene hydrocarbon (d-limonene) with a very light citrus note, one alcohol (1-hexanol) with green/grass note, and a rare compound, methoxy-phenyl oxime which has been reported sporadically without a clear flavor descriptor [60].

Table 5. Effect of soil treatment and storage time on volatile profile of winter melon juice.

Storage Time (Days)	Concentration (ng mL^{-1})				ANOVA (Prob > |t|)		
	1		120		Soil Treatment (S)	Storage Time (T)	S × T
Soil Treatment	ASD	Control	ASD	Control			
Acetaldehyde	1.38	3.33	1.40	3.97	0.0176 * [z]	0.7099	0.7322
Methanethiol	1.63	1.65	1.42	1.51	0.8270	0.4611	0.8703
Dimethyl sulfide	0.93	1.50	0.95	0.53	0.8121	0.1443	0.1266
Pentanal	2.04	2.49	2.03	2.44	0.0160 *	0.8678	0.9045
Dimethyl disulfide	1.21	1.70	1.12	1.46	0.0097 **	0.2641	0.6028
(*Z*)-3-Hexenal	4.34	6.32	4.31	6.22	0.0010 ***	0.9059	0.9391
Hexanal	299.26	340.17	293.92	340.42	0.0075 **	0.8643	0.8512
(*E*)-2-Hexenal	190.65	242.69	190.57	242.93	0.0004 ***	0.9946	0.9897
1-Hexanol	74.30	179.65	74.72	198.77	0.0265 *	0.8405	0.8472
Methoxy-phenyl oxime	6.13	5.31	6.18	5.09	0.2104	0.9081	0.8548
(*E*,*E*)-2,4-Hexadienal	4.06	5.39	3.95	5.52	0.0203 *	0.9908	0.8339
D-Limonene	8.58	1.70	8.71	1.69	0.0100 **	0.9806	0.9797
Nonanal	1.58	4.07	1.60	4.11	<0.0001 ***	0.9479	0.9917
(*E*,*Z*)-2,6-Nonadienal	13.98	22.37	14.01	22.44	0.0907	0.9917	0.9970
(*E*)-2-Nonenal	3.59	7.76	3.59	7.81	<0.0001 ***	0.9737	0.9742
Total	613.66	826.11	608.49	844.91	0.0002 ***	0.9532	0.9100

[z] *, **, *** represent significant levels at 0.05, 0.01, and 0.001, respectively.

Most compounds were affected by soil treatment, with the ASD fruit having lower volatile concentration in 11 of 15 compounds, and the total concentration was 25% lower than in the control fruit (Table 5). Those volatiles generally contribute to "green/vegetable" notes, which is not desirable for fruit juice; thus, ASD fruit and juice are presumed to have better flavor quality. Lower volatile abundance is preferred regardless of whether the winter melon juice is used for stand-alone or blended fruit juice. Volatiles were not affected by storage duration, and there was no interaction between soil treatment and storage times (Table 5). PCA analysis confirmed the conclusion that volatile profiles were discriminated by ASD treatment, but not storage time (Figure 4). The PCA discriminated ASD-derived fruit juice samples from the control samples on Component 1, which explained 56.1% of the variation (Figure 4a,b). Most juice volatiles were associated with the control samples, indicating more off-odor volatiles in the control juice (Figure 4).

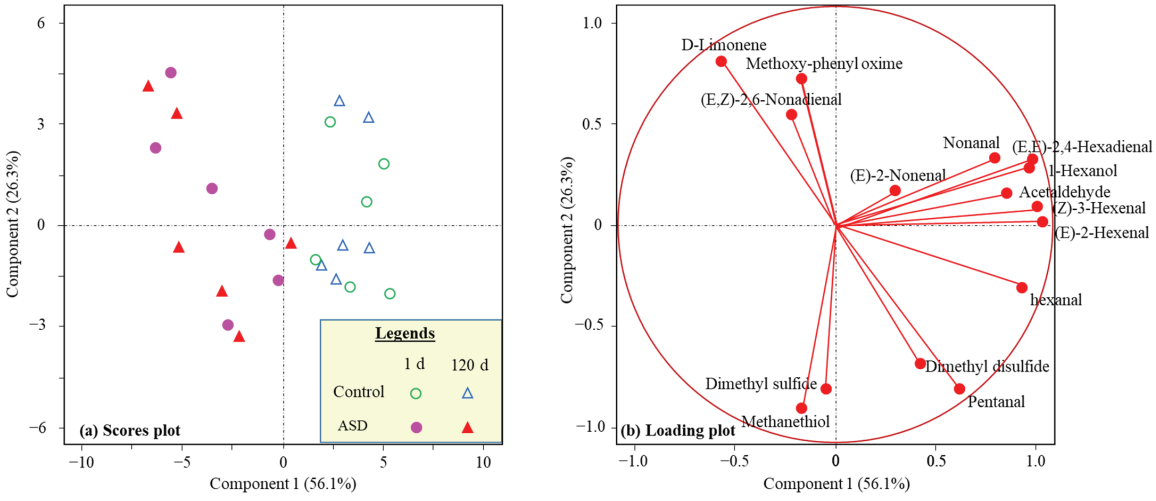

Figure 4. Principal component analysis (PCA) of 16 volatile compounds in winter melon juice samples extracted from ASD treated or control fruit that were stored at 20 °C for 1 or 120 d. (**a**) Scores plot and (**b**) Loading plot.

From this work, we conclude that the gap in fresh fruit supply during the four-month off season in winter melon could be made up by long-term, room temperature stored fruit. The long-term storage resulted in substantial water loss, but there was no loss due to decay. The long storage also did not cause consistent loss of flavor or nutritional quality. This research provides strong evidence to the industry that low-cost room temperature storage would ensure stable fruit supplies for the winter melon juice industry.

4. Conclusions

Fruit harvested from the ASD soil amendment treatment had higher juice yield due to reduced core and peel waste. However, ASD fruit lost more weight during 120 d storage at room temperature. Juice from ASD treated fruit was more stable with a greater magnitude of zeta potential, and had lower SSC, non-soluble dry matter, and total volatiles. The volatile components were primarily sulfur compounds, and carbon-6 aldehydes, principally associated with off-flavor in juice. Juice samples resulting from ASD-produced fruit had higher vitamin B5 and cytidine in their nutritional profiles. Storing fruit at 20 °C for 120 d caused fruit weight loss of 12.4 to 15.6%. However, storage did not cause significant changes in the volatile profiles, although it increased juice pulp, non-soluble dry matter, and dramatically increased TA content, which was due primarily to an increase in citric acid. Storage also decreased SSC and pH. Six out of 16 free amino acids increased and only one decreased; however, three out of five nucleosides decreased. Vitamins B1 and B6 increased, but vitamins B2, B3, and C decreased. The results clearly support the conclusion that 120 d storage at 20 °C did not cause an increase in SSC or flavor deterioration, and the juice's nutritional quality was comparable to that obtained from fresh fruit. Fruit juice from the ASD treatment was physically more stable.

From this work, we conclude that the gap in fresh fruit supply during the four-month off season in winter melon could be made up by long-term, room temperature stored fruit. The long-term storage resulted in substantial water loss, but there was no loss due to decay. The long storage also did not cause consistent loss of flavor or nutritional quality. This research provides strong evidence to the industry that low-cost room temperature storage would ensure stable fruit supplies for the winter melon juice industry.

Supplementary Materials: The following supporting information can be downloaded at: https://www.mdpi.com/article/10.3390/foods12010209/s1, Table S1: LC-MS/MS MRM transitions and compound specific parameters.

Author Contributions: Conceptualization, J.B. and E.N.R.; methodology, J.B., E.N.R., K.A.J., W.Z. and A.P.; statistical analysis and the analysis of the results, J.B., E.N.R., K.A.J. and W.Z.; writing—original draft preparation, J.B., E.N.R., K.A.J. and W.Z.; writing—review and editing, J.B., E.N.R., K.A.J., W.Z. and A.P. All authors have read and agreed to the published version of the manuscript.

Funding: This research received no external funding.

Institutional Review Board Statement: Not applicable.

Informed Consent Statement: Not applicable.

Data Availability Statement: The datasets generated in this study are available on request to the corresponding author.

Conflicts of Interest: The authors declare no conflict of interest.

References

1. Epstein, L.H.; Gordy, C.C.; Raynor, H.A.; Beddome, M.; Kilanowski, C.K.; Paluch, R. Increasing fruit and vegetable intake and decreasing fat and sugar intake in families at risk for childhood obesity. *Obes. Res.* **2001**, *9*, 171–178. [CrossRef]
2. Malik, V.S.; Hu, F.B. Sweeteners and risk of obesity and type 2 diabetes: The role of sugar-sweetened beverages. *Curr. Diabetes Rep.* **2012**, *12*, 195–203. [CrossRef]
3. Hu, F.B. Resolved: There is sufficient scientific evidence that decreasing sugar-sweetened beverage consumption will reduce the prevalence of obesity and obesity-related diseases. *Obes. Rev.* **2013**, *14*, 606–619. [CrossRef]
4. Bray, G.A.; Popkin, B.M. Dietary sugar and body weight: Have we reached a crisis in the epidemic of obesity and diabetes? Health be damned! Pour on the sugar. *Diabetes Care* **2014**, *37*, 950–956. [CrossRef]
5. Hung, H.-C.; Joshipura, K.J.; Jiang, R.; Hu, F.B.; Hunter, D.; Smith-Warner, S.A.; Colditz, G.A.; Rosner, B.; Spiegelman, D.; Willett, W.C. Fruit and vegetable intake and risk of major chronic disease. *J. Natl. Cancer Inst.* **2004**, *96*, 1577–1584. [CrossRef]
6. Joshipura, K.J.; Ascherio, A.; Manson, J.E.; Stampfer, M.J.; Rimm, E.B.; Speizer, F.E.; Hennekens, C.H.; Spiegelman, D.; Willett, W.C. Fruit and vegetable intake in relation to risk of ischemic stroke. *JAMA* **1999**, *282*, 1233–1239. [CrossRef]
7. Joshipura, K.J.; Hu, F.B.; Manson, J.E.; Stampfer, M.J.; Rimm, E.B.; Speizer, F.E.; Colditz, G.; Ascherio, A.; Rosner, B.; Spiegelman, D. The effect of fruit and vegetable intake on risk for coronary heart disease. *Ann. Intern. Med.* **2001**, *134*, 1106–1114. [CrossRef]
8. Dennison, B.A.; Rockwell, H.L.; Baker, S.L. Excess fruit juice consumption by preschool-aged children is associated with short stature and obesity. *Pediatrics* **1997**, *99*, 15–22. [CrossRef]
9. Wojcicki, J.M.; Heyman, M.B. Reducing childhood obesity by eliminating 100% fruit juice. *Am. J. Public Health* **2012**, *102*, 1630–1633. [CrossRef]
10. Gill, J.M.; Sattar, N. Fruit juice: Just another sugary drink? *Lancet Diabetes Endocrinol.* **2014**, *2*, 444–446. [CrossRef]
11. De Oliveira Pineli, L.d.L.; de Aguiar, L.A.; Fiusa, A.; de Assunção Botelho, R.B.; Zandonadi, R.P.; Melo, L. Sensory impact of lowering sugar content in orange nectars to design healthier, low-sugar industrialized beverages. *Appetite* **2016**, *96*, 239–244. [CrossRef]
12. Badami, K.; Daryono, B.; Amzeri, A.; Khoiri, S. Combining ability and heterotic studies on hybrid melon (*Cucumis melo* L.) populations for fruit yield and quality traits. *SABRAO J. Breed. Genet.* **2020**, *52*, 402–417.
13. Mohosina, F.; Mehedi, M.N.H.; Mahmud, E.; Hasan, M.K.; Noor, M.M.A.; Rahman, M.H.S.; Chowdhury, A.K. Genetic diversity of commercially cultivated watermelons (Citrullus lanatus) hybrids in Bangladesh. *SABRAO J. Breed. Genet* **2020**, *52*, 418–434.
14. Zaini, N.A.M.; Anwar, F.; Hamid, A.A.; Saari, N. Kundur [Benincasa hispida (Thunb.) Cogn.]: A potential source for valuable nutrients and functional foods. *Food Res. Int.* **2011**, *44*, 2368–2376. [CrossRef]
15. Pandey, A.; Bhardwaj, D.; Dubey, R.K.; Singh, V.; Pandey, S. Botany, diversity, utilization and improvement of ash gourd (Benincasa hispida Thunb. Ex Murray Cogn)-A review. *Ann. Hortic.* **2015**, *8*, 1–15.
16. Morton, J.F. The wax gourd, a year-round Florida vegetable with unusual keeping quality. *Proc. Fla. State Hortic. Soc.* **1971**, *84*, 104–109.
17. Tiwari, A.; Anusha, I.; Sumangali, M.; Anand Kumar, D.; Madhusudana, K.; Agawane, S. Preventive and therapeutic efficacies of Benincasa hispida and Sechium edule fruit's juice on sweet-beverages induced impaired glucose tolerance and oxidative stress. *Pharmacologia* **2013**, *4*, 197–207. [CrossRef]
18. Sun, X.; Baldwin, E.; Plotto, A.; Cameron, R.; Manthey, J.; Dorado, C.; Bai, J. The effect of cultivar and processing method on the stability, flavor, and nutritional properties of winter melon juice. *LWT* **2018**, *97*, 223–230. [CrossRef]
19. Wesson, L.G. The effect of tartronic acid on abnormal fat formation from carbohydrate. *Endocrinology* **1950**, *47*, 302–304. [CrossRef]
20. Wesson, L.G. Possible Sources of Tartronate Deficiency in Man. *Nature* **1961**, *189*, 147–148. [CrossRef]

21. Doharey, V.; Kumar, M.; Upadhyay, S.K.; Singh, R.; Kumari, B. Pharmacognostical, physicochemical and pharmaceutical paradigm of ash gourd, Benincasa hispida (Thunb.) fruit. *Plant Arch.* **2021**, *21*, 249–252. [CrossRef]
22. Ramesh, M.; Gayathri, V.; Rao, A.A.; Prabhakar, M.; Rao, C.S. Pharmacological actions of fruit juice of Benincasa hispida. *Fitoterapia* **1989**, *60*, 241–247.
23. Sun, X.; Baldwin, E.A.; Plotto, A.; Manthey, J.A.; Duan, Y.; Bai, J. Effects of thermal processing and pulp filtration on physical, chemical and sensory properties of winter melon juice. *J. Sci. Food Agric.* **2017**, *97*, 543–550. [CrossRef]
24. Rosskopf, E.; Di Gioia, F.; Hong, J.C.; Pisani, C.; Kokalis-Burelle, N. Organic amendments for pathogen and nematode control. *Annu. Rev. Phytopathol.* **2020**, *58*, 277–311. [CrossRef]
25. Paudel, B.R.; Di Gioia, F.; Zhao, X.; Ozores-Hampton, M.; Hong, J.C.; Kokalis-Burelle, N.; Pisani, C.; Rosskopf, E.N. Evaluating anaerobic soil disinfestation and other biological soil management strategies for open-field tomato production in Florida. *Renew. Agric. Food Syst.* **2020**, *35*, 274–285. [CrossRef]
26. Shah, H.; Tariq, A.; Noreen, R.; Rahman, A.; Shafique, H.A.; Ara, J.; Ehteshamul-Haque, S. Effects of fungicides and storage temperature in maintaining the shelf life and fruit quality of stored mango (Mangifera indica L.). *Pak. J. Bot.* **2021**, *53*, PJB2021–PJB2024.
27. Imahori, Y.; Takemura, M.; Bai, J. Chilling-induced oxidative stress and antioxidant responses in mume (*Prunus mume*) fruit during low temperature storage. *Postharvest Biol. Technol.* **2008**, *49*, 54–60. [CrossRef]
28. Soga, A.; Yoshida, M.; Watanabe, S.; Manago, M. *Low Temperature Limit on Storage of Wax Gourd [Benincasa hispida]*; Bulletin of the Agricultural Research Institute of Kanagawa Prefecture: Hiratsuka, Japan, 2004.
29. Sun, X.; Baldwin, E.A.; Manthey, J.; Dorado, C.; Rivera, T.; Bai, J. Effect of Preprocessing Storage Temperature and Time on the Physicochemical Properties of Winter Melon Juice. *J. Food Qual.* **2022**, *2022*, 3237639. [CrossRef]
30. Pandey, S.; Jha, A.; Rai, M. Screening of advance breeding lines/cultivars for shelf-life and biochemical changes during storage of ash gourd (Benincasa hispida). *Acta Hortic.* **2009**, *806*, 249–255. [CrossRef]
31. Di Gioia, F.; Ozores-Hampton, M.; Hong, J.; Kokalis-Burelle, N.; Albano, J.; Zhao, X.; Black, Z.; Gao, Z.; Wilson, C.; Thomas, J. The effects of anaerobic soil disinfestation on weed and nematode control, fruit yield, and quality of Florida fresh-market tomato. *HortScience* **2016**, *51*, 703–711. [CrossRef]
32. Butler, D.M.; Kokalis-Burelle, N.; Muramoto, J.; Shennan, C.; McCollum, T.G.; Rosskopf, E.N. Impact of anaerobic soil disinfestation combined with soil solarization on plant–parasitic nematodes and introduced inoculum of soilborne plant pathogens in raised-bed vegetable production. *Crop Prot.* **2012**, *39*, 33–40. [CrossRef]
33. Bai, J.; Baldwin, E.A.; Plotto, A.; Cameron, R.; Ford, B.L.; Luzio, G.; Manthey, J.; Narciso, J.; Dea, S. A comparison of processed and fresh squeezed 'Hamlin' orange juice-flavor quality. *Proc. Fla. State Hortic. Soc.* **2010**, *123*, 199–206.
34. Bai, J.; Mielke, E.A.; Chen, P.M.; Spotts, R.A.; Serdani, M.; Hansen, J.D.; Neven, L.G. Effect of high-pressure hot-water washing treatment on fruit quality, insects, and disease in apples and pears: Part I. System description and the effect on fruit quality of 'D'Anjou' pears. *Postharvest Biol. Technol.* **2006**, *40*, 207–215. [CrossRef]
35. Bai, J.; Baldwin, E.; Stover, E.; Driggers, R.; Hearn, J. Volatile profile comparison of USDA sweet orange-like hybrids versus 'Hamlin' and 'Ambersweet'. *HortScience* **2014**, *49*, 1262–1267. [CrossRef]
36. Wang, L.; Baldwin, E.A.; Zhao, W.; Plotto, A.; Sun, X.; Wang, Z.; Brecht, J.K.; Bai, J.; Yu, Z. Suppression of volatile production in tomato fruit exposed to chilling temperature and alleviation of chilling injury by a pre-chilling heat treatment. *LWT Food Sci. Technol.* **2015**, *62*, 115–121. [CrossRef]
37. Bai, J.; Hagenmaier, R.D.; Baldwin, E.A. Volatile response of four apple varieties with different coatings during marketing at room temperature. *J. Agric. Food Chem.* **2002**, *50*, 7660–7668. [CrossRef]
38. Bai, J.; Baldwin, E.; Tsantili, E.; Plotto, A.; Sun, X.; Wang, L.; Kafkaletou, M.; Wang, Z.; Narciso, J.; Zhao, W. Modified humidity clamshells to reduce moisture loss and extend storage life of small fruits⋆. *Food Packag. Shelf Life* **2019**, *22*, 100376. [CrossRef]
39. Bai, J.; Plotto, A. Coatings for fresh fruits and vegetables. In *Edible Coatings and Films to Improve Food Quality*, 2nd ed.; Baldwin, E., Hagenmaier, R., Bai, J., Eds.; CRC Press: Boca Raton, FL, USA, 2011; pp. 185–242.
40. Rahman, M.; Miaruddin, M.; Khan, M.; Masud, M.; Begum, M. Effect of storage periods on postharvest quality of pumpkin. *Bangladesh J. Agric. Res.* **2013**, *38*, 247–255. [CrossRef]
41. Li, Q.; Li, T.; Baldwin, E.A.; Manthey, J.A.; Plotto, A.; Zhang, Q.; Gao, W.; Bai, J.; Shan, Y. Extraction Method Affects Contents of Flavonoids and Carotenoids in Huanglongbing-Affected "Valencia" Orange Juice. *Foods* **2021**, *10*, 783. [CrossRef]
42. Ellerbee, L.; Wicker, L. Calcium and pH influence on orange juice cloud stability. *J. Sci. Food Agric.* **2011**, *91*, 171–177. [CrossRef]
43. Ackerley, J.; Wicker, L. Floc formation and changes in serum soluble cloud components of fresh Valencia orange juice. *J. Food Sci.* **2003**, *68*, 1169–1174. [CrossRef]
44. Salehi, F. Physico-chemical and rheological properties of fruit and vegetable juices as affected by high pressure homogenization: A review. *Int. J. Food Prop.* **2020**, *23*, 1136–1149. [CrossRef]
45. Hiemenz, P.C.; Rajagopalan, R. *Principles of Colloid and Surface Chemistry, Revised and Expanded*; CRC Press: Boca Raton, FL, USA, 2016.
46. Bai, J.; Baldwin, E.A.; Goodner, K.L.; Mattheis, J.P.; Brecht, J.K. Response of four apple cultivars to 1-methylcyclopropene treatment and controlled atmosphere storage. *HortScience* **2005**, *40*, 1534–1538. [CrossRef]
47. Yahia, E.M.; Carrillo-López, A.; Bello-Perez, L.A. Carbohydrates. In *Postharvest Physiology and Biochemistry of Fruits and Vegetables*; Yahia, E.M., Ed.; Woodhead Publishing: Sawston, UK, 2019; pp. 175–205. [CrossRef]

48. Wills, R.B.; Wong, A.W.; Scriven, F.M.; Greenfield, H. Nutrient composition of Chinese vegetables. *J. Agric. Food Chem.* **1984**, *32*, 413–416. [CrossRef]
49. Gross, K.C.; Sams, C.E. Changes in cell wall neutral sugar composition during fruit ripening: A species survey. *Phytochemistry* **1984**, *23*, 2457–2461. [CrossRef]
50. Gao, J.; Qin, Z.; Zhou, X.; Xin, M. Screening of germplasm with high content of tartronic acid in cucumber. *China Veg.* **2012**, *22*, 30–34.
51. Le Gall, H.; Philippe, F.; Domon, J.-M.; Gillet, F.; Pelloux, J.; Rayon, C. Cell wall metabolism in response to abiotic stress. *Plants* **2015**, *4*, 112–166. [CrossRef]
52. Ratnayake, R.M.S.; Melton, L.D.; Hurst, P.L. Influence of Cultivar, Cooking, and Storage on Cell-Wall Polysaccharide Composition of Winter Squash (Cucurbita maxima). *J. Agric. Food Chem.* **2003**, *51*, 1904–1913. [CrossRef]
53. Fatariah, Z.; Tengku Zulkhairuazha, T.; Wan Rosli, W. Ascorbic acid quantification in Benincasa hispida fruit extracted using different solvents. *Int. Food Res. J.* **2015**, *22*, 208–212.
54. Dong, M.; Yin, Q.; Feng, W.; Xu, J.; Xu, W. Study of Benincasa hispida contents effective for protection of kidney. *Jiangsu J. Agric. Sci.* **1995**, 46–55.
55. Hu, G.; Yang, F.-Q. Biological activities of nucleosides and their analogues in dietary foods. *Chem. Rapid Commun.* **2014**, *2*, 22–28.
56. AlJahani, A.; Cheikhousman, R. Nutritional and sensory evaluation of pumpkin-based (*Cucurbita maxima*) functional juice. *Nutr. Food Sci.* **2017**, *47*, 346–356. [CrossRef]
57. McGorrin, R.J. Character-impact flavor and off-flavor compounds in foods. In *Flavor, Fragrance, and Odor Analysis*, 2nd ed.; Marsili, R., Ed.; CRC Press: Boca Raton, FL, USA, 2012; pp. 207–262.
58. Pang, X.; Zhang, Y.; Qiu, J.; Cao, J.; Sun, Y.; Li, H.; Kong, F. Coupled multidimensional GC and odor activity value calculation to identify off-odors in thermally processed muskmelon juice. *Food Chem.* **2019**, *301*, 125307. [CrossRef]
59. McGorrin, R.J. The significance of volatile sulfur compounds in food flavors: An overview. In *Volatile Sulfur Compounds in Food*; Chapter 1; American Chemical Society: Washington, DC, USA, 2011; pp. 3–31.
60. Chipps, E.S.; Jayini, R.; Ando, S.; Protzman, A.D.; Muhi, M.Z.; Mottaleb, M.A.; Malkawi, A.; Islam, M.R. Cytotoxicity analysis of active components in bitter melon (Momordica charantia) seed extracts using human embryonic kidney and colon tumor cells. *Nat. Prod. Commun.* **2012**, *7*, 1934578X1200700926. [CrossRef]

foods

MDPI

Article

Investigations into Determinants of Blueberry Coating Effectiveness

David Obenland [1,*], Francisco M. A. Leyva-Gutierrez [2] and Tong Wang [2]

[1] USDA, Agricultural Research Service, San Joaquin Valley Agricultural Sciences Center, 9611 South Riverbend Avenue, Parlier, CA 93648, USA
[2] Department of Food Science, University of Tennessee, 2510 River Drive, Knoxville, TN 37996, USA
* Correspondence: david.obenland@usda.gov; Tel.: +1-559-596-2801

Abstract: Coatings have been investigated as a means of slowing weight loss and helping to preserve quality in blueberries but reported results have been inconsistent with the inadequate presentation of the impact of coatings on blueberry appearance. In this study, we compare the ability to limit weight loss, along with the effect on appearance, of several previously studied coatings for blueberries and attempt to identify reasons why coatings have not been more successful in limiting weight loss in blueberries. In a two-year study, coatings were applied either as a spray or a dip, depending on the nature of the coating, and included 1% chitosan (CH) with and without either 1% or 2% oleic acid (OA), 1% Semperfresh (SF), 2% sodium caseinate (SC), and carnauba wax (CAR). None of the coatings reduced weight loss in either year of the study and sometimes enhanced it. CH, CH + OA, CAR, and SF greatly altered the appearance of the berries by removing all or a part of the waxy bloom. SC also did this to some degree but was generally better at maintaining the natural appearance. It was found that coating application did not effectively limit weight loss through either the cuticle or stem end of the blueberries. Loss of the bloom on the blueberry surface, confirmed visually and by scanning electron microscopy, occurred during coating application, but was found to not influence coating effectiveness. Using CH + OA as an example, it was found that increasing the amount of handling during the drying process significantly increased subsequent weight loss relative to blueberries with minimal handling. This indicates that careful handling during the coating process is important for coating success.

Keywords: weight loss; shrivel; decay; waxy bloom; stem end; handling

Citation: Obenland, D.; Leyva-Gutierrez, F.M.A.; Wang, T. Investigations into Determinants of Blueberry Coating Effectiveness. *Foods* **2023**, *12*, 174. https://doi.org/10.3390/foods12010174

Academic Editors: Imahori Yoshihiro and Jinhe Bai

Received: 19 November 2022
Revised: 22 December 2022
Accepted: 26 December 2022
Published: 30 December 2022

1. Introduction

Weight loss during storage is a critical factor in determining blueberry quality with 5% to 8% being the level at which blueberries can become unmarketable [1]. This is primarily mediated by a loss of water through the cuticle, although a large proportion also occurs through the stem scar [2]. Cultivar differences exist in the degree of water loss that occurs, and these differences have been found to be linked to both size of the stem scar and cuticle composition [1,3]. Water loss is related linearly to loss in firmness, except when minor water loss occurs where firmness can transiently increase [4,5]. Firmness at harvest and whether the fruit have been damaged, as by the utilization of mechanical harvesting, also impact the degree of softening that may occur in storage. Blueberries that are perceived as being soft when eaten are less preferred by consumers [6], this attribute being of major importance to blueberry quality. In addition, the decline in visual quality in the form of shriveling that accompanies the loss of firmness is considered a major quality defect of blueberries [7]. Minimizing water loss to maintain firmness is, therefore, critical to preserving blueberry quality following harvest.

The cuticular wax coating acts as a critical component to maintain blueberry quality. Chu et al. [8] demonstrated that the removal of the epicuticular wax (bloom) of blueberries

exacerbated both weight loss and decay, leading to a decline in sensory and nutritional quality. They further found that fruit so treated had reduced levels of antioxidants and evidence of oxidative damage. While the natural wax layer is thought to be vital to maintaining the quality of blueberries, experimentation has been conducted on the effectiveness of supplementing the natural wax layer after harvest with an additional coating to try to further minimize water loss and slow the rate of senescence. Prior research in blueberries has been most focused on evaluating the performance of polysaccharide-based coatings, such as sodium alginate, chitosan, hydroxypropyl methylcellulose, pectin, or pullulan [9–13]. Caseinates, which are protein-based coatings, have also been studied [9]. Often combination coatings have been utilized to try to enhance coating functionality. Examples of this are high-oleic acid sunflower oil and Aloe vera combined with chitosan to lower water vapor permeability [14,15].

Unfortunately, a great deal of the reported research on blueberries has indicated that the studied coatings have been either inconsistent or ineffective in reducing weight loss for reasons that are unclear. The purpose of this study was to evaluate the performance of a variety of coatings following simulated commercial storage and marketing to obtain a comparison of their effects on blueberry weight loss and quality and, more importantly, to examine potential reasons that may influence their effectiveness. The work also included evaluations on the effect of coating applications on the surface bloom, a characteristic that is indicative of fresh blueberry quality [16] and had received inadequate attention in prior work with blueberry coatings.

2. Materials and Methods

2.1. Fruit

Varieties Snowchaser and Jewel were picked at commercial maturity from a research field at the USDA San Joaquin Valley Agricultural Sciences Center (USDA-SJVASC) on May 19 and 26, respectively, in season 1 (2020) and season 2 (2021). The field was established in 2016 with 3 m row spacing and 0.9 m between plants in a row. Both irrigation and fertilization were supplied with drip irrigation. Care was taken to pick blueberries that had no visible disorders. Fruit for scanning electron microscopy (SEM) work as well as for the examination of stem end effect were also harvested from the USDA-SJVASC research field. Fruit were obtained in the off-season from a local grocery store to perform a small subsidiary test examining the influence of handling and double coating. Variety could not be obtained in this case.

2.2. Coatings

Most coatings were selected due to their prior use in blueberry research. The coatings used were as follows: chitosan (CH, high molecular weight class, $\geq$75% deacylation, Sigma, St. Louis, MO, USA); Semperfresh (SF, combination of sucrose esters of fatty acids, sodium carboxymethyl cellulose, and mono- and diglycerides of fatty acids, Pace International, Wapato, WA, USA); sodium caseinate (SC, Sigma), and a carnauba wax (CAR) microemulsion (Sta-Fresh 2109, JBT, Riverside, CA, USA). Chitosan was prepared as a 1% (*w/v*) solution in 1% acetic acid using a Tekmar Tissumizer (Cincinnati, OH, USA) to homogenize the mixture, increasing speed as the mixture thickened. When CH was completely incorporated, Tween 20 and glycerol were added to final concentrations of 0.1% (*w/v*) and 50% (*w/w* of chitosan) [9], respectively. In addition, either 1% or 2% of oleic acid (OA) was added in season 1, using high-speed homogenization [17]. SF was made to 1% of the active ingredients (a combination of ingredients as listed above) by dilution in water. A 2% concentration of SC was made in water followed by the addition of glycerol to make a concentration of 50% (*w/w* of SC) and Tween 20 to 0.15% (*w/v*) as reported earlier [9] but substituting calcium caseinate with SC. CAR was used in undiluted form. Controls of water or acetic acid only were included to better estimate true treatment effects.

2.3. Coating Application and Packaging

Coatings were applied either as a dip or, in the case of Semperfresh, both dip and spray at ambient temperature of (23 °C). When applied as a dip the berries were immersed for 15 s, removed from the solution, and then spread out on a screen and allowed to dry under ambient conditions. Care was taken during the coating and drying process to minimize handling and the mechanical impact of the coating process on the fruit. Spraying was accomplished by placing the berries in a single layer on a screen and using a paint sprayer (Wagner, Plymouth, MN, USA) set on a fine spray setting to simulate a potential commercial operation of coating the fruit. Drying in ambient conditions was completed on a screen. In season 1, the fruit were dip-coated a single time while in season 2, the fruit were coated twice to ensure complete coverage and potentially enhance effectiveness. In season 2 the first coating was dried on a screen for 30 min prior to recoating. The effectiveness of recoating and of utilizing additional handling during the coating process was examined in season 1 using CH + OA. In this case, there was a comparison made between minimal handling (normal procedure to apply coating) and one where the fruit were continually turned during drying. After final drying, the fruit from both years were placed into vented plastic clamshells (170 g) and the clamshells placed into boxes capable of holding 12 clamshells. Each clamshell was considered a replication and there were 4 replications per treatment for each storage time.

2.4. Storage

In season 1 blueberries were stored at either 3 weeks or 6 weeks at 1 °C and 85% relative humidity in a 7.9 m^2 storage chamber equipped with a TELSEC 2000 environmental control system (Quest Controls, Palmetto, FL, USA). To better simulate commercial storage and marketing, the storage regimes in season 2 were altered to: (1) 3 weeks at 1 °C, (2) 3 weeks 1 °C + 1 week 10 °C, (3) 3 weeks 1 °C + 1 week 10 °C + 2 d 20 °C. Relative humidity was approximately 95% at 1 °C, 93% at 10 °C and 73% at 20 °C. The same storage chamber was used as in season 1.

2.5. Fruit Quality

Percent weight loss was determined by comparing the weights of the individual clamshells at the end of each of the two storage times with the initial values in the experiment. There was no removal of decayed fruit during storage. The appearance of the waxy bloom was rated from 0 to 3, where 0 = perfect, unchanged; 1 = slight loss, acceptable; 2 = moderate loss, not acceptable; 3 = severe loss, not acceptable. Berries that had visible decay, or with softening characteristics of decay, were counted as decays. Those berries that had shriveling that would be objectionable to consumers upon close examination were counted as being shriveled. The shriveling generally occurred at the stem end. Firmness was measured by the use of a FirmTech 2 (BioWorks, Wamego, KS, USA) in season 1 and a FirmTech FT7 (UP Umweltanallytische Produkte GmbH, Ibbenbürn, Germany) in season 2. Both instruments were similar in design and measured the force required in g to cause a 1 mm deflection of the berry. Twenty berries were measured for firmness from each clamshell in both years. After the removal of decayed berries, all the fruit from each clamshell were juiced to measure soluble solids concentration (SSC) and titratable acidity (TA), each clamshell being a replication. The juice was centrifuged at 8100× *g* for 10 min and the resulting clear supernatant was used for the measurements. SSC was determined with a digital refractometer (Atago, Tokyo, Japan) and TA with an automatic titrator (Mettler model T50, Columbus, OH, USA).

2.6. Stem end Contribution to Weight Loss

Eighty berries of similar size and no blemishes were selected from fruit (cv. San Joaquin) that were harvested at the SJVASC when the berries were commercially mature. Twenty berries were used for each of the 4 treatments which were as follows: (1) Untreated; (2) Stem ends covered, no coating; (3) Stem ends not covered, coating; (4) Stem ends

covered, coating. Nail polish was used to cover and seal stem ends as in previous work [2] and SC was the coating. Nail polish was applied to the appropriate treatments and allowed to dry, followed by the application of coating if needed. Each berry was individually coated, using forceps to dip the berries into the coating, and carefully placed to dry on Eppendorf tube racks. After drying each berry was individually weighed and reweighed daily for 4 days, after which the fruit were again weighed on day 7. From this data it was possible to estimate changes in weight loss or gain due to SC application from either the cuticle or stem end.

2.7. Scanning Electron Microscopy (SEM)

Coated and uncoated blueberries were carefully packed at the SJVASC in 50-mL Falcon tubes to allow little or no movement of the individual berries, placed into an insulated container with ice packs and sent to the University of Tennessee (Knoxville, TN, USA) by overnight mail. Some of the berries were half-coated to examine the coated/uncoated interface. The surfaces of coated, half-coated, and uncoated fruit were imaged using a Zeiss EVO (Zeiss, Oberkochen, Germany) SEM. Samples were mounted on aluminum holders with double-sided copper tape and analyzed directly (no gold sputter-coating needed) under variable pressure mode (40 Pa) at 200 pA. Images were processed using Microscopy Suite software (version 3.4.3, Gaitan, Pleasanton, CA, USA). All analyses were performed at the University of Tennessee Institute for Advanced Materials and Manufacturing Electron Microscopy facilities (Knoxville, TN, USA).

2.8. Blueberry Bloom Removal Experimentation

Twenty berries, that were free of injury and with substantial bloom, were selected for each of the treatments. Berries with the natural bloom present were used in half of the treatments, while berries for the other half of the treatments had the bloom removed by using Blu Tack adhesive putty (Bostik, Wauwatosa, WI, USA) as previously described [8]. Both sets of berries had the same control and coatings applied: uncoated, CH, SF, SC, and CAR. Coatings were applied by dipping individual berries and then carefully placing them in Eppendorf tube racks to dry. The berries were then transferred to a new rack for storage at 20 °C for 4 days. Weights of the individual berries were taken after the berries had dried and then daily until the end of storage.

2.9. Statistical Analysis

Blueberry weight loss and bloom data for seasons 1 and 2 were analyzed by a completely randomized design, using a one-way ANOVA within both variety and storage time using statistical software (SPSS version 24, IBM, Chicago, IL, USA). Similarly, data examining the influence of handling on weight loss were analyzed by ANOVA within storage time and data on the impact of the epicuticular bloom by ANOVA within bloom condition and storage time, both with SPSS. Both of these analyses used a completely randomized design. Mean separations for all analyses in this manuscript were determined using Tukey's test ($p \leq 0.05$).

3. Results

3.1. Effect of Coatings on Weight Loss and Quality

'Snowchaser' and 'Jewel' were harvested from the same field in both seasons 1 and 2 and subjected to coating treatments prior to storage. In season 1 the blueberries were stored for either 3 or 6 weeks at 1°C prior to evaluation (Table 1). Presentation of results will focus on coatings and not the associated controls unless the controls indicated that it may have not been just the coating that causes the effect. Weight loss was not different between the untreated control and any coating after both storage times for either variety. For the most part, the waxy bloom was not altered to any sizeable extent by the control treatments throughout the experiments, although 'Jewel' after 6 weeks was judged to have enough natural wax removal that marketability might be impacted, indicating that even the

control treatments could at times cause substantial damage to the fragile bloom. CH-OA coatings had a strong impact and caused almost complete removal of the bloom, leaving the blueberries to be nearly black in color. Both dip and spray versions of SF caused much less bloom loss and, although the loss was evident, it was in most cases thought not to alter the marketability of the fruit. Two exceptions to this were SF spray following 3 weeks for 'Snowchaser' and both dip and spray treatments for 'Jewel' after 6 weeks. Examples of the appearance of blueberries with partial or full bloom removal following treatment (applied in season 2) are shown in Figure 1. There was no consistent change due to coating application in decay, shrivel or firmness (Supplementary Table S1).

Table 1. Influence of dip or spray coatings on weight loss and berry bloom rating following 3 weeks or 6 weeks at 1 °C in season 1.

Treatment [y]	Weight Loss (%)	Bloom (Rating) [z]	Weight Loss (%)	Bloom (Rating) [z]
	Loss (%) (Rating [z])		Loss (%) (Rating [z])	
3 weeks 1 °C	'Snowchaser'		'Jewel'	
Untreated	3.47 a	0.0	2.39 a	0.0
Water dip	3.63 a	0.5	3.18 a	1.0
Water spray	3.75 a	0.5	3.23 a	1.0
Acetic acid dip	3.64 a	0.5	3.04 a	1.0
CH + 1% OA dip	3.41 a	3.0	3.26 a	3.0
CH + 2% OA dip	3.52 a	3.0	2.98 a	3.0
SF dip	3.34 a	1.5	3.19 a	1.0
SF spray	3.65 a	2.0	3.40 a	1.0
6 weeks 1 °C				
Untreated	8.74 ab	0.0	6.08 ab	0.0
Water dip	8.43 ab	0.0	3.61 b	2.0
Water spray	7.91 c	0.0	7.96 a	2.0
Acetic acid dip	8.22 ab	0.0	7.32 a	2.0
CH + 1% OA dip	8.63 ab	3.0	6.56 ab	3.0
CH + 2% OA dip	7.70 b	3.0	6.63 ab	3.0
SF dip	7.90 b	1.0	7.49 a	2.0
SF spray	9.60 a	1.5	7.77 a	2.0

[y] C = chitosan, OA = oleic acid, SF = Semperfresh. [z] Waxy bloom coverage: 0 = equivalent to control; 1 = slight loss but acceptable; 2 = moderate loss, not acceptable le; 3 = severe loss, not acceptable. The same letter within the same variety and storage time indicates no significant difference with $p \leq 0.05$.

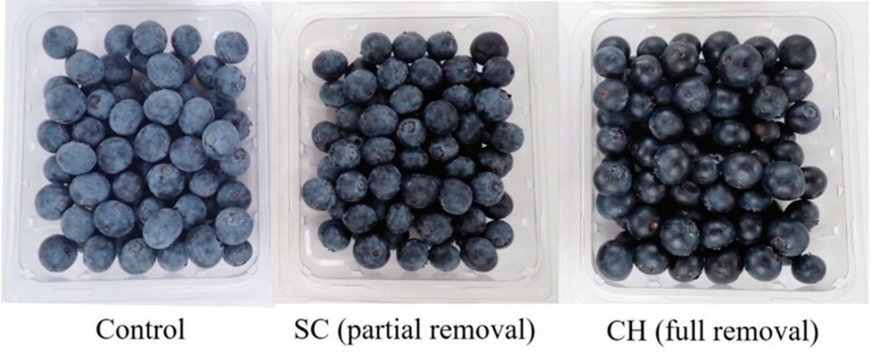

Figure 1. Differential removal of waxy bloom due to coating application. SC being an example of partial and CH of full removal of the waxy bloom.

In season 2, the coating experimentation was altered to include a new storage regime to better approximate handling and marketing. In addition, different coatings were evaluated to find ones that might be more effective than those tested in the prior year. In both varieties, there were no coatings that significantly reduced weight loss below that of the

untreated control and the effect of the coatings was often to increase weight loss (Table 2). In contrast to the prior year, there was often seen a negative effect of either the water or acetic acid controls, particularly in 'Snowchaser'. This may have been due to there being two applications in season 2 rather than one in season 1. As evidenced by the bloom ratings, the waxy bloom was strongly reduced by CH, SF and CAR in both varieties, but in 'Jewel' all the coatings negatively altered the bloom to a level that might limit marketability (example photos in Figure 1). The control treatments did not alter the bloom in 'Snowchaser' but did occasionally in 'Jewel'. Fruit coated with CAR often had less decay, and all coatings tended to reduce SSC, but results for shrivel, firmness and TA were inconsistent (Supplementary Table S2).

Table 2. Influence of dip coatings on weight loss and berry bloom rating following simulated storage and marketing in season 2.

Treatment [y]	Weight Loss (%)	Bloom (Rating) [z]	Weight Loss (%)	Bloom (Rating) [z]
	Loss (%) (Rating [z])		Loss (%) (Rating [z])	
3 weeks 1 °C	'Snowchaser'		'Jewel'	
Untreated	2.53 d	1.0	1.83 d	1.0
Water	3.10 ab	1.0	1.98 cd	1.0
Acetic acid	3.18 ab	1.0	2.00 cd	2.0
CH	3.23 ab	3.0	2.50 b	3.0
SF	2.90 bc	2.0	2.10 cd	2.0
SC	2.63 cd	1.0	2.18 bc	2.0
CAR	3.45 a	3.0	2.98 a	3.0
3 weeks 1 °C + 1 week 10 °C				
Untreated	3.35 bc	1.0	2.55 d	1.0
Water	4.05 a	1.0	2.90 cd	1.0
Acetic acid	4.13 a	1.0	2.83 cd	1.0
CH	4.13 a	3.0	3.45 b	3.0
SF	3.88 ab	2.0	2.83 cd	2.0
SC	3.20 c	1.0	3.03 c	2.0
CAR	4.30 a	3.0	4.03 a	3.0
3 weeks 1 °C + 1 week 10 °C + 2 d 20 °C				
Untreated	5.43 c	1.0	3.83 d	1.0
Water	6.78 b	1.0	4.46 bc	1.0
Acetic acid	6.64 b	1.0	4.09 cd	1.0
CH	6.69 b	3.0	4.98 b	3.0
SF	6.56 b	2.0	4.60 bc	2.0
SC	5.71 c	1.0	4.84 b	2.0
CAR	7.69 a	3.0	5.94 a	3.0

[y] CH = chitosan, SF = Semperfresh, SC = sodium caseinate, CAR = carnauba (undiluted Stafresh 2109). [z] Waxy bloom coverage: 0 = equivalent to control; 1 = slight loss but acceptable; 2 = moderate loss, not acceptable; 3 = severe loss, not acceptable. The same letter within the same variety and storage time indicates no significant difference with $p \leq 0.05$.

3.2. Effect of Handling and Additional Coating

An experiment was conducted to examine whether the amount of handling that the blueberries experienced during the coating process or the number of coats applied would alter the coating performance (Table 3). Chitsosan + OA was the coating combination tested. Minimal handling during coating application, which was equivalent to the normal application practice, resulted in a reduction in weight loss from that of the untreated control after 3 weeks but not after 6 weeks. Fruit that received extra handling had increased weight loss above that of the fruit that received minimal handling, although the weight loss was not different than the untreated control for both storage times. The application of an additional coat did not help reduce weight loss.

Table 3. Influence of handling and multiple coats on the effectiveness of a chitosan (CH) + oleic acid (OA) dip on the prevention of weight loss following 3 weeks or 6 weeks at 1 °C using purchased blueberries.

Coating	Weight Loss (%) [y]	
	3 weeks	6 weeks
Untreated	3.82 ab	7.49 bc
CH + OA minimal handling	2.85 c	6.47 c
CH + OA extra handling [z]	4.31 b	8.42 ab
CH + OA double coat	4.88 a	9.17 a

[y] Letters indicate statistical significance ($p \leq 0.05$) within week. [z] Blueberries continually turned while drying.

3.3. Influence of Coating on Cuticle and Stem end Weight Loss

As prior work had demonstrated the importance of the blueberry stem end to weight loss [2], it was of interest to examine the potential effect of a selected coating on this region of the blueberry. SC was chosen as the coating to use based upon its slightly better effectiveness seen in this experiment than the other coatings on preventing weight loss. Blocking the stem end (sealed) of both uncoated and coated fruit dramatically reduced the amount of weight loss by approximately 50%, regardless of the presence of coating (Figure 2A). SC had no effect on limiting weight loss of either sealed or non-sealed fruit. Calculated relative change over time in weight over time due to SC in either the cuticle or the stem end of the fruit is indicated in Figure 2B. Interestingly, SC induced a slight increase in weight loss from the cuticle that linearly increased over time while weight loss from the stem end slightly declined.

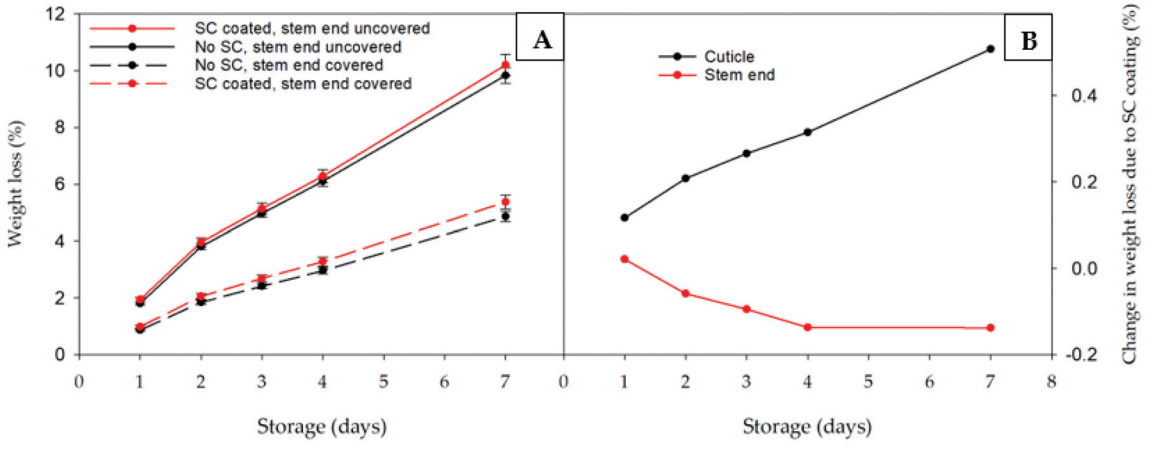

Figure 2. Effect of coating with sodium caseinate (SC) and coverage of the stem end of 'San Joaquin' blueberries with nail polish on weight loss during 7 d storage at 20 °C (**A**) and change in weight loss due to SC in either the cuticle or stem end (**B**).

3.4. SEM imaging of Coated Fruit

Coated blueberries were imaged to better understand the poor performance of the coatings in limiting weight loss. SEM images of the various coatings and controls indicated that the coatings were generally continuous and relatively featureless on the fruit surface (images not shown). An exception to this was CAR which tended to crack (Figure 3A). This coating was formulated for citrus fruit and apparently is not appropriate for blueberries even though CAR is an excellent coating in terms of its low water vapor permeability [18]. The representative images in Figure 3B,C were of half-coated fruit to be able to better determine the contrast between coated and uncoated areas. It was hoped that it might be possible to observe additional evidence (beyond darkening of the skin) of the degree that

the coatings alter the waxy bloom with the idea that alteration of the bloom may have some role in applied coating performance. In Figure 3C, waxy rodlets that make up the waxy bloom are visible on the uncoated but not the coated side of the fruit. This contrasts with a blueberry dipped in 1% acetic acid, the control for CH, where waxy rodlets are visible throughout (Figure 3D). Since chitosan is transparent then it would have been expected that the wax would have been visible under the coating had the wax been present.

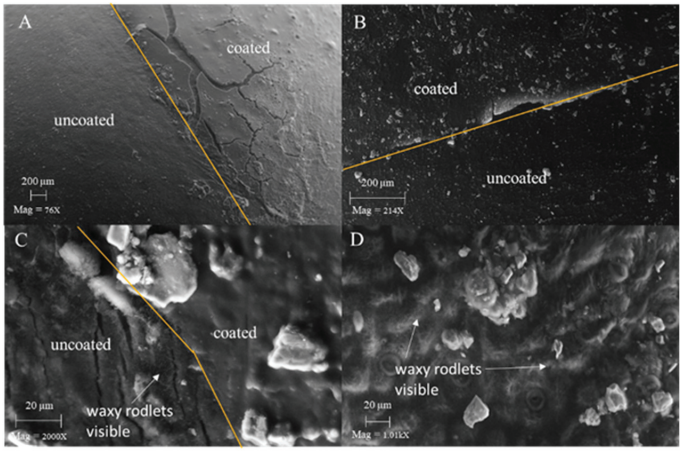

Figure 3. SEM images of blueberries with only one half of the fruit coated (**A**–**C**) or fully coated (**D**) to help better understand coating effects. Carnauba (CAR) coating illustrating the propensity of this coating to crack (**A**). Two magnifications of the chitosan (CH) coating (**B**,**C**) showing its appearance in contrast to the uncoated portion of the fruit. An image of blueberry treated with acetic acid (1%), the control for CH, is shown in a treated area of the berry (**D**).

3.5. Blueberry Bloom Removal

Weight loss from blueberries that were coated over the natural bloom or after it had been manually removed was examined to further explore the involvement of loss of the bloom in determining coating effectiveness. Gently wiping the surface of the blueberries with Blu Tack appeared to remove a substantial portion of the bloom as judged by the dark appearance of the berries after wiping. The effectiveness of Blu Tack adhesive for this purpose was previously demonstrated by [8] using SEM imaging. The amount of bloom removed by this process was determined to be an average of 2.9 mg per blueberry as estimated by weight loss. The overall weight loss across treatments was significantly higher ($p \leq 0.05$) in blueberries with the bloom removed in contrast with those with intact bloom. Except for CAR, which lost significantly less weight relative to the untreated control on days 3 and 4, CH, SF and SC were ineffective in limiting weight loss (Table 4). This was true regardless of whether the bloom had been present prior to coating.

Table 4. Influence of prior epicuticular bloom removal on coating performance during storage at 20 °C.

			Weight Loss (%) [z]		
Treatment [x]	Bloom [y]	Days:	1	2	3
Uncoated	Present		1.44 ab	3.11 a	4.52 a
CH			1.68 a	3.49 a	5.16 a
SC			1.65 a	3.40 a	5.03 a
SF			1.58 ab	3.27 a	4.87 a
CAR			1.39 b	2.90 a	3.82 b
Uncoated	Removed		2.24 ab	4.44 ab	6.48 ab

Table 4. *Cont.*

	Weight Loss (%) [z]		
CH	2.31 a	4.60 a	6.65 a
SC	2.09 ab	4.20 ab	5.84 ab
SF	1.87 b	3.84 b	5.64 b
CAR	2.02 ab	3.87 ab	5.57 b

[x] CH = chitosan, SF = Semperfresh, SC = sodium caseinate, CAR = carnauba. [y] Bloom present or removed by wiping with Blu-Tack prior to coating application. [z] Letters indicate statistical significance ($p \leq 0.05$) within day and bloom removal status.

4. Discussion

Experimentation was undertaken in this study to thoroughly characterize the performance of several coatings that had been used in prior research with blueberries and some that had not yet been tried with this commodity. This was used to set the stage for experimentation to better understand why blueberry coatings have often been ineffective in prior research. All the coatings evaluated in this study were ineffective in reducing weight loss, a result that was consistent in both years of the research using two different varieties. In fact, in the second season, weight loss was accelerated by some of the coatings. The only positive results were with CAR when treating individual berries, an impractical procedure commercially. The lack of positive effect in our research on weight loss of chitosan-based coatings agrees with much of the prior research on this coating on blueberries [9,11,14,19,20], although there are some reports that do indicate a benefit [15,21]. The relatively high water vapor permeability of chitosan film [18] likely contributed to the poor or inconsistent results. Although components such as oleic acid are sometimes added to improve water vapor resistance [17], this did not help lower weight loss in the first season of this study where this was tried. SF, a hydrophobic coating in contrast to the hydrophilic CAR, was reported to slow weight loss in blueberries [9], but the results in that study were inconsistent within the duration of the test. In our experiments, SF was not effective in preventing weight loss at any time. Duan et al. [9] also found that calcium caseinate was a poor coating to limit weight loss, the same as our findings with SC. To try to find any coating that would reduce weight loss in blueberries we also tried CAR, a coating with relatively low water vapor permeability [18,22]. This coating also failed, although the fact that the coating was formulated for citrus and not blueberries could have played a part. In addition, unlike in this case, citrus fruit are heat-dried after wax application which may act to soften or partially melt the wax and make its coverage more continuous. Cracking developed during storage may have also limited its effectiveness (Figure 3A). Sodium alginate, pectin, and pullulan, other coatings that have been shown to be of no use in lessening weight loss in blueberry, were not tried [12,13].

It is recognized that coatings have other functions than just lessening weight loss. Since firmness can be reduced by weight loss [5], coatings could potentially make blueberries more firm. Although firmness has been positively impacted in blueberries by coatings in some studies [9,21], often there have been no or inconsistent effects such as those obtained in this study (Supplementary Tables S1 and S2). Our results were not surprising given the poor ability of our coatings to limit weight loss. This was the same situation with shrivel, another quality attribute directly related to weight loss. Decay can cause a severe loss in the marketability of the fruit and, accordingly, this has been an important target of most of the prior studies with blueberry coatings. In the second season, the inhibitory effect of CH on decay was clear in both varieties as has been often noted in various commodities by others [23]. Antioxidant capacity may potentially also be altered by coatings but was not evaluated in this study that focuses on weight loss and external factors due to their greater importance.

The appearance of coated blueberries has not been commented on in almost all prior studies yet is very likely important. Mannozzi et al. [13] mentioned that blueberries treated with sodium alginate or pectin were bluer than the controls. The loss of waxy

bloom is responsible for this as was acknowledged in Duan et al. [9]. In this study, we performed visual evaluations for the condition of the bloom to gauge the impact of the different coatings more completely on this quality parameter. Most treatments, including the controls, had some negative impact, although sometimes not to the degree that would likely impact consumer preference. Some coatings, such as CH (with or without OA) and CAR, always were very damaging and caused a complete or near complete removal of the bloom (Tables 1 and 2; Figure 1). Other coatings, such as SF and SC were more intermediate in effect, causing only a partial bloom removal. A recent study by our laboratory found that partial bloom removal was acceptable to sensory panelists, but full removal was not [24]. This means that a bloom-damaging coating such as CH, despite its benefits in reducing decay, is likely not acceptable for fresh blueberries unless some more gentle means of application can be devised.

After confirmation of the ineffectiveness of the coatings tested in this study, the research moved to experimentation designed to have a better understanding of potential factors for why the coatings were not more efficacious. One of the first areas of the investigation was to examine the impact of handling during the application process as handling was required to both coat and dry the fruit. Using CH + OA as the test coating, it was found that if the amount of handling during the drying process was increased beyond what was normally practiced (minimal handling) the weight loss was significantly greater (Table 3). The results were also similar to CAR (results not shown). This indicates that the methodology of application can influence the success of the coating. The reason for this observation is not known but it is supposed that the coverage of the coating may be compromised by excessive handling. Indeed, SEM observations of blueberries coated with CH, SF, or SC indicated that these coatings formed films with a tendency to flake off (Supplementary Figure S1). Attempts to alter the application method to improve coating performance by spraying instead of dipping were not successful (Table 1). Further experimentation using an air-brush to delicately apply the coating and then drying without handling were also not successful. Surprisingly, it was found that with the CH + OA coating, even the application of an additional coat (using minimal handling during drying) did not lessen weight loss and, in fact, weight loss was even greater than the single coat with minimal handling (Table 3). In one of the few mentions of the mode of coating application for blueberries, Duan et al. [9] noted in their conclusion that dipping may have reduced the effectiveness of their coatings but offered no explanation of why that may have been so.

The stem end, although small in area relative to the cuticle, was found to be responsible for an average of 40% of the total weight loss in a study that examined a range of highbush blueberry genotypes [2]. To gain insight whether the stem end may be more difficult to coat, and negatively affect coating effectiveness, SC was applied to both blueberries that had the stem end completely blocked using nail polish [2] and control blueberries where the stem end had not been blocked. Eliminating water loss through the stem end eliminated approximately 50% of the total weight loss (Figure 2A), like the findings of Moggia et al. [2]. Same as the research presented earlier in this study, SC did not reduce weight loss in either sets of blueberries. In this case, the handling of the coated blueberries cannot be blamed for the ineffectiveness as each fruit was carefully coated and dried individually. Calculated estimates of the relative effect of SC on both regions indicated the cuticle weight loss was slightly increased over time while that from the stem end does not change much or even slightly declined due to SC application. It appears that, at least with SC, that poor coverage of the stem end was not the reason of the ineffectiveness of the coating in limiting weight loss.

In this study application of coating often led to a visible darkening of the blueberries (Figure 1) due to the loss of epicuticular bloom (Figure 3C). Prior research had shown that removal of the bloom increased weight loss in blueberries [8] and indicated the possibility that damage to the bloom due to coating application may be at least partially responsible for the poor coating performance that we observed. To examine this possibility coatings were applied to natural blueberries (bloom present) and to others that had the bloom artificially

removed (Table 4). It should also be noted here that the berries were all individually coated and dried, eliminating the effect of handling. Analysis across treatments indicated that removal of the bloom did result in greater weight loss ($p \leq 0.5$) as had been previously seen [8], the difference being up to 1.36% by day 3. If damage to the bloom would have played a significant role in the failure of the coatings to prevent weight loss, however, there should have been significant differences between the uncoated and coated blueberries in the group that had the bloom removed as the bloom, in that case, was not a factor. This was not observed, however, indicating that loss of bloom did not influence coating performance.

5. Conclusions

Additional confirmation was provided in this study to support previous research indicating the poor effectiveness of coatings to reduce blueberry weight loss. This paper also highlights the fact that coatings alter the appearance by partial or total removal of the waxy bloom. This somewhat neglected aspect needs to be considered in the development and testing of coatings as we have recently shown that consumers prefer blueberries that have at least partial bloom present [24]. Much of this study focused on determining potential reasons why the coatings used in this work performed so poorly to provide means of enhancing the effectiveness of these or other coatings for use for blueberries. Out of all the factors studied only excessive handling during coating was clearly linked to a worsening of coating results. This indicates that careful handling is needed during the coating process, but even with the coating of individual berries where handling was not an issue, we almost never saw that the coatings were effective in reducing weight loss. If coatings are to be used for blueberries it may be that novel formulations, specifically designed for this fruit, are needed for them to be successful. It is also important that consideration be made to ensure that the coatings can be successfully integrated into the commercial packing process that currently exists for blueberries.

Supplementary Materials: The following supporting information can be downloaded at: https://www.mdpi.com/article/10.3390/foods12010174/s1, Table S1: Influence of dip or spray coatings on other key quality parameters following 3 weeks or 6 weeks at 1 °C in season 1; Table S2: Influence of dip coatings on other key quality parameters following simulated storage and marketing in season 2.; Figure S1: Example of sodium caseinate flaking visualized by SEM.

Author Contributions: Conceptualization, D.O. and F.M.A.L.-G.; methodology, D.O. and F.M.A.L.-G.; validation, D.O.; formal analysis, D.O.; investigation, D.O. and F.M.A.L.-G.; resources, D.O, F.M.A.L.-G. and T.W.; data curation, D.O.; writing—original draft preparation, D.O.; writing—review and editing, D.O., F.M.A.L.-G. and T.W; visualization, D.O.; supervision, D.O. and T.W.; project administration, D.O. and T.W. All authors have read and agreed to the published version of the manuscript.

Funding: This research received no external funding.

Institutional Review Board Statement: Not applicable.

Informed Consent Statement: Not applicable.

Data Availability Statement: The datasets generated in this study are available on request to the corresponding author.

Acknowledgments: Thanks to Paul Neipp for his assistance in conducting coating applications and blueberry quality evaluation.

Conflicts of Interest: The authors declare no conflict of interest.

References

1. Retamales, J.B.; Hancock, J.F. *Blueberries. Crop Production Science in Horticulture*; Cabi: Cambridge, MA, USA, 2011.
2. Moggia, C.; Beaudry, R.M.; Retamales, J.B.; Lobos, G.A. Variation in the impact of stem scar and cuticle on water loss in highbush blueberry fruit argue for the use of water permeance as a selection criterion in breeding. *Postharvest Biol. Technol.* **2017**, *132*, 88–96. [CrossRef]
3. Moggia, C.; Graell, J.; Lara, I.; Schmeda-Hirschmann, G.; Thomas-Valdés, S.; Lobos, G.A. Fruit characteristics and cuticle triterpenes as related to postharvest quality of highbush blueberries. *Sci. Hortic.* **2016**, *211*, 449–457. [CrossRef]
4. Miller, W.R.; McDonald, R.E.; Cracker, T.E. Quality of Two Florida Blueberry Cultivars after Packaging and Storage. *HortScience* **1993**, *28*, 144–147. [CrossRef]
5. Paniagua, A.C.; East, A.R.; Hindmarsh, J.P.; Heyes, J.A. Moisture loss is the major cause of firmness change during postharvest storage of blueberry. *Postharvest Biol. Technol.* **2013**, *79*, 13–19. [CrossRef]
6. Lobos, G.A.; Callow, P.; Hancock, J.F. The effect of delaying harvest date on fruit quality and storage of late highbush blueberry cultivars (Vaccinium corymbosum L.). *Postharvest Biol. Technol.* **2014**, *87*, 133–139. [CrossRef]
7. United States Standards for Grades of Blueberries. Available online: https://www.ams.usda.gov/grades-standards/blueberries-grade-and-standards (accessed on 3 March 2022).
8. Chu, W.; Gao, H.; Chen, H.; Fang, X.; Zheng, Y. Effects of cuticular wax on the postharvest quality of blueberry fruit. *Food Chem.* **2018**, *239*, 68–74. [CrossRef] [PubMed]
9. Duan, J.; Wu, R.; Strik, B.C.; Zhao, Y. Effect of edible coatings on the quality of fresh blueberries (Duke and Elliott) under commercial storage conditions. *Postharvest Biol. Technol.* **2011**, *59*, 71–79. [CrossRef]
10. Osorio, F.A.; Molina, P.; Matiacevich, S.; Enrione, J.; Skurtys, O. Characteristics of hydroxy propyl methyl cellulose (HPMC) based edible film developed for blueberry coatings. *Procedia Food Sci.* **2011**, *1*, 287–293. [CrossRef]
11. Chiabrando, V.; Giacalone, G. Anthocyanins, phenolics and antioxidant capacity after fresh storage of blueberry treated with edible coatings. *Int. J. Food Sci. Nutr.* **2015**, *66*, 248–253. [CrossRef] [PubMed]
12. Kraśniewska, K.; Ścibisz, I.; Gniewosz, M.; Mitek, M.; Pobiega, K.; Cendrowski, A. Effect of Pullulan Coating on Postharvest Quality and Shelf-Life of Highbush Blueberry (Vaccinium corymbosum L.). *Materials* **2017**, *10*, 965. [CrossRef] [PubMed]
13. Mannozzi, C.; Cecchini, J.P.; Tylewicz, U.; Siroli, L.; Patrignani, F.; Lanciotti, R.; Rocculi, P.; Dalla Rosa, M.; Romani, S. Study on the efficacy of edible coatings on quality of blueberry fruits during shelf-life. *Food Sci. Technol.* **2017**, *85*, 440–444. [CrossRef]
14. Abugoch, L.; Tapia, C.; Plasencia, D.; Pastor, A.; Castro-Mandujano, O.; López, L.; Escalona, V.H. Shelf-life of fresh blueberries coated with quinoa protein/chitosan/sunflower oil edible film. *J. Sci. Food Agric.* **2016**, *96*, 619–626. [CrossRef] [PubMed]
15. Vieira, J.M.; Flores-López, M.L.; de Rodríguez, D.J.; Sousa, M.C.; Vicente, A.A.; Martins, J.T. Effect of chitosan—*Aloe vera* coating on postharvest quality of blueberry (*Vaccinium corymbosum*) fruit. *Postharvest Biol. Technol.* **2016**, *116*, 88–97. [CrossRef]
16. U.S. Highbush Blueberry Council, 2021. Fresh Blueberries. Available online: https://blueberry.org/about-blueberries/forms-of-blueberries/#fresh-blueberries (accessed on 5 March 2022).
17. Vargas, M.; Albors, A.; Chiralt, A.; González-Martínez, C. Quality of cold-stored strawberries as affected by chitosan–oleic acid edible coatings. *Postharvest Biol. Technol.* **2006**, *41*, 164–171. [CrossRef]
18. Bai, J.; Plotto, A. Coatings for fresh fruits and vegetables. In *Edible Coatings and Films to Improve Fruit Quality*; Baldwin, E.A., Hagenmaier, R.D., Bai, J., Eds.; CRC Press: Boca Raton, FL, USA, 2012; pp. 185–242.
19. Mannozzi, C.; Tylewicz, U.; Chinnici, F.; Siroli, L.; Rocculi, P.; Dalla Rosa, M.; Romani, S. Effects of chitosan based coatings enriched with procyanidin by-product on quality of fresh blueberries during storage. *Food Chem.* **2018**, *251*, 18–24. [CrossRef]
20. Yang, G.; Yue, J.; Gong, X.; Qian, B.; Wang, H.; Deng, Y.; Zhao, Y. Blueberry leaf extracts incorporated chitosan coatings for preserving postharvest quality of fresh blueberries. *Postharvest Biol. Technol.* **2014**, *92*, 46–53. [CrossRef]
21. Jiang, H.; Sun, Z.; Jia, R.; Wang, X.; Huang, J. Effect of Chitosan as an Antifungal and Preservative Agent on Postharvest Blueberry. *J. Food Qual.* **2016**, *39*, 516–523. [CrossRef]
22. Leyva-Gutierrez, F.M.A.; Wang, T. Crystallinity and Water Vapor Permeability of n-Alkane, Alcohol, Aldehyde, and Fatty Acid Constituents of Natural Waxes. *Ind. Eng. Chem.* **2021**, *60*, 14651–14663. [CrossRef]
23. Romanazzi, G.; Feliziani, E.; Baños, S.B.; Sivakumar, D. Shelf life extension of fresh fruit and vegetables by chitosan treatment. *Crit. Rev. Food Sci. Nutr.* **2017**, *57*, 579–601. [CrossRef] [PubMed]
24. Asensio, C.; Arpaia, M.L.; Obenland, D. University of California: Parlier, CA, USA, 2022; *manuscript in preparation*.

foods

MDPI

Article

Dynamic Change of Carbon and Nitrogen Sources in Colonized Apples by *Penicillium expansum*

Di Gong [1,2], Yang Bi [1,*], Yuanyuan Zong [1], Yongcai Li [1], Edward Sionov [2] and Dov Prusky [1,3]

[1] College of Food Science and Engineering, Gansu Agricultural University, Lanzhou 730070, China
[2] Department of Food Science, Agricultural Research Organization, The Volcani Center, Rishon LeZion 7505101, Israel
[3] Department of Postharvest Science, Agricultural Research Organization, The Volcani Center, Rishon LeZion 7505101, Israel
* Correspondence: biyang@gsau.edu.cn; Tel.: +86-931-763-1113; Fax: +86-931-7631201

Abstract: *Penicillium expansum* is a necrotrophic pathogen, which actively kills host cells and obtains nutrients from dead cells to achieve infection. However, few reports have elucidated the differential levels of carbon and nitrogen sources over increasing distances of the leading edge in fungal colonized fruit tissues during colonization. Our results showed that the highest consumption of sucrose and fructose, as well as the accumulation of glucose, were found in the decayed region of *P. expansum*-colonized 'Delicious' apple fruit compared with the healthy region at the leading edge and the healthy region 6 mm away from the leading edge. As nitrogen sources, the contents of methionine, glutamate, leucine, valine, isoleucine and serine were the lowest in the decayed region compared with the healthy regions during colonization. In addition, the titratable acidity, oxalic acid, citric acid, succinic acid and malic acid showed the highest accumulation in the decayed region compared with the healthy regions. *P. expansum* colonization induced the accumulation of saturated fatty acids in the decayed region, while the level of unsaturated fatty acids was the lowest. These changes were not observed in the healthy regions. These results indicated that *P. expansum* kills cells in advance of its colonization in order to obtain the nutrients of the apple tissue from the distal leading tissue of the colonized apple. It is understood that more carbon and nitrogen sources are required for fungal colonization, and a stronger defense response against colonization occurred in the fruit, causing the transit of nutrients from the distal tissue to the infected sites.

Keywords: *Penicillium expansum*; apple; fungal infection; carbon source; nitrogen source

Citation: Gong, D.; Bi, Y.; Zong, Y.; Li, Y.; Sionov, E.; Prusky, D. Dynamic Change of Carbon and Nitrogen Sources in Colonized Apples by *Penicillium expansum*. *Foods* **2022**, *11*, 3367. https://doi.org/10.3390/foods11213367

Academic Editors: Imahori Yoshihiro and Jinhe Bai

Received: 4 October 2022
Accepted: 22 October 2022
Published: 26 October 2022

1. Introduction

Penicillium expansum is one of the major postharvest pathogens, which causes the blue mold in pomes, stones and berries [1]. As a necrotrophic fungal, *P. expansum* kills the host cells in the colonized sites by secreting extracellular enzymes and acquires nutrients from these dead cells [2]. Subsequently, due to more demands for nutrients to facilitate colonization, the healthy tissues around the colonized sites are gradually destroyed, causing the expansion of the decay [3–5]. Therefore, the development of decay in fruit is a dynamic process that gradually develops outward from the initial colonized sites to the healthy tissue around it during fungal colonization [6,7].

During the process of colonization, fungi usually face nutrient limitations. The sugars and amino acids in fruit are considered as major carbon and nitrogen sources for fungi, which are utilized by sugar or amino acid transporters located in the fungal hyphae to achieve the fungal colonization of fruits [8]. The contents of sucrose, fructose, methionine and glutamate were decreased in the decayed tissue of *P. expansum*-infected apple fruit [9]. A reduced sucrose content and increased glucose and fructose content, as well as the total soluble solid content, were observed in the healthy tissue of *Monilinia fructicola*-infected peach fruit [10]. Moreover, a decreased glucose and sucrose content was found in the

healthy tissues of citrus fruit after *P. digitatum* infection [11]. In addition, higher contents of amino acids were found in the healthy tissue of *P. expansum*-infected apple fruit [12].

Organic acids contribute to the pH of fruit [13]. Compared with the healthy tissue of fruit infected by *P. digitatum* and *P. expansum*, higher concentrations of malic and citric acid were found in the tissue at the leading edge of apple and orange fruit [14]. Moreover, higher concentrations of citric acid accumulated in the decayed region of *P. expansum*-infected apple fruit and *P. digitatum*-infected grapefruit [13]. Our previous results indicated that *P. expansum* inoculation decreased the titratable acid content in the healthy tissue of apple fruit [15]. Fatty acids form the main composition of the cell membrane in fruit tissue and, together with the high level of unsaturated fatty acids (USFAs)/saturated fatty acids (SFAs), contribute to maintaining the fluidity and integrity of the cell membrane [16,17]. However, fungal infection reduced the ratio of USFAs/SFAs in the healthy tissue of fruit, resulting in an impaired integrity of the cell membrane of the host [18,19], which enabled the release of primary metabolites from the cells and their use for fungal colonization. *Phomopsis longanae* infection decreased the integrity of the cell membrane by increasing the levels of palmitic acid and stearic acid and reducing the levels of oleic acid, linoleic acid and linolenic acid in the healthy tissue of longan fruit [20,21]. In addition, lower contents of oleic acid and linoleic acid were observed in the decayed tissue of *P. expansum*-infected apple fruit [9].

The latest results illustrated differences in the contents of sugars, organic acids, amino acids and fatty acids in the decayed tissue at the leading edge of the center region of decay in *P. expansum*-infected 'Fuji' apple fruit [9]. However, the changes in these essential compounds between the colonized and healthy regions of fruit during fungal colonization are poorly understood. Therefore, the objective of the present study was to analyze changes in the contents of major sugars, organic acids, amino acids and fatty acids in three different regions of the 'Delicious' apple fruit during *P. expansum* inoculation, including the decayed tissue at the leading edge of decay, the healthy tissue at the leading edge and the healthy tissue 6 cm away from the leading edge, in order to understand the contributions of these essential metabolites in fruit to fungal colonization. Understanding the dynamic change in carbon and nitrogen sources in *P. expansum*-colonized apples can help us to further investigate the infection mechanism of *P. expansum*, contributing to the control of blue mold in apple fruit.

2. Materials and Methods

2.1. Fruit

Apple fruit (*Malus domestica* Borkh. cv. Delicious) was harvested from a commercial orchard in Jingtai, Gansu Province, China. Fruits of a uniform size and similar maturity that were free from wounds and fungal infection were collected from different apple trees. Subsequently, the fruits were individually covered with foam net bags, put into corrugated boxes and transferred to the lab on the day of harvest and stored in a cool room (5 ± 2 °C, with a RH 80–90%) until further use.

2.2. Preparation of the Spore Suspension

P. expansum (T01) was supplied by Prof. Shiping Tian of the Institute of Botany, Chinese Academy of Sciences. The strain was grown on potato dextrose agar plates (PDA) at 25 °C for 7 days. For the spore collection, the plates were flooded with 5 mL sterile water, and the spores removed by gentle rubbing with a sterile glass rod, followed by filtration through four layers of sterile cheesecloth. The concentration of the spore suspension was determined using a hemocytometer and then diluted to a final concentration of 1×10^6 spore mL^{-1}.

2.3. Fruit Inoculation

The fruits were taken out of cool storage. After warming to an ambient temperature (22 ± 2 °C) for 24 h, they were washed with tap water and surface-sterilized in 1% $NaClO_3$ for 2 min, and then washed again with sterile water and dried at an ambient temperature for 1 h. Two wounds were created with a sterile nail (2 mm depth and 2 mm diameter)

on opposite sides of the apple along the equator on each fruit before inoculation. Then, the apple fruit was inoculated with 10 μL of spore suspension in each wound. Sterile water inoculation was used as a control. After air-drying, all the fruits were placed into polyethylene bags and stored at an ambient temperature (22 ± 2 °C, RH 55–65%).

2.4. Sampling

According to the method of Gong et al. [15], at 2, 4 and 6 days after inoculation, 3 mm-thick tissues of the peel and pulp in the decayed region at the leading edge (DE), the healthy region at the leading edge (HE) and the healthy region 6 mm away from the leading edge (OE) were sampled from each fruit, respectively, as shown in Figure 1. In the experiment, tissues from the same region were blended, and 3 g of them were weighted and packaged with tinfoil and then immediately frozen in liquid nitrogen. The samples were stored at −80 °C until the time of analysis. A total of 36 apple fruits were contained in each group, and 12 apple fruits in each group were used for each sampling time. For each measurement, 3 packages of the samples of the same tissues were used, and 3 replicates were performed for the measurements.

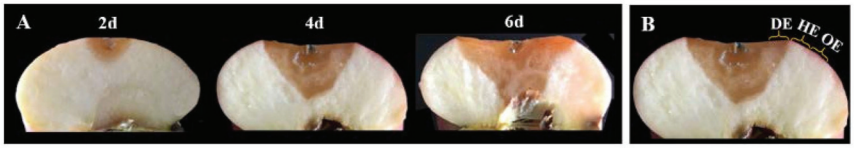

Figure 1. Pictures of lesion development in *P. expansum*-colonized apple fruit at 2, 4 and 6 days of colonization (**A**). Three regions of the tissues were collected (**B**). DE, the decayed region at the leading edge; HE, the healthy region at the leading edge; OE, the healthy region 6 mm away from the leading edge.

2.5. Measurement of the Total Soluble Solids (TSS) and Titratable Acidity (TA) Contents

The TSS content of the fresh tissues was determined using a digital refractometer (TD-45, Hangzhou, China) and expressed as %. Ten grams of frozen tissues were ground and diluted to 100 mL with distilled water for the TA determination. Ten mL of solution was taken and titrated with 0.2 M NaOH until a pH of 8.2 was reached, and the result was expressed as % [22].

2.6. Analysis of the Sugar and Organic Acid Contents

The sugars and organic acids were extracted using the method of Zhang et al. [23] with modifications. Three grams of frozen tissue were finely ground and homogenized in the presence of 10 mL of cold HPLC-grade ethanol (Sigma-Aldrich Products, St. Loui, MO, USA) and then incubated at 35 °C for 20 min and centrifuged at 10,000× *g* for 10 min. The supernatant was transferred to a tube, and the residues were extracted again using the extraction protocol. Supernatants were added up to volume of 25 mL with ethanol. Subsequently, 1 mL of the solution was dried using nitrogen at 55 °C, and then the residue was resuspended in 0.5 mL of distilled water and filtered through a 0.22 μm syringe filter (Agela Technologies, Torrance, CA, USA). The filtered solution was used for the sugar and organic acid analysis by ACQUITY HPLC (Waters Beckman Coulter Inc., Milford, MA, USA).

The sugars (fructose, glucose and sucrose) were analyzed as described by Gancedo and Luh [24], with modifications. A chromatographic separation of the sugars was carried out using a ZORBAX carbohydrate column (4.5 μm, 4.6 mm × 250 mm, Agilent GL Sciences Inc., Santa Clara, CA, USA). The mobile phase consisted of acetonitrile:water (80:20, *v*/*v*), and the flow rate was 1.4 mL min^{-1}. Eluted peaks were detected with a refractive index detector, and the data were analyzed with a Waters Empower system. Organic acids (oxalic acid, citric acid, succinic acid and malic acid) were analyzed as described by López-Hernández et al. [25], with modifications. The chromatographic separation of the organic

acids was carried out using an ODS C18 column (4.6 mm × 250 mm, Waters Beckman Coulter Inc., Milford, MA, USA). The mobile phase consisted of $(NH_4)_2HPO_4$ and the flow rate was 0.5 mL min^{-1}. Eluted peaks were detected with a refractive index detector, and the data were analyzed with a Waters Empower system. The sugars and organic acids were detected at 210 nm. The peak area of each sugar and organic acid was quantified by comparison with the calibration curve of the corresponding standards. The concentrations of sugars and organic acids were expressed as mg g^{-1}.

2.7. Analysis of the Amino Acid Contents

The amino acid contents were analyzed using the method of Li et al. [26], with some modifications. One gram of frozen tissue was ground and homogenized with 10 mL of 5% (*v*/*v*) sulfosalicylic acid. Subsequently, the mixture was centrifuged at 12,000× *g* for 20 min at 4 °C, and the supernatant was transferred to a new tube. The amino acid content was quantified by reference to 17 amino acid mixed standards using a Hitachi L-8800 Amino Acid Automatic Analyzer (Hitachi-Hitec, Omuta-shi, Japan) equipped with a Hitachi custom ion exchange resin (4.6 mm ID × 60 mm). The quantity of each amino acid was expressed as mg kg^{-1}.

2.8. Analysis of the Fatty Acid (FA) Contents

The FAs were analyzed using the method of Valero-Garrido et al. [27], with some modifications. Three grams of frozen tissue were ground, and 9 mL hexane:isopropanol (3:2, *v*/*v*) and 100 µL heptadecanoic acid were added into it as an internal standard. The mixture was heated at 85 °C for 1 h and then cooled and supplemented with 1 mL hexane. After 1 h, 100 µL of supernatant was adjusted to 1 mL of hexane. The lipids were quantified as the FA methyl esters using a Trace 1310 gas chromatograph (ThermoFisher Scientific Inc., Waltham, MA, USA) equipped with a TG-5MS column (30 m × 0.25 mm × 0.25 µm, ThermoFisher Scientific Inc., Waltham, MA, USA). The initial oven temperature was 85 °C, which was held for 2 min and then increased by 25 °C min^{-1} to 220 °C, by 5 °C min^{-1} to 250 °C and by 2 °C min^{-1} to 270 °C, and then held for 5 min. The injector and detector were maintained at 290 °C. The splitter ratio was 50:1, the injection volume 1 µL, and the hydrogen flow was 1.2 mL min^{-1}. The FA content was quantified against the internal standard, and the quantity of each FA was expressed as mg kg^{-1}. The double bond index (DBI) was calculated using the following equation: DBI = ([18:1] + 2 × [18:2] + 3 × [18:3])/([16:0] + [18:0]).

2.9. Statistical Analysis

All the data are expressed as the mean ± standard error of the 3 replicates. A statistical analysis was performed using SPSSv19.0 (SPSS Inc., Chicago, IL, USA). Significant differences between the samples were calculated using one-way ANOVA followed by Duncan's test at $p < 0.05$.

3. Results and Discussion

3.1. Effects of P. expansum Colonization on the Contents of TSS and Individual Sugars in Different Regions of the Apple Fruit

Sugars are considered as an important form of carbohydrates in fruit, which are stored in the vacuoles of cells in harvested fruit [28]. During colonization, sugars are taken up from the fruit by pathogens as carbon sources to participate fungal development [29]. In the present study, the contents of TSS increased in the three regions of fruit, but the TSS content declined from the distal healthy region to the decayed region of the fruit during incubation. The sucrose content in the DE region was 88.1% and 94.6% lower than that in the HE and OE regions by the 2nd day of inoculation, respectively (Figure 2). The accumulation of fructose declined in the DE region, being 30.8%, which was 17% lower than that in the HE and OE regions by the 6th day of inoculation, respectively (Figure 2). A different pattern was observed in the consumption of glucose. The content of this sugar was lower in both the DE and HE regions compared to the OE region on the 2nd of inoculation. However,

after that, the glucose content increased in both the DE and HE regions and declined in the OE region (Figure 2). These results may indicate that *P. expansum* mostly consumed sucrose and fructose as carbon sources for colonization.

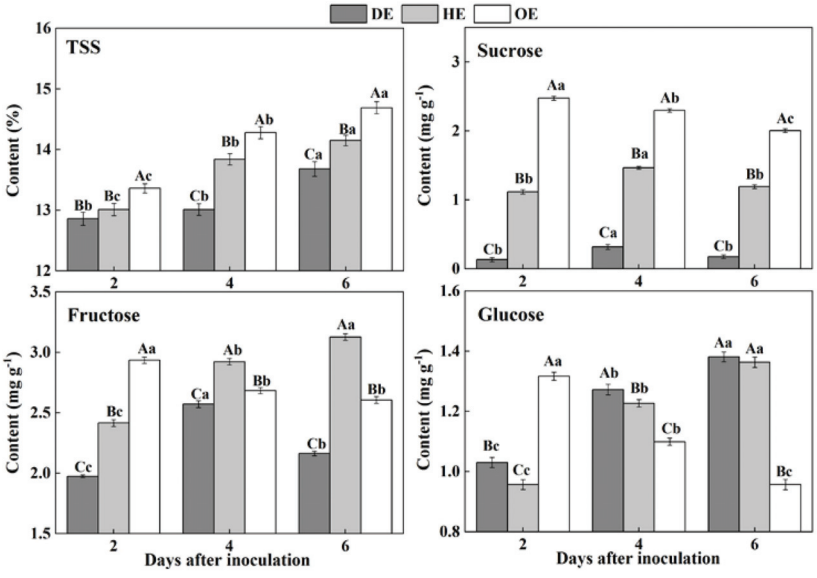

Figure 2. The contents of TSS, sucrose, fructose and glucose in different regions of *P. expansum*-inoculated apples during incubation. DE: the decayed tissue at the leading edge; HE: the healthy tissue at the leading edge; OE: the healthy tissue 6 mm away from the leading edge. The error bar indicates the standard error (±SE). Capitals indicate a significant difference between different groups at the same time point, and small letters indicate a significant difference in the same group at the different time points ($p < 0.05$).

The accumulation of TSS, sucrose, fructose and glucose in the decayed region is closely related to the disruption of the fruit's cell structure caused by fungal colonization. Various extracellular enzymes are secreted into the decayed tissue by the fungus to disassemble the cell wall of the fruit during colonization [30], causing the degradation of the cell wall polysaccharide and the increase in the soluble sugar contents [31]. Moreover, fungal colonization facilitates the breakdown of the vacuole of fruit [32], which causes the leakage of the stored fructose and glucose into to the apoplasmic space in the fruit cells [33]. Our results showed that fungus prefers to degrade or directly use sucrose as a carbon source during colonization, which caused a rapid decrease in the sucrose content in the decayed tissue. The cell wall degradation enzymes secreted by the tips of the fungal mycelium degrade the cellular components of fruit during colonization, leading to the accumulation of TSS, sucrose, fructose and glucose in the healthy regions of the leading edge. Moreover, fungal infection improves the ethylene production of fruit, which accelerates the polysaccharide degradation of the fruit [34], elevating the sugar contents. Additionally, the higher accumulation of glucose and fructose in the healthy tissues of the leading edge may be the results of the transportation of these sugars from the distal tissues in order to defend against pathogen infection [35,36]. Sucrose can be degraded to create glucose and fructose [37], which also enhanced the contents of fructose and glucose in the healthy tissues of the leading edge. The increase in the TSS in the healthy tissues away from the leading edge may be due mainly to the polysaccharide degradation caused by fungal-induced ethylene production. Moreover, the decrease in the sucrose, fructose and glucose contents may relate to the increase in the respiration of the inoculated fruit, which leads to more demands for energy and a reduced activity for the defense response of the fruit.

3.2. Effects of P. expansum Colonization on the Contents of Amino Acids in Different Regions of Apple Fruit

In fruit, amino acids are mainly stored in the vacuole, and they take part in various biological and metabolic processes in the fruit. Moreover, pathogenic fungi utilize amino acids as nitrogen sources during colonization [38,39]. Two differential accumulations of amino acids were observed in the colonized tissue. While there was a decreased accumulation of methionine, isoleucine, serine, valine, leucine and glutamate, another group of amino acids, including aspartate, threonine, lysine, arginine, alanine, glycine, cystine, phenylalanine, histidine and tyrosine, showed an increased accumulation in comparison to the healthy tissue (Figures 3 and 4). Except for leucine, methionine, glutamate, valine, isoleucine and serine contents increased in the healthy tissues (HE and OE) during incubation (Figure 3). The range of the decrease comparing the healthy with the decayed tissues in the contents of these amino acids was from 0- to 11.3-fold. The observations of the lowest contents of methionine, glutamate, leucine, valine, isoleucine and serine in the colonized tissue, in comparison to the healthy tissues, indicate the consumption of these amino acids by the pathogen (Figure 3).

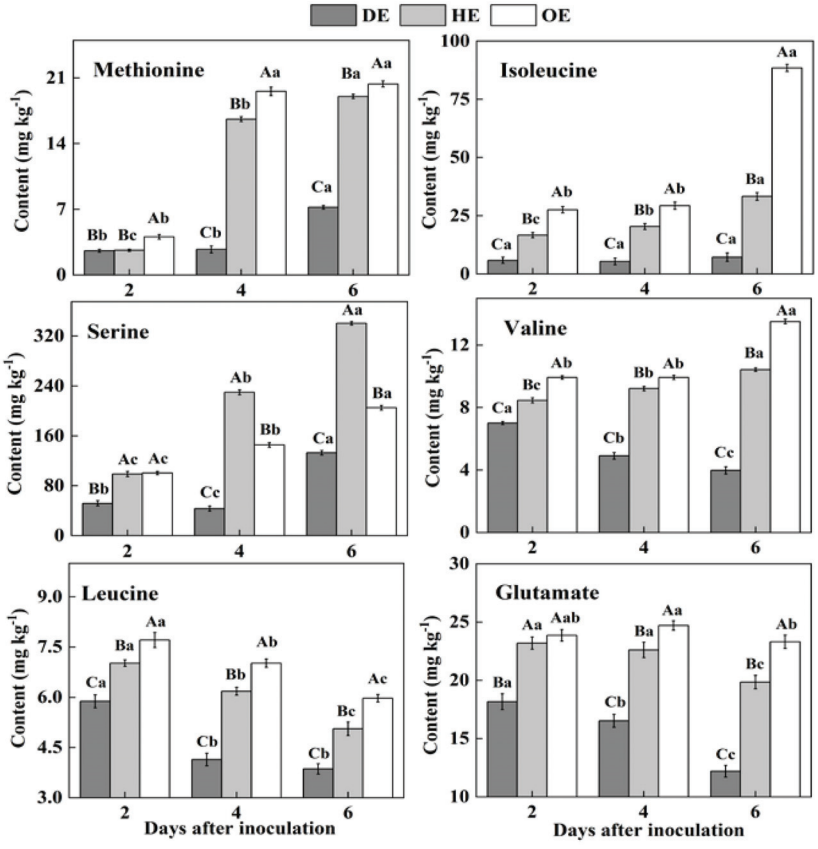

Figure 3. The decreased contents of amino acids in the decayed region compared with the healthy regions of *P. expansum*-inoculated apples during incubation. DE: the decayed tissue at the leading edge; HE: the healthy tissue at the leading edge; OE: the healthy tissue 6 mm away from the leading edge. The error bar indicates the standard error (±SE). Capitals indicate a significant difference between different groups at the same time point, and small letters indicate a significant difference in the same group at the different time points ($p < 0.05$).

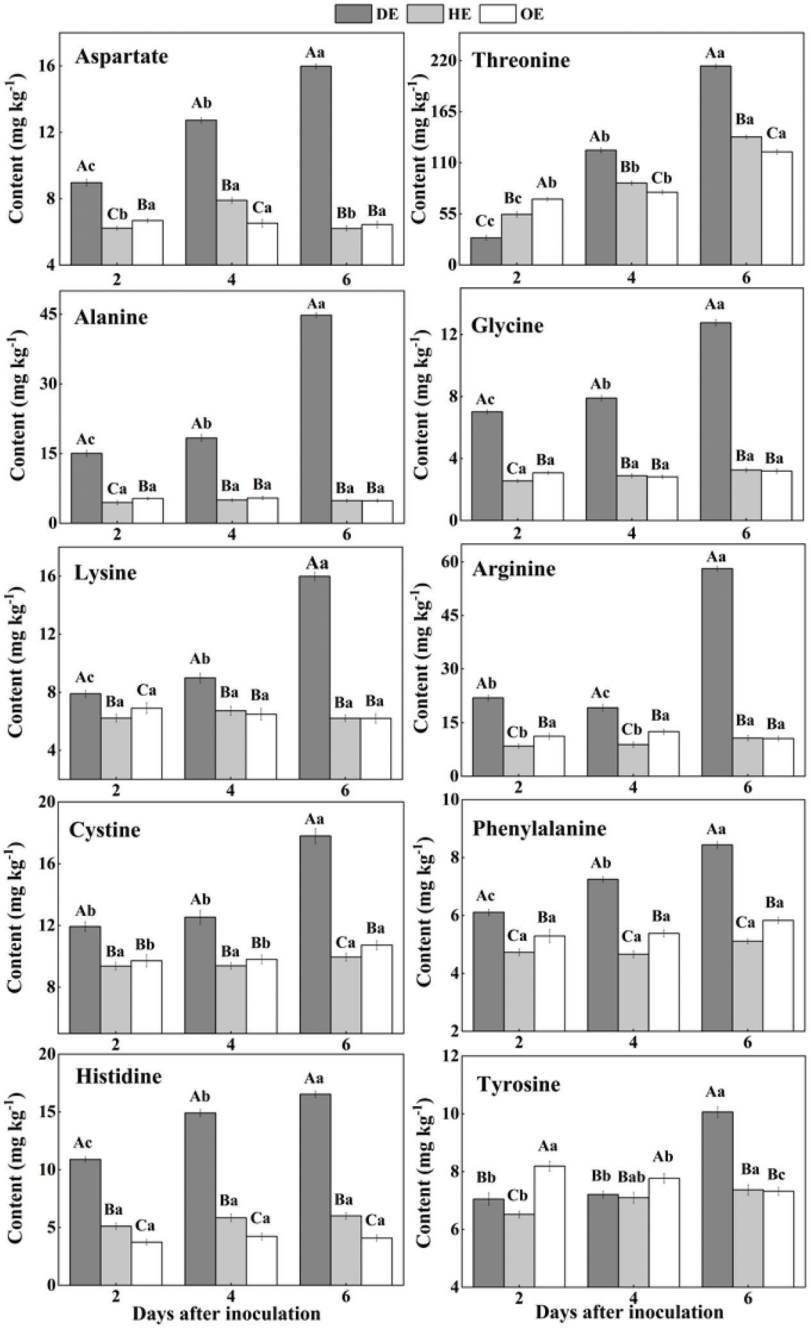

Figure 4. The increased contents of amino acids in the decayed region compared with the healthy regions of *P. expansum*-inoculated apples during incubation. DE: the decayed tissue at the leading edge; HE: the healthy tissue at the leading edge; OE: the healthy tissue 6 mm away from the leading edge. The error bar indicates the standard error (±SE). Capitals indicate a significant difference between different groups at the same time point, and small letters indicate a significant difference in the same group at the different time points ($p < 0.05$).

On the contrary, after the 2nd day of inoculation, the highest content of aspartate was observed in the decayed region, which increased by 55.4% and 75.9% compared with the HE and OE regions by the 6th day of inoculation, respectively (Figure 4). The threonine, lysine, arginine, alanine, glycine, cystine and tyrosine contents showed no significant difference between the HE and OE regions during colonization. By the 6th day of inoculation, the range of the contents of threonine, lysine, arginine, alanine, glycine, cystine and tyrosine comparing the healthy with the decayed tissues was from 0- to 8.3-fold (Figure 4). The increased accumulation of amino acids suggested a metabolic response of the fruit to the pathogen, inducing a specific accumulation in the apple tissues.

Pathogenic fungi secrete proteases into the host during colonization, which causes proteolysis at the infected sites of the fruit, leading to the accumulation of amino acids in the decayed tissues of fruit [40]. Moreover, due to the fact that most of the amino acids are stored in the vacuole of the fruit [39], we hypothesized that fungal colonization may destroy the vacuole of the fruit, causing the release of amino acids into apoplasmic space and their accumulation in the decayed region. In the present study, the lowest contents of methionine, isoleucine, serine, valine, leucine and glutamate and the accumulated contents of aspartate, threonine, lysine, arginine, alanine, glycine, cysteine, phenylalanine and histidine were observed in the decayed tissue (Figures 3 and 4). It has been indicated that fungi can selectively take up amino acids from fruit as nitrogen sources in order to meet the demands for colonization [41]. Therefore, the decrease in those amino acids in the decayed region may be more beneficial for *P. expansum* colonization. Additionally, the accumulation of methionine, isoleucine, serine, valine, glutamate and aspartate in the healthy tissue of the leading edge may be involved in their participation in the defense response of the fruit [42]. Methionine is the precursor of ethylene biosynthesis in fruit, and ethylene, as a signal, participates in the defense resistance of fruit [43]. Moreover, serine, isoleucine, aspartate and valine, as signals, can also contribute to the resistance response of fruit [44–46]. In addition to being related to the defense response, the accumulations of methionine, isoleucine, serine, valine, glutamate and aspartate during colonization may be also related to infection-induced ethylene production, which causes protein degradation.

3.3. Effects of P. expansum Colonization on the Contents of TA and Individual Organic Acids in Different Regions of the Apple Fruit

Organic acids such as citric acid, malic acid and succinic acid participate in the TCA cycle and are mostly stored in the vacuole of fruit [47]. The TA content accumulated mostly in the decayed tissue, reaching the most significant difference by the 6th day of inoculation, which was 23.80% and 76.77% higher than that in the HE and OE regions, respectively (Figure 5). The HE region had the highest content of malic acid in the first 4 days of inoculation compared with the other two regions, but it was the highest in the DE region by the 6th day of inoculation, increasing by 1.4- and 2.7-fold compared to that in the HE and OE regions, respectively (Figure 5). By the 6th day of inoculation, the citric acid content in the DE region was 1.5- and 1.9-fold higher than that in the HE and OE regions, respectively (Figure 5). The succinic acid content increased by 4.3- and 3.4-fold in the DE region compared to that in the HE and OE regions, respectively (Figure 5). The content of oxalic acid showed a higher amount in the decayed tissues, which increased by 73.1% and 42.7% compared to that in the HE and OE regions on the 4th of inoculation, respectively (Figure 5). These results indicated that *P. expansum* increased the accumulation of organic acid in the decayed tissues compared with the healthy tissues of the infected fruit.

The accumulations of TA, malic acid, citric acid, succinic acid and oxalic acid in the decayed region of the fruit are related to the breakdown of the fruit vacuole by the fungal infection. Due to the fact that most of the organic acids are stored in the vacuole, fungal colonization destroys the membrane of the vacuole, leading to the leakage of these organic acids into the apoplasmic space and causing the accumulation of these organic acids in the decayed tissues [47]. Malic acid predominates among the organic acids of apple fruit, which can enter into the gluconeogenesis pathway to produce glucose [48]. This may explain the

accumulation of glucose and the reduction in malic acid in the decayed region. *P. expansum* is described as an "acidifying fungi" that reduces the host pH by secreting gluconic and citric acid during colonization, which may contribute to citric acid accumulation in the decayed tissues [49]. Moreover, the citric and succinic acids in fruit are mainly produced by the TCA cycle [48]. Fungal colonization may improve the TCA cycle in the decayed region of the fruit, increasing the contents of citric and succinic acids. The oxalic acid in fruit is derived from the TCA cycle and ascorbic acid degradation [50]. The accumulation of oxalic acid in the decayed tissues may relate to the increased TCA cycle and induction of the antioxidant system of ascorbic acid by the pathogen infection. In addition, the accumulation of TA and organic acids in the healthy tissues of the leading edge is the result of the enhanced TCA cycle and tissue acidification caused by fungal colonization. Furthermore, during colonization, the slight decrease in the TA and organic acid contents is mainly related to infection-induced ethylene production, accelerating the TAC cycle of the fruit [15].

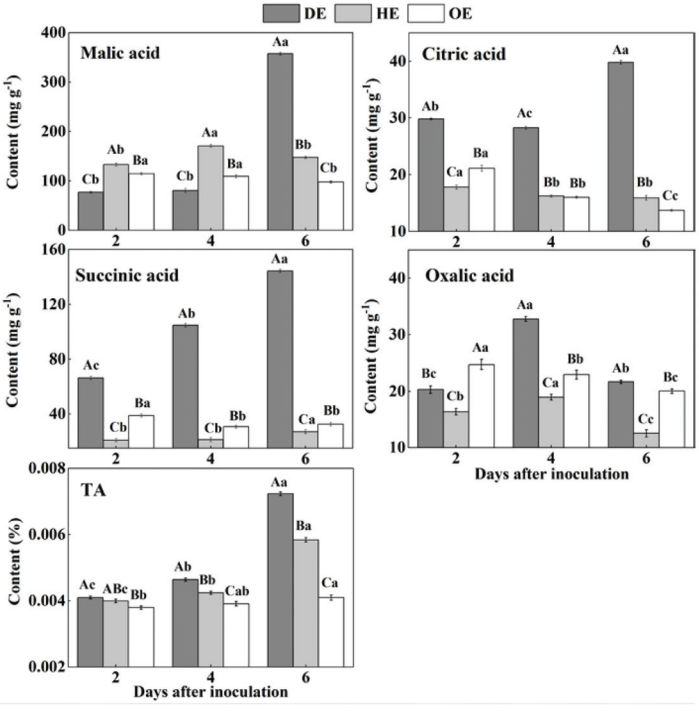

Figure 5. The contents of TA, malic acid, citric acid, succinic acid and oxalic acid in different regions of *P. expansum*-inoculated apples during incubation. DE: the decayed tissue at the leading edge; HE: the healthy tissue at the leading edge; OE: the healthy tissue 6 mm away from the leading edge. The error bar indicates the standard error (±SE). Capitals indicate a significant difference between different groups at the same time point, and small letters indicate a significant difference in the same group at the different time points ($p < 0.05$).

3.4. Effects of P. expansum Colonization on the Contents of Fatty Acids in the Different Regions of Apple Fruit

Fatty acids are an important component of cell membranes [20]. Our results showed that SFAs, stearic acid and palmitic acid accumulated from the distal healthy region to the decayed region (Figure 6). The stearic acid content in the DE region was 22.5% and 81.1% higher than that in the HE and OE regions by the 4th day of inoculation, respectively. Similarly, the palmitic acid content in the DE region was 8.7% and 22.6% higher compared with the HE and OE regions by the 6th day of inoculation, respectively. On the contrary,

the content of USFAs, including oleic acid, linoleic acid and linolenic acid, and the DBI values declined from the distal healthy region to the decayed region (Figure 6). The oleic acid content in the DE region was 9.2- and 9.4-fold lower compared with the HE and OE regions by the 4th day of inoculation, respectively. A similar pattern was observed on the 6th day of inoculation, whereupon the linoleic acid content in the DE region was 35.4% and 51.9% lower compared with the HE and OE regions, respectively. Similarly, the linolenic acid content was 45.3% and 68.2% lower in the DE region than the HE and OE regions by the 6th day of inoculation, respectively. Additionally, the DBI value showed a similar pattern, with a 38.8% and 61.3% lower content in the DE region than the HE and OE regions. These results suggest that *P. expansum* may consume the USFAs present in the decayed and healthy regions at the leading edge of the fruit more effectively.

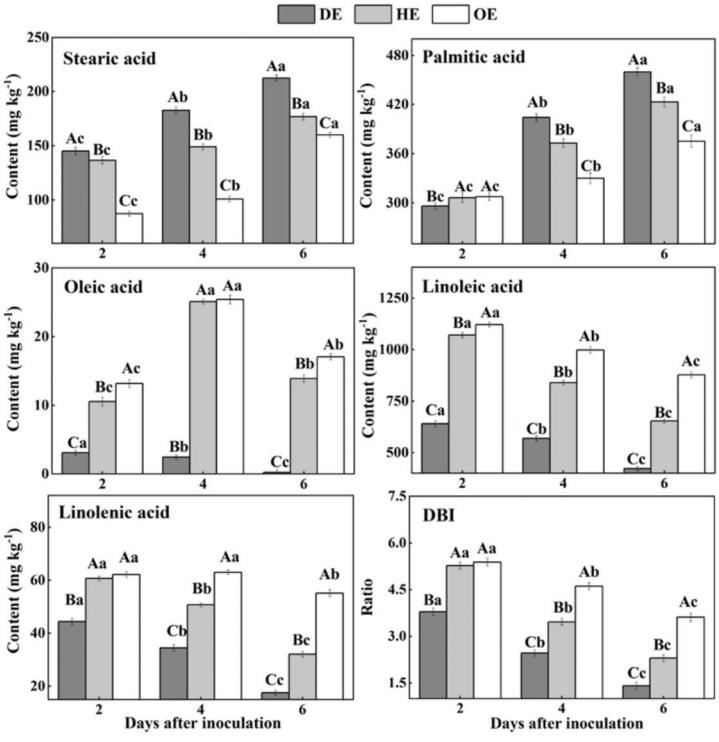

Figure 6. The contents of fatty acids in different regions of *P. expansum*-inoculated apples during incubation. DE: the decayed tissue at the leading edge; HE: the healthy tissue at the leading edge; OE: the healthy tissue 6 mm away from the leading edge. The error bar indicates the standard error (±SE). Capitals indicate a significant difference between different groups at the same time point, and small letters indicate a significant difference in the same group at the different time points ($p < 0.05$).

During colonization, the increase in the SFA (stearic acid and palmitic acid) contents and the decrease in the USFA (oleic acid, linoleic acid and linolenic acid) contents can be observed in the decayed tissues. Fungal colonization causes excess reactive oxygen species (ROS) accumulation in the fruit cells, while ROS can trigger phospholipase A2 that catalyzes the membrane lipid, releasing USFAs [51,52]. Moreover, ROS can oxidize USFAs to SFAs, decreasing the degree of unsaturation in the decayed region [53]. The accumulation of stearic acid and palmitic acid in the healthy tissue of the leading edge or that away from the decayed region may be involved in the activation of phospholipase A1 caused by infection [54]. Additionally, the reduction in the contents of linoleic acid, linolenic acid and DBI may relate mainly to the oxidation of USFAs to SFAs by ROS. In the middle stage

of colonization, the increase in the oleic acid content in the healthy tissue of the leading edge or that away from the decayed region is mainly due to the activation of lipase activity caused by the infection, which accelerates the hydrolysis of the phospholipid membrane, releasing oleic acid [17]. In addition, compared with the decayed tissue, a higher content of USFAs was observed in the healthy tissue of the leading edge or that away from the decayed region during colonization. Linoleic acid and linolenic acid participated directly or indirectly in the fruit defense via jasmonic-acid-mediated signaling [17,55].

4. Conclusions

Fungal colonization is a dynamic process, which develops in the colonized sites and spreads to the surrounding healthy tissue of the fruit. Based on the results, we identified changes in the essential metabolites in different regions of *P. expansum*-colonized apple during incubation, as shown in Figure 7. *P. expansum* preferred to use sucrose and fructose as carbon sources in the decayed region of the fruit during colonization. The accumulation of fructose and glucose in the healthy tissues of the leading edge may be related to the degradation of starch and sucrose. The breakdown of the vacuole and defense response of the fruit were caused by *P. expansum* colonization, while the decrease in the sugars in the healthy tissues away from the decayed region may be mainly involved in the improved ripening caused by colonization. Moreover, *P. expansum* selectively took up amino acids in the fruit as nitrogen sources during colonization. The accumulation of amino acids in the two healthy regions is mainly the result of protein degradation by pathogen-secreted proteases. In addition, the accumulation of organic acids in the decayed tissues is mainly related to the breakdown of the fruit vacuole and accelerated TCA cycle during colonization. The changes in the fatty acid contents in different tissues suggested that the membrane lipid metabolism and ROS production are increased from the distal healthy region to the decayed region, while the defense response of the fruit induced by USFAs may decrease in the same direction. Therefore, *P. expansum* kills cells in advance of its infection of the fruit in order to obtain carbon and nitrogen sources in the distal leading tissue of the infected apple. It is believed that more nutrients are required for the infection and a stronger defense response of the fruit to the fungal infection, causing the transit of nutrients from the distal tissue to the infected sites.

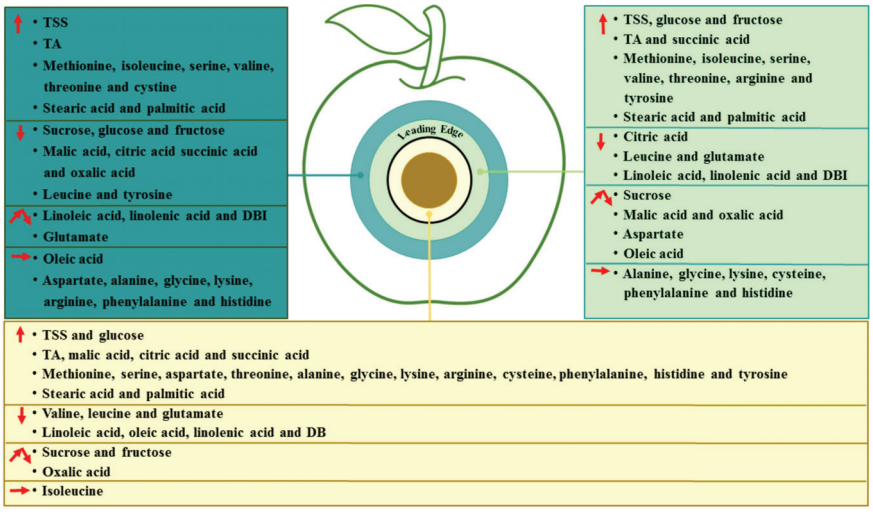

Figure 7. Proposed model of changes in the essential metabolites in different regions of *P. expansum*-colonized apple during incubation. An upward arrow indicates an increase, a downward arrow indicates a decrease, a polyline arrow indicates an increase followed by a decrease and a horizontal arrow indicates no change.

Author Contributions: Writing—original draft preparation, D.G.; writing—review and editing, Y.B.; methodology, Y.Z.; data curation, Y.L.; supervision, D.P. and E.S. All authors have read and agreed to the published version of the manuscript.

Funding: This research was funded by the Israel–China Project of the National Natural Science Foundation of China (31861143046). And The APC was funded by 31861143046.

Data Availability Statement: Data is contained within the article.

Acknowledgments: This work was supported by the Israel–China Project of the National Natural Science Foundation of China (31861143046).

Conflicts of Interest: The authors declare no conflict of interest.

References

1. Luciano-Rosario, D.; Keller, N.P.; Jurick, W.M. *Penicillium expansum*: Biology, omics, and management tools for a global postharvest pathogen causing blue mould of pome fruit. *Mol. Plant Pathol.* **2020**, *21*, 1391–1404. [CrossRef] [PubMed]
2. Yu, L.L.; Qiao, N.Z.; Zhao, J.X.; Zhang, H.; Tian, F.W.; Zhai, Q.X.; Chen, W. Postharvest control of *Penicillium expansum* in fruits: A review. *Food Biosci.* **2020**, *36*, 100633. [CrossRef]
3. Prusky, D.; Alkan, N.; Mengiste, T.; Fluhr, R. Quiescent and necrotrophic lifestyle choice during postharvest disease development. *Annu. Rev. Phytopathol.* **2013**, *51*, 155–176. [CrossRef] [PubMed]
4. Xylia, P.; Chrysargyris, A.; Ahmed, Z.F.R.; Tzortzakis, N. Application of rosemary and eucalyptus essential oils and their main component on the preservation of apple and pear fruits. *Horticulturae* **2021**, *7*, 479. [CrossRef]
5. Xylia, P.; Chrysargyris, A.; Shahwar, D.; Ahmed, Z.F.R.; Tzortzakis, N. Application of rosemary and eucalyptus essential oils on the preservation of cucumber fruit. *Horticulturae* **2022**, *8*, 774. [CrossRef]
6. García-Guzmán, G.; Heil, M. Life histories of hosts and pathogens predict patterns in tropical fungal plant diseases. *New Phytol.* **2014**, *201*, 1106–1120. [CrossRef]
7. Ahmed, Z.F.; Kaur, N.; Maqsood, S.; Schmeda-Hirschmann, G. Preharvest applications of chitosan, salicylic acid, and calcium chloride have a synergistic effect on quality and storability of date palm fruit (*Phoenix dactylifera* L.). *HortScience* **2022**, *57*, 422–430. [CrossRef]
8. Schmidt, S.M.; Panstruga, R. Pathogenomics of fungal plant parasites: What have we learnt about pathogenesis? *Curr. Opin. Plant Biol.* **2011**, *14*, 392–399. [CrossRef]
9. Shen, Y.M.; Liu, M.Y.; Nie, J.Y.; Ma, N.; Xu, G.F.; Zhang, J.Y.; Li, Y.P.; Li, H.F.; Kuang, L.X.; Li, Z.Y. Metabolite changes of apple *Penicillium expansum* infection based on a UPLC-Q-TOF metabonomics approach. *Postharvest Biol. Technol.* **2021**, *181*, 111646. [CrossRef]
10. Kou, J.; Wei, Y.Y.; He, X.X.; Xu, J.Y.; Xu, F.; Shao, X.F. Infection of post-harvest peaches by *Monilinia fructicola* accelerates sucrose decomposition and stimulates the Embden-Meyerhof-Parnas pathway. *Hortic. Res.* **2018**, *5*, 46. [CrossRef]
11. Tang, N.; Chen, N.; Hu, N.; Deng, W.; Chen, Z.X.; Li, Z.G. Comparative metabolomics and transcriptomic profiling reveal the mechanism of fruit quality deterioration and the resistance of citrus fruit against *Penicillium digitatum*. *Postharvest Biol. Technol.* **2018**, *145*, 61–73. [CrossRef]
12. Gong, D.; Bi, Y.; Zong, Y.Y.; Li, Y.C.; Sionov, E.; Prusky, D. *Penicillium expansum*-induced release of branched-chain volatile compounds in apple fruit by increasing amino acids accumulation. *Postharvest Biol. Technol.* **2021**, *173*, 111432. [CrossRef]
13. Prusky, D.; McEvoy, J.L.; Saftner, R.; Conway, W.S.; Jones, R. Relationship between host acidification and virulence of *Penicillium* spp. on apple and citrus fruit. *Phytopathology* **2004**, *94*, 44–51. [CrossRef] [PubMed]
14. Vilanova, L.; Viñas, I.; Torres, R.; Usall, J.; Buron-Moles, G.; Teixidó, N. Acidification of apple and orange hosts by *Penicillium digitatum* and *Penicillium expansum*. *Int. J. Food Microbiol.* **2014**, *178*, 39–49. [CrossRef]
15. Gong, D.; Bi, Y.; Li, Y.C.; Zong, Y.Y.; Han, Y.; Prusky, D. Both *Penicillium expansum* and *Trichothecium roseum* infections promote the ripening of apples and release specific volatile compounds. *Front. Plant Sci.* **2019**, *10*, 338. [CrossRef]
16. Lin, Y.F.; Chen, M.Y.; Lin, H.T.; Lin, M.S.; Hung, Y.C.; Lin, Y.X.; Chen, Y.H.; Wang, H.; Ritenourd, M.A. *Phomopsis longanae*-induced pericarp browning and disease development of longan fruit can be alleviated or aggravated by regulation of ATP-mediated membrane lipid metabolism. *Food Chem.* **2018**, *269*, 644–651. [CrossRef]
17. Walley, J.W.; Kliebenstein, D.J.; Bostock, R.M.; Dehesh, K. Fatty acids and early detection of pathogens. *Curr. Opin. Plant Biol.* **2013**, *16*, 520–526. [CrossRef]
18. Wang, H.; Chen, Y.H.; Sun, J.Z.; Lin, Y.F.; Lin, Y.X.; Lin, M.S.; Hung, Y.C.; Lin, H.T. The changes in metabolisms of membrane lipids and phenolics induced by *Phomopsis longanae* Chi infection in association with pericarp browning and disease occurrence of postharvest longan fruit. *J. Agric. Food Chem.* **2018**, *66*, 12794–12804. [CrossRef]
19. He, Y.Z.; Li, Z.R.; Tan, F.Q.; Liu, H.; Zhu, M.; Yang, H.B.; Bi, G.L.; Wan, H.L.; Wang, J.Q.; Xu, R.W.; et al. Fatty acid metabolic flux and lipid peroxidation homeostasis maintain the biomembrane stability to improve citrus fruit storage performance. *Food Chem.* **2019**, *292*, 314–324. [CrossRef]

20. Lin, Y.X.; Lin, H.T.; Chen, Y.H.; Wang, H.; Ritenour, M.A.; Lin, Y.F. Hydrogen peroxide-induced changes in activities of membrane lipids-degrading enzymes and contents of membrane lipids composition in relation to pulp breakdown of longan fruit during storage. *Food Chem.* **2019**, *297*, 124955. [CrossRef]
21. Chen, Y.H.; Sun, J.Z.; Lin, H.T.; Lin, M.S.; Lin, Y.F.; Wang, H.; Hung, Y.C. Salicylic acid treatment suppresses *Phomopsis longanae* Chi-induced disease development of postharvest longan fruit by modulating membrane lipid metabolism. *Postharvest Biol. Technol.* **2020**, *164*, 111168. [CrossRef]
22. Lee, J.; Jeong, M.C.; Ku, K.H. Chemical, physical, and sensory properties of 1-MCP-treated Fuji apple (*Malus domestica* Borkh.) fruits after long-term cold storage. *Appl. Biol. Chem.* **2017**, *60*, 363–374. [CrossRef]
23. Zhang, W.S.; Chen, K.S.; Zhang, B.; Sun, C.D.; Cai, C.; Zhou, C.H.; Ferguson, I.B. Postharvest responses of Chinese bayberry fruit. *Postharvest Biol. Technol.* **2005**, *37*, 241–251. [CrossRef]
24. Gancedo, M.C.; Luh, B. HPLC analysis of organic acids and sugars in tomato juice. *J. Food Sci.* **1986**, *51*, 571–573. [CrossRef]
25. López-Hernández, J.; Oruña-Concha, M.; Simal-Lozano, J.; Vázquez-Blanco, M.; González-Castro, M. Chemical composition of Padrón peppers (*Capsicum annuum* L.) grown in Galicia (NW Spain). *Food Chem.* **1996**, *57*, 557–559. [CrossRef]
26. Li, Y.; Qi, H.; Jin, Y.; Tian, X.; Sui, L.; Qiu, Y. Role of ethylene in biosynthetic pathway of related-aroma volatiles derived from amino acids in oriental sweet melons (*Cucumis melo* var. makuwa Makino). *Sci. Hortic.* **2016**, *201*, 24–35. [CrossRef]
27. Valero-Garrido, D.; López-Frías, M.; Llopis, J.; López-Jurado, M. Influence of dietary fat on the lipid composition of perirenal adipose tissue in rats. *Ann. Nutr. Metab.* **1990**, *34*, 327–332. [CrossRef]
28. Kim, J.Y.; Loo EP, I.; Pang, T.Y.; Lercher, M.; Frommer, W.B.; Wudick, M.M. Cellular export of sugars and amino acids: Role in feeding other cells and organisms. *Plant Physiol.* **2021**, *187*, 1893–1914. [CrossRef]
29. Divon, H.H.; Fluhr, R. Nutrition acquisition strategies during fungal infection of plants. *FEMS Microbiol. Lett.* **2007**, *266*, 65–74. [CrossRef]
30. Petrasch, S.; Silva, C.J.; Mesquida-Pesci, S.D.; Gallegos, K.; van den Abeele, C.; Papin, V.; Fernandez-Acero, F.J.; Knapp, S.J.; Blanco-Ulate, B. Infection strategies deployed by *Botrytis cinerea*, *Fusarium acuminatum*, and *Rhizopus stolonifer* as a function of tomato fruit ripening stage. *Front. Plant Sci.* **2019**, *10*, 223. [CrossRef]
31. Juge, N. Plant protein inhibitors of cell wall degrading enzymes. *Trends Plant Sci.* **2006**, *11*, 359–367. [CrossRef] [PubMed]
32. Huang, Y.; Sun, C.; Guan, X.; Lian, S.; Li, B.; Wang, C. Butylated hydroxytoluene induced resistance against *Botryosphaeriadothidea* in apple fruit. *Front. Microbiol.* **2021**, *11*, 599062. [CrossRef] [PubMed]
33. Bezrutczyk, M.; Yang, J.; Eom, J. Sugar flux and signaling in plant-microbe interactions. *Plant J.* **2018**, *93*, 675–685. [CrossRef] [PubMed]
34. Sun, Y.J.; Shi, Z.D.; Jiang, Y.P.; Zhang, X.H.; Li, X.; Li, F.J. Effects of preharvest regulation of ethylene on carbohydrate metabolism of apple (*Malus domestica* Borkh cv. Starkrimson) fruit at harvest and during storage. *Sci. Hortic.* **2021**, *276*, 109748. [CrossRef]
35. Moghaddam, M.R.B.; Van den Ende, W. Sugars and plant innate immunity. *J. Exp. Bot.* **2012**, *63*, 3989–3998. [CrossRef]
36. Luna, E.; Flandin, A.; Cassan, C.; Prigent, S.; Chevanne, C.; Kadiri, C.F.; Gibon, Y.; Pétriacq, P. Metabolomics to exploit the primed immune system of tomato fruit. *Metabolites* **2020**, *10*, 96. [CrossRef]
37. Yao, S.X.; Cao, Q.; Xie, J.; Deng, L.L.; Zeng, K.F. Alteration of sugar and organic acid metabolism in postharvest granulation of Ponkan fruit revealed by transcriptome profiling. *Postharvest Biol. Technol.* **2018**, *139*, 2–11. [CrossRef]
38. Jin, L.F.; Cai, Y.T.; Sun, C.; Huang, Y.N.; Yu, T. Exogenous L-glutamate treatment could induce resistance against *Penicillium expansum* in pear fruit by activating defense-related proteins and amino acids metabolism. *Postharvest Biol. Technol.* **2019**, *150*, 148–157. [CrossRef]
39. Yang, G.; Wei, Q.; Huang, H.; Xia, J. Amino acid transporters in plant cells: A brief review. *Plants* **2020**, *9*, 967. [CrossRef]
40. Xue, Q. Pathogen proteases and host protease inhibitors in molluscan infectious diseases. *J. Invertebr. Pathol.* **2019**, *166*, 107214. [CrossRef]
41. Huang, H.; Nguyen Thi Thu, T.; He, X.; Gravot, A.; Bernillon, S.; Ballini, E.; Morel, J.B. Increase of fungal pathogenicity and role of plant glutamine in nitrogen-induced susceptibility (NIS) to rice blast. *Front. Plant Sci.* **2017**, *8*, 265. [CrossRef] [PubMed]
42. Dinkeloo, K.; Boyd, S.; Pilot, G. Update on amino acid transporter functions and on possible amino acid sensing mechanisms in plants. *Semin. Cell Dev. Biol.* **2018**, *74*, 105–113. [CrossRef] [PubMed]
43. Mäkinen, K.M.; Swarnalok, D. The significance of methionine cycle enzymes in plant virus infections. *Curr. Opin. Plant Biol.* **2019**, *50*, 67–75. [CrossRef] [PubMed]
44. Wang, W.; Xu, M.; Wang, G.; Galili, G. New insights into the metabolism of aspartate-family amino acids in plant seeds. *Plant Reprod.* **2018**, *31*, 203–211. [CrossRef] [PubMed]
45. Benstein, R.M.; Ludewig, K.; Wulfert, S.; Wittek, S.; Gigolashvili, T.; Frerigmann, H.; Krueger, S. *Arabidopsis* phosphoglycerate dehydrogenase 1 of the phosphoserine pathway is essential for development and required for ammonium assimilation and tryptophan biosynthesis. *Plant Cell* **2013**, *25*, 5011–5029. [CrossRef] [PubMed]
46. Binder, S. Branched-chain amino acid metabolism in *Arabidopsis thaliana*. *Arab. Book* **2010**, *8*, e0137. [CrossRef] [PubMed]
47. Famiani, F.; Battistelli, A.; Moscatello, S.; Cruz-Castillo, J.G.; Walker, R.P. The organic acids that are accumulated in the flesh of fruits: Occurrence, metabolism and factors affecting their contents-a review. *Rev. Chapingo Ser. Hortic.* **2015**, *21*, 97–128. [CrossRef]
48. Etienne, A.; Génard, M.; Lobit, P.; Mbéguié-A-Mbéguié, D.; Bugaud, C. What controls fleshy fruit acidity? A review of malate and citrate accumulation in fruit cells. *J. Exp. Bot.* **2013**, *64*, 1451–1469. [CrossRef]

49. Prusky, D.; Bi, F.; Moral, J.; Barad, S. How does host carbon concentration modulate the lifestyle of postharvest pathogens during infection? *Front. Plant Sci.* **2016**, *7*, 1306. [CrossRef]
50. Chakraborty, N.; Ghosh, R.; Ghosh, S.; Narula, K.; Tayal, R.; Datta, A.; Chakraborty, S. Reduction of oxalate levels in tomato fruit and consequent metabolic remodeling following overexpression of a fungal oxalate decarboxylase. *Plant Physiol.* **2013**, *162*, 364–378. [CrossRef]
51. Gong, D.; Bi, Y.; Zhang, X.M.; Han, Z.H.; Zong, Y.Y.; Li, Y.C.; Sionov, E.; Prusky, D. Benzothiadiazole treatment inhibits membrane lipid metabolism and straight-chain volatile compound release in *Penicillium expansum*-inoculated apple fruit. *Postharvest Biol. Technol.* **2021**, *181*, 111671. [CrossRef]
52. Peng, H.; Gong, D.; Wei, Y.N.; Yang, Q.; Zong, Y.Y.; Prusky, D.; Sionov, E.; Bi, Y. Changes of membrane phospholipid metabolism in apple fruit infected by Penicillium expansum. *Food Sci.* **2020**. Available online: http://kns.cnki.net/kcms/detail/11.2206.TS.20200330.1406.048.html (accessed on 30 January 2020).
53. Hasanuzzaman, M.; Bhuyan, M.H.M.B.; Zulfiqar, F.; Raza, A.; Mohsin, S.M.; Mahmud, J.A.; Fujita, M.; Fotopoulos, V. Reactive oxygen species and antioxidant defense in plants under abiotic stress: Revisiting the crucial role of a universal defense regulator. *Antioxidants* **2020**, *9*, 681. [CrossRef] [PubMed]
54. Chen, G.Q.; Greer, M.S.; Weselake, R.J. Plant phospholipase A: Advances in molecular biology, biochemistry, and cellular function. *BioMolecular Concepts* **2013**, *4*, 527–532. [CrossRef] [PubMed]
55. Lim, G.H.; Singhal, R.; Kachroo, A.; Kachroo, P. Fatty acid-and lipid-mediated signaling in plant defense. *Annu. Rev. Phytopathol.* **2017**, *55*, 505–536. [CrossRef]

foods

MDPI

Review

Postharvest Biology and Technology of Loquat (*Eriobotrya japonica* Lindl.)

Hafiz Muhammad Shoaib Shah [1], Ahmad Sattar Khan [2], Zora Singh [1,*] and Saqib Ayyub [2]

[1] Horticulture, School of Science, Edith Cowan University, 270 Joondalup Drive, Joondalup 6027, Australia
[2] Postharvest Research and Training Centre, Institute of Horticultural Sciences, University of Agriculture, Faisalabad 38040, Pakistan
* Correspondence: author: z.singh@ecu.edu.au

Abstract: Loquat (*Eriobotrya japonica* Lindl.) fruit is a rich source of carotenoids, flavonoids, phenolics, sugars, and organic acids. Although it is classified as a non-climacteric fruit, susceptibility to mechanical and physical bruising causes its rapid deterioration by moisture loss and postharvest decay caused by pathogens. Anthracnose, canker, and purple spot are the most prevalent postharvest diseases of loquat fruit. Cold storage has been used for quality management of loquat fruit, but the susceptibility of some cultivars to chilling injury (CI) consequently leads to browning and other disorders. Various techniques, including cold storage, controlled atmosphere storage, hypobaric storage, modified atmosphere packaging, low-temperature conditioning, heat treatment, edible coatings, and postharvest chemical application, have been tested to extend shelf life, mitigate chilling injury, and quality preservation. This review comprehensively focuses on the recent advances in the postharvest physiology and technology of loquat fruit, such as harvest maturity, fruit ripening physiology, postharvest storage techniques, and physiological disorders and diseases.

Keywords: browning; chilling injury; *Eriobotrya japonica*; fruit ripening; postharvest physiology

Citation: Shah, H.M.S.; Khan, A.S.; Singh, Z.; Ayyub, S. Postharvest Biology and Technology of Loquat (*Eriobotrya japonica* Lindl.). *Foods* **2023**, *12*, 1329. https://doi.org/10.3390/foods12061329

Academic Editors: Imahori Yoshihiro and Jinhe Bai

Received: 9 February 2023
Revised: 14 March 2023
Accepted: 17 March 2023
Published: 20 March 2023

1. Background

Loquat fruit is believed to have originated during the Han Dynasty in southeast China approximately 2000 years ago [1]. Currently, it is cultivated in many countries around the globe, while China, the United States, Japan, Turkey, Spain, Pakistan, India, Brazil, Greece, and Cyprus are the top producers around the globe [2]. Loquat fruit is a rich source of vitamins, phenolics, minerals, sugars, organic acids, and antioxidants which protect the consumer against many diseases. Moreover, loquat fruit reduces the levels of free lipoproteins, which narrow the arteries and increase blood cholesterol. Flavonoids are only present in the peel tissues of loquat fruit, while in addition, phenolics and carotenoids are present in the fruit flesh [3]. The highest total phenolic contents (TPC) have been reported in 'Mizauto' fruit as compared to other cultivars [4]. Loquat fruit ripening is a complex process of different physiological and metabolic changes, mainly including: ethylene biosynthesis and respiratory modifications [5], colour modifications due to carotenoid biosynthesis [6], sugar and acid metabolism contributing to the variation in fruit sensory attributes [7] and changes in the lignin, polysaccharide, and pectin contents during fruit ripening resulting in cell wall modifications and fruit firmness changes during ripening [8]. These changes are associated with complex transcriptional elucidations and interlinked metabolic changes in loquat fruit. Carotenoid biosynthesis is the main constituent of fruit colour and fully mature loquat fruit may exhibit an orange to yellow colour due to the level and type of carotenoids [9]. Based on the flesh colour, loquat cultivars are divided into two main groups, including white and yellow- to orange-fleshed cultivars (Table 1).

Table 1. Some important loquat cultivars grown in the world [10,11].

Cultivar	Harvest Season	Flesh Colour	Fruit Shape	Peel Colour	Fruit Flavour
Advance	Mid	White	Pear	Yellow	Acidic sweet
Ahdar	Late	White	Oval	Greenish yellow	Sweet Tart
Ahmar	Early	Yellow	Pear	Radish orange	Sweet Tart
Baiyu	Early	White	Oval	Radish blushed	Sweet to subacid
Blush	Mid	White	Pear	Yellow	Subacid
Compagne	Early	Yellowish white	Elongated pear	Golden yellow	Subacid to sweet
Dahongpao	Mid	Yellow	Oval	Orange yellow	Subacid
Fire Ball	Mid	White or straw	Ovate	Orange	Acidic
Jiefangzhong	Mid	Yellow	Oval large	Yellow	Sweet to subacid
Lyuyangqing	Early to mid	Deep yellow	Ovate	Yellowish orange	Acidic
Mammoth	Mid	Orange	Rounded oval	Orange	subacid
Matchless	Mid	Pale orange	Pear	Golden yellow	Subacid
Mogi	Early	Light yellow	Elliptical	Yellow	Sweet
Premier	Mid	White	Oblong	Salmon orange with dots	Acidic
Safeda	Early to mid	White creamy	Pear	Yellow	Acidic
Tanaka	Late	Brownish orange	Ovoid or round	Orange yellow	Sweet
Thales	Late	Orange yellow	Oblong	Yellow	Sweet
Thames Pride	Early	Pale orange	Ovate	Yellow	Subacid
Victor	Very late	White	Oblong	Deep yellow	Sweet
Zhaozong	Mid	White	Pear	Yellow	Acidic
Zhaozong No. 6	Late	Yellow	Oval	Light yellow	Sweet

Chilling injury (CI) is the main constraint in the extension of the cold (<5 °C) storage life of loquat fruit, which consequently shortens the marketing window [12–14]. The application of polyamine [15,16], methyl jasmonate (MeJA) [17], modified atmospheric packaging (MAP) [18], and low-temperature conditioning (LTC) [19] have been found effective to mitigate the incidence of CI. Purple spot is another physiological disorder that is characterized by purple colour spots with irregular and depressed areas on the peel of loquat fruit due to a calcium deficiency and a sudden change in the water potential of fruit at the colour break stage. However, purple spot symptomatic fruit has less acceptability in the supply chain. Gariglio, et al. [20] have reported that the incidence of the purple spot may be reduced by the application of calcium ethylenediaminetetraacetic acid, calcium chloride, and calcium nitrate before the colour break stage in loquat fruit. Moreover, direct sunlight exposure at the onset of colour break is also helpful to lower the purple spot incidence. Postharvest flesh browning incidence is an important constraint during postharvest handling of various fruits, including loquat, which is caused by cellular decompartmentalization. Loquat fruit is highly susceptible to the incidence of internal flesh browning during the postharvest supply chain. The application of 1-methylcyclopropene (1-MCP) [21], acetylsalicylic acid [12], oxalic acid [22], calcium chloride [23], MeJA [24], nitric oxide (NO) [25], and L-cysteine [26] has been reported to lessen the incidence of browning in loquat. Many other non-chemical alternatives, including controlled atmosphere (CA) storage [27], MAP [28,29], LTC [13], cold storage [30], and edible coatings [31] have also been reported to reduce the incidence of postharvest internal browning in loquat fruit.

Previously, the metabolic changes during fruit ripening and the postharvest quality management of loquat fruit have been summarized in different reviews [2,32]. Moreover, the mechanism and control strategies of major fungal diseases in loquat fruit have also been presented in a recent review [33]. However, comprehensive information explaining harvest maturity indices, harvest and handling at the farm, postharvest quality management techniques, postharvest disorders and their management, as well as major diseases in the loquat fruit were not discussed in detail. Hence, the present review focuses on detailed information on harvest maturity indices, fruit ripening, postharvest disorders and diseases, and the application of various postharvest technologies to maintain the quality of loquat fruit during the supply chain.

2. Determination of Harvest Maturity

In loquat fruit, many physiological and physical attributes have been used to determine the optimum harvest maturity in different regions of the world. However, fruit colour is the most adopted technique to determine the harvest maturity of loquat fruit, depending upon the cultivar [34,35]. Fruit aroma volatiles, total soluble solids (TSS), titratable acidity (TA), and the TSS/TA ratio have also been reported to estimate the optimum maturity of loquat fruit [36]. The level of sugars has also been reported to estimate the harvesting stage of loquat, as there is a higher concentration of fructose and glucose at maturity stage as compared to the immature fruit [37]. The optimum sugar level in the loquat fruit at maturity is 10° Brix [38]. The harvest stage has a significant direct association with the postharvest physiology and storage potential of loquat fruit. However, harvesting before the fully ripe stage is advised by different scientists for commercial purposes, and this stage can be identified by the eating ripe stage along with the yellowish orange colour of loquat fruit. On the other hand, the bruising quality of loquat is directly associated with the degree of ripening, as fully ripened loquat is more susceptible to mechanical damage than fruit harvested at earlier stages [39].

Due to a higher demand in the markets, loquat fruit is advised to be harvested before 100% colour development, as it is a widely accepted commercial practice. The other reason to harvest at the early ripe stage is that the incidence of mechanical damage is very high in the fruit harvested at the fully ripe stage. There may be mechanical bruising and postharvest losses in loquat fruit when harvested at a fully ripe stage due to soft fruit flesh [40]. However, there may be an unpleasant fruit taste if loquat is harvested at an immature stage. Consumer acceptance is the main indicator that should be considered during the harvesting of fruit. Harvest maturity has been found to significantly influence postharvest bruising incidence and consumer acceptability. 'Algerie' loquat fruit, harvested with yellow-orange colour stage with 10° Brix TSS, exhibited the best eating quality [34].

3. Fruit Physiology Modifications during Ripening

Loquat fruit ripening is the sum of some structural and biochemical changes, including an increase in fruit size and weight, modifications in fruit firmness, colour development due to carotenoid biosynthesis, and a decrease in the levels of organic acids [41]. Hamauzu, et al. [42] investigated the physiological and compositional changes in 'Mogi' loquat at different maturity stages. Ethylene production, respiration rate, flesh firmness, surface colour, TPC, organic acids and sugar content were observed in fruit harvested at different maturity stages. They observed that harvesting at the faded green colour stage resulted in a decline in fruit firmness, decreasing the sugar and organic acid contents. Malic acid was found to be the most abundant organic acid in loquat at maturity, although there was also a considerable amount of succinic, fumaric, and citric acids. There was a simultaneous increase in ethylene biosynthesis at maturity with a considerable decline in respiration rate and this was the optimum stage for harvest.

The relationship between loquat fruit ripening and ethylene biosynthesis is somewhat inconclusive, as there have been varied assessments made by different researchers. However, it is believed to be non-climacteric in nature due to the lack of a sharp rise in ethylene biosynthesis and respiration rate at harvest maturity [42–44]. Moreover, fruit maturation is independent on exogenous ethylene application [45], and irregular patterns of relationships between respiration and ethylene biosynthesis are not evident in loquat fruit despite being reported for many climacteric fruits [46]. Three genes, including *EjACO1*, *EjACO2,* and *EjACS1* from 'Luoyanqing' loquat fruit, have been cloned at various ripening stages and shown to account for endogenous ethylene production. The expression of *EjACO2* was observed in petals and leaves, whereas *EjACO1* and *EjACS1* appear in fruit. The ethylene production peaked at the colour break stage, where the *EjACO2* expression pattern was consistent with ethylene biosynthesis [47]. Respiration is another important factor associated with loquat fruit ripening and is catalyzed by ethylene biosynthesis. The rate of respiration during maturation is also correlated with the cultivars. The lowest respiration

has been reported in 'Centenaria' loquat while 'Mizauto' and 'Mizumo' loquat exhibited a higher respiration rate up to two days after harvest, and declined thereafter [48]. However, the pattern of respiration and ethylene biosynthesis is still unknown in many cultivars and requires future investigations.

Loquat fruit undergoes colour modifications, which is an important maturity index based on the type of cultivar (yellow or white), contributed by the endogenous carotenoids production. The major constituent of ripe loquat fruit is β-carotene in the pulp, while β-cryptoxanthin has been found in the peel tissues [49]. There is a consistent increase in carotenoid biosynthesis with the advancement in the maturation of loquat fruit [50]. The advancement of fruit growth causes a reduction in organic acids, except for malic acid, which is the main acid at the ripe stage, and carotenoids increase in pulp tissues, which leads to the colour development in loquat fruit. During ripening, fruit softening increases due to the degradation and hydrolysis of pectin and lignin contents. Immature fruit exhibits a higher activity of phenylalanine ammonia lyase (PAL) enzyme, which catalyzes lignin biosynthesis in immature fruit. There was a gradual decline in PAL enzyme activity with the advancement in fruit maturation, leading to less lignin deposition in the cell walls of loquat fruit, resulting in fruit softening [51]. Cell wall depolymerizing enzymes play a significant role in the downregulation of fruit firmness with the advancement in fruit development. Pectin methyl esterase and polygalacturonase are the principal enzymes leading to the demethylation and misfunctioning of cross-linkages between the cell wall components, increasing the hydrolysis of pectin molecules in the cell wall. Similarly, the cellulase enzyme deteriorates the cell wall polysaccharides and causes fruit softening during fruit maturation [52].

Sugars and organic acids contribute to the fruit flavour and texture at the ripe stage. The level of sorbitol is at its maximum in unripe loquat fruit and decreases with the advancement of fruit maturation. However, sucrose accumulation is very high during the early fruit maturation phase and is also the predominant sugar in mature loquat fruit [2]. Similarly, glucose and fructose contents also increase with the advancement of loquat fruit maturation [7]. During ripening, the accumulation of sucrose by the metabolism of polysaccharide molecules is triggered by a series of sugar-metabolizing enzymes including sucrose phosphate synthase (SPS), sucrose synthase (SS), and acid invertase (AI), while the major enzymes catalyzing the metabolism of sorbitol in ripening loquat are sorbitol-6-phosphate dehydrogenase (S6PDH), sorbitol dehydrogenase (SDH), and sorbitol oxidase (SOX) [53–55]. The TSS/TA ratio contributes to the sensory attributes of loquat fruit, including flavour and texture, while approximately seventy-eight various aroma volatiles have also been identified in loquat fruit [56]. Although the primary aroma volatiles have also been reported in the literature, changes in the levels of conjugated and non-conjugated aroma volatiles have not been determined in different loquat fruit cultivars and warrant further investigation.

4. Harvest and Handling

Harvest and handling are directly associated with the postharvest quality of loquat, as about 50% of losses are due to the harvest and handling operations of the fruits. Mostly, the fruit is harvested at 100% colour development for the local markets. In Cyprus, the fruit is mainly harvested at an early stage (50–75% colour development) and exhibited better shelf life than late harvesting at 100% colour development [36]. The harvesting stage of loquat fruit may be judged based on certain physical, physiological, and biochemical attributes (Table 2). Loquat fruit is harvested manually, using gloves to avoid contamination of the fruit with germs. Fruit should be cut from the nearby stalk and should not be pulled to avoid skin bruising, and then gently placed with care in the container. Rough handling causes bruising and bursting of the peel with sap flow, where later fungal and bacterial growth leads to deterioration of the fruit [57]. The best time for harvesting loquat is the morning after sunrise because there is less ethylene production, respiration rate, and lower fruit internal temperature, which can enhance the shelf life and postharvest quality of the

fruit [58]. After harvest, fruit should be packed in a container with shock absorber material to avoid bruising during transport to the packhouse [59]. Package house practices include many operations, such as the grading of fruit based on colour and quality free from decay, the removal of insect pest symptoms, exposing the fruit to a low temperature, throwing out decayed fruit, and packaging. Shading for harvesting fruit is necessary with proper aeration to remove field heat, followed by transport to the packhouse. Packhouse operations start with the removal of fruit from containers after the sorting of fruit based on decayed and healthy fruit. Fruits are mainly graded based on their size and colour, free from any physical damage, bruising, and disease symptoms. Pre-cooling should also be practiced for fruit preservation because it reduces postharvest losses by reducing the ethylene and respiration rate [41]. Physical damage is the first constraint in fruit deterioration that initiates a stress condition, leading to a subsequent increase in malondialdehyde (MDA) content, polyphenol oxidase (PPO) enzyme, ethylene, and respiration rate, with a browning index [60]. Stem cutting with a clipper or sharp knife can help reduce physical damage. Possible operations from harvest to consumer are listed in Figure 1.

Table 2. Physical, physiological, and biochemical characteristics of loquat fruit at maturity [34,47,48,61].

Parameter	Ripe Fruit Concentration
Respiration rate at 20 °C (μL CO_2 g^{-1} h^{-1})	36.59–48.13
Ethylene production at 20 °C (nL g^{-1} h^{-1})	0.62–1.00
Fruit firmness (N)	3.33–3.83
Lightness	61.56–63.11
a *	8.82–10.57
b *	49.64–52.05
Total soluble solids (°Brix)	7.63–12.97
Titratable acidity (%)	7.04–9.78
TSS/TA ratio	0.86–1.11
Glucose (g 100 g^{-1} FW)	1.4–1.7
Fructose (g 100 g^{-1} FW)	3.08–3.60
Sucrose (g 100 g^{-1} FW)	5.2–5.4
Malic acid (mg 100 g^{-1} FW)	101.97–150.14
Citric acid (mg 100 g^{-1} FW)	895.58–988.05
Ascorbic acid (μg g^{-1} FW)	15.7–18.3
Total phenolic content (μg GAE/g FW)	427.9–450.7
Total antioxidant content (% inhibition DPPH)	60–65
Total flavonoid content (μg rutin/g FW)	43.5–51.0
Total carotenoids (β-carotene/g FW)	35.7–48.3

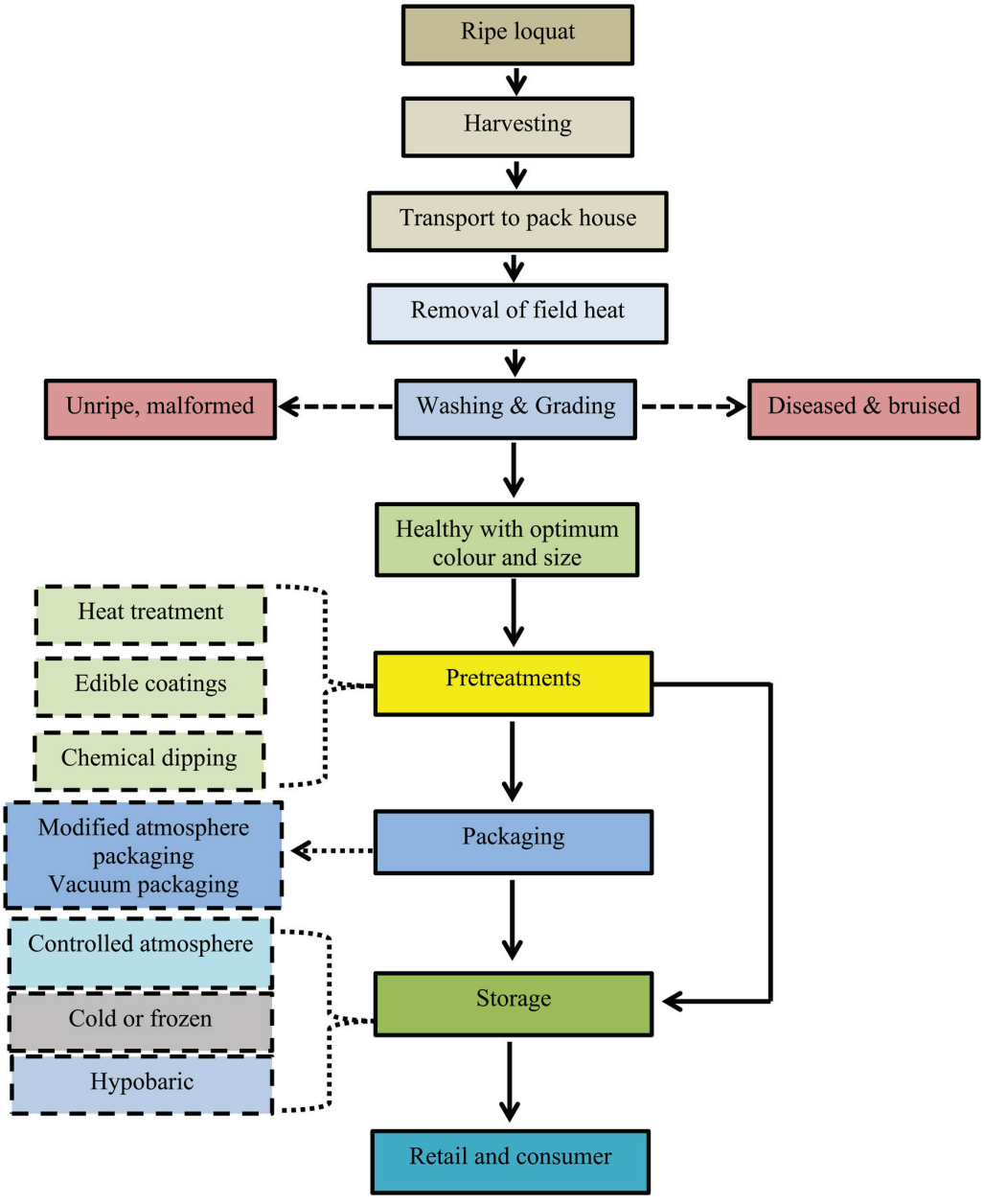

Figure 1. Process flow chart for the harvesting and postharvest handling of loquat fruit is described based on the literature.

5. Postharvest Handling and Storage Techniques

5.1. Heat Treatment

Heat treatment (HT), conducted either alone or in combination with other techniques such as cold storage, MAP, and chemical application, has been shown to be effective for the quality maintenance of loquat fruit [14]. Hot air treatment is an effective technique to control CI in loquat fruit (Table 3). Hot air treatment at 38 °C for 5 h, followed by cold storage at

1 °C for 35 days, is very effective against chilling stress in 'Jiefangzhong' loquat fruit. The above study also showed a significant decline in electrolyte leakage and MDA content with reduced activities of the lipoxygenase (LOX) and phospholipase D (PLD) enzymes. Further, linoleic and linolenic acid levels were maintained, which delayed the production of oleic, stearic, and palmitic acids, in turn leading to a higher unsaturated-to-saturated fatty acid ratio [62]. Similarly, loquats exposed to hot air treatment (45 °C) for 3 h maintained a higher saturated/unsaturated fatty acid ratio, and inhibited membrane leakage by reducing the levels of MDA and hydrogen peroxide (H_2O_2) radicals [14]. Further, HT delayed activities of polygalacturonase (PG), PPO, peroxidase (POD), and PAL enzymes, maintained higher juice content, and lowered fruit decay incidence in loquat fruit. Moreover, fruit firmness was maintained due to the higher pectin and lignin content in the peel of HT-treated loquat fruit [63]. Similar hot air (35 °C, 5 h) treatment in cultivar 'Jiefangzhong' was useful in maintaining higher activities of ascorbate peroxidase (APX), catalase (CAT), and superoxide dismutase (SOD) with condensed POD enzyme, H_2O_2 content, and superoxide anion leading to lesser LOX activity and MDA production, with higher juice content and alleviation of fruit firmness [64]. Combined hot air and hot water dip applications before cold storage in 'Jiefangzhong' efficiently delayed the senescence of the fruit with a delayed reduction in TSS and TA, reduced decay, browning index, rot incidence, and improved sensory qualities with higher juice content [65]. The efficiency of hot air (37 °C) for 3 and 6 h, followed by cold storage for 60 days, demonstrated that heat application for 3 h was very helpful in lowering the internal browning of 'Fukuhara' loquat fruit pulp compared to 6 h with lower activities of PAL, POD, and PPO enzymes, which were negatively correlated with HT, and an intermittent exposure for 3 h with no effect on fruit firmness [66]. Similarly, hot air exposure at 48–52 °C, with cold storage at 2–5 °C, reduced CI symptoms, plasma membrane permeability, and respiration rate, and maintained higher activities of CAT, POD, and PAL enzymes. Heat shock-induced defence mechanisms ultimately alleviated chilling stress and respiration rate while enhancing the activities of CAT and POD enzymes and reducing the activity of the PAL enzyme [67].

Table 3. Effect of heat treatment on postharvest quality management of loquat.

Cultivar	Treatment	Inference	Reference
'Fukuhara'	Hot air treatment 37 °C for 3- and 6 h	Higher AsA, TA, and TSS content with less activity of PAL, POD, and PPO enzymes were observed. CI was suppressed.	[66]
'Jiefangzhong'	Hot air (38 °C) for 36- and 48 h	Less fruit rot, FWL, FD, and internal browning with higher TA and TSS content. Burning symptoms were observed when stored for 48 h.	[65]
'Jiefangzhong'	Hot air exposure (38 °C) for 5 h	Reduced MDA and H_2O_2 contents, higher juice content and less fruit firmness, enhanced APX, SOD, and CAT enzyme activities. Lowered LOX and superoxide radical production.	[63]
'Jiefangzhong'	Hot air treatment (38 °C) for 5 h	Delayed the activities of PG, PPO, POD, and PAL enzymes, reduced lignin deposition and FD, maintained higher sensory quality.	[64]
'Jiefangzhong'	Exposure to hot air at 38 °C for 5 h	Inhibition of PLD and LOX enzymes, decline in membrane leakage, higher linolenic and linoleic acid content with less stearic and oleic acid. Maintained higher unsaturated/saturated fatty acid content with less MDA content.	[62]
'Jiefangzhong'	Hot air (38 °C) for 36 h + *Pichia guilliermondii*	*C. acutatum* was lowered with higher SOD and CAT enzymes and less ROS. Higher lignin deposition due to higher PAL enzyme.	[68]
'Jiefangzhong'	Hot air treatment at 38 °C for 36 h	Reduced FWL, FD, internal browning, and POD, PPO, and PAL enzymes. Higher APX, CAT, and SOD enzymes with less membrane leakage. Higher TPC with less CI and ROS.	[69]
'Jiefangzhong'	Hot air exposure (35 °C) for 3 h	Lowered MDA and H_2O_2 contents, maintained membrane integrity, higher NI, AI, SS, and SPS enzyme assays with less sucrose and higher fructose and glucose level. Alleviated CI symptoms.	[70]

Table 3. *Cont.*

Cultivar	Treatment	Inference	Reference
'Jiefangzhong'	Hot air (38 °C, 5 h) + MeJA 16 μmol L^{-1}	Less protopectin, pectin, and lignin content, less PPO, POD, and PAL with higher PG, APX, CAT and SOD enzyme activities.	[71]
'Jiefangzhong'	Hot water treatment (45 °C) for 10 min + GB 10 mmol L^{-1}	Reduced MDA content and electrolyte leakage, higher CAT, SOD, and APX enzymes, higher proline, and GABA due to higher OAT, P5CS, and GAD enzymes.	[72]

FD = fruit decay, FWL = fruit weight loss, GABA = γ-aminobutyric acid, GAD = glutamate decarboxylase, GB = glycine betaine, NI = neutral invertase, OAT = ornithine δ-aminotransferase, P5CS = Δ^1-pyrroline-5-carboxylate synthetase, RSM = response surface methodology.

5.2. Postharvest Chemical Treatments

Several chemicals have been used as potential inhibitors against senescence and physiological disorders to extend the storage life of loquat fruit (Table 4). 1-MCP is an ethylene inhibitor that is used for quality management and extending the shelf life of many horticultural commodities [73–77]. 1-MCP has been found to be very effective against internal browning and fruit decay incidence, with better sensory attributes in 'Luoyangqing' loquat during storage as well as maintained membrane integrity, reduced oxidation of polyphenols, superoxide anion accumulation, and activities of PPO and LOX enzymes [21]. Similarly, 1-MCP application lowered fruit decay in 'Qingzhong' loquat by inhibiting reactive oxygen species (ROS) production due to effective 1,1-diphenyl-2-picrylhydrazyl (DPPH) radical scavenging activity and lower activity of the PPO enzyme [78]. The application of 1-MCP before cold storage alleviated CI symptoms with a considerable decrease in electrolyte leakage, H_2O_2, superoxide radicals, and MDA content by maintaining lower activities of phospholipase C (PLC) and LOX enzymes and higher CAT enzyme activities [79]. The application of 1-MCP treated 'Fuyang' loquat fruit maintained a higher unsaturated to saturated fatty acid ratio, leading to higher membrane integrity and reduced CI symptoms. Moreover, 1-MCP treated fruit reduced the levels of cellulose, hemicellulose, and cyclohexanediaminetetraacetic acid (CDTA) soluble pectin than control [80]. The relationship between cell wall metabolism and CI is the key factor in the chilling susceptibility of loquat fruit and is mainly influenced by upstream activities of the phenylpropanoid pathway, including the activities of coenzyme A ligase:4 coumarate (4CL), the endomembrane-bound cinnamate 4-hydroxylase (C4H), and PAL enzymes. Exogenous application of 1-MCP suppressed the activities of PAL, C4H, and 4CL coenzyme A and maintained higher PG enzyme activity, leading to less pectin and lignin deposition in cold-stored loquat fruit and hence lowered the CI index [81].

Table 4. Effect of chemical treatments on postharvest quality management of loquat fruit.

Chemical	Cultivar	Treatment	Inference	Reference
1-MCP	'Baisha', 'Luoyangqing'	1 μL L^{-1} + LTC at 5 °C for 6d	Less G-POD, CAD, and PAL enzyme activities with less superoxide radicals, lignin deposition, FD at 5 °C LTC, and 1-MCP in both cultivars. 'Luoyangqing' was a better respondent than 'Baisha'	[82]
	'Claudia'	1, 2, 3, 4 and 5 μL L^{-1}	CI, browning, FD, and fruit softening were delayed with better fruit sensory attributes. Best treatment was 1 μL L^{-1} 1-MCP.	[83]
	'Claudia' 'Nespolone di Trabia'	0.50 and 1 μL L^{-1}	Fruit firmness was maintained with better TA and lower browning in both cultivars. However, better results were presented by 'Nespolone di Trabia' with 1 μL L^{-1} 1-MCP treatment.	[84]

Table 4. *Cont.*

Chemical	Cultivar	Treatment	Inference	Reference
	'Fuyang'	10, 50 and 100 nL L^{-1}	CI was inhibited with a decrease in MDA, H_2O_2, and superoxide radicals, lower LOX, and PLC enzymes. However, CAT enzyme activity was maintained.	[79]
	'Fuyang'	2.32 nmol L^{-1}	CI was reduced. Higher linolenic and linoleic acid content, leading to higher unsaturated/saturated fatty acid ratio. Less hemicellulose and cellulose content with higher water- and CDTA-soluble pectin content.	[80]
	'Fuyang'	50 nL L^{-1}	Suppressed PAL, CAD, C4H, 4CL coenzyme A, POD, and PPO enzymes, and high PG enzyme activity. CI was also lowered. Inhibition of FD, browning, and lignin deposition were observed.	[85]
	'Jiefangzhong'	50 nL L^{-1}	Suppressed browning, FD, H_2O_2 content, and superoxide radicals. Improved APX, SOD, and CAT enzymes with higher chitinase and β-1,3-glucanase enzymes. Higher juice content, TSS, and TA were also exhibited. *C. acutatum* infection was inhibited.	[81]
	'Luoyangqing'	0.5, 5 and 50 μL L^{-1}	Inhibited browning and ethylene production. Lowered PPO and LOX enzymes. Maintained higher TPC and polyphenol content with reduced superoxide anion radicals.	[21]
	'Qingzhong'	50 nL L^{-1}	Lowered FD, enhanced TSS, TA, sucrose, glucose and TPC. Reduced PPO activity with higher DPPH-radical scavenging activity. Inhibited ROS production.	[78]
BTH	'Jiefangzhong'	10, 30 and 60 mg L^{-1}	Higher TSS and TA were maintained. Suppressed *C. acutatum* infestation and PAL enzyme activity. Lignin deposition was minimized, and there was aggravation of the disease tolerance mechanism.	[86]
	'Jiefangzhong', 'Zhaozhong 6'	10, 30 and 60 mg L^{-1}	Higher chitinase and β-1,3-glucanase, SOD, CAT, POD, and PPO enzyme activities but suppressed PAL enzyme. Reduced LOX and ROS production.	[87]
		2, 3 and 4% $CaCl_2$	Maintained a lower browning index, weight loss, and TA while increasing juice content, pH, and TSS.	[88]
	'Advance'	4% $CaCl_2$ + 11 m*M* AsA + 5 m*M* CA + 5 mmol SA	Higher hue angle was exhibited. Less FWL, DI, FD, and firmness were seen. There was higher TA, TSS, and AsA content.	[89]
	'Changhong'	1% $CaCl_2$	Reduced CI, superoxide anion, H_2O_2, and MDA content while exhibiting higher activities of DHAR, GR, MDHAR, APX, CAT, and SOD enzymes, as well as a higher DPPH radical assay.	[90]
	'Changhong'	1% $CaCl_2$, 10 mmol L^{-1} EGTA	Prevented CI, ion leakage, and MDA content with higher ATP, ADP, and EC. Increased Ca^{2+}-ATPase and H^+-ATPase, CCO, SDH, PAO, DAO, GAD, OAT, and P5CS enzymes. There were higher proline, polyamine, and GABA contents.	[91]
	'Surkh'	1, 2 and 3% $CaCl_2$	Reduction in EC, FWL, browning, and firmness increase. Higher TA, TSS, and AsA contents.	[23]
	'Trouloti'	2% $CaCl_2$	Sweetness was increased, and acidity declined with a lower TPC level. There was no impact on FWL and dry matter. There was a reduction in respiration rate.	[92]
	'Qingzhong'	0.8% $CaCl_2$ + 0.2, 0.4 and 0.8% PAA	DI, FD, FWL, respiration rate, and membrane leakage was decreased. Higher TSS, TA, and AsA content with better sensory attributes were observed.	[93]

Table 4. *Cont.*

Chemical	Cultivar	Treatment	Inference	Reference
Ethanol	'Jiefangzhong'	300 μL L^{-1}	Boosted activities of PAL, SOD, PPO, POD, chitinase, and β-1,3-glucanase enzymes. H_2O_2 was increased which initiated a defense mechanism against spores and mycelium of *C. acutatum*.	[94]
GB	'Jiefangzhong'	10 mmol L^{-1} GB + HT 45 °C for 10 min	Higher CAT, SOD, APX, P5CS, OAT, and GAD enzymes with higher GABA and proline content. Reduction in MDA content and CI symptoms.	[72]
	'Jiefangzhong'	1, 5, 10, 20 mmol L^{-1} GB	Higher TFC and TPC content, less FWL, and browning. Higher CAT and SOD enzymes with less MDA content. A 10 mmolL^{-1} concentration was best.	[95]
MeJA	'Fuyang'	10 mmol L^{-1} MeJA	Reduction in respiration, ethylene production, PPO, and PAL enzymes activities. Higher total sugar and organic acid content with higher TPC and TFC was maintained. Browning and FD were lessened.	[96]
	'Fuyang'	10 mmol L^{-1} MeJA	Reduced CI, saturated fatty acids, H_2O_2 content, and superoxide radicals. Fruit firmness and colour was maintained.	[97]
	'Fuyang'	10 mmol L^{-1} MeJA	CI was lowered with less pectin, hemicellulose, pectin, alcohol content, and lignin deposition by suppressing PAL and PPO enzymes. CDTA and water soluble pectin were increased. ROS production was lowered with a remarkable decline in the POD enzyme.	[98]
	'Jiefangzhong'	10 μmol L^{-1} MeJA	Exhibited higher level of chitinase and β-1,3-glucanase enzymes, higher TSS and TA content, less browning, FD, and spore germination of *C. acutatum*.	[24]
	'Jiefangzhong'	10 μmol L^{-1} MeJA	Reduced lignin deposition, inhibited PPO and PAL enzyme activities. MeJA induced H_2O_2 content that suppressed the fungal growth of *C. acutatum* with higher CAT and APX enzymes.	[99]
	'Jiefangzhong'	10 μmol L^{-1} MeJA + *Pichia membranefaciens* 1×10^8 colony-forming units mL^{-1}	Inhibited spore germination and germ tube elongation of *C. acutatum*. There was less disease incidence and higher chitinase and β-1,3-glucanase enzymes activities were maintained.	[100]
	'Jiefangzhong'	10 μmol L^{-1} MeJA	GSH-POD, APX, and GST enzymes were enhanced with a higher AsA content. GSH content was decreased due to more MDHAR, DHAR, and GR enzyme activities, and inhibition of AO enzyme activity. Browning was also delayed.	[101]
	'Jiefangzhong'	10 μmol L^{-1} MeJA	Higher GABA and proline content were shown with higher P5CS, OAT, and GAD enzymes and reduced PDH enzyme. CI was suppressed with less browning.	[102]
	'Jiefangzhong'	10 μmol L^{-1} MeJA	Higher ATP, Put, Spd, and Spm content was maintained. Suppressed AMP and ADP production by increasing energy status with less anthracnose symptoms.	[103]
	'Jiefangzhong'	MeJA 16 μmol L^{-1} + HT at 38 °C for 5 h	Less protopectin, pectin and lignin content, less PPO, POD, and PAL with higher PG, APX, CAT, and SOD enzyme activities.	[71]
	'Luoyangqing'	10 μmol L^{-1}	Induced *EjbHLH14*, *EjHB1*, and *EjPRX12* gene expression, thereby decreasing CI and lignin content.	[17]

Table 4. *Cont.*

Chemical	Cultivar	Treatment	Inference	Reference
NO	'Luoyangqing'	0.5 mmol L^{-1} cPTIO, 0.1 mmol L^{-1} TUN, 10 m mmol L^{-1} Gln, 0.5 m mmol L^{-1}, *L*-NAME and 0.5 m mmol L^{-1} PBITU	All these NO inhibitors reduced APX, CAT, POD, and SOD enzyme activities with higher MDA and H_2O_2 content. Membrane leakage and browning were increased. The role of NO in fruit quality has been confirmed.	[25]
Melatonin	'Dawuxing'	50 μL melatonin	Reduced weight loss and MDA content while maintaining higher firmness, ABTS, FRAP, and DPPH radical assays	[104]
SA		1500, 2000 and 3000 ppm	Reduced browning and increased TSS, TA, and pH.	[105]
	'Jiefangzhong'	1 gL^{-1} SA	FD, lignin deposition, and browning were decreased. Reduction in CAD, PAL, and PPO enzymes were also observed.	[106]
	'Luoyangqing'	1 mmol L^{-1} ASA	Reduced the CI symptoms with reduced G-POD, CAD, and PAL enzyme activities and prohibited superoxide radical accumulation.	[12]
	'Zaozhong'	40 and 70 mg L^{-1} SA	GSH was increased with higher GST, G-POD, MDHAR, DHAR, and APX enzymes, which alleviated the POD enzyme and decreased MDA and H_2O_2 contents with less DHA activities.	[107]
2, 4-epib-rassinolide	'Changhong'	10 μmol L^{-1} EBR	The symptoms of lignification were alleviated because of the delay in the rise in lignin concentration in loquat fruit.	[108]
Short term N_2	'Dahongpao'	100% N_2	Changes in membrane permeability, MDA levels, and ROS production rates were all significantly slowed down. Furthermore, SOD and CAT activities were considerably higher, whereas LOX activity was significantly lower, in N_2-treated fruits compared to control fruits.	[109]

ADP = adenosine diphosphate, AMP = adenosine monophosphate, AO = ascorbate oxidase, ASA = acetyl-salicylic acid, ATP = adenosine triphosphate, BTH = benzothiadiazole, CA = citric acid, Ca^{2+}-ATPase = Ca^{2+}-adenosine triphosphate, CCO = cytochrome *c* oxidase, DAO = diamine oxidase, DHA = dehydroascorbic acid, DI = disease incidence, EC = electrical conductivity, EBR = epibrassinolide, EGTA = ethylene glycol bis (2-aminoethyl ether) tetraacetic acid, FD = fruit decay, FWL = fruit weight loss, GABA = γ-aminobutyric acid, GAD = glutamate decarboxylase, GB = glycine betaine, Gln = glutamine, GSH = glutathione, GSSG = oxidized glutathione, GST = glutathione-*S*-transferases, H^+-ATPase = H^+-adenosine triphosphate, H_2O_2 = hydrogen peroxide, HT = heat treatment, *L*-NAME = NG-nitro-l-Arg methyl ester, OAT = ornithine δ-aminotransferase, P5CS = Δ^1-pyrroline-5-carboxylate synthetase, PAA = peracetic acid, PAO = polyamine oxidase, PBITU = S,S'-1,3-phenylene-bis(1,2-ethanediyl)-bis-isothiourea, PDH = proline dehydrogenase, PE = polyethylene, ppb = parts per billion, Put = putriscine, SA = salicylic acid, Spd = spermidine, Spm = Spermine, TUN = tungstate.

MeJA, an ester of jasmonic acid, is a cyclopentanone compound known to regulate plant growth and is effective against physical and physiological stresses [110]. Recently, the role of MeJA in the alleviation of CI and quality deterioration in horticultural commodities has been examined [17,98,102]. MeJA induces chilling tolerance, mainly by inducing gene expression in *EjbHLH14*, *EjHB1*, and *EjPRX12* genes, which lowers lignin biosynthesis [17]. The mechanism of MeJA against chilling stress is mainly due to the activation of oxidative enzymes such as CAT, SOD, POD, and APX, which are mainly initiated by the higher H_2O_2 level and delay in the oxidation of unsaturated to saturated fatty acids during storage. Exogenous MeJA application lowered the ethylene biosynthesis, respiration rate, and PAL and PPO enzyme activities with higher DPPH-radical scavenging and SOD enzyme activities [96]. Moreover, there were a delay in H_2O_2 and superoxide anion production that inhibited LOX enzyme activity and elevated activities of APX, CAT, and SOD enzymes, leading to higher membrane integrity due to an increase in unsaturated fatty acids, hence inducing chilling tolerance in MeJA-treated 'Fuyang' loquat than control [97]. MeJA treatment inhibited the activity of the PAL enzyme and increased the activity of

the PG enzyme, which lowered ROS production and fruit firmness due to a reduction in lignin, pectin, hemicellulose alcohol residues, and cellulose elevation, thereby inducing CI tolerance in 'Fuyang' loquat during cold storage. Additionally, CDTA- and water-soluble pectin were reduced with improved solubility of polysaccharides in the cell wall [98].

NO is the major bioactive signaling compound during abiotic and biotic stresses in plants that triggers a defense response and itself is the major scavenger of ROS during CI [111]. The inhibition of endogenous NO accumulation is the main factor that makes a fruit susceptible to oxidative stress and higher membrane leakage due to the activities of oxidative enzymes such as PPO and POD, with higher lignin deposition due to PAL enzyme activity. Alternatively, a 50 mmol·L^{-1} sodium nitroprusside (SNP) dip treatment maintained a lower activity of LOX and MDA content, leading to a reduction in lipid peroxidation with higher activities of APX, CAT, and SOD enzymes in 'Dawuxing' loquat, thereby maintaining cell membrane integrity and the suppression of POD and PPO enzymes. Additionally, the confirmation of the NO role in low-temperature tolerance and the signal transduction of jasmonic acid (JA) was confirmed by the exogenous application of 2-(4-carboxyphenyl)-4,4,5,5-tetramethylimidazoline-1-oxyl-3-oxide (cPTIO), an NO scavenger, and the NO inhibitors NaN_3 and *L-NAME* in 'Zaozhong No. 6′ young loquat fruit [112]. Chilling stress increased with the application of a NO inhibitor and scavenger with suppressed activities of SOD, POD, and CAT enzymes while MDA and H_2O_2 contents were aggravated. The application of cPTIO not only stimulated CI symptoms but also lowered endogenous NO biosynthesis during cold storage with reduced membrane integrity [25].

Sulphur is an essential nutrient required for plant growth and development and plays a crucial role in various physiological processes. It has been shown that improved plant resilience is directly connected to the increasing levels of sulphur dioxide (SO_2) uptake and SO_2 metabolism in plants. The application of SO_2 helps to maintain the equilibrium between the production of ROS and their detoxification, which in turn helps to suppress ROS formation and prevent the lignification of the flesh of loquat fruit [33]. The treatment of loquat fruit with an SO_2-releasing agent (SO_2-releasing pad) substantially reduced the prevalence of decay and browning. The TSS and TA levels were observed to be higher than in control fruits [113]. Similarly, after 35 days of storage, loquat fruit treated with SO_2 exhibited acceptable quality and a significantly lower reduction in total acidity and percentage of juice [15].

Several studies have reported that short-term N_2 treatment delayed fruit ripening by reducing respiration and ethylene production [114,115]. A substantial delay in the rise in fruit decay rate, less reduction in TSS and TA, improved eating quality, and extended shelf life were observed in loquat fruits treated with short-term N_2 for 6 h at 20 °C. Furthermore, increases in membrane permeability, MDA concentration, and superoxide anion generation rate were all significantly slowed by short-term exposure to N_2. SOD, CAT, and POD activities were all substantially increased in N_2-treated fruits compared to control fruits, which led to a decrease in CI [109].

Ozone is an allotropic species of oxygen that has powerful disinfection capabilities; as a result, its use in the postharvest processing of fruits is becoming more widespread. Under the right conditions during the production process, ozone will activate mechanisms that are involved in the protection of cellular structures against oxidative stress. This will increase the concentration of vitamin C, and consequently, the product will have more antioxidant properties [116]. Loquat fruit, treated with ozone, showed significantly less rise in lignin content and cell membrane permeability, as well as a decreased fruit deterioration rate [117].

Calcium is a very important nutrient that not only stimulates the growth of plants but also enhances the defense mechanism against many physiological and physical stresses [118]. It has been widely used to alleviate CI in cold-stored loquat fruit by triggering the suppression of ROS accumulation through the Helliwell-Asada pathway. Higher activities of dehydroascorbate reductase (DHAR), monodehydroascorbate reductase (MDHAR),

glutathione reductase (GR), APX, CAT, and SOD were also exhibited by the calcium chloride ($CaCl_2$)-treated fruit [90]. Calcium is also effective in inhibiting flesh and peel browning [105]. $CaCl_2$ pre-storage treatment induced *EjCAMTA5*-mediated transcriptional regulation of *EjPLC6*-like and *EjLOX5* genes, which delayed membrane lipid hydrolysis and maintained cell membrane integrity, preventing loquat fruit browning during chilling stress [119]. The exogenous application of calcium compounds reduced membrane permeability, suppressed ethylene production and the respiration rate in loquat fruit, resulting in better fruit quality compared to the control [120]. Recently, melatonin has been found to be effective in the downregulation of MDA content and oxidative stress due to higher levels of DPPH, ferric ion reducing antioxidant power (FRAP), and 2,2′-azinobis (3-ethylbenzothiazoline-6-sulfonic acid) (ABTS) assays. In addition, higher phenolic content in melatonin-mediated loquat fruit was noted with higher activities of PAL, 4CL, C4H, and cinnamyl alcohol dehydrogenase (CAD) enzymes [104].

5.3. Edible Coatings

Edible coatings play a key role in the postharvest management of loquat fruit [31]. Carbohydrate-based edible coatings have been widely used to extend the shelf life of loquat fruit. The coating of loquat fruit with chitosan, a polysaccharide, maintained higher catechin and quercetin polyphenols while reducing ROS accumulation during cold storage [121]. Moreover, chitosan coating suppressed the respiration rate, ethylene production, internal browning, fruit firmness, and weight loss [122]. The application of a 1% chitosan coating in 'Golden Nugget', 'Nespolone Rosso di Trabia', and 'Algerie' loquat fruit was beneficial to delay changes in skin colour, TA, TSS, and sugar content, with lower fruit weight loss and internal browning, which were correlated with higher ascorbic acid (AsA) content, carotenoid, flavonoids, polyphenols, and reduced ROS production [123]. The packaging of loquat fruits with 3% myrtle leaves and exposing them to myrtle leaf vapour for 2 min inhibited weight loss, decay incidence, and fruit browning [124]. The total phenolic contents of loquat fruit, coated with an edible coating made from cactus pear mucilage, were higher than uncoated fruits, which indicated that the coating showed a beneficial effect in scavenging ROS, protecting cell membrane peroxidation, and delaying the senescence of loquat fruit [125]. Biomaterials with 0.5% *Nigella sativa* oil and 0.5% propolis extract reduced weight loss, maintained fruit firmness, and reduced fruit browning and decay in loquat fruits during cold storage [126]. The CI symptoms were downregulated in 'Baiyu' loquat fruit by the combination of a nano-silica and chitosan coating through maintaining higher cell wall integrity, leading to a subsequent decline in fruit weight loss and internal browning throughout the cold storage period with higher TSS, TA, and sugars [127]. Similarly, alleviation in CI incidence consequently reduced the activities of the LOX enzyme with lower MDA production and maintained membrane integrity by reducing the unsaturated fatty acids in fruit tissues by the chitosan and nano-montmorillonite composite film in loquat fruit [123]. Natural plant tree extracts from apricot and cherry were also effective in reducing microbial decay, bacterial colonies, and mycelia growth in loquat and strawberry fruits during postharvest storage. Moreover, there were no residual chemicals in coated fruits that may be harmful to consumer health [128]. Although the effectiveness of edible coatings has been reported in the literature, the production of fermented products is the major issue in the prolonged storage of edible coated loquat fruit [129]. Moreover, consumer acceptance toward coated fruit is the main hindrance to commercial usage of edible coatings for loquat fruit.

5.4. Cold Storage

Cold storage is widely used as it not only reduces the incidence of fruit decay and internal browning but also significantly extends storage life and maintains loquat fruit quality [127]. However, CI symptoms are shown to be elevated with low-temperature storage, which is associated with higher lignin biosynthesis in loquat fruit [27]. Moreover, some studies have shown that cold storage intensified CI with higher lignin deposition

and juiceless flesh in cold-stored loquat fruit [85,98]. Tian, et al. [130] have outlined the minimum temperature to avoid chilling stress to loquats, which varies from 0 to 10 °C, depending upon the cultivars. They investigated chilling tolerance in 'Wuxing', 'Zhaozhong', and 'Jiefangzhong' loquat cultivars, observing the optimum temperature for these cultivars to be 1 °C, 8–10 °C, and 6–8 °C, respectively, for a maximum of 4 weeks of storage. However, cell wall integrity was maintained at lower temperatures (4 °C), while there was a higher PG correlation with higher temperature storage in 'Karantoki' and 'Morphitiki' loquat fruit stored at 20 °C [52]. Among cultivars, 'Karantoki' exhibited less phenolic content, antioxidative capacity, and acidity during storage. Similarly, there was an increase in fruit firmness throughout storage at 20 °C, with the increase in lignin content caused by the persistent rise in the activities of POD, CAD, and PAL enzymes in 'Luoyangqing' loquat fruit [13]. There was a higher rate of lignin deposition and firmness in fruit during the early days of cold storage while there was very little difference in loss of firmness after 3 weeks of storage [29]. The activities of sucrose hydrolysing enzymes were higher in chilling tolerant cultivars with higher activities of hexokinase and fructokinase enzymes involved in sugar generation signalling and hexose phosphorylation. Both of these enzymes maintained lower ethylene synthesis and respiration rates with better fruit quality after 35 days of cold storage [131].

5.5. Modified Atmosphere Packaging (MAP) and Controlled Atmosphere (CA) Storage

MAP is an effective postharvest strategy to enhance the shelf life and maintain loquat fruit quality by maintaining a higher CO_2 and a lower O_2 atmosphere around the fruit [130]. Several studies have outlined the efficacy of MAP in shelf life extension and quality management of loquats during postharvest storage (Table 5). The MAP storage of 'Hafif Çukurgöbek' loquat was beneficial in maintaining higher flavonoid, phenolic content, total sugars, organic acid, TA, and TSS with better skin colour and reduced internal browning and fruit decay at 5 °C for 30 days. There was significant inhibition in ethylene production in MAP stored over the control fruit [132]. Similarly, 'Champagne de Grasse' loquat fruit treated with 1-MCP followed by MAP storage at 5 °C for 4 weeks reduced ethylene production and maintained fruit quality [133]. Postharvest MAP storage in Xtend® bags maintained higher levels of organic acids and sugars in 'Morphitiki' loquat fruit [18]. MAP, using biodegradable polymer polylactic acid bags, was effective in reducing internal browning, fruit weight loss, and the quality attributes of 'Golden Nugget' and 'Algerie' loquat fruit during low-temperature storage; however, there was an abrupt rise in the deterioration of fruit during the shelf period [134]. The MAP of biodegradable polymer polyactic acid on the postharvest sensory quality and storability of 'Golden Nugget' and 'Algerie' loquat fruits was effective in lowering internal browning, fruit weight loss, and quality attributes of both cultivars during low-temperature storage; however, there was an abrupt rise in deterioration of fruits during the shelf period [135]. 'Ottawianni' loquat fruit stored at 5 °C in active MAP with gas combinations (3% CO_2 + 12% O_2 +85% Ar) showed better quality attributes, along with a lower decay incidence as compared to the control [132].

Table 5. Effect of modified atmospheric packaging storage on postharvest quality management of loquat.

Cultivar	Treatment	Inference	Reference
'Algerie, 'Golden Nugget',	PLA tray at 5 or 10 °C	Reduced browning, weight loss, and sugar content with improved organoleptic attributes.	[135]
'Algerie'	Microperforated PE at 2 °C storage and a 4 day shelf life at 20 °C	Lowered fruit weight loss, reduced firmness increase, and maintained higher sugar and acid levels.	[29]
'Champagne de Grasse'	(I) 312.5 ppb of 1-MCP+MAP (II) 625.5 ppb of 1-MCP+MAP	Reduced internal browning, microbial activity, better fruit colour, and higher TSS content.	[133]

Table 5. *Cont.*

Cultivar	Treatment	Inference	Reference
'Golden Nugget' 'Syeda'	12.5 μm, 14 μm, or 16 μm thick PVC films at 0 °C	Browning increased with increased PE film thickness, lowered weight loss, and firmness increase maintained higher TSS and TA content.	[136]
'Hafif Çukurgöbek'	MAP (20 μm thick; LifePack) with 3- and 6-mM OA	Higher TPC, TFC, organic acids, and delayed browning and firmness increase was maintained, especially in 6 m*M* and MAP storage.	[132]
'Japanese Azalea'	MAP with CA (0.5, 1.0%), AsA (1, 2%), NaHMP (0.5, 1.0%)	Higher DPPH radical scavenging activity with a better TPC, TFC, TA, TSS, and TSS/TA ratio was exhibited with less browning and weight loss.	[137]
'Jiefangzhong'	PE packaging with 6 at 10 °C	Less respiration and fruit weight loss at 10 °C than at 6 °C with better sensory attributes.	[27]
'Jiefangzhong'	Perforated low density PE with (4.8 ± 0.67)% CO_2 and (11.5 ± 0.85)% O_2.	Reduced weight loss, respiration rate, firmness increased, and maintained higher TSS, TA, and vitamin C content.	[60]
'Karantoki' 'Morphitiki'	Xtend® packaging + 4 °C storage + 20 °C for 2d.	'Morphitiki' was better in colour, TSS, TA, and higher browning was observed in 'Karantoki'	[18]
'Mogi'	0.15% perforated PE + 1, 5, 10, 20 and 30 °C	Suppressed respiration rate and ethylene production, reduction in malic acid and sucrose content, fruit weight loss and fruit decay were lowered.	[28]
'Ottawianni'	MAP with (12% O_2 + 3% CO_2 + 85% Ar), (12% O_2 + 3% CO_2 + 85% N), (15% O_2 + 5% CO_2 + 80% Ar), (15% O_2 + 5% CO_2 + 80% N)	Ar-treated MAP stored fruits exhibited higher TPC and TFC content, while there was less browning in N treated MAP stored fruits.	[132]
'Surkh'	HDPE (0.09 mm), LDPE (0.03 mm), 0.25% LDPEP at 4 °C	LDPE exhibited the least browning, HDPE maintained the lowest TSS and firmness, and LDPEP maintained the lowest TA and highest firmness.	[134]
'Qingzhong' 'Dawuxing'	Nano-SiO_2 packing (0.10% of nano-SiO_2 with film thickness of 40 mm	Substantial reduction in the rate of internal browning, as well as slowed declines in TSS, TA, and vitamin C contents and extractable juice in both cultivars.	[138]
'Palermitana'	PVC plastic film, transmission rates of water vapor, O_2 and CO_2 through CX film are 350 g m^{-2}·24 h at 38 °C, 18,000 cm^3 m^{-2}·24 h,and 47,000 cm^3 m^{-2}·24 h at 23 °C.	Loquat fruits kept in cold storage and SL with film packaging significantly prevented shriveling and maintained interior quality and flavour.	[139]

Ar = argon, HDPE = high density polyethylene, LDPE = low density polyethylene, LDPEP = perforated low density polyethylene, N = nitrogen, NaHMP = sodium haxamataphosphate, OA = oxalic acid, ppb = parts per billion, PE = polyethylene, TFC = total flavonoids content.

CA storage is a specific gaseous composition around the fruit, with a higher concentration of CO_2 and a lower O_2. Atmospheric ethylene, CO_2, O_2, storage temperature and time, ripening stage, and commodity are key factors that determine the ethylene biosynthesis and respiration rates in CA storage. The CA storage with 10% O_2 + 1% CO_2 and 70% O_2 for 24 h first, followed by CA storage with 10% O_2 + 1% CO_2 at 1 °C was effective in delaying fruit decay and maintained a TSS: TA ratio with higher endo-polygalacturonase (Endo-PG) and exo-polygalacturonase (Exo-PG) levels that also mitigated oxidative stress and internal browning [27]. It was observed that with higher O_2 combined with polythene packaging, the activity of PPO was inhibited, resulting in lower oxidative stress and a browning index with better TSS and TA content in 'Jiefangzhong' loquat fruit [140]. The cost of CA storage and MAP bags and their unavailability in developing countries is the major limitation in their commercial use. Extensive research is required to develop the cost-effective and easily

available MAP bags to lower the fruit quality deterioration and extend the shelf life of loquat fruit during postharvest storage and the supply chain.

5.6. Hypobaric Storage

Another very important storage technique that has been used to extend the shelf life by reducing senescence and delay in the ripening of loquat fruit is hypobaric storage. This technique is described by quick heat loss, reduced pressure, and oxygen levels during storage. Quality management and shelf life of loquat stored at 2–4 °C and 40–50 kPa for 7 weeks exhibited lower fruit flesh browning and fruit decay and higher juice contents with higher AsA content and TA [141]. The storage period can be increased up to 50 days when loquat is stored at 10 kPa pressure with low fruit decay and normal fruit flavour [142]. However, there is less information about the efficacy of hypobaric storage on the quality maintenance and postharvest storage life of loquat, which warrants further investigation.

6. Postharvest Physiological Disorders

6.1. Chilling Injury (CI)

Loquat is a highly perishable fruit that exhibits a very limited shelf life of about 10 days at ambient temperature due to excessive moisture loss and microbial decay. The desiccation of the fruit is a critical factor that determines the shelf life of any fresh commodity. Cold storage is a common way to lower the constraints related to ambient storage. However, some cultivars, such as the red-fleshed 'Luoyangqing' loquat cultivar, are very perishable due to CI, that can be determined by internal browning, juiceless texture, hardening of pulp, and stuck peel [143]. Yang, Sun, Wang, Shan, Cai, Zhang, Zhang, Li, Ferguson and Chen [82] determined the efficacy of different cultivars for CI and reported that 'Baisha' was the most susceptible among white-fleshed cultivars. There was increased lignification accompanied by the browning of pulp tissues and decreased juice content. Moreover, the activities of lignification enzymes, including guaiacol peroxidase (G-POD), CAD, and PAL were also increased with higher superoxide-free radical development. The incidence of CI is directly correlated with the abnormal metabolism of the fruit tissues due to increased PG and pectin methyl esterase (PME) enzyme activities [16]. Alterations in the levels of putrescine, spermidine, and spermine in fruit pulp have also been correlated with chilling stress and severe damage to loquat fruit [15]. Another physiological cause of CI might be a reduction in unsaturated fatty acids in the cell membrane of the fruit pulp due to oxidative stress followed by lipid peroxidation [144].

There is a direct correlation between the ethylene biosynthesis signalling and the expression of CI symptoms in loquat fruit. This role was demonstrated both in chilling sensitive red-fleshed 'Luoyangqing' and chilling tolerant white-fleshed 'Baisha' loquat cultivars [145]. Transcription records of both cultivars showed enhanced expression of *EjCTR1*, *EjETRS1b*, and *EjETR1* genes in both cultivars, while *EjEIL1* was expressed in 'Baisha' only at the middle stage of development; over the course of fruit ripening, there was a characteristic decrease in the expression of *EjEIL1* and *EjERS1a* genes in both cultivars. The development of the CI symptoms may be ascribed to oxidative stress, leading to the formation of MDA [97]. The mechanism in the CI resistance of loquat fruit was primarily due to higher levels of anti-oxidative enzymes, including APX, glutathione peroxidase (GSH-POD), SOD, and CAT activities that ultimately lowered H_2O_2 and superoxide radicals, leading to a significant decline in lipid peroxidation [146].

Another important physiological aspect which correlated with CI is lignin deposition in the cell wall of fruit tissues which causes the hardening of pulp and peel tissues. There are different mechanisms in both white- and red-fleshed loquat cultivars for lignin deposition [147]. Two genes, *EjMYB1* and *EjMYB2*, isolated from chill-stressed fruit, play important regulatory roles in lignification and promote the transcription rate for lignin synthesizing genes. Similarly, the role of *EjNAC1*, *EjNAC2*, and *EjODO1* genes in lignified stems and roots indicated that there was a decline in expression during the fruit development process [148]. Lignin biosynthesis increased due to increased *EjCL5*, *Ej4CL1*, and

EjPAL1 gene expression caused by trans-activation of the promoter with the overexpression of *EjODO1* [149].

Control of CI

Cold storage is the common technique to store loquat fruit, and some cultivars are susceptible to CI during low-temperature storage. LTC is an alternative technique for fruit quality management that regulates biochemical and physiological responses by suppressing CI incidence [150]. An antagonistic examination of LTC and HT based on the RNA-seq transcription database with the expression of *EjHSF* exhibited an abundance in *EjHSF1* transcription with a higher HSP *EjHsp* level in heat-treated loquat fruit, while there was a higher transcription of *EjHSF3* in LTC. Both *EjHSF1* and *EjHSF3* activated promoters of lignin biosynthesis-related genes and *EjHsp*. Therefore, *EjHSF* induced two distinct mechanisms in fruit regarding lignin deposition and transcription of *EjHSF3* induced in LTC was positively correlated with lignin biosynthesis, although *EjHSF1* induced chilling resistance in heat-treated loquat fruit [151]. The expression of genes involved in lignin deposition leading to CI was suppressed by LTC and HT, exhibiting a better quality of cold-stored loquat fruit [152]. LTC induces higher H_2O_2 accumulation at an early stage of loquat fruit storage and induces the chilling tolerance by regulating higher activities of antioxidant enzymes, including GSH-POD, APX, CAT, and SOD [153]. A significant reduction in CI symptoms with a double shelf-life extension was observed in 'Luoyangqing' loquat fruit exposed to LTC as compared to the control. LTC increased the resistance to browning in 60 days of cold storage, followed by a 2-day shelf life at 20 °C. Improved sensory attributes and low chilling damage were induced by LTC in loquat fruit [13].

Membrane leakage and internal flesh browning are two prominent symptoms of CI in loquat fruit. HT induces chilling tolerance in cold-stored loquat fruit by reducing the conversion of unsaturated fatty acids to saturated fatty acids, inhibiting the activities of phospholipase D (PLD) and LOX enzymes [62]. The upregulation of ascorbate and glutathione contents through the higher metabolism of sugars is another possible way to control the CI in HT-treated loquat fruit. HT induced higher ascorbate and glutathione contents and reduced fruit firmness, lignin deposition, and lipid peroxidation during low-temperature storage, leading to higher membrane integrity and chilling tolerance [14]. A comparative analysis of loquat fruit showing CI symptoms indicates a higher activity of the CAD enzyme, which is regulated through the expression of *EjCAD5*. Xu, et al. [154] reported that the application of hot air treatment suppressed the activity of the CAD enzyme and the expression of *EjCAD5* via a higher transcriptional expression of the *EjHAT1* promoter, hence maintaining less CI symptoms than control loquat fruit during low-temperature storage.

The exogenous application of anti-ripening chemicals is also effective to suppress CI symptoms in loquat fruit. The application of MeJA induces chilling tolerance by regulating the arginine metabolic pathway and increases γ-aminobutyric acid and proline contents in loquat fruit [102]. Moreover, MeJA increases the activities of antioxidant enzymes in cold-stored loquat fruit, leading to the reduced conversion of liquid to gel phase. MeJA-treated loquat fruit exhibited a higher metabolism of glutathione and ascorbic acid, followed by higher activities of SOD, CAT, and APX enzymes, and fewer CI symptoms [101]. 1-MCP reduces CI symptoms in loquat fruit by maintaining a higher unsaturated to saturated fatty acid ratio and reducing the activities of phospholipases and oxidative enzymes [79,80]. NO is also reported to lower the incidence of CI in cold-stored loquat fruit by regulating sugar metabolism [25].

6.2. Enzymatic Browning

Enzymatic browning is probably one of the most pronounced disorders in fruits and vegetables [76,155]. It reduces consumer acceptability of vegetables and fruits. The most accepted mechanism of browning is the oxidation of phenolic compounds by the oxidative enzyme PPO, which involves O-diphenol and oxygen oxidoreductase activities. Phenolic compounds are naturally present in the vacuole of plant cells while the oxidative enzymes

are part of cellular cytoplasm [156]. Degradation and oxidative damage to the vacuolar membrane initiate the reaction of PPO with phenolic compounds. Monophenolase or cresolase enzymes catalyse the production of O-diphenol by the hydroxylation of monophenol, leading to further oxidation of O-diphenols to O-quinones. Both reactions are catalyzed by the PPO enzyme in the presence of O_2. PAL and POD enzymes play a supportive role in the oxidation of phenolic compounds [157]. Potentially, SO_2 fumigation was used for the inhibition of internal and pericarp browning in horticultural commodities [158]; however, due to its residual effects and carcinogenicity, it was prohibited in the fruit industry [26]. To avoid hazards caused by SO_2 fumigation, many alternative chemicals, such as 1-MCP [21], acetylsalicylic acid [12], oxalic acid [22], calcium chloride [23], MeJA [97], and NO [25], have also been reported to minimize the incidence of postharvest internal browning in loquat fruit. However, internal flesh browning is still a major constraint in the loquat fruit supply chain and warrants an investigation of the strategies to control browning.

7. Diseases

Diseases cause fruit decay, limit preharvest production and postharvest life, and deteriorate fruit quality. A variety of pathogens are involved in pre- and post-harvest diseases; the main pathogenic organisms are *C. gloeosporioides*, *C. acutatum*, *Pseudomonas syringae*, *Phytophthora palmivora*, *Diplodia natalensis*, *Diplocarpon mespili* and *Botrytis cinerea*.

7.1. Purple Spot

Purple spot, caused by *Diplocarpon mespili* fungus, is a major preharvest disease that not only deteriorates fruit production in the preharvest phase but also limits the supply chain of loquat fruit in local and distant offshore markets [159]. Purple spot has been reported in many regions of the world and reduces about 50% of the commercial and cosmetic value of loquat fruit, and adversely impacts consumer acceptability. Early maturing cultivars are more vulnerable to being affected, and symptoms appear at the colour break stage during fruit development, leading to a decline in commercial value [46]. According to Gariglio, et al. [160] the initiation of purple spot is directly associated with a modified water relationship between peel and pulp tissues, leading to the spontaneous purple colour development followed by higher sugar accumulation in loquat fruit and a simultaneous rise in growth rate. Other symptoms are juiceless hard cells, collapsed cytoplasm with a breakdown in cellular composition out of the plasmalemma, flaccid peel tissues, and deformed fruit shape [46,161]. Sunlight exposure with low temperature and higher differences between day and night temperatures increases the purple spot incidence in loquat fruit. However, there is no influence of purple spot on the transpiration from the surface of the fruit [162]. Purple spot on loquat exhibit an irregular fruit surface and a more depressed area with slight spots of purple colour at the start of the disease, resulting in a 20% loss in natural fruit colour; however, this affects the epidermal tissues, with no effects on deeper flesh tissues. A calcium deficiency accompanied by a fungus attack may also lead to the development of deeper spots because there is a characteristic decline in the calcium level in loquat fruit throughout fruit development [162]. Contrarily, Blumenfeld [57] reported that the main cause of purple spots is the sudden change in water potential at the colour break stage of the fruit. This was very clear evidence that the purple spot appearance was correlated with dehydration of peel tissues and sudden exposure to low temperatures at the fruit colour break stage. Moreover, there was no difference in the permeability of the cuticle, and there was no damage to the cuticle layer of the fruit surface, although peel tissues were damaged by purple spot [44].

Another very important phenomenon is the reduction in the levels of Cu, K, and Fe in the peel tissues of the affected fruit compared to healthy fruit [159]. Purple spot incidence is mainly dependent upon the type of cultivar, the temperature change during fruit development, and the osmotic balance of the fruit. It has been demonstrated that early-maturing cultivars are more susceptible to the development of purple spot (60%) than late-maturing cultivars (30%) [163]. A significant increase in purple spots was associated

with lower temperatures during the colour break stage, although the plants grown in a greenhouse that bear a higher night temperature compared to the open area, were less susceptible to purple spots. Direct exposure to the sunlight lessened purple spots on fruit exposed to light compared to shady areas. The management of purple spot is very important for the supply chain of loquat fruit. In this context, the efficacy of fruit thinning on the purple spot was assessed. There was higher carbohydrate accumulation with a higher growth rate in thinned fruit. Thinning led to a higher sugar content that was directly correlated with the incidence of purple spot.

In conclusion, there should be less or no fruit thinning to avoid the purple spot in loquat fruit [159]. In contrast, a higher accumulation of fructose, sucrose, glucose, and TSS lowered purple spot in the 'Karantoki' loquat. On the other hand, 'Obusa' exhibited the highest purple spot susceptibility due to the lower accumulation of sugars and TSS in fruit. Moreover, it was also proposed that there was a direct role of fruit maturity at the harvest stage on the development of purple spots, as there was the highest incidence in 'Obusa' harvested at commercial maturity. 'Morphitiki' was the most resistant cultivar against purple spots, as compared to 'Karantoki' and 'Obusa' [164]. However, there is a need to investigate the control strategies for the management of purple spot incidence.

7.2. Anthracnose

The incidence of anthracnose is caused by the fungus *Colletotrichum* genus [81,165]. There are many known species of genus *Colletotrichum*, such as *C. acutatum*, *C. eriobotryae*, *C. simmondsii*, *C. godetiae*, *C. gloeosporioides*, *C. siamense*, and *C. nymphaeae*; however, the most important are *C. gloeosporioides* and *C. acutatum* in loquat fruit, which deteriorate the fruit quality during postharvest handling [68,165,166]. The development of dark and water-soaked lesions are typical symptoms of anthracnose rot and often occur with pink gelatinous masses at the center of lesions during wet, moist, and warm temperatures. The severity of the disease is directly associated with a higher storage temperature and moisture content [94]. Different species of *Colletotrichum* were isolated in Taiwan [166]. In this regard, *β*-tubulin (TUB2), *actin* (ACT), chitin synthase (CHS-1), glyceraldehyde-3-phosphate dehydrogenase (GAPDH), and internal transcribed spacer (ITS) genes were sequenced and two different types of *C. eriobotryae* and *C. nymphaeae* were found. However, the main pathogen causing anthracnose in Taiwan is *C. eriobotryae*. Oxidative stress and the production of ROS are mainly associated with the severity of the disease, as exhibited by higher H_2O_2 assay in infected fruit with reduced activities of SOD and CAT enzymes [166]. Similarly, morphological and phylogenic identification of a new strain, *C. godetiae*, in loquat fruit was identified by an internal transcribed space region (ITS) and four housekeeping partial genes relevant to TUB2, CHS-1, ACT, and GAPDH sequences by revealing reconstruction strain clusters through an ITS4 and ITS5 assay. Typical symptoms of *Colletotrichum* were similar concerning the molecular and morphological characteristics of this new strain, but it showed a different ITS assay [165].

Different strategies have been reported in the literature to control *Colletotrichum* infestations in loquat fruit. The exogenous application of MeJA has been reported to inhibit the spore germination and lesion diameter of *C. acutatum*. MeJA-mediated anthracnose rot, either by the direct inhibition of spores or indirectly through the higher H_2O_2 accumulation, resulting in reduced activities of PAL and PPO enzymes and lignin deposition in the peel tissues of 'Jiefangzhong' loquat fruit [24]. The defense-mediated activity of MeJA against anthracnose is also associated with higher sugar and juice contents and a reduction in internal browning, leading to the higher activities of chitinase and *β*-1,3-glucanase enzymes [99]. Moreover, the disease resistance in MeJA-treated loquat fruit might also be ascribed to the higher polyamine biosynthesis and cellular ATP levels [103]. Similar results were observed in the inhibition of anthracnose rot with the application of a 1-MCP treatment to loquat fruit [81]. Although chemical treatments have been reported to control the incidence of anthracnose rot, there may be residual levels of these chemicals that may be harmful to

consumer health. Consumer concern for chemical residual effects initiated the search for biological alternatives to control the infestation of *Colletotrichum*.

Biological control is also significant in reducing the *C. gloeosporioides* infestation in loquat fruit. Yan, et al. [167] reported that there was a negative correlation between the inoculation of the *Bacillus amyloliquefaciens* MG3 strain and fungal growth, and an inhibition of spore germination. Similarly, another strain (HG_{01}) of *B. amyloliquefaciens* was found to be very effective in reducing *C. acutatum* severity and delayed oxidative stress due to a lower PAL enzyme activity in loquat fruit [168]. *Bacillus cereus* AR156 induced a higher phenolic biosynthesis and H_2O_2 accumulation when inoculated in loquat fruit with *Colletotrichum acutatum* colonies. The possible defense-oriented pathway may be ascribed to the inhibition of membrane leakage due to higher activities of POD, PPO, PAL, β-1,3-glucanase and chitinase enzymes that induced higher H_2O_2 accumulation [169]. *Pichia membranefaciens*, a yeast, was reported to inhibit spore germination by increasing the activities of chitinase and β-1,3-glucanase enzymes that played a defensive role against *C. acutatum*. MeJA played a stimulating role in the enhancement of *P. memranfaciens* colonies at an exponential rate with higher biocontrol activities against the germ tube elongation of *C. acutatum* [100]. Moreover, there was also a positive role of *Pichia membranefaciens* in the reduction of *C. acutatum* spore germination and lesion diameter in loquat fruit [170].

7.3. Loquat Canker

Loquat is very susceptible to many bacterial diseases and cankers caused by *Pseudomonas syringae* pv. *eriobotryae* is one of the most severe diseases worldwide [171]. This disease attacks almost all parts of the plant and appears as brown lesions on the leaf and fruit surfaces that damage the mesophyll cells. There is a natural defense mechanism in loquat to alleviate canker disease, and the genetic basis of the resistance was discovered by identifying the gene locus and linkage group in the wild loquat species *Eriobotrya deflexa* [172]. Hiehata, et al. [173] outlined that the loquat resistance against *Pseudomonas syringae* can only be expressed in homozygous conditions, as *Psc-c* a recessive gene that triggers the plant defense mechanism. To check the efficacy of different hybrids obtained by two resistant cultivars, 'Shiromogi' and 'Champagne', 14 different crosses of both of these cultivars were observed, and it was found that there was more resistance among the hybrids, as compared to the original parent lines. It was further suggested that there is more than one gene involved in the disease tolerance in loquat fruit that cannot be determined by the phenotype or genotype of the *Psc-c* locus gene. Based on disease symptoms, *Pseudomonas* has been classified into three potential groups, A, B, and C, from which only group C pathogens cause brown spots on the skin of leaves and fruit [174]. However, future research on the canker control strategies in loquat on its transmission, mode of action, and control strategies in loquat fruit is warranted.

8. Conclusions and Future Prospects

Loquat fruit is regarded as a minor fruit containing a wide array of phytochemicals and health-promoting compounds. Short shelf life with accelerated quality degradation remains a challenge for growers, processors, and associated industry stakeholders. It is still considered an unexploited fruit crop, presenting extensive research gaps in disease control, nutrition for fruit quality, protection of on-tree delicate ripe fruit to avoid physical and mechanical injuries, postharvest handling and storage, and supply chain. Loquat is not well documented for its harvest handling and postharvest operations and for the quantitative losses in the supply chain from farmgate to consumers. During the postharvest period, low-temperature storage is coupled with certain constraints, such as susceptibility to CI, enzymatic browning, and microbial decay, which substantially downgrade the quality and marketability of stored loquat fruit.

In conclusion, loquat is highly perishable, and future research encompassing various pre- and post-harvest factors affecting postharvest quality warrants further investigations. The fruit ripening physiology of loquat fruit is worth studying, which warrants further

research involving molecular approaches to determine alterations in fruit quality. The appropriate harvest maturity standards are yet to be determined for different types of storage conditions. Moreover, the integrated pre- and post-harvest approaches to managing the postharvest diseases of loquat warrant further investigation. Although cold storage is the most widely used practice for the storage of loquat, it causes CI. Considering the adverse impacts of CI on loquat fruit quality, the management strategies for CI must be considered for future research. The holistic approaches encompassing preharvest and postharvest practices impacting the storage of loquat fruit must be standardized on a genotype and regional basis to reduce postharvest losses.

Author Contributions: H.M.S.S. and A.S.K.; conceptualization, writing-original manuscript, writing-review and editing, Z.S.; conceptualization, writing-review and editing and S.A.; writing-review and editing. All authors have read and agreed to the published version of the manuscript.

Funding: This research received no external funding.

Data Availability Statement: No research data is associated with this review article.

Acknowledgments: The authors are thankful to Michael Stein, HDR Communication Adviser, at Edith Cowan University, Joondalup campus, Western Australia, Australia, for improving the language of the manuscript.

Conflicts of Interest: The authors declare no conflict of interest.

References

1. Martínez-Calvo, J.; Badenes, M.; Llácer, G.; Bleiholder, H.; Hack, H.; Meier, U. Phenological growth stages of loquat tree (*Eriobotrya japonica* (Thunb.) Lindl.). *Ann. Appl. Biol.* **1999**, *134*, 353–357. [CrossRef]
2. Cai, J.; Chen, T.; Zhang, Z.; Li, B.; Qin, G.; Tian, S. Metabolic dynamics during loquat fruit ripening and postharvest technologies. *Front. Plant Sci.* **2019**, *10*, 619. [CrossRef] [PubMed]
3. Koba, K.; Matsuoka, A.; Osada, K.; Huang, Y.S. Effect of loquat (*Eriobotrya japonica*) extracts on LDL oxidation. *Food Chem.* **2007**, *104*, 308–316. [CrossRef]
4. Ferreres, F.; Gomes, D.; Valentão, P.; Gonçalves, R.; Pio, R.; Chagas, E.A.; Seabra, R.M.; Andrade, P.B. Improved loquat (*Eriobotrya japonica* Lindl.) cultivars: Variation of phenolics and antioxidative potential. *Food Chem.* **2009**, *114*, 1019–1027. [CrossRef]
5. Alós, E.; Martinez-Fuentes, A.; Reig, C.; Mesejo, C.; Zacarías, L.; Agustí, M.; Rodrigo, M. Involvement of ethylene in color changes and carotenoid biosynthesis in loquat fruit (*Eriobotrya japonica* Lindl. cv. Algerie). *Postharvest Biol. Technol.* **2019**, *149*, 129–138. [CrossRef]
6. Hadjipieri, M.; Georgiadou, E.C.; Marin, A.; Diaz-Mula, H.M.; Goulas, V.; Fotopoulos, V.; Tomás-Barberán, F.A.; Manganaris, G.A. Metabolic and transcriptional elucidation of the carotenoid biosynthesis pathway in peel and flesh tissue of loquat fruit during on-tree development. *BMC Plant Biol.* **2017**, *17*, 1–12. [CrossRef]
7. Yang, J.; Zhang, J.; Niu, X.-Q.; Zheng, X.-L.; Chen, X.; Zheng, G.-H.; Wu, J.-C. Comparative transcriptome analysis reveals key genes potentially related to organic acid and sugar accumulation in loquat. *PLoS ONE* **2021**, *16*, e0238873. [CrossRef]
8. Deng, H.; Wang, X.; Wang, Y.; Xiang, Y.; Chen, M.; Zhang, H.; Luo, X.; Xia, H.; Liang, D.; Lv, X. Dynamic changes in cell wall polysaccharides during fruit development and ripening of two contrasting loquat cultivars and associated molecular mechanisms. *Foods* **2023**, *12*, 309. [CrossRef]
9. Barreto, G.P.; Benassi, M.T.; Mercadante, A.Z. Bioactive compounds from several tropical fruits and correlation by multivariate analysis to free radical scavenger activity. *J. Braz. Chem. Soc.* **2009**, *20*, 1856–1861. [CrossRef]
10. Badenes, M.L.; Janick, J.; Lin, S.; Zhang, Z.; Liang, G.L.; Wang, W. Breeding loquat. *Plant Breed. Rev.* **2013**, *37*, 259–296.
11. Janick, J. Important world cultivars of loquat. *Acta Hortic.* **2014**, *1092*, 25–32. [CrossRef]
12. Cai, C.; Li, X.; Chen, K. Acetylsalicylic acid alleviates chilling injury of postharvest loquat (*Eriobotrya japonica* Lindl.) fruit. *Eur. Food Res. Technol.* **2006**, *223*, 533–539. [CrossRef]
13. Cai, C.; Xu, C.; Shan, L.; Li, X.; Zhou, C.; Zhang, W.; Ferguson, I.; Chen, K. Low temperature conditioning reduces postharvest chilling injury in loquat fruit. *Postharvest Biol. Technol.* **2006**, *41*, 252–259. [CrossRef]
14. Shao, X.; Zhu, Y.; Cao, S.; Wang, H.; Song, Y. Soluble sugar content and metabolism as related to the heat-induced chilling tolerance of loquat fruit during cold storage. *Food Bioproc. Technol.* **2013**, *6*, 3490–3498. [CrossRef]
15. Yonghua, Z.; Xinguo, S.; Sanyu, L.; Yufang, X. Quality, active oxygen and polyamines metabolic changes in cold-stored loquat fruits as affected by postharvest SO_ (2) treatment. *Acta Phytophysiologica Sinica* **2000**, *26*, 397–401.
16. Zheng, Y.H.; Li, S.Y.; Xi, Y.F.; Su, X.G.; Yi, Y.B. Polyamine changes and chilling injury in cold-stored loquat fruits. *J. Integ. Plant Biol.* **2000**, *42*, 824.

17. Zhang, M.; Shi, Y.; Liu, Z.; Zhang, Y.; Yin, X.; Liang, Z.; Huang, Y.; Grierson, D.; Chen, K. An *EjbHLH14-EjHB1-EjPRX12* module is involved in methyl jasmonate alleviation of chilling-induced lignin deposition in loquat fruit. *J. Exp. Bot.* **2022**, *73*, 1668–1682. [CrossRef]
18. Hadjipieri, M.; Gavriel, K.; Sismanidis, G.; Manganaris, G.A. The effect of modified atmosphere packaging on postharvest performance of two loquat cultivars. *Acta Hortic.* **2016**, *1242*, 729–734. [CrossRef]
19. Jin, P.; Zhang, Y.; Shan, T.; Huang, Y.; Xu, J.; Zheng, Y. Low-temperature conditioning alleviates chilling injury in loquat fruit and regulates glycine betaine content and energy status. *J. Agric. Food Chem.* **2015**, *63*, 3654–3659. [CrossRef]
20. Gariglio, N.; Martinez-Fuentes, A.; Mesejo, C.; Agustí, M. Control of purple spot of loquat fruit (*Eriobotrya japonica*) by means of mineral compounds. *Ann. Appl. Biol.* **2005**, *146*, 415–420. [CrossRef]
21. Cai, C.; Chen, K.; Xu, W.; Zhang, W.; Li, X.; Ferguson, I. Effect of 1-MCP on postharvest quality of loquat fruit. *Postharvest Biol. Technol.* **2006**, *40*, 155–162. [CrossRef]
22. Öz, A.T.; Kafkas, N.E.; Bozdoğan, A. Combined effects of oxalic acid treatment and modified atmosphere packaging on postharvest quality of loquats during storage. *Turk. J. Agric. Fores.* **2016**, *40*, 433–440. [CrossRef]
23. Akhtar, A.; Abbasi, N.A.; Hussain, A. Effect of calcium chloride treatments on quality characteristics of loquat fruit during storage. *Pak. J. Bot.* **2010**, *42*, 181–188.
24. Cao, S.; Zheng, Y.; Yang, Z.; Tang, S.; Jin, P.; Wang, K.; Wang, X. Effect of methyl jasmonate on the inhibition of *Colletotrichum acutatum* infection in loquat fruit and the possible mechanisms. *Postharvest Biol. Technol.* **2008**, *49*, 301–307. [CrossRef]
25. Xu, M.; Dong, J.; Zhang, M.; Xu, X.; Sun, L. Cold-induced endogenous nitric oxide generation plays a role in chilling tolerance of loquat fruit during postharvest storage. *Postharvest Biol. Technol.* **2012**, *65*, 5–12. [CrossRef]
26. Ding, C.-K.; Chachin, K.; Ueda, Y.; Wang, C.Y. Inhibition of loquat enzymatic browning by sulfhydryl compounds. *Food Chem.* **2002**, *76*, 213–218. [CrossRef]
27. Ding, Z.; Tian, S.; Wang, Y.; Li, B.; Chan, Z.; Han, J.; Xu, Y. Physiological response of loquat fruit to different storage conditions and its storability. *Postharvest Biol. Technol.* **2006**, *41*, 143–150. [CrossRef]
28. Ding, C.-K.; Chachin, K.; Ueda, Y.; Imahori, Y.; Wang, C.Y. Modified atmosphere packaging maintains postharvest quality of loquat fruit. *Postharvest Biol. Technol.* **2002**, *24*, 341–348. [CrossRef]
29. Amoros, A.; Pretel, M.; Zapata, P.; Botella, M.; Romojaro, F.; Serrano, M. Use of modified atmosphere packaging with microperforated polypropylene films to maintain postharvest loquat fruit quality. *Int. J. Food Sci. Technol.* **2008**, *14*, 95–103. [CrossRef]
30. Ding, C.K.; Chachin, K.; Hamauzu, Y.; Ueda, Y.; Imahori, Y. Effects of storage temperatures on physiology and quality of loquat fruit. *Postharvest Biol. Technol.* **1998**, *14*, 309–315. [CrossRef]
31. Ghasemnezhad, M.; Nezhad, M.A.; Gerailoo, S. Changes in postharvest quality of loquat (*Eriobotrya japonica*) fruits influenced by chitosan. *Hortic. Environ. Biotechnol.* **2011**, *52*, 40–45. [CrossRef]
32. Zargar, B.; Mir, M.M.; Ganai, S.A.; Mir, S.A.; Shah, M.A.; Banday, S.A. Postharvest Biology and Technology of Loquat. *Postharvest Biol. Technol. Temp. Fruits* **2018**, 285–298. [CrossRef]
33. Zhang, S.; Sun, H.; Wang, J.; Shen, J.; He, F.; Chen, D.; Wang, Y. The regulatory mechanisms and control technologies of chilling injury and fungal diseases of postharvest loquat fruit. *Plants* **2022**, *11*, 3472. [CrossRef]
34. Cañete, M.; Hueso, J.; Pinillos, V.; Cuevas, J. Ripening degree at harvest affects bruising susceptibility and fruit sensorial traits of loquat (*Eriobotrya japonica* Lindl.). *Sci. Hortic.* **2015**, *187*, 102–107. [CrossRef]
35. Pinillos, V.; Hueso, J.J.; Marcon Filho, J.L.; Cuevas, J. Changes in fruit maturity indices along the harvest season in 'Algerie' loquat. *Sci. Hortic.* **2011**, *129*, 769–776. [CrossRef]
36. Hadjipieri, M.; Christofi, M.; Goulas, V.; Manganaris, G.A. The impact of genotype and harvesting day on qualitative attributes, postharvest performance and bioactive content of loquat fruit. *Sci. Hortic.* **2020**, *263*, 108891. [CrossRef]
37. Chen, F.X.; Liu, X.H.; Chen, L.S. Developmental changes in pulp organic acid concentration and activities of acid-metabolising enzymes during the fruit development of two loquat (*Eriobotrya japonica* Lindl.) cultivars differing in fruit acidity. *Food Chem.* **2009**, *114*, 657–664. [CrossRef]
38. Kader, A.A. *Recommendations for Maintaining Postharvest Quality*; Postharvest Technology Research and Information Center: UC Davis, CA, USA, 2009.
39. Cuevas, J.; Salvador-Sola, F.; Gavilán, J.; Lorente, N.; Hueso, J.; González-Padierna, C. Loquat fruit sink strength and growth pattern. *Sci. Hortic.* **2003**, *98*, 131–137. [CrossRef]
40. González, L.; Lafuente, M.; Zacarías, L. Maturation of loquat fruit (*Eriobotrya japonica* Lindl.) under Spanish growing conditions and its postharvest performance. *Opt. Mediterr.* **2003**, *58*, 171–179.
41. Hirai, M. Sugar accumulation and development of loquat fruit. *J. Jpn. Soc. Hortic. Sci.* **1980**, *49*, 347–353. [CrossRef]
42. Hamauzu, Y.; Chachin, K.; Ding, C.; Kurooka, H. Differences in surface color, flesh firmness, physiological activity, and some components of loquat [*Eriobotrya japonica*] fruits picked at various stages of maturity. *J. Jpn. Soc. Hortic. Sci.* **1997**, *65*, 859–865. [CrossRef]
43. Hirai, M. Accelerated sugar accumulation and ripening of loquat fruit by exogenously applied ethylene. *J. Jpn. Soc. Hortic. Sci.* **1982**, *51*, 159–164. [CrossRef]
44. Gariglio, N.; Reig, C.; Martinez-Fuentes, A.; Mesejo, C.; Agusti, M. Purple spot in loquat (*Eriobotrya japonica* Lindl.) is associated to changes in flesh-rind water relations during fruit development. *Sci. Hortic.* **2008**, *119*, 55–58. [CrossRef]

45. Undurraga, P.; Olaeta, J. Effect of ethephon (2-chloro ethylphosphonic acid) applied to the trees on ripening of Golden Nugget loquat (*Eriobotrya japonica* Lindl.). *Options Mediterr* **2004**, *58*, 123–128.
46. Reig, C.; Martinez-Fuentes, A.; Juan, M.; Gariglio, N.; Marti, G.; Mesejo, C.; Agustí, M. Tecnicas para anticipar la recoleccion del fruto del nispero japones (*Eriobotrya japonica* Lindl.). In Proceedings of the XI Congress National SECH Abstract 4D01, 2007.
47. Jiang, T.M.; Wang, P.; Yin, X.R.; Zhang, B.; Xu, C.J.; Li, X.; Chen, K.S. Ethylene biosynthesis and expression of related genes in loquat fruit at different developmental and ripening stages. *Sci. Hortic.* **2011**, *130*, 452–458. [CrossRef]
48. Hasegawa, P.N.; de Faria, A.F.; Mercadante, A.Z.; Chagas, E.A.; Pio, R.; Lajolo, F.M.; Cordenunsi, B.R.; Purgatto, E. Chemical composition of five loquat cultivars planted in Brazil. *Food Sci. Technol.* **2010**, *30*, 552–559. [CrossRef]
49. Zhou, C.H.; Xu, C.J.; Sun, C.D.; Li, X.; Chen, K.S. Carotenoids in white-and red-fleshed loquat fruits. *J. Agric. Food Chem.* **2007**, *55*, 7822–7830. [CrossRef]
50. Serrano, M.; Guillén, F.; Martínez-Romero, D.; Castillo, S.; Valero, D. Chemical constituents and antioxidant activity of sweet cherry at different ripening stages. *J. Agric. Food Chem.* **2005**, *53*, 2741–2745. [CrossRef]
51. Pinillos, V.; Cañete, M.; Sanchez, R.; Cuevas, J.; Hueso, J. Fruit development and maturation phenological stages of 'Algerie' loquat. *Acta Hortic.* **2006**, *750*, 331–336. [CrossRef]
52. Goulas, V.; Minas, I.; Kourdoulas, P.; Vicente, A.R.; Manganaris, G.A. Phytochemical content, antioxidants and cell wall metabolism of two loquat (*Eriobotrya japonica*) cultivars under different storage regimes. *Food Chem.* **2014**, *155*, 227–234. [CrossRef]
53. Iida, M.; Bantog, N.A.; Yamada, K.; Shiratake, K.; Yamaki, S. Sorbitol-and other sugar-induced expressions of the NAD^+-dependent sorbitol dehydrogenase gene in Japanese pear fruit. *J. Am. Soc. Hortic. Sci.* **2004**, *129*, 870–875. [CrossRef]
54. Sotiras, M.; Papadakis, I.; Landi, M.; Tsaniklidis, G.; Tsiantas, P.; Psychoyou, M. Allocation pattern, photosynthetic performance and sugar metabolism in hydroponically grown seedlings of loquat (*Eriobotrya japonica* Lindl.) subjected to salinity. *Photosynthetica* **2019**, *57*, 258–267. [CrossRef]
55. Bruneau, J.M.; Worrell, A.C.; Cambou, B.; Lando, D.; Voelker, T.A. Sucrose phosphate synthase, a key enzyme for sucrose biosynthesis in plants: Protein purification from corn leaves and immunological detection. *Plant Physiology* **1991**, *96*, 473–478. [CrossRef] [PubMed]
56. Takahashi, H.; Sumitani, H.; Inada, Y.; Mori, D.; Nakano, Y. Potent aroma volatiles in fresh loquat and its canned product. *J. Jpn. Soc. Food Sci. Technol.* **2000**, *47*, 302–310. [CrossRef]
57. Blumenfeld, A. Fruit growth of loquat. *J. Am. Soc. Hortic. Sci.* **1980**, *105*, 747–750. [CrossRef]
58. Sultan, M.; Khalefa, S.; Elhamamsy, S.; Mostafa, Y. Effect of postharvest anti-oxidant treatments on loquat fruit deterioration during storage at room temperature. *Acta Hortic.* **2014**, *1092*, 173–179. [CrossRef]
59. Barchi, G.; Berardinelli, A.; Guarnieri, A.; Ragni, L.; Fila, C.T. pH—Postharvest technology: Damage to loquats by vibration-simulating intra-state transport. *Biosyst. Eng.* **2002**, *82*, 305–312. [CrossRef]
60. Chen, F.; Wu, G.; Li, C. Effects of modified atmosphere packaging on respiration and quality attributes of loquat fruit during cold storage. *Trans. Chi. Soc. Agri. Engrr* **2003**, *19*, 147–151.
61. Amorós, A.; Zapata, P.; Pretel, M.; Botella, M.; Serrano, M. Physico-chemical and physiological changes during fruit development and ripening of five loquat (*Eriobotrya japonica* Lindl.) cultivars. *Int. J. Food Sci. Technol.* **2003**, *9*, 43–51. [CrossRef]
62. Rui, H.; Cao, S.; Shang, H.; Jin, P.; Wang, K.; Zheng, Y. Effects of heat treatment on internal browning and membrane fatty acid in loquat fruit in response to chilling stress. *J. Sci. Food Agric.* **2010**, *90*, 1557–1561. [CrossRef]
63. Rui, H.; Wang, K.; Shang, H.; Tang, S.; Jin, P.; Cao, S.; Zheng, Y. Effects of heat treatment on flesh leatheriness and related enzyme activities of loquat fruits during cold storage. *Trans. Chi. Soc. Agric. Engrr.* **2009**, *25*, 294–298. [CrossRef]
64. Rui, H.; Shang, H.; Wang, K.; Jin, P.; Tang, S.; Cao, S.; Zheng, Y. Effects of heat treatment on active oxygen metabolism and flesh lignification in cold-stored loquat fruits. *Food Science* **2009**, *25*, 276–281. [CrossRef]
65. Liu, F.; Shao, X.; Tu, K.; Zhao, Y. Effect of postharvest heat treatment on the quality of loquat fruit in cold storage. *J. Fruit Sci.* **2009**, *26*, 649–653.
66. Edagi, F.K.; Sestari, I.; Sasaki, F.F.; Cabral, S.M.; Meneghini, J.; Kluge, R.A. Potential increasing in the cold-storage of 'Fukuhara' loquat using heat treatments. *Pesq. Agro. Bras.* **2009**, *44*, 1270–1276. [CrossRef]
67. Wu, G.B.; Chen, F.H.; Zhang, Q.B.; Yang, J. Effects of heat shock treatment on chilling injury and physiological responses of *Eriobotrya japonica* fruit during cold storage. *J. Plant Res. Environ.* **2004**, *13*, 1–5.
68. Liu, F.; Tu, K.; Shao, X.; Zhao, Y.; Tu, S.; Su, J.; Hou, Y.; Zou, X. Effect of hot air treatment in combination with *Pichia guilliermondii* on postharvest anthracnose rot of loquat fruit. *Postharvest Biol. Technol.* **2010**, *58*, 65–71. [CrossRef]
69. Shao, X.; Tu, K. Hot air treatment improved the chilling resistance of loquat fruit under cold storage. *J. Food Proc. Pres.* **2014**, *38*, 694–703. [CrossRef]
70. Song, Y.; Liao, X.; Shao, X. Effects of postharvest heat treatment on the fatty acid composition and chilling injury of loquat fruits during the cold storage. In Proceedings of the 2011 International Conference on New Technology of Agricultural, Zibo, China, 27–29 May 2011; pp. 945–948.
71. Jin, P.; Duan, Y.; Wang, L.; Wang, J.; Zheng, Y. Reducing chilling injury of loquat fruit by combined treatment with hot air and methyl jasmonate. *Food Bioproc. Technol.* **2014**, *7*, 2259–2266. [CrossRef]
72. Zhang, Y.; Jin, P.; Huang, Y.; Shan, T.; Wang, L.; Li, Y.; Zheng, Y. Effect of hot water combined with glycine betaine alleviates chilling injury in cold-stored loquat fruit. *Postharvest Biol. Technol.* **2016**, *118*, 141–147. [CrossRef]

73. Khan, A.S.; Singh, Z. 1-methylcyclopropene application and modified atmosphere packaging affect ethylene biosynthesis, fruit softening, and quality of 'Tegan Blue' Japanese plum during cold storage. *J. Am. Soc. Hortic. Sci.* **2008**, *133*, 290–299. [CrossRef]
74. Liu, H.; Cao, J.; Jiang, W. Changes in phenolics and antioxidant property of peach fruit during ripening and responses to 1-methylcyclopropene. *Postharvest Biol. Technol.* **2015**, *108*, 111–118. [CrossRef]
75. Lee, J.; Jeong, M.C.; Ku, K.H. Chemical, physical, and sensory properties of 1-MCP-treated Fuji apple (*Malus domestica* Borkh.) fruits after long-term cold storage. *Appl. Biol. Chem.* **2017**, *60*, 363–374. [CrossRef]
76. Shah, H.M.S.; Khan, A.S.; Ali, S. Pre-storage kojic acid application delays pericarp browning and maintains antioxidant activities of litchi fruit. *Postharvest Biol. Technol.* **2017**, *132*, 154–161. [CrossRef]
77. Tomala, K.; Grzęda, M.; Guzek, D.; Głąbska, D.; Gutkowska, K. The effects of preharvest 1-methylcyclopropene (1-MCP) treatment on the fruit quality parameters of cold-stored 'Szampion' cultivar apples. *Agric.* **2020**, *10*, 80. [CrossRef]
78. Cao, S.; Zheng, Y.; Yang, Z. Effect of 1-MCP treatment on nutritive and functional properties of loquat fruit during cold storage. *NZ J. Crop Hortic Sci.* **2011**, *39*, 61–70. [CrossRef]
79. Cao, S.; Zheng, Y.; Wang, K.; Rui, H.; Tang, S. Effects of 1-methylcyclopropene on oxidative damage, phospholipases and chilling injury in loquat fruit. *J. Sci. Food Agric.* **2009**, *89*, 2214–2220. [CrossRef]
80. Cao, S.; Zheng, Y.; Wang, K.; Rui, H.; Tang, S. Effect of 1-methylcyclopropene treatment on chilling injury, fatty acid and cell wall polysaccharide composition in loquat fruit. *J. Agric. Food Chem.* **2009**, *57*, 8439–8443. [CrossRef]
81. Cao, S.; Zheng, Y. Effect of 1-methylcyclopropene on anthracnose rot caused by *Colletotrichum acutatum* and disease resistance in loquat fruit. *J. Sci. Food Agric.* **2010**, *90*, 2289–2294. [CrossRef]
82. Yang, S.; Sun, C.; Wang, P.; Shan, L.; Cai, C.; Zhang, B.; Zhang, W.; Li, X.; Ferguson, I.; Chen, K. Expression of expansin genes during postharvest lignification and softening of 'Luoyangqing'and 'Baisha' loquat fruit under different storage conditions. *Postharvest Biol. Technol.* **2008**, *49*, 46–53. [CrossRef]
83. Liguori, G.; Farina, V.; Corona, O.; Mazzaglia, A.; Barone, E.; Inglese, P. Effects of 1-MCP on postharvest quality and internal browning of white-flesh loquat fruit during cold storage. *Fruits* **2017**, *72*, 67–73. [CrossRef]
84. Liguori, G.; Farina, V.; Sortino, G.; Mazzaglia, A.; Inglese, P. Effects of 1-methylcyclopropene on postharvest quality of white-and yellow-flesh loquat (*Eriobotrya japonica* Lindl.) fruit. *Fruits* **2014**, *69*, 363–370. [CrossRef]
85. Cao, S.; Zheng, Y.; Wang, K.; Rui, H.; Shang, H.; Tang, S. The effects of 1-methylcyclopropene on chilling and cell wall metabolism in loquat fruit. *J. Hortic. Sci. Biotechnol.* **2010**, *85*, 147–153. [CrossRef]
86. Zhang, Z.; Zhu, S. Effects of benzothiadiazole on diseases and quality of postharvest loquat fruit. *Food Sci.* **2009**, *30*, 264–267. [CrossRef]
87. Zhu, S.; Zhang, Z.; Xu, J.; Ma, L.; Tang, W.; Liu, D. Effect of BTH treatment on storability and activity of related enzymes of harvested loquat fruit. *Acta Hortic.* **2006**, *750*, 445–450. [CrossRef]
88. Hussain, S.; Zahoor, H.; Khadijac, F.; Salikc, M.R.; Alia, M.; Hayatc, A.; Mustafad, G. Postharvest calcium chloride application maintains shelf life and quality of loquat (*Eriobotrya japonica* L.) fruit. *J. Hortic. Sci. Technol.* **2021**, *4*, 1–6. [CrossRef]
89. Mostafa, Y.; Sultan, M. Calcium chloride combined with antioxidants increases keeping quality and limits postharvest decay of loquat fruit. *Acta Hortic.* **2016**, *1194*, 157–164. [CrossRef]
90. Hou, Y.; Li, Z.; Zheng, Y.; Jin, P. Effects of $CaCl_2$ treatment alleviates chilling injury of loquat fruit (*Eribotrya japonica*) by modulating ROS homeostasis. *Foods* **2021**, *10*, 1662. [CrossRef]
91. Li, Z.; Wang, L.; Xie, B.; Hu, S.; Zheng, Y.; Jin, P. Effects of exogenous calcium and calcium chelant on cold tolerance of postharvest loquat fruit. *Sci. Hortic.* **2020**, *269*, 109391. [CrossRef]
92. Tzortzakis, N.; Sergentani, C. Determination of heat stress and calcium chloride application in loquat storage. *Acta Hortic.* **2014**, *1079*, 581–587. [CrossRef]
93. Song, H.; Zheng, Y.; Yuan, W.; Zhang, R.; Yang, L. Effects of peracetic acid (PAA) combined with calcium treatments on storage quality of loquat fruit. *Agric. Sci. Technol.* **2013**, *14*, 1476.
94. Wang, K.; Cao, S.; Di, Y.; Liao, Y.; Zheng, Y. Effect of ethanol treatment on disease resistance against anthracnose rot in postharvest loquat fruit. *Sci. Hortic.* **2015**, *188*, 115–121. [CrossRef]
95. Shan, T.; Sun, Y.; Jin, P.; Xu, J.; Zheng, Y. Effects of glycine betaine on loquat fruit quality during cold storage. *Acta Hortic.* **2014**, *1092*, 131–137. [CrossRef]
96. Cao, S.; Zheng, Y.; Yang, Z.; Wang, K.; Rui, H. Effect of methyl jasmonate on quality and antioxidant activity of postharvest loquat fruit. *J. Sci. Food Agric.* **2009**, *89*, 2064–2070. [CrossRef]
97. Cao, S.; Zheng, Y.; Wang, K.; Jin, P.; Rui, H. Methyl jasmonate reduces chilling injury and enhances antioxidant enzyme activity in postharvest loquat fruit. *Food Chem.* **2009**, *115*, 1458–1463. [CrossRef]
98. Cao, S.; Zheng, Y.; Wang, K.; Rui, H.; Tang, S. Effect of methyl jasmonate on cell wall modification of loquat fruit in relation to chilling injury after harvest. *Food Chem.* **2010**, *118*, 641–647. [CrossRef]
99. Cao, S.; Zheng, Y.; Yang, Z.; Tang, S.; Jin, P. Control of anthracnose rot and quality deterioration in loquat fruit with methyl jasmonate. *J. Sci. Food Agric.* **2008**, *88*, 1598–1602. [CrossRef]
100. Cao, S.; Zheng, Y.; Wang, K.; Tang, S.; Rui, H. Effect of yeast antagonist in combination with methyl jasmonate treatment on postharvest anthracnose rot of loquat fruit. *Biol. Cont.* **2009**, *50*, 73–77. [CrossRef]
101. Cai, Y.; Cao, S.; Yang, Z.; Zheng, Y. MeJA regulates enzymes involved in ascorbic acid and glutathione metabolism and improves chilling tolerance in loquat fruit. *Postharvest Biol. Technol.* **2011**, *59*, 324–326. [CrossRef]

102. Cao, S.; Cai, Y.; Yang, Z.; Zheng, Y. MeJA induces chilling tolerance in loquat fruit by regulating proline and γ-aminobutyric acid contents. *Food Chem.* **2012**, *133*, 1466–1470. [CrossRef]
103. Cao, S.; Cai, Y.; Yang, Z.; Joyce, D.C.; Zheng, Y. Effect of MeJA treatment on polyamine, energy status and anthracnose rot of loquat fruit. *Food Chem.* **2014**, *145*, 86–89. [CrossRef]
104. Wang, D.; Chen, Q.; Chen, W.; Guo, Q.; Xia, Y.; Wu, D.; Jing, D.; Liang, G. Melatonin treatment maintains quality and delays lignification in loquat fruit during cold storage. *Sci. Hortic.* **2021**, *284*, 110126. [CrossRef]
105. Hussain, Z.; Hussain, S.; Sarwar, G.; Latif, M.; Anwar, R.; Khadija, F.; Bilal, M.; Sherani, J.; Yaseen, M. Postharvest application of salicylic acid to improve the shelf life and quality of loquat (*Eriobotrya japonica* L.) fruit. *J. Pure Appl. Agric.* **2021**, *6*, 31–38.
106. Wu, J.; Chen, Q.; Tang, C.; Xia, H. Effects of exogenous salicylic acid on lignification and related enzymes activities of loquat during cold storage. *Trans. Chi. Soc. Agric. Engrr.* **2006**, *22*, 175–179.
107. Huang, Z.; Wu, J.; Chen, W.; Cai, L.; Xie, C.; Lin, L.; Huang, S.; Ye, M. Effects of SA on enzymes of ascorbate-glutathione cycle in young loquat fruits after low temperature stress. *Sci. Sil. Sin.* **2011**, *47*, 36–42.
108. Chen, G.; Hou, Y.; Zheng, Y.; Jin, P. 2, 4-epibrassinolide enhance chilling tolerance of loquat fruit by regulating cell wall and membrane fatty acid metabolism. *Sci. Hortic.* **2022**, *295*, 110813. [CrossRef]
109. Gao, H.; Tao, F.; Song, L.; Chen, H.; Chen, W.; Zhou, Y.; Mao, J.; Zheng, Y. Effects of short-term N_2 treatment on quality and antioxidant ability of loquat fruit during cold storage. *J. Sci. Food Agric.* **2009**, *89*, 1159–1163. [CrossRef]
110. Creelman, R.A.; Mullet, J.E. Biosynthesis and action of jasmonates in plants. *Annu. Rev. Plant Biol.* **1997**, *48*, 355–381. [CrossRef]
111. Besson-Bard, A.; Pugin, A.; Wendehenne, D. New insights into nitric oxide signaling in plants. *Annu. Rev. Plant Biol.* **2008**, *59*, 21–39. [CrossRef]
112. Chen, Y.; Lin, S.; Huang, Z.; Cai, B.; Wu, G.; Pan, Z.; Wu, J. Response of endogenous nitric oxide and Jasmonate acid to low temperature stress in young loquat fruits. *Plant Sci. J.* **2012**, *30*, 611–617. [CrossRef]
113. Zheng, Y.; Su, X.; Yi, Y.; Li, S.; Xi, Y. Effects of SO_2 on loquat fruits stored at 1° C. *J. Nanj. Agric. Uni.* **2000**, *23*, 89–92.
114. Tang, J.; Ren, H.; Chen, X.; Ma, F.; Jiang, F.; Sun, B. Effects of short-term N_2 anaerobic treatment on respiratory metabolism and oxidation status of *Agaricus bisporus*. *Postharvest Biol. Technol.* **2021**, *181*, 111692. [CrossRef]
115. Larbat, R.; Olsen, K.M.; Slimestad, R.; Løvdal, T.; Bénard, C.; Verheul, M.; Bourgaud, F.; Robin, C.; Lillo, C. Influence of repeated short-term nitrogen limitations on leaf phenolics metabolism in tomato. *Phytochemistry* **2012**, *77*, 119–128. [CrossRef]
116. Zhang, Z.; Fu, T.; Li, Y.; Peng, C.; Qin, W. Effects of ozone treatment on the preservation of loquat cultivar big five-pointed star during storage. *Food Sci.* **2011**, *32*, 282–285.
117. Piechowiak, T.; Grzelak-Błaszczyk, K.; Sójka, M.; Balawejder, M. One-time ozone treatment improves the postharvest quality and antioxidant activity of *Actinidia arguta* fruit. *Phytochemistry* **2022**, *203*, 113393. [CrossRef] [PubMed]
118. Zhu, X.; Perez, M.; Aldon, D.; Galaud, J.P. Respective contribution of CML8 and CML9, two arabidopsis calmodulin-like proteins, to plant stress responses. *Plant Signal. Behav.* **2017**, *12*, e1322246. [CrossRef]
119. Hou, Y.; Wang, L.; Zhao, L.; Xie, B.; Hu, S.; Chen, G.; Zheng, Y.; Jin, P. $CaCl_2$ mitigates chilling injury in loquat fruit via the CAMTA5-mediated transcriptional repression of membrane lipid degradation genes. *Food Res. Int.* **2022**, *162*, 111966. [CrossRef] [PubMed]
120. Bo, H. A preliminary report on the effect of calcium on some physiological indexes of postharvest loquat fruit. *Subt. Plant Sci.* **2000**, *29*, 31.
121. Riseh, R.S.; Vatankhah, M.; Hassanisaadi, M.; Kennedy, J.F. Chitosan-based nanocomposites as coatings and packaging materials for the postharvest improvement of agricultural product: A review. *Carbohydrate Polymers* **2023**, *309*, 120666. [CrossRef]
122. Márquez, C.J.; Cartagena, J.R.; Pérez-Gago, M.B. Effect of edible coatings on japanese loquat (*Eriobotrya japonica* T.) postharvest quality. *Vitae* **2009**, *16*, 304–310. [CrossRef]
123. Petriccione, M.; Pasquariello, M.S.; Mastrobuoni, F.; Zampella, L.; Di Patre, D.; Scortichini, M. Influence of a chitosan coating on the quality and nutraceutical traits of loquat fruit during postharvest life. *Sci. Hortic.* **2015**, *197*, 287–296. [CrossRef]
124. Bahadırlı, N.P.; Kahramanoğlu, İ.; Wan, C. Exposure to volatile essential oils of myrtle (*Myrtus communis* L.) leaves for improving the postharvest storability of fresh loquat fruits. *J. Food Qual.* **2020**, *2020*, 1–10. [CrossRef]
125. Liguori, G.; Greco, G.; Gaglio, R.; Settanni, L.; Inglese, P.; Allegra, A. Influence of cactus pear mucilage-based edible coating on marketability and edibility parameters of minimally processed loquat fruits. *Agronomy* **2022**, *12*, 2120. [CrossRef]
126. Kahramanoğlu, İ. Preserving postharvest storage quality of fresh loquat fruits by using different bio-materials. *J. Food Sci. Technol.* **2020**, *57*, 3004–3012. [CrossRef] [PubMed]
127. Song, H.; Yuan, W.; Jin, P.; Wang, W.; Wang, X.; Yang, L.; Zhang, Y. Effects of chitosan/nano-silica on postharvest quality and antioxidant capacity of loquat fruit during cold storage. *Postharvest Biol. Technol.* **2016**, *119*, 41–48. [CrossRef]
128. Ergin, S.Ö.; Yaman, H.; Dilek, M. The usage of edible films extracted from cherry and apricot tree gums for coating of strawberry (*Fragaria ananassa*) and loquat (*Eriobotrya japonica*) fruits. *Turk. J. Agric. Food Sci. Technol.* **2018**, *6*, 561–569. [CrossRef]
129. Hanif, J.; Khalid, N.; Khan, R.S.; Bhatti, M.F.; Hayat, M.Q.; Ismail, M.; Andleeb, S.; Mansoor, Q.; Khan, F.; Amin, F. Formulation of active packaging system using Artemisia scoparia for enhancing shelf life of fresh fruits. *Mat. Sci. Engnr.* **2019**, *100*, 82–93. [CrossRef]
130. Tian, S.; Li, B.; Ding, Z. *Physiological properties and storage technologies of loquat fruit. In Fresh Produce*; da Teixeira, S., Ed.; Global Science Books: Isleworth, UK, 2007; Volume 1, pp. 76–81.

131. Cao, S.; Yang, Z.; Zheng, Y. Sugar metabolism in relation to chilling tolerance of loquat fruit. *Food Chem.* **2013**, *136*, 139–143. [CrossRef]
132. Öz, T.; Kafkas, E.; Eker, T. Effects of active modified atmosphere packaging with argon and nitrogen on postharvest quality of loquat. *Acta Hortic.* **2016**, *1242*, 335–342. [CrossRef]
133. Oz, A.; Ulukanil, Z. Effects of 1-methylcylopropene (1-MCP) and modifed atmopshere packing (MAP) on postharvest browning and microbial growth of loquat fruit. *J. Appl. Bot. Food Qual.* **2012**, *84*, 125.
134. Akhtar, A.; Abbasi, N.A.; Hussain, A.; Bakhsh, A. Preserving quality of loquat fruit during storage by modified atmosphere packaging. *Pak. J. Agric. Sci.* **2012**, *49*, 419–423.
135. Palma, A.; Mura, D.; D'Aquino, S.; Continella, G.; Continella, A. Storability of 'Algerie' and 'Golden Nugget' loquats in modified atmosphere packaging. *Acta Hortic.* **2012**, *934*, 245–252. [CrossRef]
136. Çandir, E.; Polat, A.; Özdemir, A.; Caliskan, O.; Temizyürek, F. The effects of modified atmosphere packaging on quality of loquat fruits. *Acta Hortic.* **2010**, *887*, 363–367. [CrossRef]
137. Hashemabadi, D.; Najmabadi, N.; Kaviani, B.; Ghasemnejad, M.; Zaredoost, F.; Jadid Soleymandarabi, M. The effect of antioxidant compounds and packaging materials on quality and storage life of loquat (*Eriobotrya japonica*) fruits. *Ira. J. Hortic. Sci. Technol.* **2018**, *19*, 143–156.
138. Wang, L.; Shao, S.; Madebo, M.P.; Hou, Y.; Zheng, Y.; Jin, P. Effect of nano-SiO_2 packing on postharvest quality and antioxidant capacity of loquat fruit under ambient temperature storage. *Food Chem.* **2020**, *315*, 126295. [CrossRef] [PubMed]
139. Pica, A.; Continella, G.; Agabbio, M.; D'Aquino, S. Effect of packaging and coating on fruit quality changes of loquat during three cold storage regimes. *Adv. Hortic. Sci.* **1996**, *10*, 1000–1006.
140. Zheng, Y.H.; Su, X.G.; Li, Q.J.; Li, S.Y.; Xi, Y.F. Effect of high oxygen on respiration rate, polyphenol oxidase activity and quality in postharvest loquat fruits. *Plant Physiol. Commun.* **2000**, *36*, 318–320.
141. Haiyan, G.; Lili, S.; Yongjun, Z.; Ying, Y.; Wenxuan, C.; Hangjun, C.; Yonghua, Z. Effects of hypobaric storage on quality and flesh leatheriness of cold-stored loquat fruit. *Trans. Chi. Soc. Agric. Engrr.* **2008**, *24*, 245–249.
142. Chen, W.; Yang, Y.; Song, L.; Jiang, Y.; Zheng, Y.; Gao, H.; Chen, H. Effect of hypobaric storage on physiological and quality attributes of loquat fruit at low temperature. *Acta Hortic.* **2006**, *712*, 269–274. [CrossRef]
143. Zhang, W.; Jiang, H.; Cao, J.; Jiang, W. Advances in biochemical mechanisms and control technologies to treat chilling injury in postharvest fruits and vegetables. *Trands Food Sci. Technol.* **2021**, *113*, 355–365. [CrossRef]
144. Lyons, J.M. Chilling injury in plants. *Annu. Rev. Plant Physiol.* **1973**, *24*, 445–466. [CrossRef]
145. Wang, P.; Zhang, B.; Li, X.; Xu, C.; Yin, X.; Shan, L.; Ferguson, I.; Chen, K. Ethylene signal transduction elements involved in chilling injury in non-climacteric loquat fruit. *J. Exp. Bot.* **2010**, *61*, 179–190. [CrossRef] [PubMed]
146. Wei, Y.; Xu, F.; Shao, X. Changes in soluble sugar metabolism in loquat fruit during different cold storage. *J. Food Sci. Technol.* **2017**, *54*, 1043–1051. [CrossRef] [PubMed]
147. Shan, L.L.; Li, X.; Wang, P.; Cai, C.; Zhang, B.; Sun, C.D.; Zhang, W.S.; Xu, C.J.; Ferguson, I.; Chen, K.S. Characterization of cDNAs associated with lignification and their expression profiles in loquat fruit with different lignin accumulation. *Planta* **2008**, *227*, 1243–1254. [CrossRef]
148. Xu, Q.; Wang, W.; Zeng, J.; Zhang, J.; Grierson, D.; Li, X.; Yin, X.; Chen, K. A NAC transcription factor, *EjNAC1*, affects lignification of loquat fruit by regulating lignin. *Postharvest Biol. Technol.* **2015**, *102*, 25–31. [CrossRef]
149. Zhang, L.; Zhang, Z.; Zheng, T.; Wei, W.; Zhu, Y.; Gao, Y.; Yang, X.; Lin, S. Characterization of carotenoid accumulation and carotenogenic gene expression during fruit development in yellow and white loquat fruit. *Hortic. Plant. J.* **2016**, *2*, 9–15. [CrossRef]
150. Hofman, P.J.; Stubbings, B.A.; Adkins, M.F.; Corcoran, R.J.; White, A.; Woolf, A.B. Low temperature conditioning before cold disinfestation improves 'Hass' avocado fruit quality. *Postharvest Biol. Technol.* **2003**, *28*, 123–133. [CrossRef]
151. Zeng, J.K.; Li, X.; Zhang, J.; Ge, H.; Yin, X.R.; Chen, K.S. Regulation of loquat fruit low temperature response and lignification involves interaction of heat shock factors and genes associated with lignin biosynthesis. *Plant Cell Environ.* **2016**, *39*, 1780–1789. [CrossRef]
152. Li, X.; Zang, C.; Ge, H.; Zhang, J.; Grierson, D.; Yin, X.R.; Chen, K.S. Involvement of PAL, C4H, and 4CL in chilling injury-induced flesh lignification of loquat fruit. *HortScience* **2017**, *52*, 127–131. [CrossRef]
153. Jin, P.; Sun, C.; Zheng, Y.; Sun, M. Effects of methyl jasmonate in combination with low temperature conditioning on chilling injury and active oxygen metabolism in loquat fruits. *Acta Hortic. Sin.* **2012**, *39*, 461–468.
154. Xu, M.; Zhang, M.; Shi, Y.; Liu, X.; Li, X.; Grierson, D.; Chen, K. *EjHAT1* participates in heat alleviation of loquat fruit lignification by suppressing the promoter activity of key lignin monomer synthesis gene *EjCAD5*. *J. Agric. Food Chem.* **2019**, *67*, 5204–5211. [CrossRef]
155. Jiang, Y.; Duan, X.; Joyce, D.; Zhang, Z.; Li, J. Advances in understanding of enzymatic browning in harvested litchi fruit. *Food Chem.* **2004**, *88*, 443–446. [CrossRef]
156. Sapers, G.M.; Miller, R.L. Browning inhibition in fresh-cut pears. *J. Food Sci.* **1998**, *63*, 342–346. [CrossRef]
157. Walker, J.R. Enzymatic browning in fruits: Its biochemistry and control. In *Enzymatic Browning and Its Prevention*; Lee, C., Whitaker, J., Eds.; ACS Publications: Washington, DC, USA, 1995; pp. 8–22.
158. Zauberman, G.; Ronen, R.; Akerman, M.; Weksler, A.; Rot, I.; Fuchs, Y. Post-harvest retention of the red colour of litchi fruit pericarp. *Sci. Hortic.* **1991**, *47*, 89–97. [CrossRef]

159. Gariglio, N.; Fonfría, M.A. Effect of fruit thinning on the mineral composition of loquat ("*Eriobotrya japonica*" Lindl.) fruit and its connection with purple spot. *Span. J. Agric. Res.* **2005**, *4*, 439–446. [CrossRef]
160. Gariglio, N.; Almela, V.; Agusti, M. Physiological factors related to purple spot of loquat fruit. *Plant Physiol. Biochem.* **2000**, *38*, 58.
161. Gariglio, N.; Juan, M.; Castillo, A.; Almela, V.; Agustı, M. Histological and physiological study of purple spot of loquat fruit. *Sci. Hortic.* **2002**, *92*, 255–263. [CrossRef]
162. Villar, P.C. El nispero y su expansion, posibilidades y limitaciones. *Fruit. Prof.* **1993**, *54*, 35–40.
163. Ojima, M.; Rigitano, O.; Simao, S.; Ique, T. The effect of the type of fruit protection on the incidence of purple spot and fruit development in loquats. *Bragantia* **1976**, *35*, 1–44.
164. Hadjipieri, M.; Georgiadou, E.C.; Costa, F.; Fotopoulos, V.; Manganaris, G.A. Dissection of the incidence and severity of purple spot physiological disorder in loquat fruit through a physiological and molecular approach. *Plant Physiol. Biochem.* **2020**, *155*, 980–986. [CrossRef]
165. Juárez-Vázquez, S.B.; Silva-Rojas, H.V.; Rebollar-Alviter, A.; Maidana-Ojeda, M.; Osnaya-González, M.; Fuentes-Aragón, D. Phylogenetic and morphological identification of *Colletotrichum godetiae*, a novel pathogen causing anthracnose on loquat fruits (*Eriobotrya japonica*). *H. Plant Dis. Prot.* **2019**, *126*, 593–598. [CrossRef]
166. Damm, U.; Sun, Y.C.; Huang, C.J. *Colletotrichum eriobotryae* sp. nov. and *C. nymphaeae*, the anthracnose pathogens of loquat fruit in central Taiwan, and their sensitivity to azoxystrobin. *Mycol. Prog.* **2020**, *19*, 367–380. [CrossRef]
167. Yan, F.; Li, C.; Ye, X.; Lian, Y.; Wu, Y.; Wang, X. Antifungal activity of lipopeptides from *Bacillus amyloliquefaciens* MG3 against *Colletotrichum gloeosporioides* in loquat fruits. *Biol. Cont.* **2020**, *146*, 104281. [CrossRef]
168. Wang, Q.H.; Ji, Y.P.; Qu, Y.Y.; Qi, Y.K.; Li, D.W.; Liu, Z.Y.; Wu, X.Q. The response strategies of *Colletotrichum gloeosporioides* s.s. due to the stress caused by biological control agent *Bacillus amyloliquefaciens* deciphered by transcriptome analyses. *Biol. Cont.* **2020**, *150*, 104372. [CrossRef]
169. Wang, X.; Wang, L.; Wang, J.; Jin, P.; Liu, H.; Zheng, Y. *Bacillus cereus* AR156-induced resistance to *Colletotrichum acutatum* is associated with priming of defense responses in loquat fruit. *PLoS ONE* **2014**, *9*, e112494. [CrossRef] [PubMed]
170. Cao, S.; Zheng, Y.; Tang, S.; Wang, K. Improved control of anthracnose rot in loquat fruit by a combination treatment of *Pichia membranifaciens* with $CaCl_2$. *Int. J. Food Microbiol.* **2008**, *126*, 216–220. [CrossRef]
171. Lin, S.; Sharpe, R.H.; Janick, J. Loquat: Botany and horticulture. *Hortic. Rev.* **1999**, *23*, 233–276.
172. Fukuda, S.; Ishimoto, K.; Sato, S.; Terakami, S.; Yamamoto, T.; Hiehata, N. Genetic mapping of the loquat canker resistance locus in bronze loquat (*Eriobotrya deflexa*). *Tree. Gen. Geno.* **2014**, *10*, 875–883. [CrossRef]
173. Hiehata, N.; Fukuda, S.; Sato, Y.; Tominaga, Y.; Terai, O.; Yamada, M. Quantitative inheritance of resistance to loquat canker (*Pseudomonas syringae* pv. *eriobotryae, Group C) in loquat progenies from crosses between a resistant cultivar, 'Champagne', and susceptible cultivars. HortScience* **2014**, *49*, 1486–1491. [CrossRef]
174. Fukuda, S.; Ishimoto, K.; Terakami, S.; Yamamoto, T.; Hiehata, N. Genetic mapping of the loquat canker resistance gene *pse-c* in loquat (*Eriobotrya japonica*). *Sci. Hortic.* **2016**, *200*, 19–24. [CrossRef]

foods

MDPI

Review

A Review of Storage Temperature Recommendations for Apples and Pears

Robert K. Prange [1,*] and A. Harrison Wright [2]

[1] Special Graduate Faculty, School of Environmental Sciences, University of Guelph, Guelph, ON N1G 2W1, Canada
[2] Kentville Research and Development Centre, Agriculture & Agri-Food Canada, Kentville, NS B4N 1J5, Canada
* Correspondence: prangepublications@gmail.com

Abstract: An exploration of the range of expert opinions on the optimum storage temperature for apples and pears in RA (refrigerated air), CA (controlled atmosphere), and DCA (dynamic controlled atmosphere) is provided, based on the accumulated postharvest data from the last 20 years. Apple cultivars have been divided into two storage temperature groups (0 to 1 °C and >1 °C), based on chilling sensitivity. Increasingly, gradual cooling, rather than rapid cooling, is recommended for apple cultivars, especially for chilling-sensitive cultivars. European pear cultivars are held at storage temperatures close to or just below 0 °C since they are not chilling-sensitive, and most cultivars require a cold temperature to induce ethylene production and ripening, especially if picked early for long-term storage. Asian pears apparently have higher temperature requirements in CA, compared with European pears. The temperature recommendations for RA and CA storage differ in some apple and European pear cultivars. In such cases, the CA recommendation is, on average, approximately 0.9 °C higher for apple cultivars and approximately 0.5 °C higher for pear cultivars, compared with RA. Research evidence suggests that some apple and pear cultivars can be stored at higher temperatures in DCA than in CA, and if the ethylene inhibitor, 1-methylcyclopropene (1-MCP), is applied in CA and/or DCA, leading to possible energy savings and quality benefits. A cool growing season may increase postharvest disorders, depending on cultivar and region. The store or packinghouse manager may choose to mitigate potential postharvest problems by maintaining the storage temperature at or above the temperature listed here and/or using stepwise (gradual) cooling. The storage temperature can affect the humidity and vapour pressure deficit (driving force) in the storage room. Altering the vapour pressure deficit controls the water loss in stored fruit, which can affect various quality parameters and the occurrence of several storage disorders.

Keywords: apples; pears; storage temperature; refrigerated atmosphere; controlled atmosphere; dynamic controlled atmosphere; chilling-sensitive; energy savings; pre-harvest effects; storage humidity

Citation: Prange, R.K.; Wright, A.H. A Review of Storage Temperature Recommendations for Apples and Pears. *Foods* **2023**, *12*, 466. https://doi.org/10.3390/foods12030466

Academic Editors: Imahori Yoshihiro and Jinhe Bai

Received: 27 October 2022
Revised: 11 January 2023
Accepted: 16 January 2023
Published: 19 January 2023

1. Introduction

The most recent estimate of the total world fruit production was 883 million tonnes (t) in 2019 (https://www.fao.org/3/cb4477en/cb4477en.pdf, accessed on 16 December 2022). The world's apple (*Malus domestica* Borkh.) and European pear (*Pyrus communis* L.) production was estimated at approximately 104 million t (81 million t apple plus 23 million t pear) in 2021 (http://www.wapa-association.org/asp/article_2.asp?doc_id=643, accessed on 16 December 2022), which is approximately 11.8% of the total world fruit production and second only to bananas and plantains (18%). Asian pears (Nashi) (*Pyrus pyrifolia* (Burm.f.) Nak., *P. bretschneideri* Rehder, or *P. ussuriensis* Maxim.) production is historically small compared with apples and European pears and reliable production values are not available.

Storing at the lowest acceptable temperature is an essential factor in extending the storage life of apples and pears [1,2]. If stored above this temperature, fruit senescence

and associated fungal decay will shorten the storage period, and if stored below that temperature, fruit may freeze, or the fruit can develop chilling-induced disorders [1]. There are some cultivars of apples and Asian pears that are prone to chilling disorders and a solution for these cultivars is to store them at a higher temperature and/or use low-temperature conditioning, which is a gradual lowering of the temperature over a period of several days or weeks [3–8].

It should be noted that ethylene production is stimulated by chilling in some apple and European pear cultivars [9–19]. Induction of ethylene production, which hastens ripening in pears, can occur at temperatures $\leq$ 10 °C [9,15,19–21], but in at least one cultivar, Passe Crassane, it must be $\leq$5 °C [22]. Some apple cultivars, e.g., Golden Delicious, Granny Smith, Lady Williams, and Fuji, are also chilling-sensitive and can be induced to ripen by exposure to 0–10 °C in air [9,15]. Cold-induced stimulation of ethylene formation is due to the increased activity of both 1-aminocyclopropane-1-carboxylic acid (ACC) synthase and ACC oxidase, which then leads to increased ethylene production, especially when the fruit temperature is increased after removal from cold storage [12,14,15]. The low-temperature requirement varies with the cultivar, with early maturing pear cultivars having a shorter requirement, 0–20 days, while later-maturing cultivars require longer durations, >40 days. The low-temperature requirement in pears can be reduced by applying exogenous ethylene and/or delaying harvest [16–19,23–25].

Controlled atmosphere (CA) storage is based on the alteration and maintenance of gas composition different from that of air (78 kPa N_2, 21 kPa O_2, and 0.03 kPa CO_2) in the storage atmosphere of the commodity. Ripening at the lowest acceptable temperature is delayed by CA conditions in almost all apple and pear cultivars, compared with refrigerated air (RA) conditions [1,8,10,16,26]. The major benefit of CA is derived from lowering the O_2 concentration as low as possible without inducing undesirable anaerobic metabolism. A low O_2 concentration inhibits respiratory metabolism and, if sufficiently low, it also inhibits ethylene biosynthesis and perception and ripening [8,26].

Almost all the information on the recommended storage temperature for apples and pears is for fruit stored in CA, with a limited number of temperature recommendations for storage in RA. Unfortunately, there is no central repository for the recommendations and the last summary was by Kupferman at the 8th International Controlled Atmosphere Research Conference [27]. He presented a summary of the most recent (to that date) controlled atmosphere (CA) recommendations for apples and pears. It included CA requirements for 32 apple and 9 pear cultivars, from 9 different growing regions. His summary identified the optimum storage temperature, atmosphere, and storage duration for each of these cultivars. Prange [8] has updated Kupferman's CA storage recommendations with more recent data, including information on temperature and CA recommendations for 116 apple and 38 pear cultivars. The intent of this review is to provide more current storage temperature recommendations along with the factors identified by Prange [8] that can affect the recommended storage temperatures.

2. Development of a Database

A database of postharvest information generated between 2000 and 2022 was compiled from published and unpublished sources. Including the information from Kupferman [27], this database now comprises 116 apple cultivars and 42 European and Asian pear cultivars from approximately 17 growing regions (Tables 1 and 2). Each recommendation in the database included most of the following key details: cultivar(s), country/region, year, optimum RA storage temperature, optimum CA storage temperature, recommended O_2 and/or CO_2 atmospheres, and storage duration, plus any relevant notes.

Table 1. Apple cultivars included in Kupferman's work [27], and additional apple cultivars assembled from published and unpublished information available between 2000 and 2022 (from Prange [8], with permission).

32 Apple Cultivars with CA Recommendations, as Reported by Kupferman [27]	**84 Additional Apple Cultivars with CA Recommendations**
'Boskoop', 'Braeburn', 'Cortland', 'Cox's Orange Pippin', 'Delicious', 'Elstar', 'Empire', 'Fuji', 'Gala', 'Gloster', 'Golden Delicious', 'Granny Smith', 'Gravenstein', 'Idared', 'Jonagold', 'Jonathan', 'Lobo', 'Macfree', 'McIntosh', 'Moira', 'Mutsu', 'Northern Spy', 'Nova Easygro', 'Novamac', 'Novaspy', 'Prima', 'Priscilla', 'Rome', 'Sciros' ('Pacific Rose'), 'Spartan', 'Splendour', 'Stayman'	'Alwa', 'Ambrosia', 'Antàres', 'Antonovka ohuknovenaya', 'Aport', 'Aprelskoe', 'Ariane', 'Arlet', 'Belchard' ('Chantecler'), 'Belgica', 'Berkutovskoe', 'Bogatir', 'Bonita', 'Bonza', 'Bramley's Seedling', 'Caudle' ('Cameo'), 'Chopin', 'Choupette', 'CIV G198′ ('Modi'), 'Civni' ('Rubens'), 'Coobishevskoe', 'Coolikovskoe', 'Coop 38′ ('Goldrush'), 'Corichnoe Novoe', 'Cosmic Crisp', 'Cripps Pink' ('Pink Lady'), 'Cripps Red' ('Sundowner', 'Joya'), 'Delblush' ('Tentation'), 'Discovery', 'Egremont Russet', 'Firmgold', 'Glockenapfel', 'Golden Orange', 'Golden Russet', 'Honeycrisp', 'Imrus', 'Jonamac', 'Karmijn de Sonnaville' ('Carmine'), 'Ladina', 'Lady Williams', 'La Flamboyante' ('Mairac'), Ligol', 'Macoun', 'Maigold', 'Martovskoe', 'Meridian', 'Milwa' ('Diwa'), 'Nicogreen' ('Greenstar'), 'Nicoter" ('Kanzi'), 'Noris', 'Orlik', 'Orlovskoe polosatoe', 'Pamyat Michurina', 'Pamyat Voinu', 'Pazazz', 'Pepin Shafrany', 'Pinova' ('Corail'), 'Red Pippin', 'Reinette grise du Canada', 'Renet Chernenco', 'Renet Coorsky Zolotai', 'Rososhanskoe polosatne', 'Rubinette', 'Salish', 'Šampion' ('Champion'), 'Scifresh' ('Jazz'), 'Scilate' ('Envy'), 'Severni Sinap', 'Sinap Beloruski', 'Sinap Orlovski', 'Skoroplodnoe', 'Spigold', 'Summerred', 'Tambovskoe', 'Topaz', 'Veteran', 'Vishnevonee', 'Welsey', 'Winesap', 'Worcester Pearmain', 'Yellow Newtown', 'York', 'Zhigulevskoe', 'Zimnee polosatoe'

Table 2. Pear cultivars included in Kupferman's work [27], and additional pear cultivars assembled from published and unpublished information available between 2000 and 2022 (from Prange [8], with permission).

9 Pear Cultivars with CA Recommendations, as Reported by Kupferman [27]	**29 Additional Pear Cultivars with CA Recommendations**
'Beurré Bosc' ('Kaiser Alexander'), 'Beurré d'Anjou', 'Conference', 'Doyenné du Comice' ('Vereinsdechant', 'Sweet Sensation', 'Decana del Comizio'), 'Forelle', 'Josephine' ('Joséphine de Malines'), 'Packham's Triumph', 'Rosemarie', 'Williams Bon Chretien' ('Bartlett')	**25 European Pear cultivars** 'Abate Fetel', 'Alexander Lucas', 'Alexandrine Douillard', 'Amfora', 'Angélys', 'Beurré Hardy', 'Cold Snap' ('Harovin Sundown'), 'Concorde', 'Corella', 'Delbuena', 'Delmoip', 'Dr. Jules Guyot' ('Limonera'), 'Erica', 'Flamingo', 'Forelle', 'Fred' ('CH 201'), 'General Leclerc', 'Gute Louise' ('Louise Bonne d'Avranches'), 'Harrow Sweet', 'Nojabrska' ('Novembra'), 'Passe Crassane', 'Rocha', 'Selena' ('Elliott'), 'Spadona' ('Blanquilla'), 'Winter Nelis' ('Bonne de Maline')
	4 Asian Pear Cultivars 'Chojuro', 'Hosui', 'Nijisseiki', 'Ya Li'

Since 2003 when Kupferman's summary was published, the amount of information on CA recommendations for apple and pear cultivars has significantly increased. Not only has the number of cultivars greatly increased (Tables 1 and 2), but the number of recommendations for each cultivar has also grown. For example, there are more than 35 CA recommendations each for Gala and Golden Delicious.

The increase in the number of cultivars in the database is a reflection of the changes in the apple and pear industry. Not only are there new cultivars every year, but in some cultivars, there is evidence that some newly identified clones may have real differences that necessitate different harvest and storage recommendations. These clonal differences need more research. Perhaps researchers could identify the clone as well as the cultivar that they are using in future research.

Another trend in the industry is the appearance of new 'club varieties' that are protected for a number of years under plant breeders' rights in many countries. Even though

growers are being encouraged to plant these club varieties, many of them could not be included in this database due to limited, or non-existent, harvest and storage information. Part of the club variety trend is the use of a new trademarked name (and sometimes multiple names) as an alternative to the actual cultivar name. The approach employed here is to use a generally accepted cultivar name and list in parentheses the known alternative names, e.g., Cripps Pink (Pink Lady).

3. Effect of Cultivar, CA, and RA on Storage Temperature Recommendations

Several trends since Kupferman's publication can be identified by examining the postharvest database information. First, the apple cultivars listed in Tables 3 and 4 can be divided into two groups based on their chilling sensitivity, using 1 °C as the critical boundary temperature. This is believed to be the first instance of grouping apples in this way:

- Chilling-insensitive: apple cultivars that are not chilling-sensitive in CA and can be stored at 0 to 1 °C (Table 3).
- Chilling-sensitive: apple cultivars that are chilling-sensitive in CA and need to be stored > 1 °C (Table 4).

Table 3. Apple cultivars that are not chilling-sensitive in CA (can be stored between 0 and 1 °C), arranged from lowest to highest recommended storage temperature. If the number of recommendations < 4, the CA temperature recommendation should be considered provisional (from Prange [8], with permission).

Chilling-Insensitive Cultivars (Including Clones)	Mean Recommended CA Temperature (°C)	Number of Recommendations
Mutsu (Crispin)	0	5
Delicious	0.22	17
Granny Smith	0.47	14
Lady Williams	0.50	2
Spartan	0.58	6
Gala	0.61	27
Golden Delicious	0.62	22
Stayman	0.62	2
Fuji [a]	0.63	12
Rome (Rome Beauty, Morgenduft)	0.65	5
Northern Spy	0.67	5
Braeburn [a]	0.74	15
Delblush (Tentation)	0.75	2
Jonathan	0.75	4
Cripps Red (Sundowner, Joya)	0.75	4
Jonagold'	0.84	16
Šampion (Champion)	0.84	5
Ligol	0.92	3
Gloster	0.94	4
Ladina	1.00	2
Topaz	1.00	2

[a] Gradual cooling may be required.

Over the last 20 years, a trend for gradual instead of abrupt (static) cooling recommendations has developed, and this trend is likely to increase in the future. Although most of the cultivars listed in Tables 3 and 4 have only static temperature recommendations, some now also have one or more recommendations to cool gradually (stepwise) to the final CA storage temperature (noted in the tables). Most of these cultivars are in the chilling-sensitive group, i.e., those that should be stored above 1 °C.

Table 4. Apple cultivars that are chilling-sensitive in CA (must be stored > 1 °C), arranged from lowest to highest recommended storage temperature. If the number of recommendations < 4, the CA temperature recommendation should be considered provisional (from Prange [8], with permission).

Chilling-Sensitive Cultivars (Including Clones)	Mean Recommended CA Temperature (°C)	Number of Recommendations
Caudle (Cameo)	1.13	2
Cortland	1.16	9
Ambrosia	1.20	5
Civni (Rubens)	1.22	3
Elstar [a]	1.23	12
Winesap	1.25	1
Pinova (Corail) [a]	1.25	4
Coop 38 (Goldrush)	1.38	2
Alwa	1.50	2
Scilate (Envy) [a]	1.50	2
Cripps Pink (Pink Lady) [a]	1.67	12
Idared	1.77	10
Scifresh (Jazz) [a]	1.85	4
Belchard	2.00	2
Empire	2.12	10
Arlet	2.25	2
McIntosh [a]	2.79	5
Nicoter (Kanzi) [a]	2.88	5
Honeycrisp [a]	3.00	6
Cox's Orange Pippin	3.50	5
Belle de Boskoop	3.96	6
Lobo	4.12	2
Bramley's Seedling	4.38	2

[a] Gradual cooling may be required.

Interestingly, two of the cultivars in the chilling-insensitive group (Table 3), 'Fuji' and 'Braeburn', also have some gradual cooling recommendations. The collected recommendations for 'Fuji' (Table 5) and for 'Braeburn' (Table 6) illustrate the range of CA temperature recommendations for some cultivars. For both cultivars, there are several recommendations for storage above 1 °C, suggesting chilling sensitivity of the fruit grown in those regions. There are also some recommendations for gradual cooling and/or delayed introduction of CA for these cultivars (Tables 5 and 6).

Table 5. CA temperature recommendations for 'Fuji' apple (from Prange [8], with permission).

CA Temperature (°C)	Country	Year
−0.5	South Africa	2018
0	Poland	2016
	Chile	2020
0.5	Australia	2000
0–1.0	Canada	2012
	USA (California)	2000
0.5–1.0	Argentina	2012
	France	2010, 2014
1.0	USA (Washington)	2003
1.1 + gradual cooling	USA (Pennsylvania)	2008
2.0–2.5 + gradual cooling + delayed CA	Italy	2018

Table 6. CA temperature recommendations for 'Braeburn' apple (from Prange [8], with permission).

CA Temperature (°C)	Country	Year
−0.5	South Africa	2003, 2008
0.50	New Zealand	2003
0.50–1.0	Argentina	2012
	France	2010, 2014
	Switzerland	2018
1.0	Australia	2000
	Belgium	2017
	Poland	2016
	USA (Washington)	2003
1.1 + gradual cooling	USA (Pennsylvania)	2008
1.0–1.5 + delayed CA	Italy	2018
1.5–2.0 + delayed CA	UK	2017

Unlike the apple cultivars, very few of the pear cultivars have more than four temperature recommendations (Table 7). Two pear cultivars, Conference and Doyenné du Comice, do have at least one recommendation to gradually cool. Perhaps further research will determine whether these two cultivars are chilling-sensitive and could benefit from a higher storage temperature. Unless and until that happens, the mean storage temperature recommendations for European pear cultivars range from −1.0 to +0.25 °C. In contrast, the recommendations for the four Asian pear cultivars average from 0 to +0.50 °C, i.e., slightly higher than for the European pears.

Table 7. Temperature recommendations for European and Asian pear cultivars in CA, arranged from lowest to highest. If the number of recommendations is <4, the CA temperature recommendation should be considered provisional (from Prange [8], with permission).

Cultivar (Including Clones)	Mean Recommended CA Temperature (°C)	Number of Recommendations
European pears		
'Angélys'	−1.00	1
'Beurré Hardy'	−1.00	1
'Dr. Jules Guyot' ('French Bartlett', 'Limonera')	−1.00	1
'Selena' ('Elliott')	−1.00	1
'Spadona' ('Blanquilla')	−1.00	1
'Abaté Fetel'	−0.62	4
'Amfora'	−0.50	1
'Delbuena'	−0.50	1
'Delmoip'	−0.50	1
'Erica'	−0.50	1
'Forelle'	−0.50	2
'Flamingo'	−0.50	1
'Josephine'('Joséphine de Malines')	−0.50	3
'Nojabrska' ('Novembra')	−0.50	1
'Passe Crassane'	−0.50	1
'Rocha'	−0.50	1
'Rosemarie'	−0.50	2
'Winter Nelis' ('Bonne de Maline')	−0.50	1
'Conference'	−0.49	12
'Beurré Bosc' ('Kaiser Alexander')	−0.47	8
'Doyenné du Comice' ('Vereinsdechant', 'Sweet Sensation', 'Decana del Comizio')	−0.44	10
'Packham's Triumph'	−0.43	10

Table 7. *Cont.*

Cultivar (Including Clones)	Mean Recommended CA Temperature (°C)	Number of Recommendations
'Beurré d'Anjou'	−0.38	2
'Williams Bon Chretien' ('Bartlett')	−0.36	12
'Alexander Lucas'	−0.25	2
'Cold Snap ' ('Harovin Sundown')	0	1
'General Leclerc'	0	1
'Concorde'	0.12	2
'Gute Louise' ('Louise Bonne d'Avranches')	0.12	2
'Fred' ('CH 201')	0.25	1
Asian pears		
'Ya Li'	0	1
'Chojuro'	0.50	1
'Hosui'	0.50	1
'Nijisseki'	0.50	2

4. Comparison of Storage Temperatures in RA, CA, and DCA and Effect of 1-MCP

4.1. Temperature in RA vs. CA

Some of the entries in the database have only an RA or only a CA temperature recommendation. Nevertheless, among the apple cultivars, there are 109 recommendations, for 54 cultivars, that contain both RA and CA storage temperature recommendations. Among these:

- 63% of the recommendations specify the same RA and CA temperature
- 35% of the temperature recommendations are higher in CA than in RA, i.e., higher by a mean of 0.93 °C (range of 0.2 to 3.5 °C)
- 1% of the recommendations are lower in CA, i.e., lower by a mean of −0.40 °C

The higher temperature in CA is in agreement with Kupferman [27], who suggested that the CA temperature for a few specific apple cultivars can range from 0.5 to 1.0 °C higher than the RA recommendation. Interestingly, Fidler et al. [28] also stated that "the temperature used for a given cultivar kept in RA is usually 0.5 to 1.0 °C lower than that used in CA." Two explanations are offered for this difference. Fidler, Wilkinson, and Edney [28] say that it is because "apples are more susceptible to low-temperature breakdown in CA than in air," so it is necessary to use a higher temperature if CA is used. However, another more plausible explanation was offered much earlier by Davis and Blair [29] in a study on McIntosh, a chilling-sensitive cultivar. They state that using CA for this cultivar in combination with a non-chilling temperature, e.g., 4.4 °C, not only increases the storage period, compared with RA, but actually reduces the hazards associated with storage at a colder temperature.

For European pear cultivars, there are 34 recommendations for 17 cultivars that included both RA and CA storage temperature recommendations:

- 62% of the recommendations specify the same RA and CA temperature
- 38% of the recommendations are higher in CA than RA, i.e., higher by a mean of 0.52 °C (range of 0.1 to 0.7 °C)

There have been no studies of Asian pears that include both RA and CA storage temperatures. Therefore, at this time, it is assumed that the recommended storage temperature in RA and CA should be the same.

4.2. Temperature in DCA vs. CA

To date, commercial recommendations for storage temperatures in a dynamic controlled atmosphere (DCA) are the same as for conventional CA. However, physiological studies show that lowering the O_2 concentration below 1.0 kPa, as in DCA, reduces apple and pear metabolic rates compared with the rates in CA (where typical O_2 > 1.0 kPa).

This allows storage temperatures in DCA to be higher than in CA, possibly up to approximately 5 °C, without incurring any negative metabolic effects (see Prange [8] for oxygen recommendations).

In support of this, the research on increasing storage temperatures in DCA, compared with CA, reports a number of possible benefits (Table 8). These include energy and cost savings, fewer storage disorders (especially chilling disorders), reduction in storage rot, less weight loss, and improved flavour. More research may be required to define the benefits of higher storage temperatures for specific cultivars of interest, perhaps also with higher commercial DCA temperature recommendations.

Table 8. Benefits of elevated storage temperature for apples stored in DCA (from Prange [8], with permission).

Cultivar(s)	Condition	Benefit	Reference
'Royal Gala', 'Cripps Pink' ('Pink Lady')	DCA-CF at 5 °C vs. CA at 3 °C	35% energy saving during cooling and 15% during storage.	[30]
'Cripps Pink' ('Pink Lady')	DCA-CF at 3 °C vs. CA at 3 °C	Reduced flesh browning.	[30]
'Golden Delicious', 'Jonagold', 'Pinova'	DCA-CF at 3–4 °C vs. ULO at 1 °C	15–50% energy saving, less weight loss, less storage rot (Pinova), improved taste, no quality loss.	[31,32]
'Elstar', 'Jonagold', 'Gloster'	DCA-CF (with or without 1-MCP) at 3.5–10 °C vs. ULO at 2 °C	Combination of DCA-CF +1-MCP is more favourable than either alone, especially at higher storage temperatures. Benefits include better firmness, and control of watercore, internal browning, and skin spots.	[33]
Galaxy Gala	DCA-RQ 1.3 and DCA-RQ 1.5 at higher temperatures (2.0 or 2.5 °C), compared with 1.5 °C	Galaxy Gala can be stored at higher temperatures (2.0 or 2.5 °C), because of lower mealiness, ethylene production, ACC oxidase, and higher flesh firmness, than at 1.5 °C.	[34]
Nicoter (Kanzi)	DCA-CF or DCA-RQ 1.5 at 3 vs. 1 °C	Both DCA methods at 3 °C produced better quality and fewer disorders, compared with 1 °C.	[35]
Royal Gala and Galaxy Gala	for both clones: 1.2 kPa O_2 and 2 kPa CO_2 vs. 0.8 k Pa O_2 and 1.6 kPa CO_2 for Galaxy only: 0.4 kPa O_2 and 1.2 kPa CO_2 at 1.0 vs. 1.5 °C	Storage of both Gala clones at extremely low O_2 at 1.5 °C provided better quality, compared with 1 °C	[36]

4.3. Effect of 1-Methylcyclopropene (1-MCP) on Storage Temperature Recommendations

The growth regulator 1-methylcyclopropene (1-MCP) is a vapour under physiological conditions and acts by inhibiting the binding of the hormone ethylene to its binding site [37,38]. Exposure to 1-MCP can temporarily render plant material insensitive to ethylene when applied at the parts-per-billion level. It is applied as a postharvest treatment but is sometimes applied on trees pre-harvest. The 1-MCP can reduce several serious storage disorders that cause fruit loss, such as senescent breakdown and superficial scald, but the incidence of others, including carbon dioxide injury and flesh browning, can be increased by 1-MCP [38]. Since apple fruit in storage can respond well to 1-MCP treatment, it is recommended for use on most apple cultivars, whereas recommendations for its use in stored pears has been more limited to a few selected cultivars.

Mir and Beaudry [39] were the first to propose the use of 1-MCP to reduce the requirement for refrigeration. They stored Delicious apples in RA at temperatures between 0 and 20 °C. They concluded that storage of 1-MCP-treated apple fruit at elevated temperatures will be limited to relatively short durations (<50 days) without some means of controlling storage decay.

Mattheis [40] stated that, in Washington State, some storage operators have altered CA conditions based on the reduced rates of fruit ripening after 1-MCP treatment. Higher O_2 and temperature set points have been used in some warehouses, but widespread adoption of these changes has not yet occurred. The use of higher O_2 and higher temperatures lowers the risk of low O_2 or low-temperature injuries. An additional benefit is a decrease in power costs. McCormick et al. [41,42] examined the effect of adding 1-MCP to Gala and Jonagold apples in commercial rooms under CA conditions in Germany. The setpoint temperature of the control rooms without 1-MCP was 1.5 °C and, in the 1-MCP rooms, it was 2.5 °C higher at 4.0 °C. Assessment of the Gala and Jonagold fruit removed from storage at various times and evaluated for quality after seven days at ambient temperature to simulate marketing showed that 1-MCP-treated fruit at the higher storage temperature had similar or better quality attributes, compared with the fruit not treated with 1-MCP. An energy audit after 6 and 8 months showed that a 35% ('Gala' experiment) and 26% reduction (Jonagold experiment) in energy was achieved by storage at the higher temperature. In the UK, a trial with Gala apples using a storage temperature of 3.5 °C in the 1-MCP-treated CA room, compared with 0.5 °C in the control CA room, yielded similar results as in Germany [43,44]. Harz-Pitre [45] reported on similar commercial trials with CA-stored Golden Delicious, Granny Smith, Gala, Delicious, and Cripps Pink in South Africa. The 1-MCP-treated fruit were stored at 1.5 °C warmer than fruit not treated with 1-MCP. The report claimed that the findings at the various packhouses turned out to be excellent, with an average of 16% kWh saving for each degree Celsius of temperature increase. Kittemann, McCormick, and Neuwald [31] stored Golden Delicious, Jonagold, and Pinova for seven months in either CA at 1 °C without 1-MCP or CA at 5 °C with 1-MCP. Storing at 4 °C higher with 1-MCP resulted in an energy saving of 70%. The effect of storing in CA at 5 °C with 1-MCP on fruit quality and decay varied with the cultivar, with no consistent negative effects.

Despite these commercially sponsored results, there are few recommendations of higher storage temperatures when using 1-MCP. Zanella [45] suggests that CA storage of Cripps Pink in Italy is possible at 4 °C with 1-MCP, compared with 2.5 °C without 1-MCP. In Belgium, there are recommendations for CA with and without 1-MCP for five apple and three pear cultivars [46]. For the five apple cultivars, if 1-MCP is used, the CA storage temperature recommendation does not change for Gala and Greenstar, increases 0.2 °C for Pinova, and increases 0.5 °C for Golden Delicious and Jonagold. For the three pear cultivars, if 1-MCP is used, the CA storage temperature recommendation does not change for Comice, increases 0.2 °C for Conference, and increases 1.0 °C for Alexander Lucas.

It may be possible to achieve energy saving by increasing the storage temperature in CA if 1-MCP is used but there needs to be more research on how much of an increase is acceptable for specific cultivars in each growing region. Köpcke [33] examined the effect of combining 1-MCP with DCA on German-grown Elstar, Jonagold, and Gloster apples stored at 2.0, 3.5, and 8.7 °C for 140 days plus a 10-day shelf-life. Their overall conclusion was that the combination of 1-MCP and DCA storage is more favourable than 1-MCP or DCA alone, especially at higher storage temperatures. de Oliveira Anese et al. [34] tested this assumption with Brazilian-grown Galaxy Gala apples stored at 1.5, 2.0, and 2.5 °C in CA and DCA, with and without 1-MCP. They concluded that Galaxy Gala apples can be stored at more elevated temperatures (2.0 and 2.5 °C) under DCA, with no extra benefit with the addition of 1-MCP application. The 1-MCP was only beneficial if CA was used, rather than DCA. Vanoli et al. [47] conducted a similar study with Abate Fetel pear using 2 storage temperatures (−0.5 and 1 °C), 3 atmospheres (RA, CA, and DCA), and 2 storage times (20 and 28 weeks), with the aim of finding a better strategy to ensure ethylene-induced softening without inducing storage disorders. Although fruit treated with 1-MCP reduced or stopped softening, especially at −0.5 °C, they concluded that 90–95% of 1-MCP-treated fruit stored in CA and DCA was saleable, regardless of storage temperature and storage. They recommended that further research is needed to develop an optimum strategy.

These results suggest that further research is needed on the benefit of combining 1-MCP with DCA to allow for higher storage temperatures and thereby achieve greater energy savings.

5. Effects of Growing Season Temperature on Storage Temperature

Examination of the variations in storage guidelines employed around the world for widely grown cultivars reveals that the recommended storage temperature in production regions with a relatively warm growing season is often lower than the temperature recommended in regions with cooler climates. This is consistent with the findings of Wright et al. [48]. It suggests that lower growing season temperatures, especially during the latter part of the season, are associated with increased susceptibility to low-temperature breakdown (LTB) of apples in storage, which can be avoided by increasing the storage temperature [48–50]. For example, in Cripps Pink apples, fruit can develop two types of flesh browning, both of which vary depending on the heat units during the growing season (Tables 9 and 10 [51,52]). Diffuse flesh browning (DFB) is a chilling disorder which behaves like LTB, i.e., it occurs when the growing degree days (GDD, 10 °C base temperature) are below 1100–1200, and it can be controlled with a higher storage temperature, e.g., 3 °C (Table 11). Radial flesh browning (RFB) is a senescent disorder that may occur in regions or seasons that accumulate between 1100 and 1800 GDD (Tables 9 and 10 [53]), although there is no clear predictable relationship between RFB and GDD [53]. This is not surprising since senescent breakdown can occur in all apple cultivars and is affected by a number of factors [14,18]. In contrast with DFB, RFB is controlled by a lowered storage temperature, either by storing directly at 1 °C, or by stepwise cooling to 1 °C (Table 11). However, fruit from a region or season that accumulates >1700–1800 GDD has little or no risk of developing either of these disorders during storage.

Table 9. Relationship between growing degree days (GDD) from full bloom to harvest and the incidence of diffuse and radial types of flesh browning (FB) in Cripps Pink apples (from [8,51], with permission).

Type of Flesh Browning	GDD	Incidence of Flesh Browning, %
Diffuse	888	95.4
	888	99.4
	904	75.7
	904	76.0
	930	8.1
Radial	1462	57.5
	1462	54.2
	1567	27.8
	1641	10.0
	1679	0

Table 10. The effect of growing degree days (GDD) on the two types of flesh browning in Cripps Pink apples. The chilling disorder or diffuse flesh browning develops in cool regions, whereas senescent disorder or radial flesh browning develops in warm regions. Neither of these develop in hot regions. Although Cripps Pink is also susceptible to CO_2 injury, this is not dependent on GDD (from [8,52], with permission).

District	$GDD_{10\,°C}$ (2005 Data)	Type of Flesh Browning		
		Radial	Diffuse	CO_2 Injury
				

Table 10. *Cont.*

District	$GDD_{10\,°C}$ (2005 Data)		Type of Flesh Browning		
			Radial	Diffuse	CO_2 Injury
Tasmania, Australia	807	**Cool**		Y	Y
Nelson, New Zealand	1026			Y	Y
Hawkes Bay, New Zealand	1102			Y	Y
Yarra Valley, Australia	1162		Y	Y	Y
Manjimup, Australia	1405		Y		Y
Batlow, Australia	1556		Y		Y
Goulburn Valley, Australia	1688		Y		Y
California	1840	**Hot**			Y

Table 11. Overall recommendations for control of diffuse and radial flesh browning in Cripps Pink apples (from [8,51,52], with permission).

	Diffuse Flesh Browning	Radial Flesh Browning
Classification	Chilling injury	Senescent breakdown
Climatic range	<1100 GDD	>1100 GDD [1]
Maturity	SPI [2] 3.5	SPI 3.5
Storage temperature	3.0 °C [3]	1 °C [4] or stepwise cooling [5]
Storage atmosphere	<1% CO_2	<1% CO_2
Orchard management	Ensure calcium levels are adequate	Best commercial practice [6]

[1] Since insufficient data in the climatic range of 1100–1400 growing degree days (GDD) > 10 °C are currently available, the type of flesh browning that develops in this range has not been determined. However, the general recommendations for radial flesh browning (RFB) may be suitable as a guide. [2] The starch pattern index (SPI) recommendation is based on the Centre Technique Interprofessionnel des Fruits et Légumes (CTIFL) 10-point scale. [3] Storage at 3 °C will prevent the development of diffuse flesh browning (DFB), however storage at 1 °C will reduce symptoms. Storage at 3 °C will reduce the period of storage before loss of quality occurs. [4] Storage at 1 °C successfully prevented RFB, however this was in a low-risk season. In a high-risk season, storage at a higher temperature may be required. [5] The stepwise cooling recommendation is: 2 weeks at 3 °C, followed by 2 weeks at 2 °C, then the remainder of the storage period at 1 °C. [6] Use best commercial practices for management of crop load and fruit nutrition.

If no local expert advice is available and the growing season is cooler than 'normal' for a cultivar that is prone to cool season disorders, the store/packinghouse manager should consider mitigating potential postharvest problems by avoiding storage temperatures below those listed in Table 9, and/or by implementing stepwise cooling over 1–2 months. Climate change, which is slowly increasing the growing temperature over the course of many decades, may alter what is a 'normal' growing season. However, this change is gradual, relies on averaging over the course of many disparate years, and can be associated with other changes, such as increased frequency of drought and extreme temperature events. This makes it difficult to predict how climate change will affect storage temperature recommendations and this remains poorly studied.

6. Interaction between Storage Temperature and Humidity

The rate at which water is lost from a single apple or pear fruit is a function of three factors, i.e., the surface area of the fruit, the vapour permeance of the fruit surface, and the difference in water vapour pressure between the inside and the outside of the fruit (see [8] for more detail). The difference in water vapour pressure between the inside of the fruit and the room air is also known as the driving force.

Water leaves the fruit in the form of water vapour. The water vapour pressure inside the fruit is assumed to be 100% RH at the temperature of the fruit. If the room air is also at 100% relative humidity (RH), then there is no difference, and thus no net loss of water from the fruit. Therefore, in theory, as much water enters the fruit as leaves it. In practice, however, the room air cannot be maintained at 100% RH because of the need to cool the fruit.

In all modern apple and pear storerooms, cooling is accomplished using the cooling coils of a mechanical refrigeration system to cool the room air and fans to distribute the cool air throughout the room. This type of cooling system increases the water vapour difference (driving force) because the cold temperature of the evaporation coils reduces the water-holding capacity of the room air. To achieve cooling, the temperature of the discharged air from the evaporation coils must be lower than the room air. This reduces its moisture-holding capacity and excess moisture condenses onto the evaporation coils. Thus, the relationship between the temperature of the room air and the temperature of the air discharged from evaporation coils dictates the maximum room air RH (Figure 1). Using the graph in Figure 1, one can estimate the maximum room air RH from two temperature measurements, i.e., room air and evaporation discharge temperatures, without measuring the actual RH in the room.

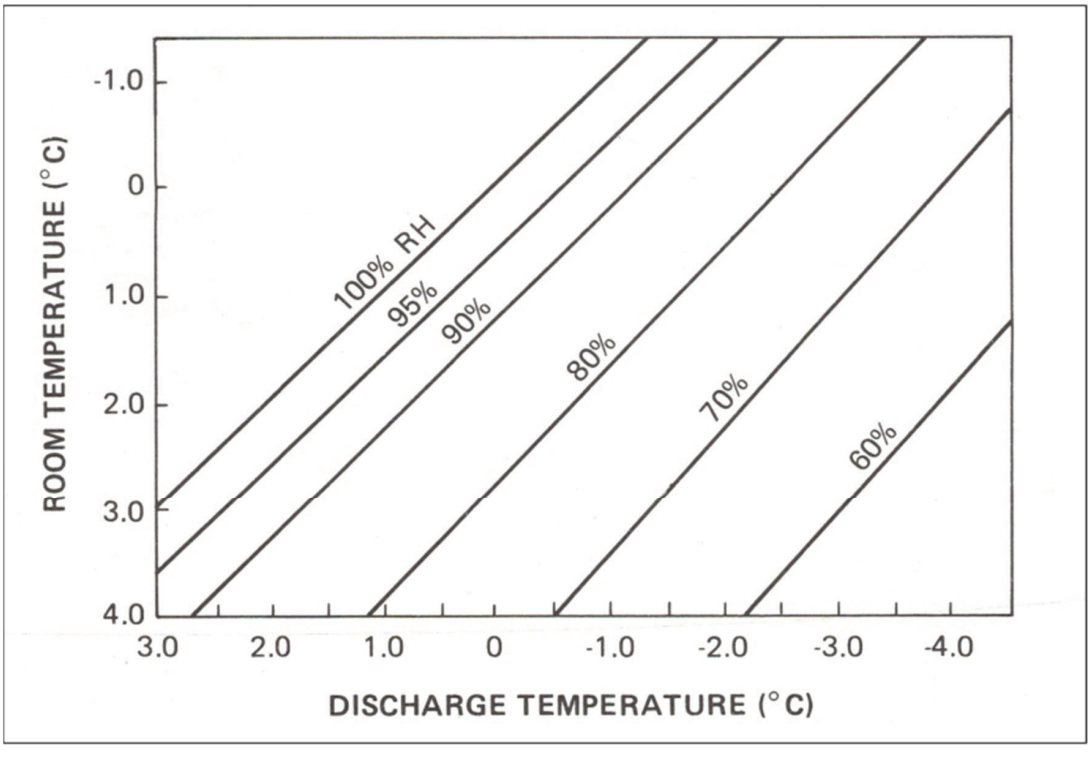

Figure 1. Relationship of the relative humidity (RH) of the room air to the temperature of the discharge air from the evaporation coils (from [8], with permission).

During the room-filling stage and RA storage, the only reliable method to measure weight loss is by repeated weighing of fruit samples since the room humidity can be quite variable due to variable bin numbers, bin material (plastic vs. wood), and repeated room opening. For example, the use of dry wood bins, compared with plastic bins, results in a depression in storeroom humidity that can last for weeks (Figure 2).

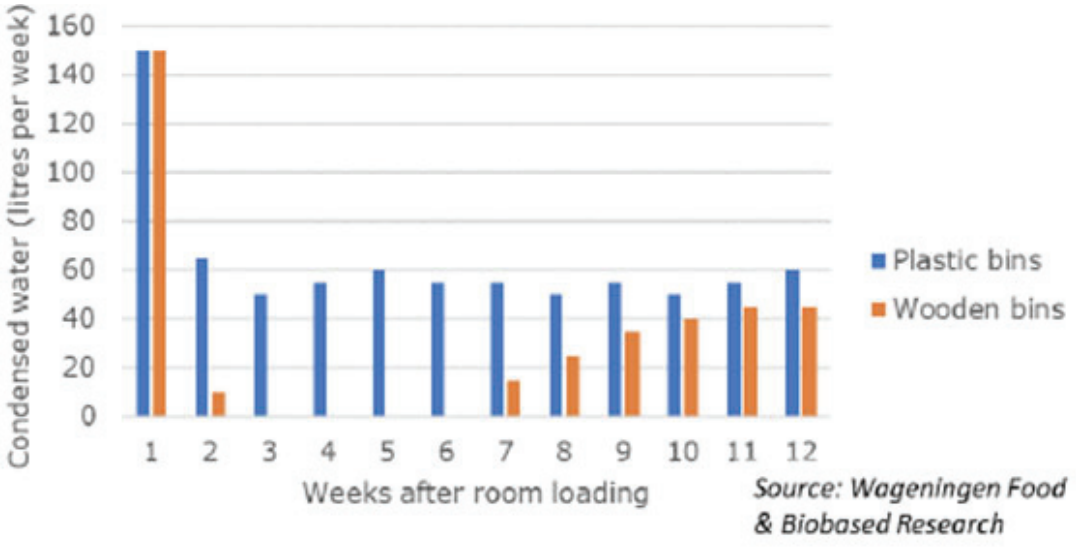

Figure 2. The amount of condensed water (litres per week) from a room with plastic bins and a room with wooden bins (150 tons of pears per room) (from [8,54], with permission).

Note that, in a sealed CA room, one can measure the amount of condensation from the evaporation coils to determine if the room air RH is at its maximum. This can be measured manually (Figure 3a) or electronically (Figure 3b). If there is no condensate, then the room air is actually below the maximum possible RH (Figure 1). In such a situation, the fruit will be subject to greater weight loss. The RH can be increased by adding water to the room floor, or by misting, or by adding more fruit if the room is only partially filled. If condensate is present, the amount collected can be used to estimate weight loss in the storage room, assuming that 1 L of condensate water equals 1 kg of weight loss. This is expressed as litres/1000 kg/month, i.e., 1 L/1000 kg/month equals 0.10% weight loss per month.

Altering the water loss in stored fruit affects various quality parameters and the occurrence of several storage disorders [8,55]. Consequently, some specialists recommend an amount of weight loss during long-term CA storage which varies with the cultivar, e.g., 1.5–2.5% for Golden Delicious apple and Conference pear, 2.0–2.5% for Gala apple, and 2.5–3.0% for Elstar apple [55].

(**a**) (**b**)

Figure 3. (**a**) Manual collection of water outside a CA room from the evaporation coils inside the room. There is a drain trap on the water pipe inside the CA room, to maintain airtight conditions. The volume collected in the green container is measured to determine moisture loss from the fruit, since 1 L collected equals 1 kg of weight loss from the fruit in the room. (**b**) Device for computerised electronic collection of water outside a CA room, from the evaporation coils inside the room (https://storage.isolcell.com/en/sentinel/). This system can redirect drainage water either back into the storeroom (onto the floor) or outside, according to the humidity requirements.

7. Conclusions

There is no single storage temperature that can be used for apples or pears. The choice of storage temperature is dependent on several factors. An exploration of the range of expert opinions on the optimum storage temperature for apples and pears in RA, CA, and DCA was provided in this study, based on the accumulated postharvest data from the last 20 years. Apple cultivars have been divided into two storage temperature groups (0 to 1 °C and >1 °C), based on chilling sensitivity. Increasingly, gradual cooling, rather than rapid cooling, is recommended, especially for chilling-sensitive cultivars. European pears are not chilling-sensitive and most of the cultivars can be stored between −1 and 0 °C. European pears also require a period of chilling, especially if harvested early, to stimulate ethylene production and ripening. There is limited information on the recommended storage temperature for Asian pear species. The current information suggests the storage temperature should be 0 to 0.5 °C in either RA or CA, with some cultivars needing gradual cooling to avoid chilling injury. The temperature recommendations for RA and CA storage differ in some cultivars. In such cases, the CA recommendation is, on average, approximately 0.9 °C higher for apple cultivars and approximately 0.5 °C higher for pear cultivars, compared with RA. Research evidence indicates that apples can be stored at higher temperatures in DCA than in CA, leading to possible energy savings and quality benefits. Applying 1-MCP

to some cultivars of apples and pears may also provide similar benefits. A cool growing season may increase the chilling sensitivity and increase certain disorders, depending on the cultivar and region. The store or packinghouse manager may choose to mitigate potential postharvest problems by maintaining the storage temperature at or above the temperature listed here and/or using stepwise (gradual) cooling. The storage temperature can affect the humidity and vapour pressure deficit (driving force) in the storage room. Altering the vapour pressure deficit controls the water loss in stored fruit, which can affect various quality parameters and the occurrence of several storage disorders.

Author Contributions: Conceptualization, R.K.P. and A.H.W.; methodology, R.K.P. and A.H.W.; validation, R.K.P. and A.H.W.; formal analysis, R.K.P. and A.H.W.; investigation, R.K.P. and A.H.W.; resources, R.K.P. and A.H.W.; data curation, R.K.P. and A.H.W.; writing—original draft preparation, R.K.P. and A.H.W.; writing—review and editing, R.K.P. and A.H.W.; visualization, R.K.P. and A.H.W.; supervision, R.K.P. and A.H.W.; project administration, R.K.P. and A.H.W.; funding acquisition, R.K.P. and A.H.W. All authors have read and agreed to the published version of the manuscript.

Funding: This research received no external funding.

Data Availability Statement: Not applicable.

Acknowledgments: The authors acknowledge the editorial assistance of Barbara Daniels-Lake.

Conflicts of Interest: The authors declare no conflict of interest.

References

1. Kidd, F.; West, C.; Kidd, M.N. *Gas Storage of Fruit*; Department of Science and Industrial Research: London, UK, 1927; p. 87.
2. Porritt, S.W. The effect of temperature on postharvest physiology and storage life of pears. *Can. J. Plant Sci.* **1964**, *44*, 568–579. [CrossRef]
3. DeLong, J.M.; Prange, R.K.; Harrison, P.A. The influence of pre-storage delayed cooling on quality and disorder incidence in 'Honeycrisp' apple fruit. *Postharvest Biol. Technol.* **2004**, *33*, 175–180. [CrossRef]
4. Wang, J.; Zhou, X.; Zhou, Q.; Cheng, S.; Wei, B.; Ji, S. Low temperature conditioning alleviates peel browning by modulating energy and lipid metabolisms of 'Nanguo' pears during shelf life after cold storage. *Postharvest Biol. Technol.* **2017**, *131*, 10–15. [CrossRef]
5. Li, D.; Cheng, Y.; Dong, Y.; Shang, Z.; Guan, J. Effects of low temperature conditioning on fruit quality and peel browning spot in 'Huangguan' pears during cold storage. *Postharvest Biol. Technol.* **2017**, *131*, 68–73. [CrossRef]
6. Toivonena, P.M.A. Factors affecting internal browning of new apple cultivars during storage. *Acta Hortic.* **2020**, *1275*, 1–6. [CrossRef]
7. Xu, F.; Zhang, K.; Liu, S. Evaluation of 1-methylcyclopropene (1-MCP) and low temperature conditioning (LTC) to control brown of Huangguan pears. *Sci. Hortic.* **2020**, *259*, 108738. [CrossRef]
8. Prange, R.K. *Controlled Atmosphere Storage of Apples and Pears*; Prange Publications: Wolfville, NS, Canada, 2022.
9. Knee, M.; Looney, N.E.; Hatfield, S.G.S.; Smith, S.M. Initiation of rapid ethylene synthesis by apple and pear fruits in relation to storage temperature. *J. Exp. Bot.* **1983**, *34*, 1207–1212. [CrossRef]
10. Richardson, D.G.; Gerasopoulos, D. Controlled atmosphere recommendations for pear fruits and storage chilling satisfaction requirements for ripening winter pears. *Acta Hortic.* **1994**, *367*, 452–454. [CrossRef]
11. Lelièvre, J.M.; Tichit, L.; Fillion, L.; Larrigaudière, C.; Vendrell, M.; Pech, J.C. Cold-induced accumulation of 1-aminocyclopropane 1-carboxylate oxidase protein in Granny Smith apples. *Postharvest Biol. Technol.* **1995**, *5*, 11–17. [CrossRef]
12. Lèlievre, J.M.; Latché, A.; Jones, B.; Bouzayen, M.; Pech, J.C. Ethylene and fruit ripening. *Physiol. Plant* **1997**, *101*, 727–739. [CrossRef]
13. Johnston, J.W.; Hewett, E.W.; Hertog, M.L.A.T.M.; Harker, F.R. Temperature and ethylene affect induction of rapid softening in 'Granny Smith' and 'Pacific Rose™' apple cultivars. *Postharvest Biol. Technol.* **2002**, *25*, 257–264. [CrossRef]
14. Lelièvre, J.M.; Tichit, L.; Dao, P.; Fillion, L.; Nam, Y.W.; Pech, J.C.; Latché, A. Effects of chilling on the expression of ethylene biosynthetic genes in Passe-Crassane pear (*Pyrus communis* L.) fruits. *Plant Mol. Biol.* **1997**, *33*, 847–855. [CrossRef]
15. Jobling, J.; Pradhan, R.; Morris, S.C.; Wade, N.L. Induction of chill-induced ripening in Fuji apples is a function of both temperature and time. *Aust. J. Exp. Agric.* **2003**, *43*, 1255–1259. [CrossRef]
16. Villalobos-Acuña, M.; Mitcham, E.J. Ripening of European pears: The chilling dilemma. *Postharvest Biol. Technol.* **2008**, *49*, 187–200. [CrossRef]
17. Sugar, D.; Basile, S.R. Low-temperature induction of ripening capacity in 'Comice' and 'Bosc' pears as influenced by fruit maturity. *Postharvest Biol. Technol.* **2009**, *51*, 278–280. [CrossRef]
18. Sugar, D.; Einhorn, T.C. Conditioning temperature and harvest maturity influence induction of ripening capacity in 'd'Anjou' pear fruit. *Postharvest Biol. Technol.* **2011**, *60*, 121–124. [CrossRef]

19. Sugar, D.; Basile, S.R. Induction of ripening capacity in 'Packham's Triumph' and 'Gebhard Red D'Anjou' pears by temperature and ethylene conditioning. *Postharvest Biol. Technol.* **2014**, *91*, 84–89. [CrossRef]
20. Sfakiotakis, E.M.; Dilley, D.R. Induction of Ethylene Production in 'Bosc' Pears by Postharvest Cold Stress1. *HortScience* **1974**, *9*, 336–338. [CrossRef]
21. Gerasopoulos, D.; Richardson, D.G. Storage temperature and fruit calcium alter the sequence of ripening events of 'd'Anjou' pears. *HortScience* **1999**, *34*, 316–318. [CrossRef]
22. Mitalo, O.W.; Tosa, Y.; Tokiwa, S.; Kondo, Y.; Azimi, A.; Hojo, Y.; Matsuura, T.; Mori, I.C.; Nakano, R.; Akagi, T.; et al. 'Passe Crassane' pear fruit (*Pyrus communis* L.) ripening: Revisiting the role of low temperature via integrated physiological and transcriptome analysis. *Postharvest Biol. Technol.* **2019**, *158*, 110949. [CrossRef]
23. Agar, I.T.; Biasi, W.V.; Mitcham, E.J. Temperature and Exposure Time during Ethylene Conditioning Affect Ripening of Bartlett Pears. *J. Agric. Food Chem.* **2000**, *48*, 165–170. [CrossRef] [PubMed]
24. Makkumrai, W.; Sivertsen, H.; Sugar, D.; Ebeler, S.E.; Negre-Zakharov, F.; Mitcham, E.J. Effect of Ethylene and Temperature Conditioning on Sensory Attributes and Chemical Composition of 'Comice' Pears. *J. Agric. Food Chem.* **2014**, *62*, 4988–5004. [CrossRef] [PubMed]
25. Makkumrai, W.; Anthon, G.E.; Sivertsen, H.; Ebeler, S.E.; Negre-Zakharov, F.; Barrett, D.M.; Mitcham, E.J. Effect of ethylene and temperature conditioning on sensory attributes and chemical composition of 'Bartlett' pears. *Postharvest Biol. Technol.* **2014**, *97*, 44–61. [CrossRef]
26. Maage, F.; Richardson, D.G. Winter pear chilling requirements for autocatalytic ethylene synthesis and ripening: Delaying effects of controlled atmosphere storage. *Acta Hortic.* **1998**, *475*, 625–632. [CrossRef]
27. Kupferman, E. Controlled Atmosphere Storage of Apples and Pears. In Proceedings of the VIII International Controlled Atmosphere Research Conference, Rotterdam, The Netherlands, 10 March 2003; Volume 600, pp. 729–735.
28. Fidler, J.C.; Wilkinson, B.G.; Edney, K.L. The Biology of Apple and Pear Storage. In *Research Review of the Commonwealth Bureaux of Horticulture and Plantation Crops*; Commonwealth Agricultural Bureaux Farnham Royal: Slough, England, 1973; Volume 3, p. xiii+235.
29. Davis, M.B.; Blair, D.S. Cold storage problems with Apples. *Sci. Agric.* **1936**, *17*, 105–114.
30. Prange, R.K.; Wright, A.H.; DeLong, J.M.; Zanella, A. History, current situation and future prospects for dynamic controlled atmosphere (DCA) storage of fruits and vegetables, using chlorophyll fluorescence. *Acta Hortic.* **2013**, *1012*, 905–916. [CrossRef]
31. Kittemann, D.; McCormick, R.; Neuwald, D.A. Effect of high temperature and 1-MCP application or dynamic controlled atmosphere on energy savings during apple storage. *Eur. J. Hortic. Sci.* **2015**, *80*, 33–38. [CrossRef]
32. Neuwald, D.A.; Spuhler, M.; Wunsche, J.; Kittemann, D. New apple storage technologies can reduce energy usage and improve storage life. In Proceedings of the Ecofruit 17th International Conference on Organic Fruit Growing, Hohenheim, Germany, 15–17 February 2016; pp. 184–187.
33. Köpcke, D. 1-methylcyclopropene (1-MCP) and dynamic controlled atmosphere (DCA) applications under elevated storage temperatures: Effects on fruit quality of 'Elstar', 'Jonagold' and 'Gloster' apple (*Malus domestica* Borkh.). *Eur. J. Hortic. Sci.* **2015**, *80*, 25–32. [CrossRef]
34. de Oliveira Anese, R.; Brackmann, A.; Wendt, L.M.; Thewes, F.R.; Schultz, E.E.; Ludwig, V.; Berghetti, M.R.P. Interaction of 1-methylcyclopropene, temperature and dynamic controlled atmosphere by respiratory quotient on 'Galaxy' apples storage. *Food Packag. Shelf Life* **2019**, *2020*, 100246. [CrossRef]
35. Weber, A.; Thewes, F.R.; Sellwig, M.; Brackmann, A.; Wünsche, J.N.; Kittemann, D.; Neuwald, D.A. Dynamic controlled atmosphere: Impact of elevated storage temperature on anaerobic metabolism and quality of 'Nicoter' apples. *Food Chem.* **2019**, *298*, 125017. [CrossRef]
36. Ludwig, V.; Thewes, F.R.; Wendt, L.M.; Berghetti, M.R.P.; Schultz, E.E.; Schmidt, S.F.P.; Brackmann, A. Extremely low-oxygen storage: Aerobic, anaerobic metabolism and overall quality of apples at two temperatures. *Bragantia* **2020**, *79*, 458–471. [CrossRef]
37. Watkins, C.B. Overview of 1-methylcyclopropene trials and uses for edible horticultural crops. *HortScience* **2008**, *43*, 86–94. [CrossRef]
38. Watkins, C.B. Current and future research and uses of 1-MCP in apples. In Proceedings of the 36th Annual Meeting of the Plant Growth Regulation Society of America, Asheville, NC, USA, 2–6 August 2009; pp. 14–26.
39. Mir, N.A.; Beaudry, R.M. Use of 1-MCP to reduce the requirement for refrigeration in the storage of apple fruit. *Acta Hortic.* **2001**, *553*, 577–580. [CrossRef]
40. Mattheis, J.P. How 1-methylcyclopropene has altered the Washington State apple industry. *HortScience* **2008**, *43*, 99–101. [CrossRef]
41. McCormick, R.; Neuwald, D.A.; Streif, J. Commercial apple CA storage temperature regimes with 1-MCP (SmartFresh™): Benefits and risks. *Acta Hortic.* **2012**, *934*, 263–270. [CrossRef]
42. McCormick, R.; Neuwald, D.A.; Streif, J. A case study: Potential energy savings using 1-MCP with 'Gala' apples in commercial CA storage. *Acta Hortic.* **2010**, *877*, 323–326. [CrossRef]
43. Saving Energy and Carbon Footprint with Smartfresh Quality English Gala. Available online: https://www.agrofresh.com/saving-energy-and-carbon-footprint-with-smartfresh-quality-english-gala/ (accessed on 11 December 2022).
44. Harz-Pitre, Y. Greater Energy Efficiency and Reduced Carbon Footprint for SmartFresh™ Fruits from South Africa—Quality Remains Consistent. Available online: https://www.agrofresh.com/greater-energy-efficiency-and-reduced-carbon-footprint-for-smartfreshsm-fruits-from-south-africa-quality-remains-consistent/ (accessed on 11 December 2022).

45. Zanella, A. *Postharvest Physiologist*; Laimburg Research Centre: Laimburg, Italy, 2020.
46. Anonymous. Bewaarcondities Appel en Peer. Available online: https://vcbt.be/bewaarcondities_appel_en_peer/ (accessed on 14 December 2022).
47. Vanoli, M.; Grassi, M.; Rizzolo, A. Ripening behavior and physiological disorders of 'Abate Fetel' pears treated at harvest with 1-MCP and stored at different temperatures and atmospheres. *Postharvest Biol. Technol.* **2016**, *111*, 274–285. [CrossRef]
48. Wright, A.H.; Delong, J.M.; Arul, J.; Prange, R.K. The trend toward lower oxygen levels during apple (Malus × domestica Borkh) storage—A review. *J. Hortic. Sci. Biotechnol.* **2015**, *90*, 1–13. [CrossRef]
49. Meheriuk, M.; Prange, R.K.; Lidster, P.D.; Porritt, S.W. *Postharvest Disorders of Apples and Pears*; Agriculture and Agri-Food Canada: Ottawa, ON, Canada, 1994.
50. Johnson, D.S.; Ridout, M.S. Prediction of storage quality of 'Cox's Orange Pippin' apples from nutritional and meteorological data using multiple regression models selected by cross validation. *J. Hortic. Sci. Biotechnol.* **1998**, *73*, 622–630. [CrossRef]
51. James, H.; Jobling, J. The Flesh Browning Disorder of 'Pink Lady' Apples. *N. Y. Fruit Q.* **2008**, *16*, 23–28.
52. Jobling, J.; James, H. *Managing the Flesh Browning Disorder of Cripps Pink Apples: A Summary of Australian Research Investigating the Causes and Management of the Problem*; Applied Horticultural Research: Sydney, Australia, 2008; p. 15.
53. Rogers, G. *Managing the Risk of Flesh Browning for 'Cripps Pink' Apples Using a Climate Model*; Horticulture Australia Ltd.: Sydney, Australia, 2014; p. 36.
54. de Wild, H. Water Loss of Horticultural Produce: Measurements in (CA) Storage Rooms. Available online: https://www.linkedin.com/pulse/water-loss-horticultural-produce-measurements-ca-storage-hans-de-wild/ (accessed on 10 March 2021).
55. de Wild, H. How to Control Water Loss of Horticultural Produce during Storage. Available online: https://www.linkedin.com/pulse/how-control-water-loss-horticultural-produce-during-storage-de-wild/ (accessed on 23 February 2021).

foods

MDPI

Article

Effects of Genotype and Modified Atmosphere Packaging on the Quality of Fresh-Cut Melons

Ranjeet Shinde [1,2,†], Yakov Vinokur [1], Elazar Fallik [1] and Victor Rodov [1,*]

[1] Department of Postharvest Science, Agricultural Research Organization (ARO), The Volcani Institute, Rishon LeZion 7505101, Israel; rshinde@uoguelph.ca (R.S.); yvinokur@agri.gov.il (Y.V.); efallik@agri.gov.il (E.F.)
[2] The Robert H. Smith Faculty of Agriculture, Food and Environment, The Hebrew University of Jerusalem, Rehovot 7610001, Israel
* Correspondence: vrodov@agri.gov.il
† Current address: Crop Diseases, Pests and Genetics Research, USDA-ARS, Parlier, CA 93648, USA.

Abstract: Marketing melons (*Cucumis melo*) as convenient fresh-cut products is popular nowadays. However, damage inflicted by fresh-cut processing results in fast quality degradation and food safety risks. The life of fresh-cut produce can be extended by a modified atmosphere (MA), either generated in a package by tissue respiration (a passive MA) or injected by gas flushing (an active MA). This work investigated the effect of passive and active MA formed in packages of different perforation levels on the quality of fresh-cut melons of two genetic groups: *C. melo var. cantalupensis*, characterized by climacteric fruit behavior, and non-climacteric *C. melo inodorus*. The best product preservation was achieved in passive MA packages: non-perforated for *inodorus* melons and micro-perforated for *cantalupensis* ones. The optimal packages allowed for the preservation of both genotypes for 14 days at 6–8 °C. The major factors limiting the shelf life of fresh-cut melons were microbial spoilage, translucency disorder and hypoxic fermentation associated with *cantalupensis* melons with enhanced ethyl acetate accumulation. *Inodorus* melons were found to be preferable for fresh-cut processing since they were less prone to fermented off-flavor development.

Keywords: *Cucumis melo*; cultivar groups; ready-to-eat; shelf life; MAP; package perforation; headspace; fermentation volatiles; ethyl acetate

Citation: Shinde, R.; Vinokur, Y.; Fallik, E.; Rodov, V. Effects of Genotype and Modified Atmosphere Packaging on the Quality of Fresh-Cut Melons. *Foods* **2024**, *13*, 256. https://doi.org/10.3390/foods13020256

Received: 2 December 2023
Revised: 8 January 2024
Accepted: 9 January 2024
Published: 13 January 2024

1. Introduction

Melons (*Cucumis melo* L.) are popular with consumers due to their high nutritional value, pleasant flavor and texture [1]. At the same time, melon is relatively inconvenient for consumption due to its large size and the presence of a considerable inedible part [2]. Therefore, marketing melons as convenient ready-to-eat sliced or cubed fresh-cut products is an attractive option for both consumers and retailers.

However, fresh-cut processing renders the fruit highly perishable, promoting physiological deterioration and providing a favorable environment for spoilage microorganisms and human pathogens [3]. In fresh-cut melons, cutting induces changes in texture, firmness and color that may result in a water-soaked appearance (translucency) of the tissues [4,5]. It affects respiration and ethylene production rates [6], as well as the profile of aroma volatiles [7,8]. Selecting the proper raw material in terms of genotype [9–11] and maturity [12] is important for ensuring the sufficient shelf life of fresh-cut melons. Product preparation should include efficient precut decontamination [11,13], aseptic processing with sharp tools [14,15], the storage of the final products under appropriate temperatures [16,17] and atmosphere composition [5,18].

A modified atmosphere (MA) with reduced oxygen and enhanced carbon dioxide levels can slow down produce deterioration via reduced respiration, inhibited ethylene biosynthesis and/or action and microbiostatic activity [19,20]. In traditional equilibrium (so-called

"passive") systems, the MA is generated due to produce respiration within semipermeable plastic modified atmosphere packaging (MAP). Such "passive" MA buildup may take a few days (a transient period) when the produce is exposed to non-optimal conditions and keeps deteriorating. In addition, a misbalance between high produce respiratory activity and insufficient package gas permeability may result in oxygen depletion and off-flavor development associated with the accumulation of fermentation volatiles, e.g., ethanol, acetaldehyde and ethyl acetate [21,22]. A micro-perforated MAP can prevent oxygen depletion by ensuring sufficient gas exchange, but it expands the transient period even more. On the other hand, in the case of "active" MAP systems, the package is flushed with an optimal gas mixture, diminishing the transient period. However, it does not eliminate and even aggravates the risk of hypoxia in the packages of highly respiring produce. The approach of micro-perforated active modified atmosphere (MAMA) packaging combines an active MA with the use of laser-micro-perforated plastic films in order to minimize the transient period and at the same time prevent hypoxia [23,24].

Cucumis melo is very diverse in fruit characteristics such as size, shape, color, texture, taste, composition and physiological behavior [25]. Based on fruit traits and uses, the species includes six cultivar groups, two of them being the most important commercially [2,26]. *C. melo var. cantalupensis* is characterized by medium–large-sized climacteric fruit with a netted, smooth or scaly rind of variable color. The fruits are aromatic, have sweet, juicy flesh and easily detach from the vine ("slip") at maturity. The group includes dessert melon types such as Galia, Ananas, Charentais, 'American shipper' cantaloupes (muskmelons), etc. In contrast, *C. melo var. inodorus* is characterized by large-sized melons with non-aromatic, non-climacteric and relatively long-stored fruit with a thick, smooth, warty or wrinkled rind. This group includes sweet dessert melons, such as Honeydew, Piel-de-Sapo and Casaba types. Each of these types is represented by numerous cultivars. For example, over sixty Galia-type cultivars are available in the market [27].

The major objective of the present study has been investigating the performance of different MA packaging types as a means to preserve the quality of fresh-cut melons of the *cantalupensis* and *inodorus* groups during a simulated shelf life.

2. Materials and Methods

2.1. Plant Material and Fruit Processing

Green-fleshed Galia-type melons (*C. melo var. cantalupensis*, cv. 'Raanan', HaZera Genetics, Israel) and pink-fleshed Piel-de-Sapo-type melons (*C. melo var. inodorus*, cv. 'Sorbeto', Catom Seeds, Israel) were harvested at commercial maturity from commercial plots in the northern Arava Valley, Israel. The melons were selected for uniformity and maturity based on ground color, appearance and firmness and brought to the ARO—The Volcani Institute—in an air-conditioned vehicle on the day of harvest. The fruits were pre-cooled and kept at 6 °C for about 2 days until the processing. The melons were aseptically processed at the pilot fresh-cut facility at the Department of Postharvest Science, ARO—The Volcani Institute, Israel. They were soaked in a sodium hypochlorite solution (100 ppm active chlorine) for 10 min, brushed within this solution for 2 min with a stiff plastic brush, rinsed with tap water and allowed to dry under the flow of sterile air. During processing, the fruits were cut with a sharp, cleaned knife to prepare melon flesh chunks of approximately 2.5 cm in size.

2.2. Packaging and Storage

Chunks from the same melon were randomly distributed between polyethylene terephthalate (CPET) trays of 171 × 127 × 50 mm dimensions (MCP Performance Plastics, Kibbutz Hama'apil, Israel), ca. 100 g per tray. The trays were sealed to obtain different package types. In the case of a passive MA, the trays were sealed without gas flushing and contained regular air as the initial atmosphere. In the case of an active MA, the trays, before sealing, were flushed with a gas mix of 5% O_2, 10% CO_2 and 85% N_2. Typically, the initial in-package atmosphere contained, in that case, 6 kPa of O_2 and 9 kPa of CO_2. The heat-sealing of both

the active and passive MA trays and the gas flushing of the active MA trays were carried out with an ILPRA Food Basic packaging machine (ILPRA, Vigevano, Italy). The trays were sealed with a 35 μm thick polyester-based medium-barrier laminate lidding film Topaz-335 (Plastopil, Kibbutz Hazorea, Israel) of the following perforation levels: (a) non-perforated, (b) with one laser micro-hole of ca. 70 μm per tray, or (c) with two micro-holes of the same size per tray. To obtain pinhole-perforated packages (d), one thin-needle (0.5 mm) hole was created manually in the active-MA trays sealed with a non-perforated lidding film. In (e) the control macro-perforated packages, MA generation was prevented by the manual perforation of two opposite walls of the sealed trays (air as the initial atmosphere) using a hot instrument, 2.5 mm in diameter, altogether creating two holes per tray. Typically, at least ten replicate packages were prepared per treatment, each from a different melon. All packages were stored under simulated cooled shelf-life conditions (temperature of 7 ± 1 °C, relative humidity of ca. 90%). The packages were sampled on day 0 and after one and two weeks of storage. With *inodorus* melons, the amount of material allowed an additional sampling point after 12 days of storage.

2.3. In-Package Atmosphere Composition Analysis

The atmosphere composition inside the packages was measured for O_2 and CO_2 by using an OXYBABY 6.0 gas analyzer (WITT-GASETECHNIK GmbH & Co. KG, Witten, Germany) comprising an infrared sensor for CO_2 measurements and an electrochemical sensor for O_2. The instrument's needle was inserted into the packages through adhesive rubber septa attached to the lidding film.

Headspace atmosphere samples of 8 mL were withdrawn from the packages via the above-mentioned septa using 10 mL gas-tight syringes with hypodermic 25 G needles (0.5 mm × 16 mm). The concentrations of acetaldehyde, ethanol and ethyl acetate were analyzed simultaneously with a Varian 3300 gas chromatograph (Varian, Inc., Palo Alto, CA, USA) equipped with a flame ionization detector and a 20% Carbowax 20 M packed column using helium as the carrier gas. The column, injector and detector temperatures were 80, 110 and 180 °C, respectively, as described by Poverenov et al. [28]. The concentration of ethylene was measured as described by Freiman et al. [29] by using a Varian 3300 GC instrument with a flame-ionization detector and a stainless steel column (length: 1.5 m; outside diameter: 3.17 mm; internal diameter: 2.16 mm) packed with HayeSep T, with a particle size of 0.125–0.149 mm (Alltech Associates, Inc., Deerfield, IL, USA). Helium was used as the carrier gas (5 mL/min).

2.4. Quality Assessment

The product quality was evaluated visually and organoleptically by three expert panelists (including one representing the industry) according to a scoring method as described by Van Oirschot and Tomlins [30]. For each quality parameter, the scores were assigned by a consensus decision of the panel according to the evaluation form received from the industry. The evaluated quality parameters included off-odor (severe to no), off-flavor (severe to no), piece shape (misshapen to clean-cut), translucency, i.e., water-soaked appearance (severe to no), decay, i.e., external signs of microbial spoilage (severe to no) and texture (mushy to crunchy). For all quality parameters, a uniform 5-grade scale was used, in which the scores of 1, 2.5 and 5 were, respectively, the worst, the marketability threshold and the best quality grade. The general quality decline was determined by the lowest score received by a sample in any category evaluated, i.e., a sample that obtained a score below 2.5 in any category was judged non-marketable. At least three typical packages were evaluated at each sampling point for each packaging type, and their scores were used as replications.

First, the panelists partially peeled off the plastic film and evaluated the off-odor intensity. Second, visual evaluations were conducted for piece shape, color, translucency and decay. In addition, the drip loss was measured with a pipette. At last, if samples were visually acceptable, the panelists performed off-flavor and texture evaluations. The

panelists used water between samples to cleanse their palates. The experimental samples were presented in random order.

The soluble solids content (SSC, %) of the juice was determined with a digital refractometer (Atago Co. Ltd., 3210 Huncho, Itabashi Ku, Tokyo, Japan). The analysis was performed in triplicate using, as replication, a juice sample obtained by squeezing three pooled melon chunks in a cloth pouch. The flesh firmness (N) was measured with a penetrometer (Chatillon Digital Force Guage, New York, NY, USA) equipped with a 6 mm conical probe on three cubes from each replication tray, for a total of nine measurements per sampling point. The probe was inserted into the side surfaces of the melon chunk to omit the effect of the natural firmness gradient within the melon when the skin-facing side is firmer than the seed-cavity-facing one.

2.5. Statistical Analysis

The experiments were performed in triplicate and repeated at least twice for each melon cultivar. The results of a typical trial are presented in this paper. Microsoft Office Excel spreadsheets were used to calculate the means, standard deviations and 95% t-based confidence intervals. The statistical analyses used JMP Version 5.0.1 software (SAS Institute, 2003, Cary, NC, USA). The significant differences among the sample means were evaluated by a one-way analysis of variance (ANOVA) and, where appropriate, the means were differentiated post hoc by the Tukey honestly significant difference (HSD) test.

3. Results

3.1. Headspace Atmosphere Composition

3.1.1. Oxygen

Similar oxygen dynamics were observed in the packages of the two melon genotypes. Package perforation was the major factor determining the oxygen level. In the non-perforated packages, complete oxygen depletion was reached in the active MA packages after one week of storage, and in the passive MA packages, after two weeks, i.e., at the end of the trial (Figure 1A,B). In the micro-perforated passive and active MA packages, the O_2 steady-state concentrations varied between 15 and 18 kPa, depending on the perforation level. There was no change in the oxygen concentration of the macro-perforated control packages.

3.1.2. Carbon Dioxide

The CO_2 accumulation in the non-perforated active MA packages steadily increased and exceeded 21 kPa, indicating hypoxic fermentation [20]. Although the CO_2 dynamics were generally similar in the packages of the two genotypes, the final CO_2 level in these packages was slightly higher for the *cantalupensis* melons than for the *inodorus* ones, 25 vs. 22 kPa, respectively. On the other hand, in the non-perforated passive MA packages of both genotypes, the CO_2 level stabilized at 17 kPa (Figure 1C,D). The steady-state CO_2 ranges were 2.5–3, 5–6 and 7–8 kPa for pinhole, two-micro-hole and one-micro-hole perforated packages, respectively, both in the passive and active MAs (Figure 1C,D). Practically no CO_2 accumulation was observed in the macro-perforated packages.

3.1.3. Ethylene

In contrast to oxygen and carbon dioxide, the headspace ethylene concentrations differed markedly between the two genotypes, being approximately one order of magnitude higher in the packages of the climacteric *cantalupensis* melons than in those of the non-climacteric *inodorus* ones. Interestingly, the ethylene level was strongly affected by the MA type. The most drastic contrast was observed in the non-perforated packages, where the highest ethylene accumulation was observed in the non-perforated passive MA packages (0.5 and 5 ppm for the *inodorus* and *cantalupensis* genotypes, respectively), while the non-perforated active MA packages contained negligible ethylene levels (Figure 1E,F). Irrespective of perforation, the accumulation of ethylene in all the active MA packages did

not exceed 0.1 ppm for the *inodorus* melons and 1 ppm for the *cantalupensis* ones. In the passive MA packages with one micro-hole, ethylene actively accumulated during the first week of storage but subsequently declined (Figure 1E,F). Apparently, the headspace ethylene level was affected by the interplay between the tissue biosynthetic activity suppressed by CO_2 and ethylene diffusion from the packages to the outside atmosphere, depending on the film perforation.

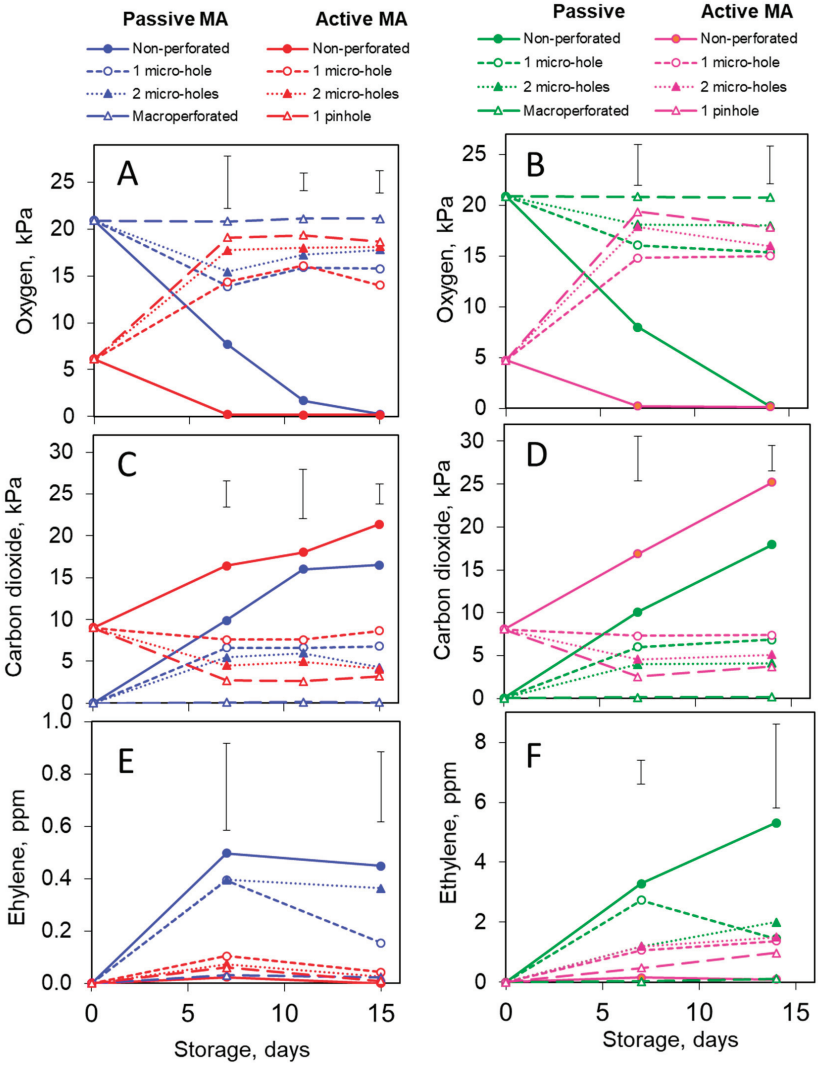

Figure 1. Effects of passive and active MA packaging on oxygen (**A**,**B**), carbon dioxide (**C**,**D**) and ethylene (**E**,**F**) levels in the headspace of packages containing 100 g of fresh-cut *inodorus* (**A**,**C**,**E**) or *cantalupensis* (**B**,**D**,**F**) melons during storage at 6–8 °C. Individual data points are the means of three replications. Vertical bars represent honest significant differences (HSDs) ($p \leq 0.05$) for each sampling period determined by the Tukey HSD test.

3.1.4. Fermentation Volatiles

In the samples of *inodorus* melon, during the first week of storage, there was no significant difference in the content of fermentative volatiles, especially in the passive MA

packages, where similar results were observed in the non-perforated and macro-perforated packages (Figure 2A). At the same time, in the active MA packages, the least perforated packages (zero or one micro-hole) showed a trend toward somewhat higher ethanol levels. During the second week, the patterns of fermentation volatiles in the *inodorus* packages stabilized, showing significantly a higher accumulation of fermentation volatiles in the non-perforated packages than in all the perforated ones. Interestingly, ethanol was the most prevalent volatile in the non-perforated active MA packages, while acetaldehyde prevailed in the non-perforated passive MA packages. At the same time, in the perforated packages, the accumulation of fermentation volatiles in the active MA was somewhat higher than in the passive MA, mainly due to the enhanced acetaldehyde levels (Figure 2A). Ethyl acetate was observed in small amounts in the *inodorus* passive MA packages but was practically absent in the active MA packages.

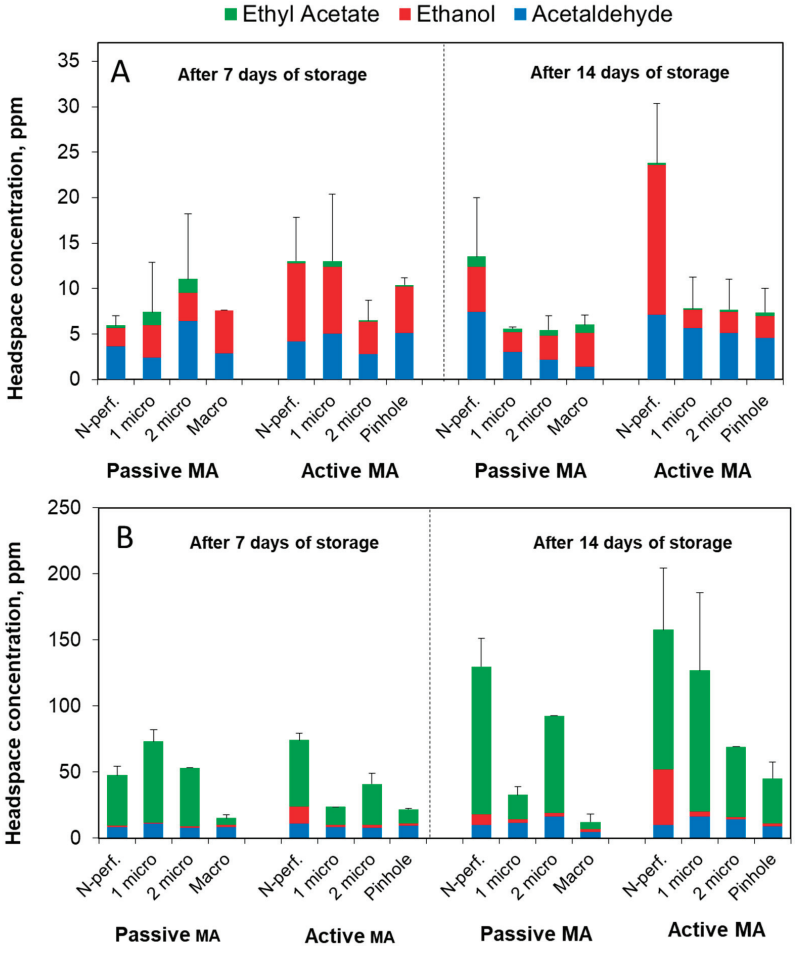

Figure 2. Effects of passive and active MA packaging on the content of fermentation volatiles (ppm) in the headspace of packages containing 100 g of fresh-cut *inodorus* (**A**) and *cantalupensis* (**B**) melons after one and two weeks of storage at 6–8 °C. Package perforation levels: non-perforated (N-perf.), a single 70 μm micro-hole (1 micro), two 70 μm micro-holes (2 micro), a single 0.5 mm hole (Pinhole), two 2.5 mm holes (Macro). Individual data points are the means of three replications. Vertical bars represent 95% t-based confidence intervals in the total content of fermentation volatiles.

The amount of fermentation volatiles in the headspace of the MA-packaged *cantalupensis* melons was typically 5–10 times greater than that of the *inodorus* ones. This difference was primarily due to the accumulation of ethyl acetate that prevailed in the headspace of all the MA-packaged *cantalupensis* melon samples but was just a minor ingredient in *inodorus* volatiles (Figure 2A,B). On the other hand, in the absence of MA, the macro-perforated packages of both genotypes showed relatively little ethyl acetate and similar total-level fermentation volatiles (ca. 5–10 ppm). The largest concentrations of fermentation volatiles were produced by the *cantalupensis* fresh-cut melons in the non-perforated active MA packages, ca. 80 and 150 ppm after 7 and 14 days of storage, respectively. In addition to ethyl acetate, these packages accumulated enhanced amounts of ethanol (Figure 2B). Interestingly, the *cantalupensis* passive MA packages with two micro-holes contained, after 14 days of storage, much more ethyl acetate vapor than those with one micro-hole.

3.2. Quality: Inodorus Melons

No decay was observed in the fresh-cut *inodorus* melons during the first 7 days of storage. Later on, the macro-perforated packages showed the most obvious decay development (Figure 3A), accompanied by a certain piece shape loss (Figure 3B). On the other hand, the non-perforated passive and active MA packages had no decay throughout the whole storage period. In all the perforated packages, the severity of decay was aggravated after 12 days of storage, except for the active MA package with 1 micro-hole, where the decay was minimal (Figure 3A).

The passive MA packages (non-perforated or single-micro-hole-perforated) showed the best odor (Figure 3C) and taste (Figure 3D) stability of the fresh-cut *inodorus* melons. Certain fermented off-odor and off-flavor (Figure 3C,D) notes were sensible in the non-perforated active MA packages and, during the last days of storage, in the active MA packaged with a single micro-hole. At the same time, a moldy off-odor was detected in the macro-perforated and pinhole-perforated packages. However, it should be noted that the off-odor and off-flavor scores in the tested *inodorus* melon samples never reached prohibitively strong scores and never declined below the marketability threshold of 2.5. The samples with visible decay were not tasted, so there were not enough replications for a statistical analysis of the off-flavor severity at a 15-day time point (Figure 3D).

Figure 3E clearly demonstrates that the active MA enhanced the translucency. This effect was especially evident in the non-perforated packages, although the difference in translucency between the various active MA treatments was not statistically significant. In addition, at the end of storage, an enhancement in translucency (water-soaked appearance) was observed in the macro-perforated packages as one of the decay manifestations. Practically no translucency was detected in the non-perforated passive MA packages (Figure 3E). The firmness and SSC levels in the fresh-cut *inodorus* melons were within 7–9 N and 9–11% ranges, respectively. No significant changes were detected during the storage of healthy melon pieces (Supplementary Material, Tables S1 and S2). However, the decay obviously resulted in tissue maceration and softening.

An integral characteristic of a product's quality decline during storage is presented in Figure 3F. The fastest and most severe deterioration was observed in the macro-perforated packages containing no MA, primarily due to the decay development. The best quality preservation was ensured by the non-perforated passive MA. While the non-perforated active MA also showed good decay control, its positive effect was jeopardized by translucency aggravation.

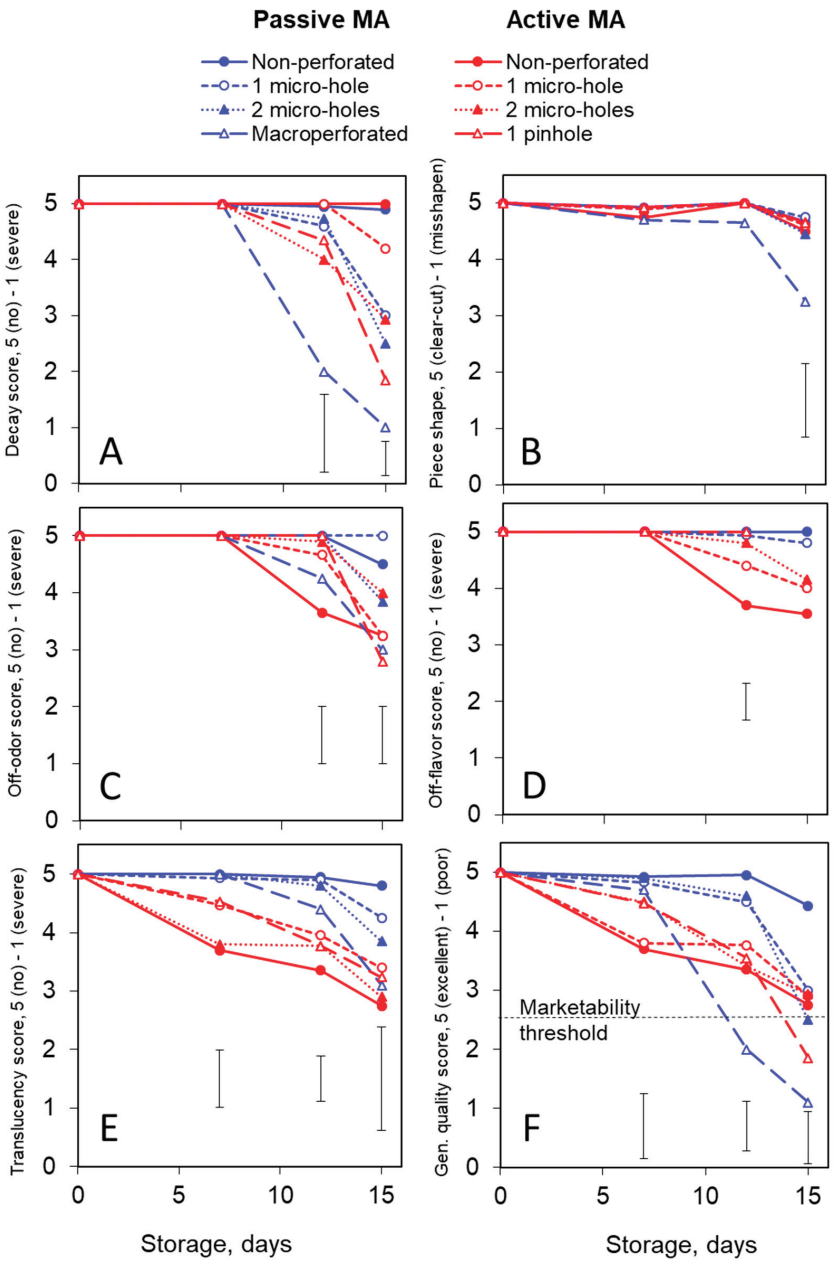

Figure 3. Effects of passive and active MA packaging on the quality scores of 100 g portions of fresh-cut *inodorus* melons stored for up to 15 days at 6–8 °C. Quality parameters: decay (**A**), piece shape (**B**), off-odor (**C**), off-flavor (**D**), translucency (**E**) and general quality/marketability (**F**). All quality parameters were evaluated according to a 5-grade visual scale, where a score of 5 corresponded to the highest quality, and a score of 1 to the lowest one. Individual data points are the means of three replications. Vertical bars represent honest significant differences (HSDs) ($p \leq 0.05$) for each sampling period determined by the Tukey HSD test.

3.3. Quality: Cantalupensis Melons

The trends in the microbial decay of the fresh-cut *cantalupensis* melons were similar to those observed with the *inodorus* type. The greatest microbial spoilage was evident in the macro-perforated packages containing no MA (Figure 4). During the second week of storage, mold-caused decay developed in the packages less protected by MA, i.e., the packages that were macro-perforated, pinhole-perforated and micro-perforated with two holes (Figure 5A). At similar perforation levels, the active MA packages showed lower decay severity than the passive MA ones. This decay was associated with a slight piece deformation (Figure 5B). On the other hand, the non-perforated or single-hole micro-perforated packages had no or negligible decay (Figure 5A).

Figure 4. Effects of package perforation level on the appearance of 100 g portions of fresh-cut *cantalupensis* melons stored for 14 days at 6–8 °C. Perforation levels: a single micro-hole (ca. 70 μm) per package (**A**); two micro-holes (ca. 70 μm) per package (**B**); two macro-holes (2.5 mm) per package (**C**); and non-perforated package (**D**).

In contrast to the *inodorus* samples, the fresh-cut *cantalupensis* melons had a distinct smell, combining the typical melon aroma with that or another degree of off-odor. A moldy off-odor was sensible during the second week of storage in the headspace of the macro-perforated packages, characterized by severe decay (Figure 4). Noticeable fermented off-odor and off-flavor appeared in the non-perforated active MA packages and, to a lesser extent, in the non-perforated passive MA and active MA packages with a single micro-hole (Figure 5C,D). Off-flavor was also registered in the active MA packages with two micro-holes (Figure 5D). Similar to the *inodorus* melons, the samples showing visible decay during the second week of storage (see Figure 5A) were not tasted at the 14-day time point. Therefore, the only treatment that showed acceptable edible quality throughout the storage period was passive MA with a single micro-hole (Figure 5D).

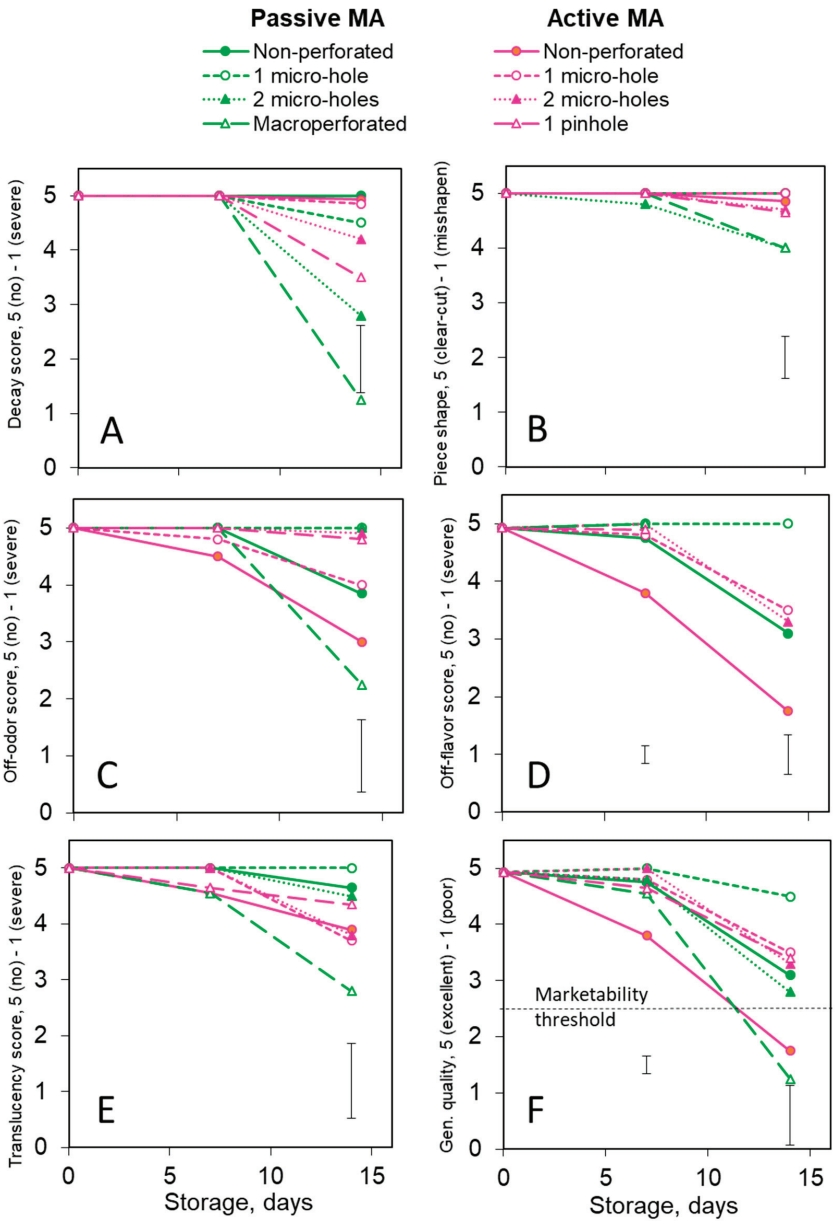

Figure 5. Effects of passive and active MA packaging on the quality scores of 100 g portions of fresh-cut *cantalupensis* melons stored for up to 14 days at 6–8 °C. Quality parameters: decay (**A**), piece shape (**B**), off-odor (**C**), off-flavor (**D**), translucency (**E**) and general quality/marketability (**F**). All quality parameters were evaluated according to a 5-grade visual scale, where a score of 5 corresponded to the highest quality, and a score of 1 to the lowest one. Individual data points are the means of three replications. Vertical bars represent honest significant differences (HSDs) ($p \leq 0.05$) for each sampling period determined by the Tukey HSD test.

The translucency in the *cantalupensis* melons was less evident than in the *inodorus* ones, except for the macro-perforated packages, where water soaking was one of the signs of decay development. At similar perforation levels, the active MA packages had somewhat higher translucency scores than the passive MA ones, although the difference was usually statistically insignificant (Figure 5E). The firmness and SSC levels of the *cantalupensis* melons were within the ranges of 6–8 N and 9–10%, respectively. These values did not change significantly during storage, provided the fresh-cut pieces remained free from microbial decay (Supplementary Material, Tables S1 and S2).

Figure 5F summarizes all the deterioration phenomena in the fresh-cut *cantalupensis* melons as an integral general quality parameter. The most severe quality degradation took place in the macro-perforated packages due to the decay development and in the non-perforated active MA packages due to the prohibitive off-flavor and off-odor. On the other hand, the passive MA packages with a single micro-hole allowed for the best quality preservation of the fresh-cut *cantalupensis* melons during the 14-day storage period (Figure 5F). In a separate trial, we found that such packaging could extend the shelf life of fresh-cut *cantalupensis* melons up to 21 days.

4. Discussion

Modified atmosphere packaging (MAP) is defined as 'the packaging of a perishable product in an atmosphere which has been modified so that its composition is other than that of air' [31,32], and the resulting environment minimizes the physiological and microbial deterioration of the foods [33]. With respiring foods such as fresh produce, atmosphere modification is based on restricting gas exchange between the package interior and the environment [34]. The MA composition is determined by the balance between food's respiration and gas diffusion through a package [33]. However, different commodities require diverse atmospheric compositions for their best preservation, and the barrier properties of available plastic films are not always suitable for reaching these conditions [35]. In particular, packaging highly respiring fresh-cut fruits and vegetables in existing plastic films may lead to undesirable hypoxic fermentation, and therefore perforation is required to avoid this condition. At the same time, excessive perforation may preclude MA formation, making the in-package atmosphere identical to the surrounding air [36]. Using micro-porous or micro-perforated packaging materials helps modulate the package barrier properties in order to create a desirable atmosphere [34,37,38]. To reach this purpose, the perforation size should not exceed 100–500 μm, and the perforation level should be optimized, preferably based on mathematical modeling [36]. Perforation-mediated MAP serves, nowadays, as the basis for modern industrially applied technologies for the preservation of fresh produce [39,40].

A modified atmosphere in a package can be created either solely by the respiratory activity of the product (so-called "passive MAP") or actively ("active MAP") by displacing air with a desired gas mixture and/or by using additives that absorb or release gases or volatile compounds [33,41]. In both the "passive" and "active" MAP versions, the equilibrium steady-state concentrations are determined by the balance between the respiration rate of the product and the diffusion characteristics of the packaging material. However, flushing a package with a gas mix can shorten the time needed to attain a desirable MA that may be critical for the preservation of products highly sensitive to oxygen or with a low respiration rate [33]. Nowadays, active MAP is a postharvest technology commonly applied to maintain the quality and extend the shelf life of fresh produce [41]. At first glance, the idea of combining the active MAP technique with micro-perforated packaging (micro-perforated active modified atmosphere, or MAMA packaging) seems paradoxical because it allows for a partial escape of the injected gas mix through perforations. However, it in face allows the MAP to be stabilized without a risk of hypoxia [24]. The positive effects of micro-perforated active MAP on produce preservation have been demonstrated with fresh-cut strawberries [23], cabbage [42], litchi [43] and rocket leaves [44].

The results of this work have confirmed the efficacy of MAs for the preservation of fresh-cut *cantalupensis* and *inodorus* melons [5,45]. The optimal MA solutions adjusted in our trials for each one of the two genotypes tested allowed their quality to be maintained for up to 14 days. Microbial decay and physiological disorders (fermentation and translucency development) were the major factors limiting the shelf life of the produce [5,9]. The major MA advantage was related to the control of microbial spoilage, primarily due to the fungistatic effect of the elevated CO_2 levels [19,20].

At the same time, using a low-oxygen MA was associated with the risk of hypoxic fermentation due to eventually passing the anaerobic compensation point (ACP), resulting in flavor deterioration [21,22]. The two genotypes differed markedly in the amount and composition of volatiles generated under low-oxygen conditions. Ethyl acetate prevailed in the fermentation volatiles produced by the fresh-cut *cantalupensis* melons exposed to hypoxia. Ethyl acetate is a characteristic melon fermentation marker associated with an unpleasant solvent-like off-flavor [22,46]. The *inodorus* melons produced very little ethyl acetate, while their ethanol and acetaldehyde levels were comparable (typically, 1.5–2 times lower) with those of the *cantalupensis* packages. The difference in ethyl acetate production was most probably related to the genetically determined low expression of genes responsible for alcohol acetyl transferase (AAT) enzymes in the non-climacteric *inodorus* melon types [47,48]. Due to this difference, the total accumulation of fermentation volatiles in the headspace of the oxygen-deficient MA packages of the *inodorus* melons was 5–10 times lower than in the *cantalupensis* melons. Therefore, the fresh-cut *inodorus* melons could benefit from the decay control provided by non-perforated MA with a low risk of prohibitive off-flavor. Altogether, *inodorus* melon varieties may be preferable for fresh-cut processing since they are less prone to fermented off-flavor development.

The effects of micro-perforated packaging on the storage of fresh-cut melons are poorly presented in the literature. Aguayo et al. [49] showed no advantage of micro-perforated polypropylene passive MA packages for the preservation of fresh-cut *inodorus*-type 'Amarillo' melons compared with non-perforated ones, as was also found for *inodorus* melons in our study. On the other hand, with the MA-packaged *cantalupensis* melons, micro-perforation was essential for keeping their sensory quality at an acceptable level under the given storage conditions. Moreover, choosing an appropriate perforation level was critical for the realization of the MA potential, as illustrated by the significant difference in decay severity between the packages bearing one vs. two micro-holes. A minimal micro-perforation level (a single 70 μm hole per 100 g package) was helpful for the efficient preservation of the *cantalupensis* melons in the passive MA packages, simultaneously controlling decay and off-flavor generation.

In this study, we compared passive and active MAs as a means of preserving fresh-cut melons of two genetic types: *inodorus* and *cantalupensis*. Furthermore, the performance of the novel approach of MAMA packaging combining active MA with micro-perforation [24] was tested with fresh-cut melons. The difference in the atmosphere composition between the active and passive MA packages was evident during the first week of storage, while during the second week, the packages of the same perforation level reached similar steady-state concentrations of oxygen and carbon dioxide, irrespective of their initial atmospheric compositions. This observation was in line with the model prediction that the steady-state O_2 and CO_2 levels in MA packages depend on the product's respiration rate and the packaging material's permeability, but not on the initial atmosphere [23,24]. On the other hand, the initial atmosphere determined the conditions during the transient period and its duration. Thus, the non-perforated active MA packages reached hypoxia after one week of storage, while in the non-perforated passive MA packages, it took twice as long and happened just at the end of storage. Understandably, the non-perforated active MA resulted in stronger fermentation and flavor deterioration than the passive one, although the differences were not always statistically significant.

The combination of active MA with micro-perforation (MAMA packaging) was supposed to prevent the risk of hypoxia and, at the same time, stabilize the MA composition

within a desirable range, ensuring efficient spoilage control. Indeed, the active MA packages with a single micro-hole allowed for the maintenance of a steady 8–9 kPa CO_2 level throughout the storage period, which is close to the recommendations [50] and sufficient to control the microbial decay of the product for two weeks. In addition, the active MA packaging, either perforated or not, inhibited ethylene production by both melon genotypes, most probably due to the effects of CO_2 [51] and/or ethanol vapor [52] on ethylene biosynthesis. This ethylene inhibition might have a positive effect on product preservation because fresh-cut melon deterioration is associated with ethylene effects [53,54].

At the same time, in contrast to reports by Bai et al. [9,18], the active MA in our trials tended to aggravate translucency development in both genotypes, especially in the *inodorus* melons. This trend toward higher translucency was observed in all the active MA packages, including the pinhole-perforated ones that had a very moderate degree of atmosphere modification (2–3 kPa CO_2 and 18–19 kPa O_2). We suggest, therefore, that the translucency in this case might be enhanced not by a certain atmosphere composition but by the gas flushing procedure per se, which included vacuum application. Pressure fluctuations may cause translucency in fruit tissues [55]. Water soaking and translucency in fresh-cut melons and watermelons are associated with tissue disruption and cell wall degradation [56,57]. *Inodorus* Sorbeto cv. flesh might be especially susceptible to this disorder due to its crispy texture and high turgidity. If our suggestion is true, the translucency development in active MA packaging might be alleviated by packaging machinery performing gas flushing without vacuum application.

The MAMA packages with a single micro-hole ensured that the headspace oxygen level remained well above the ACP, about 15 kPa. Nevertheless, the *cantalupensis* melons kept in these packages demonstrated an enhanced accumulation of fermentation volatiles, in particular ethyl acetate, and noticeable off-flavor. This phenomenon might be a result of local hypoxia caused by tissue water-soaking, as shown for fruit watercore disorder [58,59], possibly in combination with an elevated headspace carbon dioxide level. Altogether, the performance of the active MA and, in particular, the MAMA packaging observed in this study did not justify their advantage over the passive MA for the preservation of fresh-cut melons, in contrast to the results obtained previously with topped strawberries [23]. Furthermore, the most successful packaging solutions revealed by this study were a non-perforated passive MA for the *inodorus*-type melon and a single-micro-hole passive MA for the *cantalupensis*-type melon. Additional advantages of these packaging solutions for the industry are their technical simplicity and relative cost efficiency. Naturally, the choice of packaging solutions should reflect the respiratory activity of the object affected by its physiological peculiarities and storage environment, in particular observing the cold chain conditions.

5. Conclusions

The study has confirmed the efficacy of MA packaging for the preservation of fresh-cut melons, primarily due to the control of microbial spoilage.

Fermented off-flavor associated with ethyl acetate accumulation was the major risk of using a low-oxygen MA with fresh-cut *cantalupensis* melons.

Inodorus melons were found to be preferable for fresh-cut processing since they were less prone to fermented off-flavor development.

The active MA tended to aggravate translucency development, especially in the *inodorus* melons, presumably due to the effect of the vacuum-driven gas flushing procedure on the flesh tissue integrity.

No advantages justifying the application of active MA packaging to fresh-cut melons as compared to a passive MA were observed in this study.

The non-perforated passive MA packaging was suitable for the preservation of the fresh-cut *inodorus* melons, while a minimal micro-perforation level was needed for the *cantalupensis* melons in order to preserve their sensory quality.

The optimal packaging methods allowed for the good quality preservation of both genotypes for 14 days of shelf life at 6–8 °C.

Supplementary Materials: The following supporting information can be downloaded at https://www.mdpi.com/article/10.3390/foods13020256/s1: Table S1. Effect of genotype, packaging conditions and storage duration on the soluble solids content (SSC, %) in fresh-cut melons. Table S2. Effect of genotype, packaging conditions and storage duration on the firmness (N) of fresh-cut melons.

Author Contributions: Conceptualization, V.R. and E.F.; methodology, Y.V. and V.R.; validation, Y.V. and R.S.; formal analysis, R.S.; investigation, R.S. and Y.V.; resources, V.R. and E.F.; writing—original draft preparation, R.S.; writing—review and editing, V.R.; visualization, R.S. and V.R.; supervision, E.F. and V.R.; project administration, V.R.; funding acquisition, V.R. All authors have read and agreed to the published version of the manuscript.

Funding: This research received funding from the European Union Seventh Framework Programme under grant agreement no. 289719 (Project QUAFETY).

Institutional Review Board Statement: Not applicable.

Informed Consent Statement: Not applicable.

Data Availability Statement: Data is contained within the article or supplementary material.

Acknowledgments: The authors are grateful to Reuben Vaida (Einat Food Industries, Kibbutz Einat, Israel) for his participation in the product quality examination and to Benny Avni (Catom Seeds, Ein Tamar, Israel) for the provision of Sorbeto melons (*inodorus* type) for the experiments.

Conflicts of Interest: The authors declare no conflicts of interest.

References

1. Torres, A.; Langenhoven, P.; Behe, B.K. Characterizing the US melon market. *HortScience* **2020**, *55*, 795–803. [CrossRef]
2. Amaro, A.L.; Beaulieu, J.C.; Grimm, C.C.; Stein, R.E.; Almeida, D.P. Effect of oxygen on aroma volatiles and quality of fresh-cut cantaloupe and honeydew melons. *Food Chem.* **2012**, *130*, 49–57. [CrossRef]
3. Iturralde-García, R.D.; Cinco-Moroyoqui, F.J.; Martínez-Cruz, O.; Ruiz-Cruz, S.; Wong-Corral, F.J.; Borboa-Flores, J.; Cornejo-Ramírez, Y.I.; Bernal-Mercado, A.T.; Del-Toro-Sánchez, C.L. Emerging technologies for prolonging fresh-cut fruits' quality and safety during storage. *Horticulturae* **2022**, *8*, 731. [CrossRef]
4. Portela, S.I.; Cantwell, M.I. Quality changes of minimally processed honeydew melons stored in air or controlled atmosphere. *Postharvest Biol. Technol.* **1998**, *14*, 351–357. [CrossRef]
5. Rodov, V.; Shinde, R. Fresh-cut fruits: Melons. In *Controlled and Modified Atmospheres for Fresh and Fresh-Cut Produce*; Academic Press: Cambridge, MA, USA, 2020; pp. 501–509.
6. Aguayo, E.; Escalona, V.; Artés, F. Quality of minimally processed *Cucumis melo* var. *saccharinus* as improved by controlled atmosphere. *Eur. J. Hortic. Sci.* **2007**, *72*, 39–45.
7. Beaulieu, J.C. Effect of cutting and storage on acetate and nonacetate esters in convenient, ready-to-eat fresh-cut melons and apples. *HortScience* **2006**, *41*, 65–73. [CrossRef]
8. Beaulieu, J.C. Volatile changes in cantaloupe during growth, maturation, and in stored fresh-cuts prepared from fruit harvested at various maturities. *J. Am. Soc. Hortic. Sci.* **2006**, *131*, 127–139. [CrossRef]
9. Bai, J.H.; Saftner, R.A.; Watada, A.E. Characteristics of fresh-cut honeydew (*Cucumis melo* L.) available to processors in winter and summer and its quality maintenance by modified atmosphere packaging. *Postharvest Biol. Technol.* **2003**, *28*, 349–359. [CrossRef]
10. Saftner, R.A.; Lester, G.E. Sensory and analytical characteristics of a novel hybrid muskmelon fruit intended for the fresh-cut industry. *Postharvest Biol. Technol.* **2009**, *51*, 327–333. [CrossRef]
11. Silveira, A.C.; Aguayo, E.; Artés, F. The suitability of three Galia melon cultivars and different types of cuts for the fresh-cut industry. *J. Sci. Food Agric.* **2013**, *93*, 3826–3831. [CrossRef]
12. Oms-Oliu, G.; Soliva-Fortuny, R.; Martín-Belloso, O. Effect of ripeness on the shelf-life of fresh-cut melon preserved by modified atmosphere packaging. *Eur. Food Res. Technol.* **2007**, *225*, 301–311. [CrossRef]
13. Sapers, G.; Miller, R.; Pilizota, V.; Mattrazzo, A. Antimicrobial treatments for minimally processed cantaloupe melon. *J. Food Sci.* **2001**, *66*, 345–349. [CrossRef]
14. Portela, S.I.; Cantwell, M.I. Cutting blade sharpness affects appearance and other quality attributes of fresh-cut cantaloupe melon. *J. Food Sci.* **2001**, *66*, 1265–1270. [CrossRef]
15. Silveira, A.C.; Conesa, A.; Aguayo, E.; Artes, F. Alternative sanitizers to chlorine for use on fresh-cut "Galia"(*Cucumis melo* var. *cantalupensis*) melon. *J. Food Sci.* **2008**, *73*, M405–M411. [CrossRef] [PubMed]

16. Bett-Garber, K.L.; Lamikanra, O.; Lester, G.E.; Ingram, D.A.; Watson, M.A. Influence of soil type and storage conditions on sensory qualities of fresh-cut cantaloupe (*Cucumis melo*). *J. Sci. Food Agric.* **2005**, *85*, 825–830. [CrossRef]
17. Amaro, A.L.; Spadafora, N.D.; Pereira, M.J.; Dhorajiwala, R.; Herbert, R.J.; Müller, C.T.; Rogers, H.J.; Pintado, M. Multitrait analysis of fresh-cut cantaloupe melon enables discrimination between storage times and temperatures and identifies potential markers for quality assessments. *Food Chem.* **2018**, *241*, 222–231. [CrossRef] [PubMed]
18. Bai, J.H.; Saftner, R.A.; Watada, A.E.; Lee, Y. Modified atmosphere maintains quality of fresh-cut cantaloupe (*Cucumis melo* L.). *J. Food Sci.* **2001**, *66*, 1207–1211. [CrossRef]
19. Wilson, M.D.; Stanley, R.A.; Eyles, A.; Ross, T. Innovative processes and technologies for modified atmosphere packaging of fresh and fresh-cut fruits and vegetables. *Crit. Rev. Food Sci. Nutr.* **2019**, *59*, 411–422. [CrossRef]
20. Saltveit, M.E. Biological basis for CA and MA. In *Controlled and Modified Atmospheres for Fresh and Fresh-Cut Produce*; Academic Press: Cambridge, MA, USA, 2020; pp. 3–22.
21. Oms-Oliu, G.; Raybaudi-Massilia Martínez, R.; Soliva-Fortuny, R.; Martín-Belloso, O. Effect of superatmospheric and low oxygen modified atmospheres on shelf-life extension of fresh-cut melon. *Food Control* **2008**, *19*, 191–199. [CrossRef]
22. Amodio, M.L.; Pati, S.; Derossi, A.; Mastrandrea, L.; Colelli, G. Reaction mechanisms for volatiles responsible of off-odors of fresh cut melons. *Acta Hortic.* **2021**, *1311*, 15–22. [CrossRef]
23. Rodov, V.; Horev, B.; Goldman, G.; Vinokur, Y.; Fishman, S. Model-driven development of microperforated active modified-atmosphere packaging for fresh-cut produce. In Proceedings of the International Conference on Quality Management of Fresh Cut Produce, Bangkok, Thailand, 6–8 August 2007; Volume 746, pp. 83–88.
24. Shinde, R.; Rodov, V.; Krishnakumar, S.; Subramanian, J. Active and intelligent packaging for reducing postharvest losses of fruits and vegetables. In *Postharvest Biology and Nanotechnology*; Paliyath, G., Subramanian, J., Lim, L.T., Subramanian, K.S., Handa, A.K., Mattoo, A.K., Eds.; John Wiley and Sons, Inc.: Hoboken, NJ, USA, 2019; pp. 171–189.
25. Stepansky, A.; Kovalski, I.; Perl-Treves, R. Intraspecific classification of melons (*Cucumis melo* L.) in view of their phenotypic and molecular variation. *Plant Syst. Evol.* **1999**, *217*, 313–332. [CrossRef]
26. Robinson, R.W.; Decker-Walters, D. *Cucurbits*; CAB International: Wallingford, UK, 1997; 226p.
27. Mitchell, J.M.; Cantliffe, D.J.; Sargent, S.A.; Datnoff, L.E.; Stoffella, P.J. Fruit yield, quality variables, and powdery mildew susceptibility of Galia melon cultivars grown in a passively ventilated greenhouse. *Fla. State Hortic. Soc.* **2007**, *120*, 162–167.
28. Poverenov, E.; Danino, S.; Horev, B.; Granit, R.; Vinokur, Y.; Rodov, V. Layer-by-layer electrostatic deposition of edible coating on fresh cut melon model: Anticipated and unexpected effects of alginate–chitosan combination. *Food Bioprocess Technol.* **2014**, *7*, 1424–1432. [CrossRef]
29. Freiman, Z.E.; Rodov, V.; Yablovitz, Z.; Horev, B.; Flaishman, M.A. Preharvest application of 1-methylcyclopropene inhibits ripening and improves keeping quality of 'Brown Turkey'figs (*Ficus carica* L.). *Sci. Hortic.* **2012**, *138*, 266–272. [CrossRef]
30. Van Oirschot, Q.E.; Tomlins, K.I. Applying analytical sensory evaluation techniques, which translate qualitative perceptions to numerical data to research on development issues. In Proceedings of the Conference on Combining Qualitative and Quantitative Methods in Development Research, Centre for Development Studies, University of Wales, Swansea, UK, 1–2 July 2002; pp. 1–30.
31. Hintlian, C.B.; Hotchkiss, J.H. The safety of modified atmosphere packaging: A review. *Food Technol.* **1986**, *40*, 70–76.
32. Soltani, M.; Alimardani, R.; Mobli, H.; Mohtasebi, S.S. Modified atmosphere packaging: A progressive technology for shelf-life extension of fruits and vegetables. *J. Appl. Packag. Res.* **2015**, *7*, 33–59.
33. Gorris, L.G.; Peppelenbos, H.W. Modified-atmosphere packaging of produce. In *Handbook of Food Preservation*; CRC Press: Boca Raton, FL, USA, 2020; pp. 349–362.
34. McMillin, K.W. Modified atmosphere packaging. In *Food Safety Engineering*; Demirci, A., Feng, H., Krishnamurthy, K., Eds.; Springer: Cham, Switzerland, 2020; pp. 693–718.
35. Exama, A.; Arul, J.; Lencki, R.W.; Lee, L.Z.; Toupin, C. Suitability of plastic films for modified atmosphere packaging of fruits and vegetables. *J. Food Sci.* **1993**, *58*, 1365–1370. [CrossRef]
36. Oliveira, J.C.; Ramos, A.V.; Sousa-Gallagher, M.J. A meta-study of the permeance of perforated packaging films to oxygen and carbon dioxide. *Food Eng. Rev.* **2022**, *14*, 328–352. [CrossRef]
37. Beaudry, R.M. Responses of horticultural commodities to low oxygen: Limits to the expanded use of modified atmosphere packaging. *HortTechnology* **2000**, *10*, 491–500. [CrossRef]
38. Hussein, Z.; Caleb, O.J.; Opara, U.L. Perforation-mediated modified atmosphere packaging of fresh and minimally processed produce—A review. *Food Packag. Shelf Life* **2015**, *6*, 7–20. [CrossRef]
39. Falagán, N.; Terry, L.A. Recent advances in controlled and modified atmosphere of fresh produce. *Johns. Matthey Technol. Rev.* **2018**, *62*, 107–117. [CrossRef]
40. Bishop, D.; Schaefer, J.; Beaudry, R. Industrial advances of CA/MA technologies: Innovative storage systems. In *Controlled and Modified Atmospheres for Fresh and Fresh-Cut Produce*; Academic Press: Cambridge, MA, USA, 2020; pp. 265–276.
41. Belay, Z.A.; Caleb, O.J.; Opara, U.L. Influence of initial gas modification on physicochemical quality attributes and molecular changes in fresh and fresh-cut fruit during modified atmosphere packaging. *Food Packag. Shelf Life* **2019**, *21*, 100359. [CrossRef]
42. Hu, W.Z.; Jiang, A.L.; Pang, K.; Qi, H.P. Atmospheric compositions, respiration rate and quality of fresh-cut cabbages in active modified atmosphere packaging. In Proceedings of the International Conference on Quality Management of Fresh Cut Produce, Bangkok, Thailand, 6–8 August 2007; Volume 746, pp. 69–76.

43. De Reuck, K.; Sivakumar, D.; Korsten, L. Effect of passive and active modified atmosphere packaging on quality retention of two cultivars of litchi (*Litchi chinensis* Sonn.). *J. Food Qual.* **2010**, *33*, 337–351. [CrossRef]
44. Hadjilouka, A.; Polychronopoulou, M.; Paramithiotis, S.; Tzamalis, P.; Drosinos, E.H. Effect of lemongrass essential oil vapors on microbial dynamics and Listeria monocytogenes survival on rocket and melon stored under different packaging conditions and temperatures. *Microorganisms* **2015**, *3*, 535–550. [CrossRef] [PubMed]
45. Kale, P.M.; Patil, S.S.; Palghadmal, U.B. Effect of different modified atmosphere packaging on physico-chemical, microbiological and sensorial attributes of fresh-cut muskmelon. *Int. J. Environ. Agric. Biotechnol.* **2020**, *5*, 1226–1233. [CrossRef]
46. Fallik, E.; Shalom, Y.; Alkalai-Tuvia, S.; Larkov, O.; Brandeis, E.; Ravid, U. External, internal and sensory traits in Galia-type melon treated with different waxes. *Postharvest Biol. Technol.* **2005**, *36*, 69–75. [CrossRef]
47. Shalit, M.; Katzir, N.; Tadmor, Y.; Larkov, O.; Burger, Y.; Shalekhet, F.; Lastochkin, E.; Ravid, U.; Amar, O.; Edelstein, M.; et al. Acetyl-CoA: Alcohol acetyltransferase activity and aroma formation in ripening melon fruits. *J. Agric. Food Chem.* **2001**, *49*, 794–799. [CrossRef]
48. Burger, Y.; Sa'ar, U.; Paris, H.S.; Lewinsohn, E.; Katzir, N.; Tadmor, Y.; Schaffer, A.A. Genetic variability for valuable fruit quality traits in Cucumis melo. *Isr. J. Plant Sci.* **2006**, *54*, 233–242. [CrossRef]
49. Aguayo, E.; Allende, A.; Artés, F. Keeping quality and safety of minimally fresh processed melon. *Eur. Food Res. Technol.* **2003**, *216*, 494–499. [CrossRef]
50. Gorny, J.R. A summary of CA and MA requirements and recommendations for fresh-cut (minimally processed) fruits and vegetables. In Proceedings of the VIII International Controlled Atmosphere Research Conference, Rotterdam, The Netherlands, 10 March 2003; Volume 600, pp. 609–614.
51. Mathooko, F.M. Regulation of ethylene biosynthesis in higher plants by carbon dioxide. *Postharvest Biol. Technol.* **1996**, *7*, 1–26. [CrossRef]
52. Jin, Y.Z.; Liu, W.W.; Qi, H.Y.; Bai, X.H. Ethanol vapor treatment maintains postharvest storage quality and inhibits internal ethylene biosynthesis during storage of oriental sweet melons. *Postharvest Biol. Technol.* **2013**, *86*, 372–380. [CrossRef]
53. Ergun, M.; Jeong, J.; Huber, D.J.; Cantliffe, D.J. Physiology of fresh-cut 'Galia' (*Cucumis melo* var. *reticulatus*) from ripe fruit treated with 1-methylcyclopropene. *Postharvest Biol. Technol.* **2007**, *44*, 286–292. [CrossRef]
54. Supapvanich, S.; Tucker, G.A. The effect of 1-methylcyclopropene (1-MCP) on quality and cell wall hydrolases activities of fresh-cut muskmelon (*Cucumis melo* var. *reticulatus* L.) during storage. *Food Bioprocess Technol.* **2013**, *6*, 2196–2201. [CrossRef]
55. Denoya, G.I.; Vaudagna, S.R.; Polenta, G. Effect of high pressure processing and vacuum packaging on the preservation of fresh-cut peaches. *LWT-Food Sci. Technol.* **2015**, *62*, 801–806. [CrossRef]
56. Fundo, J.F.; Amaro, A.L.; Madureira, A.R.; Carvalho, A.; Feio, G.; Silva, C.L.; Quintas, M.A. Fresh-cut melon quality during storage: An NMR study of water transverse relaxation time. *J. Food Eng.* **2015**, *167*, 71–76. [CrossRef]
57. Wang, Y.; Li, W.; Cai, W.; Ma, Y.; Xu, Y.; Zhao, X.; Zhang, C. Visible light exposure reduces the drip loss of fresh-cut watermelon. *J. Food Sci. Technol.* **2018**, *55*, 1816–1822. [CrossRef]
58. Pesis, E. The role of the anaerobic metabolites, acetaldehyde and ethanol, in fruit ripening, enhancement of fruit quality and fruit deterioration. *Postharvest Biol. Technol.* **2005**, *37*, 1–19. [CrossRef]
59. Liu, X.; Ma, H.; Liu, J.; Liu, D.; Wang, C. The γ-Aminobutyric Acid (GABA) Synthesis Gene Regulates the Resistance to Water Core-Induced Hypoxia Stress for Pear Fruits. *Agronomy* **2023**, *13*, 1062. [CrossRef]

MDPI
St. Alban-Anlage 66
4052 Basel
Switzerland
www.mdpi.com

Foods Editorial Office
E-mail: foods@mdpi.com
www.mdpi.com/journal/foods

Academic Open
Access Publishing

mdpi.com

ISBN 978-3-7258-1364-3